

U.S. DEPARTMENT OF COMMERCE
National Technical Information Service

AD-A031 659

INVESTIGATION OF ROTATING STALL PHENOMENA
IN AXIAL FLOW COMPRESSORS

VOLUME III. DEVELOPMENT OF A ROTATING
STALL CONTROL SYSTEM

CALSPAN CORPORATION, BUFFALO, NEW YORK

PREPARED FOR
AIR FORCE SYSTEMS COMMAND,
WRIGHT-PATTERSON AIR FORCE BASE, OHIO

JUNE 1976

ADA031659

AFAPL-TR-76-48
VOLUME III

314104

**INVESTIGATION OF ROTATING STALL PHENOMENA IN
AXIAL FLOW COMPRESSORS
VOLUME III-DEVELOPMENT OF A ROTATING STALL
CONTROL SYSTEM**

**CALSPAN CORPORATION
P.O. BOX 235
BUFFALO, NEW YORK 14221**

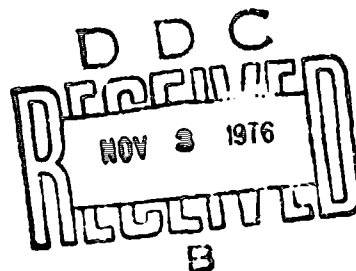
JUNE 1976

**TECHNICAL REPORT AFAPL-TR-76-48 VOLUME III
FINAL REPORT FOR PERIOD 1 MAY 1973 - 31 MAY 1976**

Approved for public release; distribution unlimited

**AIR FORCE AERO PROPULSION LABORATORY
AIR FORCE WRIGHT AERONAUTICAL LABORATORIES
AIR FORCE SYSTEMS COMMAND
WRIGHT-PATTERSON AIR FORCE BASE, OHIO 45433**

**REPRODUCED BY
NATIONAL TECHNICAL
INFORMATION SERVICE
U. S. DEPARTMENT OF COMMERCE
SPRINGFIELD, VA. 22161**



NOTICE

When Government drawings, specifications, or other data are used for any purpose other than in connection with a definitely related Government procurement operation, the United States Government thereby incurs no responsibility nor any obligation whatsoever; and the fact that the government may have formulated, furnished, or in any way supplied the said drawings, specifications, or other data, is not to be regarded by implication or otherwise as in any manner licensing the holder or any other person or corporation, or conveying any rights or permission to manufacture, use, or sell any patented invention that may in any way be related thereto.

This final report was submitted by the Calapan Corporation, under Contract F33615-73-C-2046. The effort was sponsored by the Air Force Aero-Propulsion Laboratory, Air Force Systems Command, Wright-Patterson AFB, Ohio under Project 3066, Task 306603, and Work Unit 30660334 with Mr. Marvin A. Stibich, AFAPL/TEC, as Project Engineer in charge. Dr. Gary R. Ludwig of the Calapan Corporation was technically responsible for the work.

This report has been reviewed by the Information Office, ASD/OIP, and is releasable to the National Technical Information Service (NTIS). At NTIS, it will be available to the general public, including foreign nations.

This technical report has been reviewed and is approved for publication.


MARVIN A. STIBICH
Project Engineer

FOR THE COMMANDER


MARVIN F. SCHMIDT
Tech Area Manager, Compressors

Copies of this report should not be returned unless return is required by security considerations, contractual obligations, or notice on a specific document.

FOREWORD

This is the final Technical Report prepared by the Calspan Corporation. The effort was sponsored by the Air Force Aero-Propulsion Laboratory, Air Force Systems Command, Wright-Patterson AFB, Ohio under Contract F33615-73-C-2046 for the period 1 May 1973 to 31 May 1976. The work herein was accomplished under Project 3066, Task 306603, Work Unit 30660334, "Investigation of Rotating Stall Phenomena in Axial Flow Compressors," with Mr. Marvin A. Stibich, AFAPL/TEC, as Project Engineer. Dr. Gary R. Ludwig of the Calspan Corporation was technically responsible for the work. Other Calspan personnel were: Joseph P. Nanni, John C. Erickson, John A. Lordi, Gregory F. Hecich, and Rudy H. Arendt.

ABSTRACT

This report presents the results of a research program that had two major objectives. The first objective was the development of a prototype rotating stall control system which was tested both on a low speed rig and a J-85-5 engine. The second objective was to perform fundamental studies of the flow mechanisms that produce rotating stall, surge and noise in axial flow compressors and thereby obtain an understanding of these phenomena that would aid attaining the first objective. The work is reported in three separate volumes. Volume I covers the fundamental theoretical and experimental studies of rotating stall; Volume II covers the theoretical and experimental studies of discrete-tone aerodynamic noise generation mechanisms in axial flow compressors; and, Volume III covers the development and testing of a prototype rotating stall control system on both the low speed test rig and the J-85-5 engine.

Volume I describes the theoretical and experimental investigation of the influence of distortion on the inception and properties of rotating stall for an isolated rotor row, and the effects of close coupling of a rotor and stator row on rotating stall inception. The experiments were conducted in the Calspan/Air Force Annular Cascade Facility, which is a low speed compressor research rig. In addition, the previously developed two dimensional stability theory for prediction of inception conditions was extended to include the effect of compressibility and the development of a three dimensional theory was initiated. These studies led to the following key results. The experimental studies of distortion show that for a single blade row the response of the blade row to the distortion and rotating stall are uncoupled phenomena and may be explained on the basis of a linearized analysis. The experimental studies of a closely coupled rotor-stator pair show that the addition of a closely spaced stator row downstream of a rotor row delays the onset of rotating stall. Moreover, the corresponding theoretical analysis predicts this trend although quantitative agreement is hampered by the lack of appropriate steady-state loss and turning performance for each blade row at the required operating conditions. The theoretical investigation of the effects of compressibility for wholly subsonic flows outside the blade rows indicates that the effects of

compressibility do not alter the mechanisms of rotating stall as deduced from the incompressible theory in that the rate of change of the steady state loss curve with inlet swirl is the dominant blade row characteristic affecting its stability. Therefore, if the steady state losses are known for the compressible flow condition, the linearized stability analysis is expected to apply.

Volume II describes a theoretical and experimental study of discrete-tone noise generation by the interaction of a rotor and a stator, and the development of a direct lifting surface theory for an isolated rotor. An approximate model has been developed to predict the sound pressure level and total power radiated at harmonics of the blade passage frequency for a rotor-stator stage. The analysis matches the duct acoustic modes for an annular duct with an approximate representation of the unsteady blade forces which includes compressibility effects. Measurements were made of the sound pressure levels produced on the duct wall of the annular cascade facility by a rotor-stator pair. Predictions which indicated that only the fourth and higher harmonics could be excited at conditions achievable in the facility, were borne out by the experiments. The calculations of the sound pressure levels for the propagating modes were significantly below the measured values. This discrepancy is believed to result from inaccuracies in existing models of rotor wake velocity profiles, which are shown to have a strong influence on predictions of the sound pressure levels of the higher harmonics. Volume II also contains the formulation of a direct lifting surface theory for the compressible, three-dimensional flow through a rotor row in an infinitely long annular duct. A detailed derivation is given for the linearized equations and the corresponding solutions for the blade thickness and loading contributions to the rotor flow field. The governing integral equation for the blade loading in a lifting surface theory is obtained for subsonic flow and progress on its solution is reported.

Volume III describes the development and testing of a prototype rotating stall control system. The control system was tested on the low speed compressor research rig and on a J-85-5 turbojet engine. On the low speed research compressor, the control was tested in the presence of circumferential inlet distortion. These tests were performed to demonstrate the ability of

the control to operate satisfactorily in the presence of inlet distortion and to aid in the selection of stall sensor configurations for the subsequent engine tests. The control system was then installed on a J-85-5 jet engine and its performance was tested under sea level static conditions, both with and without inlet distortion. On the engine, the stall control was installed to override the normal operating schedule of the compressor bleed doors and inlet guide vanes. The J-85-5 was stalled in two ways, first by closing the bleed doors at constant engine speed, and second by decelerating the engine with the bleed doors partially closed at the beginning of the deceleration. A total of 41 compressor stalls were recorded at corrected engine speeds between 48 and 72 percent of the rated speed. In all cases, the control took successful remedial action which limited the duration of the stall to 325 milliseconds or less.

TABLE OF CONTENTS

SECTION	PAGE
I INTRODUCTION	1
II DESCRIPTION OF THE ROTATING STALL CONTROL SYSTEM	3
III STALL CONTROL TESTS ON ROTATING ANNULAR CASCADE WITH INLET DISTORTION	10
A. INSTALLATION OF CONTROL ON ANNULAR CASCADE	10
B. STALL CONTROL TESTS	13
IV STALL CONTROL TESTS ON J-85-5 ENGINE	23
A. INSTALLATION OF CONTROL ON J-85 ENGINE	23
1. General Description	23
2. Physical Details	26
B. ADJUSTMENT OF CONTROL SYSTEM VARIABLES	30
C. STALL CONTROL TESTS	35
V SUMMARY AND CONCLUSIONS	47
REFERENCES	105

ILLUSTRATIONS

FIGURE		PAGE
1	Block Diagram of Original Rotating Stall Control System . . .	49
2	Modified Rotating Stall Control with Parallel Detector Channels	50
3	Ten Channel Rotating Stall Control System	51
4	Annular Cascade Configuration Used in Tests of Stall Control with Inlet Distortion	52
5	Geometry of Distortion Screens and Rotating Stall Sensors (Looking Upstream)	53
6	Sketch Showing Signal Conditioning of Input Reference Pressure to Remove Negative and Small Positive Reference Values and High Frequency Fluctuations	54
7	Typical Performance of Reference Pressure Conditioning System	55
8	Performance of Rotating Stall Control at Various Detector Reference Levels with Integrator Gain = 800	
(a)	Detector Signals: Sensors 1, Outer Wall 1/4 Chord Static, Stator Row 4 Detector Filter Corner Frequencies: Low = 5 Hz, High = Wideband	56
(b)	Detector Signals: Sensors 2, Outer Wall 1/4 Chord Static, Stator Row 5 Detector Filter Corner Frequencies: Low 1 Hz, High = 6 Hz	57
(c)	Detector Signals: Sensors 3, Rotor Outer Wall Detector Filter Corner Frequencies: Low = 1 Hz, High = 6 Hz	58

ILLUSTRATIONS (Cont'd)

FIGURE

PAGE

- 9 Performance of Rotating Stall Control with Constant
Compressor RPM and Variable Mass Flow-Integrator Gain = 800
 - (a) Detector Signals: Sensors 1, Outer Wall 1/4 Chord
Static, Stator Row 4
Detector Filter Corner Frequencies: Low = 5 Hz,
High = Wideband 59
 - (b) Detector Signals: Sensors 2, Outer Wall 1/4 Chord
Static, Stator Row 5
Detector Filter Corner Frequencies: Low = 1 Hz,
High = 6 Hz 60
 - (c) Detector Signals: Sensors 5, Rotor Outer Wall
Detector Filter Corner Frequencies: Low = 1 Hz,
High = 6 Hz 61
- 10 Performance of Rotating Stall Control During Rapid Acceleration
of the Rotor from 500 RPM (Normally Unstalled) to 1250 RPM
(Normally Stalled), Integrator Gain = 800
 - (a) Detector Signals: Sensors 1, Outer Wall 1/4 Chord
Static, Stator Row 4
Detector Filter Corner Frequencies: Low 5 Hz,
High = Wideband: Control Off 62
 - (b) Detector Signals: Sensors 1, Outer Wall 1/4 Chord
Static; Stator Row 4
Detector Filter Corner Frequencies: Low 5 Hz,
High = Wideband: Control On 63
- 11 Performance of Rotating Stall Control During Rapid Acceleration
of the Rotor from 500 RPM (Normally Unstalled) to 1250 RPM
(Normally Stalled), Integrator Gain = 800
 - (a) Detector Signals: Sensors 2, Outer Wall 1/4 Chord
Static, Stator Row 5

ILLUSTRATIONS (Cont'd)

FIGURE

PAGE

	Detector Filter Corner Frequencies: Low = 1 Hz, High = 6 Hz: Control Off	64
(b)	Detector Signals: Sensors 2, Outer Wall 1/4 Chord Static; Stator Row 5 Detector Filter Corner Frequencies: Low 1 Hz, High = 6 Hz: Control On	65
12	Performance of Rotating Stall Control During Rapid Acceleration of the Rotor from 500 RPM (Normally Unstalled) to 1250 RPM (Normally Stalled), Integrator Gain = 800	
(a)	Detector Signals: Sensors 3, Rotor Outer Wall Detector Filter Corner Frequencies: Low = 1 Hz, High = 6 Hz: Control Off	66
(b)	Detector Signals: Sensors 3, Rotor Outer Wall Detector Filter Corner Frequencies: Low 1 Hz, High = 6 Hz: Control On	67
13	Performance of Rotating Stall Control as Rotor Speed is Varied Slowly under Downstream Conditions Which Normally Induce Stall at all RPM's	
(a)	Detector Signals: Sensors 1, Outer Wall 1/4 Chord Static, Stator Row 4 Detector Filter Corner Frequencies: Low = 5 Hz, High = Wideband: Control Off	68
(b)	Detector Signals: Sensors 1, Outer Wall 1/4 Chord Static, Stator Row 4 Detector Filter Corner Frequencies: Low 5 Hz, High = Wideband: Control On	69
14	Modified Variable Geometry System Incorporating Rotating Stall Control on J-85 Engine	70

ILLUSTRATIONS (Cont'd)

FIGURE		PAGE
15	Schematic of Rotating Stall Control Installation on J-85 Engine	71
16	Pressure Transducers for J-85 Rotating Stall Control	72
17	Detail of Pressure Transducer Configurations	73
18	Cross Section of J-85 Compressor Casing Showing Axial Locations of Pressure Transducers	74
19	Pressure Transducer Installations in J-85 Compressor Casing Viewed from Outside	75
20	Control Pressure Transducer Installations in J-85 Compressor Casing - Viewed from Inside	76
21	Monitor Pressure Transducer Installations in J-85 Compressor Casing - Viewed from Inside	77
22	Overall View of J-85 Engine with Rotating Stall Control Mechanism Installed	78
23	Detailed View of Stall Control Mechanisms on J-85 Engine	79
24	Closeup View of Position Feedback Potentiometer and Several Pressure Transducers Used with Stall Control System on J-85 Engine	80
25	Front View of J-85 Engine with 180° Distortion Screen Installed	81
26	Tracking Performance of Stall Control System on J-85 Engine Under Normal Engine Operating Conditions	82
27	Detector Filter Characteristics Used for Stall Control Tests on J85 Engine	83
28	Compressor Inlet Dynamic Pressure and Static Pressure Rise on J85 Engine	84
29	System Reference Pressure Used in Stall Control Tests on J85 Engine	85

ILLUSTRATIONS (Cont'd)

FIGURE		PAGE
30	Performance of Rotating Stall Control on J-85 Engine Compressor Stalled by Closing Bleed Doors at Constant Engine Speed Engine Test No. 13: No Inlet Distortion	
(a)	Stall Test No. 4(b), Corrected Engine Speed, $N/N * \sqrt{\theta} = 52.3\%$	86
(b)	Stall Test No. 5, Corrected Engine Speed, $N/N * \sqrt{\theta} = 62.6\%$	87
31	Performance of Rotating Stall Control on J-85 Engine Compressor Stalled by Closing Bleed Doors at Constant Engine Speed Engine Test No. 14: 180° Circumferential Inlet Distortion	
(a)	Stall Test No. 1, Corrected Engine Speed, $N/N * \sqrt{\theta} = 52.1\%$	88
(b)	Stall Test No. 2, Corrected Engine Speed, $N/N * \sqrt{\theta} = 63.2\%$	89
(c)	Stall Test No. 3, Corrected Engine Speed, $N/N * \sqrt{\theta} = 67.4\%$	90
(d)	Stall Test No. 10, Corrected Engine Speed, $N/N * \sqrt{\theta} = 71.8\%$	91
32	Performance of Rotating Stall Control on J-85 Engine Compressor Stalled by Decelerating Engine with Bleed Doors Partly Closed Engine Test No. 13: No Inlet Distortion	
(a)	Stall Test No. 10, Initial Bleed Door Position = 30% Closed	92
(b)	Stall Test No. 12, Initial Bleed Door Position = 50% Closed	93
33	Performance of Rotating Stall Control on J-85 Engine Compressor Stalled by Decelerating Engine with Bleed Doors Partly Closed Engine Test No. 14: 180° Circumferential Inlet Distortion	

ILLUSTRATIONS (Cont'd)

FIGURE		PAGE
	(a) Stall Test No. 5, Initial Bleed Door Position = 30% Closed	94
	(b) Stall Test No. 7, Initial Bleed Door Position = 50% Closed	95
34	Rotating Stall Detector Signals (Expanded Time Scale) Engine Test No. 13: No Inlet Distortion Compressor Stalled by Closing Bleed Doors at Constant Engine Speed	
	(a) Stall Test No. 4(b), Corrected Engine Speed, $N/N * \sqrt{\theta} = 52.3\%$	96
	(b) Stall Test No. 5, Corrected Engine Speed, $N/N * \sqrt{\theta} = 62.6\%$	97
35	Rotating Stall Detector Signals (Expanded Time Scale) Engine Test No. 14: 180° Circumferential Inlet Distortion Compressor Stalled by Closing Bleed Doors at Constant Engine Speed	
	(a) Stall Test No. 1, Corrected Engine Speed, $N/N * \sqrt{\theta} = 52.1\%$	98
	(b) Stall Test No. 2, Corrected Engine Speed, $N/N * \sqrt{\theta} = 63.2\%$	99
	(c) Stall Test No. 3, Corrected Engine Speed, $N/N * \sqrt{\theta} = 67.4\%$	100
	(d) Stall Test No. 10, Corrected Engine Speed, $N/N * \sqrt{\theta} = 71.8\%$	101
36	Rotating Stall Detector Signals (Expanded Time Scale-Reduced Vertical Gain) - Engine Test No. 14, Stall Test No. 10: 180° Circumferential Inlet Distortion Compressor Stalled by Closing Bleed Doors at Constant Engine Speed $N/N * \sqrt{\theta} = 71.8\%$	102

ILLUSTRATIONS (Cont'd)

FIGURE		PAGE
37	Bleed Door Position at Rotating Stall Inception on J85 Engine with Undistorted Inlet Flow	103
38	Bleed Door Position at Rotating Stall Inception on J85 Engine with 180 Degree Circumferential Inlet Distortion	104

SYMBOLS

- β detector bias level used in conditioning of compressor static pressure rise, millivolts (see Figure 29)
- K detector level gain used in conditioning of compressor static pressure rise, see Figure 29
- N engine speed, rpm
- N^* rated speed of J-85 engine, 16,560 rpm
- P_D detection level - amplitude of conditioned pressure fluctuations from control transducers which trigger stall control into corrective action, millivolts
- P_R system reference pressure used by stall control system, millivolts, (see Figure 29)
- q_i inlet dynamic pressure measured upstream of compressor face, in. H₂O
- T ambient temperature, °R
- δ_{SM} stator stagger angle at mid-annulus, deg.
- Δ time delay factor in rotating stall control, sec.
- ΔP_{REF} compressor static pressure rise measured on outer casing, psi (millivolts)
- θ ambient temperature ratio, $\frac{T}{518.7}$

SECTION I

INTRODUCTION

The useful operating range of a turbine engine compressor is greatly influenced by its stalling characteristics. The optimum performance of a turbo-propulsion system is usually achieved when the compressor is operating near its maximum pressure ratio. However, this optimum is generally not attainable because it occurs close to compressor stall and unstable flow conditions. Because of the serious mechanical damage that may result during compressor stall cycles, a factor of safety (stall margin) must be provided between the compressor operating line and the stall boundary. This is usually done by prescheduling the primary engine controls. However, the prescheduling approach can lead to the requirement for a large stall margin in order to keep the engine from stalling under all possible transient and steady state flight conditions. It is clear, then, that an engine control system that can sense incipient destructive unsteady flow in a compressor and take corrective action would allow for reduced stall margins in the design and thus lead to large engine performance and/or efficiency gains. Recognition of this fact has been the motivation for a continuing program of research that the AFAPL has sponsored at Calspan dating back to 1962.

The work at Calspan has been both theoretical and experimental in nature and has been aimed at obtaining a sufficient understanding of the rotating stall phenomena such that its onset and its properties can be predicted and controlled. The capability of predicting the onset of rotating stall on isolated blade rows of high hub-to-tip ratios in low speed flows was demonstrated in Reference 1. In addition, the basic feasibility of developing a rotating stall control system was demonstrated in the Calspan/Air Force Annular Cascade Facility. This present report summarizes the latest three year research program at Calspan. The specific goals of the present program were to extend the fundamental studies of rotating stall to consider the effects of compressibility, blade row interaction and inlet distortion; and to extend the fundamental aerodynamic and acoustic analysis of flow through a compressor. In addition, the rotating stall control

system was validated by successful ground tests on a J-85-5 turbojet engine.

The work is reported in three separate volumes. Volume I entitled, "Basic Studies of Rotating Stall", covers the theoretical and experimental work on the effects of distortion and close coupling of blade rows on rotating stall inception and properties. In addition, the theoretical analysis of compressibility is treated in the two-dimensional approximation and the initial development of a three-dimensional theory is given. Volume II entitled, "Investigation of Rotor-Stator Interaction Noise and Lifting Surface Theory for a Rotor", describes the development of a linearized lifting surface theory for the subsonic compressible flow through an isolated rotor row. In addition, a theoretical and experimental study of the noise generated by the interaction of a rotor and stator is described. Volume III entitled, "Development of a Rotating Stall Control System", describes the development and testing of the control system installed on a low speed research compressor and on a J-85-5 turbojet engine.

Volume III is divided into three main sections. In Section II, the functional requirements for a rotating stall control system are reviewed and a description of the basic stall control system used to meet these requirements is presented. Section III presents the results of testing the control on the Calspan/Air Force Annular Cascade Facility in the presence of inlet distortion. In Section IV, the installation and testing of the control on a J-85-5 turbojet engine are described. Following these three major sections, the results of the overall development and test program for the rotating stall control are summarized in Section V.

SECTION II

DESCRIPTION OF THE ROTATING STALL CONTROL SYSTEM

As noted in the introduction, the development of an engine control system which can sense incipient destructive unsteady flow in a compressor and take corrective action would allow for reduced compressor stall margins in the design and thus lead to engine performance and/or efficiency gains. In many instances of engine failure, rotating stall has been identified as a precursor to destructive unsteady flows in an engine. Moreover, blade fatigue considerations will not allow a compressor to operate for prolonged periods in a large-amplitude rotating stall mode. It is then desirable for several reasons to develop an engine control system that would sense the onset of rotating stall and keep the engine from operating in the rotating stall mode.

The functional requirements for a rotating stall control system have been discussed in References 1 and 2. Briefly they can be summarized as follows:

1. An unambiguous signal of the presence of rotating stall must be generated.
2. The control must be capable of processing this signal so that action on some compressor variable can be taken which will eliminate rotating stall.
3. When rotating stall is detected, control action must occur within a time period on the order of milliseconds, and its effect on the compressor should be almost immediate.
4. When rotating stall is absent, the control should have no effect on the compressor operation. Return to normal compressor operation after rotating stall dies away need not be as rapid as initial control action when rotating stall first occurs.

In the work reported herein, the requirement for a fast acting control system is attacked through sensing pressure fluctuations within the compressor itself and using these signals to provide direct mechanical action on compressor geometry (such as stator stagger angle or bleed port openings). It is believed

that more indirect control action, such as fuel flow control, would not provide a fast enough response. However, such a control could be used on the indirect variables if the compressor response to these variables were fast enough.

The primary task to be treated before rotating stall control systems are feasible is the establishment of an incipient stall signature that can be sensed by such a system. In previous work (References 1 and 2) a search for suitable stall sensors was conducted in the Calspan/Air Force Annular Cascade Facility. The studies of Reference 1 indicated that a variety of unsteady pressure sensors located on or very close to the rotor or stator blades in the compressor could provide acceptable signals for use with a rotating stall control. The final selection of locations can be made on the basis of ease of installation and maintenance rather than on the basis of signal quality.

During the previous program (Reference 1), a rotating stall control which uses unsteady pressure sensor signals as inputs was designed and given limited tests in the annular cascade facility. During the current program, a number of significant modifications to the stall control were made prior to the tests. In the following paragraphs a general description of the original, less complicated system is presented first as background. This is followed by a detailed description of the major changes made during this program. In the block diagrams presented for the present system, signal points equivalent to those in the original system are identified by numbers identical to those used in Reference 1.

The control is an electro-hydraulic feed-back control system. The inputs to the control system are unsteady pressure signals produced by the sensors mounted in the compressor. The output of the control is a mechanical operation on some variable geometry feature of the compressor to be controlled. For the tests reported in Section III, the variable geometry is the stagger angle of the stators in the Calspan/Air Force Rotating Annular Cascade Facility. For the tests on the J-85 engine (Section IV), the variable geometry consists of the inlet guide vanes and bleed doors on the intermediate stages of the compressor. In the following description, stator stagger angle is used as the mechanical variable for illustrative purposes.

The signal conditioning and processing subsystem of the original design of the rotating stall control is shown in block diagram form in Figure 1. The signals at various places or stages in the circuit are shown schematically on the right hand side of the figure. In operation the system performs as follows:

- 1) Time varying electrical signals are obtained from the pressure transducers on the rotating stall sensors. These signals are summed, at appropriate gains, to form a composite stall pressure signal.
(Stage 1)
- 2) The composite signal is bandpass-filtered to remove steady state and low frequency variations (which are not associated with rotating stall) and high frequency contaminants such as instrument noise and blade passage effects. Both corners of the passband are adjustable.
(Stage 2)
- 3) The bandpass signal is then processed in an absolute value circuit (rectified) to generate a single polarity signal proportional to the absolute magnitude of the fluctuating pressure signal. (Stage 3)
Since the stall signal is a dynamic variable, pressure variations above and below the mean level are equally indicative of the presence of stall and hence the use of the absolute value circuit.
- 4) The rectified signal is then input to a voltage comparator circuit. The comparator produces two output signals. The first signal, Stage 4, is obtained by comparing the rectified input signal with an adjustable dc reference level. Only that portion of the rectified signal which exceeds the reference level is passed. The second comparator output signal, Stage 5, controls an electronic gate. This signal activates the gate whenever the input signal exceeds the reference level. The gate has been included in the circuit to ensure that the next component of the circuit, the integrator, is referenced to zero voltage when the input signal is below the reference level.
- 5) The output from the gate is fed into an integrator. The integrator gain and decay rate are independently adjustable. The integrator output is then a signal which is obtained by integrating only that portion

of the original pressure signal whose absolute value exceeds the reference level.

- 6) The output of the integrator, Stage 6, is summed in opposition with the command position signal, Stage 7. The output of the summer is fed to the servo which acts to move the stator vanes away from the stall condition (reduce angle of attack). When the vanes reduce angle of attack the original pressure signal should fall below the reference level causing the input to the integrator to drop to zero. The output voltage of the integrator then decays at a preselected, but adjustable, rate. When this signal, Stage 6, decreases sufficiently, the original command signal, Stage 7, then resumes control allowing the vanes to move towards their original position.

As discussed in Reference 1, it was found that the control system performed very well in the presence of rotating stall if the integrator decay time constant is set to large values. However operation of the control system with a long decay time constant will cause the stators to overshoot when the primary engine controls command a change from a stator stagger angle inside the rotating stall boundary to one closer to the boundary or outside of the boundary. Under this condition the undecayed portion of the stall control signal will reinforce the engine control signal. Long decay time constants will increase the magnitude and duration of the overshoot.

In order to alleviate the above problem, the control system was designed so that it operates with two time constants, that is with a long decay time constant in the presence of rotating stall and with a short time constant once it has disappeared for a specified short period.

The integrator decay circuitry consists of an electronic switch, an adjustable time delay circuit and a variable resistor that results in a short time constant when connected in parallel with the integrator feedback capacitor. The circuitry is designed to produce a short time constant when the electronic switch is closed and a long time constant when the switch is open. Stall pressures in excess of the reference level cause the electronic switch to open and thereby establish the long time constant. The long time constant is

maintained as long as the stall pressure signal is in excess of the reference level. If the stall pressure signal falls below the reference level, the integrator is switched back to the short time constant after a specific but adjustable time delay. Thus the system selects the fast recovery time (short time constant) only if the pressure signal remains below the reference level longer than the delay time. The delay time, Δ , is adjustable from 0.2 to 2.0 seconds and the short time constant is adjustable from 1.0 to 10.0 seconds. The long time constant is adjustable to values in excess of 100.0 seconds.

Although the original rotating stall control system which has just been described is functionally similar to the current configuration, there are some significant differences between the two. The major differences in the new system are the following:

- (a) A separate Detector Channel is provided for each input pressure signal.
- (b) Provisions to vary the system reference pressure as a linear function of engine pressure ratio or any other appropriate variable is incorporated.
- (c) The Detector Channel bandwidth was extended from 2 K Hz to 50 K Hz.

In the previous system the various Detector Channel signals were first summed and then the summed signal was compared to the reference pressure to generate the gate enabling signal 5 and the integrator input signal 4 as shown in Figure 1. It was believed that the noise content of the summed signal could mask the presence of a stall signal on any one channel. This is particularly unsatisfactory in the presence of circumferential inlet distortion where a sensor in one region of the flow may provide the first indication of approaching stall while the remaining sensors indicate acceptable conditions. To overcome this problem, the system was modified to incorporate a separate comparator for each detector channel. The separate comparator outputs are then combined to produce the equivalent of the integrator input and gate enabling signals labelled 4 and 5, respectively in Figure 1 but with greater noise immunity.

In the previous system, the system reference pressure was a constant level set on the control console. The present system includes circuitry to cause the pressure reference to vary as a linear function of engine pressure ratio or any other appropriate signal. This signal is processed through a one radian/sec. second order critically damped filter and therefore the reference pressure changes only in response to slowly varying parameters.

A detailed block diagram of the signal flow for two typical detector channels in the present stall control system is presented in Figure 2 and a photograph of the control console for this ten channel system is shown in Figure 3. Referring to Figure 2, each input pressure signal is amplified and bandpass filtered to remove very high and very low frequency information that is not related to rotating stall. After filtering, each signal is rectified in a precision absolute value circuit to provide a single polarity signal to compare with the system reference pressure. The bandpass filtered absolute value of each input pressure signal is connected to a gating comparator circuit and a biased analog comparator circuit. As illustrated in the block diagram of Figure 2, the gating comparator output is high when the input signal level exceeds the reference level and zero when the input level is less than the reference level. The biased analog comparator simply passes, with unity gain, that portion of the input signal in excess of the system reference level. The analog output from each analog comparator channel is summed to produce signal 4 which represents the sum of the input pressure signals in excess of the reference pressure. The gating comparator outputs are combined, with logic circuitry, to produce signal 5, the gate enabling signal. This signal is TRUE when any input signal exceeds the reference level and FALSE when all are less than the reference level. It controls the input to the integrator and also controls the integrator decay circuit. Integration is allowed only when signal 5 is TRUE. The operation of the two time constant decay circuit is identical to the original control which has been described earlier in this section. In fact, the overall system configuration from signal points 4 and 5 to the output is identical to the previous system.

In both the original and the current versions of the control system, the mechanical operation commanded by the electronic console is performed by an electro-hydraulic servo. The servo consists of a flow control valve, a feedback

potentiometer and a linear actuator. The linear actuator is of the balanced piston type (equal area on each side of piston) with an effective area of 0.2 in^2 and a stroke of 1.0 inch. The valve is a Moog Series 3 Flow Control Valve and provides a maximum flow of $26 \text{ in}^3/\text{sec}$ at a supply pressure of 3000 psi and zero load pressure. A linear potentiometer measures the actuator position. The servo was designed to meet design velocity and acceleration limits ($62.5 \text{ in}/\text{sec}$ and $3 \times 10^4 \text{ in}/\text{sec}^2$, respectively) at a supply pressure of 1000 psi. However, the servo can be operated safely to pressures of 3000 psi.

The servo loop gain (velocity constant) is 300 sec^{-1} . When used to drive the two stator rows in the tests of the rotating stall control system on the annular cascade, this gain resulted in a closed loop corner frequency (down 3 db.) of 48 Hertz. The servo was stable and well behaved at this gain. It did not require velocity or acceleration feedback to improve the damping characteristics.

During all of the tests, a small hydraulic power supply was used to drive the servo on the rotating stall control. The hydraulic power supply consisted of a $6 \text{ in}^3/\text{sec}$ fixed displacement pump, an unloading valve set to unload at 1200 psi and a 1 gallon accumulator. With this system, the hydraulic supply pressure was maintained between 1000 and 1200 psi. This was adequate for all tests which were conducted. No oil or overheating problems were encountered during operating periods up to 8 hours in length.

SECTION III

STALL CONTROL TESTS ON ROTATING ANNULAR CASCADE WITH INLET DISTORTION

The original rotating stall control system was tested previously on the Calspan/Air Force Annular Cascade Facility for undistorted inlet flow. A detailed description of the facility and the results of the tests have been reported in Reference 1. In the current program, the modified control system was tested on this same facility with circumferential inlet distortion. The latter tests were performed to demonstrate the ability of the modified control to operate satisfactorily in the presence of inlet distortion and to aid in the selection of stall sensor configurations for the subsequent control tests on a J-85-5 jet engine.

A. INSTALLATION OF CONTROL ON ANNULAR CASCADE

The annular cascade facility consists basically of the front outer casing of a J-79 jet-engine compressor with a Calspan fabricated hub. The outer casing will accept up to six variable stagger angle stator rows. The hub has provision for two rotor rows at the third- and fifth-stage rotor locations of the J-79 compressor. Speed control on each rotor hub is independently variable in either direction of rotation. The annular passage between the hub and outer casing has a constant hub-to-tip ratio of 0.80. The facility includes a bell-mouth inlet on the outer casing and a bullet nose on the hub to provide a smooth flow of air to the test section. Outlet ducting is connected to an independently variable source of suction to provide the required flow through the annulus. An electrically powered two-speed axial flow fan is used as the source of suction. Continuous control of the mass flow is achieved through the use of variable inlet guide vanes to the fan and a variable damper in the fan exit flow.

The modified rotating stall control was tested on a configuration of the annular cascade similar to that used in the tests reported in Reference 1. A sketch of the configuration is shown in Figure 4 along with a list of the sensors which were used. The only difference in the annular cascade between the current tests and those of Reference 1 is the inclusion in the current work of distortion screens just upstream of the guide vanes. These screens were configured

to generate a two lobe distortion pattern as shown in Figure 5. The circumferential locations of the sensors relative to the distortion screens are also shown in Figure 5.

In the configuration used for the tests of the control system (Figure 4), the annular cascade contained three stationary blade rows and one rotor row. In sequence from the inlet, these were: an inlet guide vane row, a stator row (stator row 4), a rotor row (rotor row 5), and finally another stator row (stator row 5). The numbering system for the rotor and stator rows is based on their locations in the original J-79 compressors. The guide vane row is Calspan fabricated. It was used to provide an inlet swirl to stator row 4. The blades in the two stator rows and the rotor row consist of shortened blades from the corresponding locations in the original J-79 compressor. In these tests, the stagger angles of the two stator rows were varied in unison by the control system servo mechanism while the rotor stagger was held fixed at 40 degrees. The controlled variable stagger angle of the stators provided the means of controlling rotating stall on themselves and on the rotor.

In operation on a compressor, the rotating stall control system would normally be used to override the primary engine control command signals. In control system tests on the annular cascade, the primary engine control command signal is simulated so that the stator vanes can be ordered to take any arbitrary position in the absence of rotating stall. The presence of rotating stall then causes the stall control system to override the primary command signal.

The types of sensors used in these stall control tests were limited to those mounted in the outer wall of the compressor casing (see Figure 4). These sensors are of the most interest because they are similar to the sensors which were used later in the control tests on the J-85 engine. For each of the types of sensors tested, two sensors were used at different circumferential locations, one in the wake of a distortion screen and one in the clear area between distortion screen lobes (Figure 5). The signals from both sensors of the same type were used simultaneously as inputs to the stall control system. However, separate tests were performed on sensors of different types.

One of the modifications to the stall control system which was described earlier (Section II) was the incorporation of provisions to vary the system reference pressure as a linear function of engine pressure ratio or any other appropriate variable. In the current tests, the static pressure rise across the compressor was chosen as the variable. Initial tests during this program pointed out a deficiency of a simple linear variation in the system reference pressure. At low rotor speeds, the system reference pressure became very small and the control took action even in the absence of rotating stall. To prevent this occurrence, the system reference pressure circuit was modified so that the reference signal was always maintained above a prescribed minimum positive value.

A sketch of the system reference pressure variation in response to a typical input pressure variation (from rotor speed changes) is shown in Figure 6. The input pressure is shown starting at a negative value and rising to some positive value. Typical fluctuations in the input pressure are also shown. These fluctuations are removed from the system reference pressure by a one radian/sec second-order critically-damped filter. While the input pressure is negative, the system reference pressure is maintained at a positive value selected by a bias control. Once the input pressure becomes positive, the system reference pressure is increased above the bias level by an amount equal to the value of the input pressure multiplied by the detector gain. Both the detector bias level and detector gain are variable in this prototype control system.

The performance of the reference pressure conditioning system under operating conditions can be seen in the records presented in Figure 7. The records were obtained by accelerating and decelerating the rotor in the annular cascade. The upper record, (a), in this figure shows the raw input pressure signal and the lower record, (b), shows the conditioned system reference pressure used by the control system. These records were taken at slightly different times but under identical operating conditions of the annular cascade.

In addition to the modifications of the conditioning circuit for the system reference pressure, one other minor modification of the control was made before initiating the main body of the tests. It was found that the presence of large amplitude rotating stall caused the new control system to act so fast that

the elasticity in the mechanical linkages to the stators caused a resonant response (chatter) of the mechanical-hydraulic system. This could be avoided by reducing the integrator gain in the control system, but at the expense of drastically slowing the response to small amplitude rotating stall signals. A satisfactory solution to the chatter was accomplished by reducing the bandwidth of the hydraulic actuator system from approximately 40 Hz to 10 Hz. With the reduction in bandwidth, it was possible to maintain a fast response to small amplitude rotating stall signals but to limit the speed of response to large amplitude signals to a value which avoided chatter.

B. STALL CONTROL TESTS

Before proceeding into the presentation of the results, some general comments which apply to all of the data will be made. In the process of testing the control on the annular cascade, over 150 data records were generated. Some of these records were used to determine final control settings and others were made to test the control operation at its final settings. For the sake of clarity and conciseness only a portion of the records will be presented. However, the selected records are representative of the performance attained.

In all of the figures which are presented (Figures 8 through 13), six recorded traces are shown as a function of time for each data run. The time increases from left to right in each figure. The time scale varies between figures and its value is indicated just above the third record from the top in each figure. Each record is discussed below starting with the top record as number one.

- (1) Rotor Speed - This is a record of the rotor speed between 500 and 1500 rpm. For the first series of tests, the rotor speed was held constant at approximately 1250 rpm (Figures 8 and 9). However, both rapid and slow variations in rotor speed are shown in the final series of tests (Figures 10 through 13).
- (2) Inlet Dynamic Pressure, q_o - This is a record of the pressure difference between the total and static pressure taps far upstream of the distortion screens. (See Figure 4.) It is

proportional to the square of the mass flow through the compressor. As noted on each figure, the top line of the dynamic pressure record corresponds to two inches of water and the bottom line to 0. Note that in some cases, this dynamic pressure can be larger than the static pressure rise across the compressor because the fan system downstream of the compressor is turned on. (The stall control was tested with the fan both on and off. The data selected for presentation are representative of the severest tests of the rotating stall control system.) In all of the figures, high frequency fluctuations in this record have been filtered through a simple first order filter with a corner frequency at 6 Hz. This filtering was performed in order to obtain a cleaner record.

- (3) Compressor Static Pressure Rise, ΔP_{REF} - This is a record of the pressure difference between static pressure taps located on the outer casing upstream and downstream of the compressor. (See Figure 4.) It is used as the input reference pressure to the control system which was discussed previously. (See Figures 6 and 7.) As with q_0 , for recording purposes the high frequency fluctuations were filtered through a simple first order filter with a corner frequency of 6 Hz.
- (4) Stator Row 4 Stagger Angle, δ_{SM_4} - This is a record of the stagger angle of stator row 4. It is representative of the response of the control to rotating stall. The scale factor for the record is 2.4 degrees per major division. As noted on each figure, the top line corresponds to $\delta_{SM_4} = 54$ degrees and the bottom line corresponds to $\delta_{SM_4} = 30$ degrees. In these tests, stator rows 4 and 5 are linked together mechanically so the record is also representative of the stagger angle of stator row 5. However, the numerical value for stator row 5 is different. For these tests, the stagger angle of stator row 5 was set to be approximately 6 degrees larger than that of stator row 4. This corresponds to the configuration designated stator row 5 "loaded" in Reference 1. In these records, the primary

compressor control is selected to provide a stagger angle on stator row 4 of 30 degrees and the occurrence of rotating stall causes the stall control system to increase the stagger angle until rotating stall disappears. In some tests the control system was turned off to provide a record of the uncontrolled compressor performance for comparison with the controlled compressor performance.

- (5) Detector Pressure Signal - This is a record of the signal obtained from the upper pressure sensor which is in the wake of the distortion screens. (See Figure 5.) This signal, along with the signal from a second sensor, (Record 6), is used by the control system to determine the presence of rotating stall. If the amplitude of the fluctuations becomes larger than the system reference pressure, the control increases the stator stagger angles until the fluctuation amplitude decreases below the reference level. After stall disappears for a specified time (1 second in these tests), the stator stagger angles return to the position selected by the primary compressor control. The rate at which the stagger angles return is specified by the decay rate of the integrator in the control system. In these tests the time constant for the decay rate was 5.8 seconds. A discussion of the control return process after stall has disappeared can be found in Section II.
- (6) Detector Pressure Signal - This record is the signal from a second sensor mounted in the clear area between the lobes of the distortion screen. The signal has the same function as that shown in Record 5. In all cases tested, both sensors were of the same type in each figure, but the results attained with different types of sensors are shown in different figures. The type of sensor used is identified in the title of each figure. In addition, the sensor signals were filtered to remove high and very low frequencies prior to insertion into the control system. Simple first order filters were used for both the low and high frequencies.

The corner frequencies of these filters are also listed in the titles. Records 5 and 6 show the signals after the high frequencies have been removed. The effects of the low frequency filters are not apparent in the records. These filters are within the control system.

The results of the control system tests will be presented in four steps. First, some records will be presented to show the steady state performance of the control system, that is operation of the control when it is required to prevent rotating stall over continuous long periods of time. Following this is a discussion of the performance of the control as the mass flow through the compressor is varied at constant rotor speed. Next, the transient performance of the control system during rapid acceleration of the rotor is presented. The final presentation is the performance of the control system as the rotor speed is varied slowly over a wide range of rpm.

In all of the results, the inlet guide vanes in the cascade were held at a fixed stagger angle of 24.5 degrees. In Reference 1, results with four different guide vane settings were presented because the rotating stall characteristics varied with guide vane stagger angle. However, preliminary tests during this program showed that with the distortion screens in place, the rotating stall characteristics were nearly independent of guide vane setting.

The procedure used in testing a particular combination of sensors and control system variables is as follows. A preliminary survey was made to determine a detector bias level setting which prevented unwarranted operation of the control at low levels of the input reference pressure (see Figure 6). With the bias level selected, the rotor speed was set to approximately 1250 rpm and the downstream flow control damper vanes were closed until continuous large amplitude stall occurred with the control turned off. With the damper vanes fixed in this position, the control was then turned on and a series of records at various detector level gain settings (see Figure 6) were recorded at slow chart speeds for periods usually exceeding thirty seconds. These records were used to assess the degree of hunting at the different detector level gain settings, and, if possible, to select one particular detector gain which appeared suitable for controlling rotating stall over long periods of time.

The criterion used in selecting the most favorable detector gain is that it should prevent repeated occurrence of large amplitude rotating stall while at the same time it should not require the stators to back off more than is necessary. As in the results reported in Reference 1, it appears that the best detector level for this purpose is one which allows occasional bursts of small amplitude rotating stall under conditions which would normally cause continuous occurrence of large amplitude rotating stall in the uncontrolled compressor.

Figure 8 presents a series of records which were used to select detector level gain settings. Each part (a, b or c) of this figure corresponds to a particular type of sensor while the various runs in each part show the performance at different detector level gain settings. On the left of each figure, the detector level gain is high and rotating stall is occurring continuously while on the right the gain is low and rotating stall has been either completely eliminated or limited to a very occasional burst. At intermediate gains, rotating stall occurs on a fairly regular basis and the controlled stator stagger angles "hunt" through a large amplitude. Note that the presence of large amplitude rotating stall is apparent not only in the detector pressure signals but also in the inlet dynamic pressure, q_o , and in the compressor static pressure rise, ΔP_{REF} .

As found in the tests with undistorted inlet conditions (Reference 1), it was found in the current tests that even when rotating stall is completely eliminated (low detector level gains), there is a certain amount of hunting in the control action on the stator blades. However, as discussed in Reference 1, this is considered acceptable for an override type of control which is being forced to operate continuously under adverse conditions when such operation should occur only transiently in practice.

Inspection of parts a, b and c of Figure 8 shows that the most satisfactory operation of the control is obtained with Sensors 1 (Figure 8a) at a detector bias level setting of 50 and a detector level gain setting of 50 or 60. Sensors 2 (Figure 8b) provided marginal performance at bias and gain settings of 50. With Sensors 3 (Figure 8c), it was necessary to use a bias level of 40 with

a gain of 40 or 50 to obtain satisfactory performance during continuous long time operation of the control.

In these tests, each type of sensor was investigated separately. The control is capable of using up to ten sensors at the same time. However, only one system reference pressure with its corresponding detector bias level and gain setting will be used. Thus, if the combined performance is to be inferred from the individual sensor tests, it is necessary to maintain the gain and bias settings in the same ratio for all three types of sensors (for example 60/50 or 48/40). Differences in absolute value of both settings can be offset by adjusting the gain of the existing amplifiers at the input of each detector channel. Thus, the final gain/bias settings which were selected for the remainder of the tests on the three types of sensors are as follows.

	<u>Detector Level Gain</u>	<u>Detector Bias Level</u>
Sensors (1)	50	50
Sensors (2)	50	50
Sensors (3)	40	40

Note that the units used to describe the detector level gain, detector bias level and the integrator gain (also listed in each figure) do not correspond to physical units. They are read from the settings of linear potentiometers on the face of the control cabinet.

Following the tests for continuous control operation under adverse conditions, the performance of the control was investigated with each type of sensor as the mass flow was varied. The rotor was held at approximately constant speed and the mass flow was varied by opening and closing a set of electrically driven damper vanes downstream of the compressor. The results are presented in Figure 9. Different parts of this figure (a, b and c) present the results for different sensor types. Two test runs are shown for each type of sensor. The run on the left shows the compressor performance with the control turned off while the run on the right shows the performance with the control turned on. Note that

the time scale in Figure 9 has been expanded by a factor of 5 over that used in Figure 8.

For each test run in Figure 9, the records were started with the damper vanes wide open, allowing a high mass flow through the compressor. The record of inlet dynamic pressure, q_0 , can be used to infer the relative mass flow, since q_0 is proportional to the square of the mass flow. Rotating stall is absent at these high mass flows. Next, the damper vanes were closed gradually. This decreased the mass flow and increased the static pressure rise,

ΔP_{aer} , up to a maximum of approximately 1.8 inches of water. Further closing of the damper vanes continued to reduce the mass flow but the compressor static pressure rise also began to decrease as the blade rows began to enter steady stall. The detector pressure signals show an increase in amplitude of the high frequency fluctuations associated with increased turbulence in this region. At very low mass flows, the uncontrolled compressor entered large amplitude rotating stall. This rotating stall is apparent in the q_0 and ΔP_{aer} records as well as in the detector pressure signals. In the final portion of each test run, the damper vanes were opened gradually and the extinction of rotating stall can be observed in the last portion of each test run.

With the control turned on, the general performance features with all three sensor types were similar. At most, the control allowed one fragmented stall cell to appear. With sensor type 1, (Figure 9a), the control began to act at the first appearance of the turbulent fluctuations associated with steady state stall. However, the mass flow was reduced to such a small value in this case that a small amplitude rotating stall (probably on the stators) was allowed to develop at these very low mass flows. It is believed that the control of these residual, very small amplitude, stalls is neither necessary nor practical since such action would probably lead to overcontrolling the compressor. With sensor types 2 and 3 (Figures 9b and 9c), the control did not act until a rotating stall cell appeared. However, the appearance of such a cell led to very rapid action of the control which eliminated its existence almost immediately. In fact, the rotating stall cell in the "control on" records of Figure 9c did not show up at all in the

ΔP_{aer} record and it is just discernible in the detector pressure signal records. The gradual decrease in control action is shown in the last portion of each record as the damper vanes are opened and rotating stall disappears.

Of the three types of sensors tested in Figure 9, the control performance appears to be best with sensor type 1, followed by sensor type 3. Sensor type 2 appears to be generating a larger control action than is required to eliminate rotating stall. If all of these sensor types were used at the same time, we would probably reduce the gain in the input amplifiers from sensor type 2 so that the control detects only the larger amplitude stalls on this sensor. The control of smaller amplitude stalls would be left to sensors of types 1 and 3. Finally, note that all three sensor types in Figure 9 generated a "control on" pressure rise across the compressor at the lowest mass flows which was equal to or larger than the maximum pressure rise during the continuous rotating stall which occurred with the control off.

In the next series of tests, each sensor type-control combination was tested for transient performance during rapid acceleration of the rotor. The results are shown in Figures 10, 11, and 12. Note that the time scale is expanded compared to those used previously. Each of these figures has two parts, a and b. Part a is a test with the control turned off and part b is a test with the control turned on. Prior to the test presented in each figure, the rotor speed was set to approximately 1250 rpm and the damper vanes were adjusted to provide a continuous large amplitude rotating stall with the control off. The damper vanes were fixed in this position for all of the tests. The fan downstream of the damper vanes kept the mass flow through the compressor high enough so that reducing the rotor speed to values substantially below 1250 rpm caused rotating stall to disappear.

All acceleration tests were initiated at 500 rpm where rotating stall was absent. The rotor was accelerated rapidly to approximately 1250 or 1300 rpm and held there for a number of seconds. The rotor was then decelerated to approximately 500 rpm. The hydraulic drive system of the rotor in the annular cascade allowed very fast accelerations. However, decelerations could not be accomplished with the same speed.

Inspection of the "control off" records, part a of Figures 10, 11 and 12 shows that inception of rotating stall usually occurred some time after the rotor reached its final top speed. Apparently, it takes a while for rotating stall to develop. Once rotating stall has developed, the maximum compressor static

pressure rise is generally slightly less than the steady pressure rise attained before inception. The decay in rotating stall as rotor speed is reduced is shown on the right side of part a of each figure.

Inspection of the "control on" records, part b of Figures 10 and 12 show that the control performance with sensor types 1 and 3 is excellent. With both of these sensor types, large amplitude rotating stall was eliminated completely while at the same time the compressor static pressure rise was maintained at levels comparable to those achieved by the uncontrolled compressor prior to rotating stall inception. The stator stagger angle records for these two cases suggest that rotating stall was controlled so completely because the control system acted on the increased turbulence signals prior to inception. Thus, inception was anticipated and eliminated. In both cases, the maximum control action on the stator stagger angles was comparable and does not appear to be excessive.

With sensors type 2 (Figure 11b), the control did not act until a stall cell appeared and then it reacted extremely rapidly to its maximum amplitude in stator stagger angle. Moreover, the compressor static pressure rise after control action was less than with the other types of sensors. This action is similar to that observed in the earlier tests of this sensor type. As mentioned previously, if this sensor type were used in combination with other types, its sensitivity would be reduced to the extent that it detected only very large amplitude rotating stalls. The majority of the control action would be contributed by sensors of types 1 and 3.

The final series of tests shows the response of the control system to rotating stalls of varying amplitude. For these tests, the damper vanes were set nearly closed and the downstream fan was turned off. With this configuration, the uncontrolled compressor experienced rotating stall at all rotor speeds. This is illustrated in Figure 13a. The rotor speed here is being varied slowly between 1250 and 500 rpm. The change in amplitude and frequency of the rotating stall is apparent in all of the pressure records. A comparable test with the control turned on is shown in Figure 13b. It can be seen that the control acts to eliminate all but the smallest amplitude rotating stalls which occur at very low rotor speeds. This result illustrates that the variable

system reference pressure is performing properly. The necessity of incorporating a positive bias in the system reference pressure makes it impossible to eliminate completely very small amplitude rotating stall. However, we believe that this limitation does not compromise the overall excellent performance of the control system. The main function of the control is to eliminate serious large amplitude stalls.

In summary, the tests of the rotating stall control system on the annular cascade with inlet distortion show that with the proper types of sensors, the performance of the control is excellent. The use of the control with sensors of types 1 or 3 provided performance characteristics which completely eliminated large amplitude rotating stall under both steady state and transient conditions. Sensors of type 2 reacted very rapidly to large amplitude rotating stall but tended to exert more control action than necessary. These latter sensors should be used only in combination with the other types and in such combinations their input gains should be adjusted so that they are sensitive only to very large amplitude rotating stalls. The control of smaller amplitude stalls should be left to sensors of types 1 and 3.

SECTION IV

STALL CONTROL TESTS ON J-85-5 ENGINE

The successful tests of the rotating stall control system on the low speed annular cascade demonstrated that the basic concept of the control was sound. However, a test of the control on an operational compressor would provide a much more convincing demonstration. This section reports the results of such tests.

The selection of a suitable operational compressor for the control tests was constrained by two requirements. First the compressor must have variable geometry features which are amenable to modification for operation by the rotating stall control system. Second, the compressor and drive system must be continuously available for installation, checkout, and testing of the control system. Both of these requirements were satisfied by the selection of a complete J-85-5 turbojet engine for the tests. The complete engine, of course, contained its own compressor drive system and was made available for long term testing by AFAPL as government furnished property. Moreover, the J-85 compressor has variable inlet guide vanes and bleed doors on the intermediate stages which are operated on a predetermined schedule by the engine fuel control system. Thus the rotating stall control system could be used to modify this schedule for stall control test purposes.

The remainder of this section is divided into three major parts. Section IV-A describes the installation of the rotating stall control system on the J-85 engine. Section IV-B describes the adjustment of the control variables to obtain the desired performance. Finally Section IV-C presents the results of testing the engine with the stall control in operation.

A. INSTALLATION OF CONTROL ON J-85 ENGINE

1. General Description

The rotating stall control is an electro-hydraulic feedback control system. Its principle of operation has been described earlier (Section II). Briefly, the inputs to the control are unsteady pressure signals produced by

sensors mounted in the compressor. The output of the control is a mechanical operation on some variable geometry feature of the compressor to be controlled. On the J-85 engine, which has an eight stage compressor, the variable geometry consists of the inlet guide vanes and bleed doors on the third, fourth, and fifth stages of the compressor. The positions of the guide vanes and bleed doors on the J-85 are normally controlled by the fuel control system as a function of engine rpm and inlet air temperature. A mechanical feedback cable between the variable geometry actuators and the fuel control is used to ensure that the proper position is maintained. The rotating stall control system was incorporated into the main J-85 control system by replacing the mechanical feedback cable with another mechanical cable which is operated by the stall control system. This cable replacement was the only change made in the original fuel control system. The variable geometry actuators continue to be operated by the fuel control but the response can be modified by action of the stall control on the feedback loop. Essentially the stall control deceives the engine fuel control into performing the desired stall control functions. The principal advantage of incorporating the stall control in this way is that it minimizes the engine modifications which are required.

A sketch of the mechanical/hydraulic feedback loop with the rotating stall control incorporated is shown in Figure 14. The lower portion of this figure shows the original variable geometry system for the J-85 engine. An operating description is presented in the J-85 Training Guide (SEI-427, August 1973). It will not be repeated here. It is sufficient to point out the above-mentioned change in the feedback cable. The rotating stall control system is shown schematically in the upper portion of Figure 14.

Under normal engine operating conditions, it is necessary that the modified engine follow a variable geometry schedule which is the same as that of the unmodified engine. This has been accomplished by mounting a precision linear potentiometer on the existing variable geometry control bellcrank (see Figure 14). The potentiometer provides an electrical signal that represents the position of the original feedback cable. In the absence of rotating stall, this electrical signal commands the stall control servo to move the new feedback cable to the normal position of the original cable. Thus, the normal operating schedule is

maintained. If a stall does occur, the stall correction signal is electrically combined with the potentiometer signal to command new bleed door (and guide vane) configurations to control the stall condition.

The installation of the stall control on the J-85 engine has a limitation generated by the overall configuration of that engine. The location of the bleed doors on the intermediate compressor stages will only allow control of stalls which originate on the first two or three compressor stages. Such stalls are most likely to occur at engine speeds between idle and approximately 80 percent of rated speed, where the bleed doors are normally scheduled to be open in order to provide matching between the front stages and rear stages. (For stall-free operation, the front stages require a higher mass flow than the rear stages can accept.) Thus, the operation of the stall control system was ultimately tested by arbitrarily closing the bleed doors at these engine speeds, and observing if the stall control prevents the occurrence of rotating stall by limiting how far the doors can be closed, or by rapidly opening the doors if a stall does begin to form. The arbitrary command for closing the bleed doors is generated by an auxiliary electrical command signal within the stall control system. This command signal, which is shown as an input to the stall control in Figure 14, is combined with the variable geometry potentiometer signal to provide off-schedule performance of the bleed doors and inlet guide vanes.

A block diagram of the overall variable geometry system with the stall control incorporated is shown in Figure 15. The signals at various stages in the complete system are sketched on the right side of this figure. These signals will be discussed shortly. For now, attention is called to the block diagram. The operation of the rotating stall control up to the generation of a stall correction signal (signal 6, Figure 15) has been described in Section II. This stall correction signal is combined with the variable geometry position feedback signal (signal 8) and a signal to generate off-schedule operation of the variable geometry (signal 7) to provide the input (signal 9) to the stall control servo. The stall control servo positions the mechanical feedback cable to the fuel control system in response to signal 9 such that the fuel control commands the final variable geometry position (signal 10) through the original engine actuators.

The signals sketched on the right side of Figure 15 for various stages in the system are divided to show two different operating conditions in the compressor. The left portions of these sketches illustrate the response during an engine acceleration and deceleration under normal (on-schedule) conditions, that is when the off-schedule command (signal 7) is zero and the bleed doors operate on their normal engine schedule without inducing rotating stall. Here no stall correction signal (signal 6) is generated. The only input to the stall control servo is the variable geometry feedback signal (signal 8). This allows the feedback cable (signal 9) and thus the variable geometry (signal 10) to follow the normal schedule programmed into the fuel control system.

The right side of the signal sketches illustrate the response with the rotating stall control in operation. Here the operating engineer has programmed an off-schedule command (signal 7) which causes the bleed doors to close far enough for the compressor to enter rotating stall. The polarity of signal 7 is negative in order to generate the correct error motion in the feedback cable (signal 9). For the situation illustrated the bleed doors were initially full open. The off-schedule command closes the doors until rotating stall occurs. When this happens, a stall correction signal (signal 6) is generated as described in Section II and the bleed doors open rapidly until the stall has disappeared. At the far right of the off-schedule sketches, the operating engineer is removing the off-schedule command in stages and the engine is reverting to normal operation.

2. Physical Details

The preceding paragraphs provide a general description of how the rotating stall control was installed on the J-85 engine. Details of the hardware associated with the installation are given below.

The inputs to the rotating stall control system are unsteady pressure signals produced by sensors mounted in the compressor. On the J-85 engine, a total of eight pressure transducers are used to provide rotating stall control signals and two additional transducers are used to monitor the unsteady pressures near the rear of the compressor. All of the transducers are mounted to measure the pressure fluctuations on the inner surface of the compressor casing at

various axial locations. A photograph of typical control and monitor pressure transducers is shown in Figure 16 and a detailed sketch of each is shown in Figure 17.

The control pressure transducers are geometrically modified versions of standard pressure transducers supplied by PCB Piezotronics, Inc. They are mounted in special housings which incorporate a ground isolation shield from the compressor casing. A recessed cavity between the compressor wall inner diameter and the transducer face is approximately 0.020 inches deep. This small clearance was chosen to provide protection of the transducer from damage without compromising the frequency response characteristics of the system.

The eight control pressure transducers are mounted at four axial locations near the front of the compressor. Two transducers, separated circumferentially, are used at each axial location. The axial locations are governed by the geometry of the existing compressor casing which includes stiffener flanges on the external surface and stator support rings on the inner surface. The four axial locations are sketched in Figure 18. They are as follows:

1. Near the first stage rotor mid-chord.
2. Near the quarter-chord of the first stage stator, as close to the stator suction surface as possible.
3. Near the trailing edge of the second stage rotor. This location is determined by the presence of a stiffener flange on the outside of the compressor casing and the second stage stator support ring on the casing inner surface.
4. Between the second stage stator trailing edge and the third stage rotor leading edge. This location is determined by the location of the compressor bleed structure on the outer surface of the compressor case.

The circumferential locations of the control pressure transducers were selected so they do not interfere with mounting of the accessories and stall control on the compressor casing. The locations selected are illustrated in the photographs of Figure 19. In final assembly on the J-85 engine, the presence of

the control transducers on the right side of the compressor casing required a slight relocation of an electrical junction box. This relocation did not cause any problems. The remaining transducers did not interfere with any of the engine accessories. The control transducers are shown in Figure 20 viewed from the inside of the compressor casing.

The two monitor pressure transducers are mounted between the seventh stage stator blades at approximately the mid-chord of these blades (axial location number 5 in Figure 18). These transducers are separated circumferentially in a fashion similar to the control pressure transducers. However, the circumferential separation in this case is less than that for the control transducers (see Figure 19, left side view). The smaller circumferential spacing was dictated by the presence of obstructing accessories on the full J-85 installation. This is not a problem since the monitor transducers are not required for any control functions. They are used only to observe the flow stability near the rear of the compressor. The monitor pressure transducers are of a design which allows for the higher temperatures which will be encountered at the rear of the compressor. The installation differs from the control transducers (Figure 17). The space available between the seventh stage stator vanes limits the allowable diameter of the holes in the compressor casing. The allowable hole diameter is less than the diameter of the transducer, requiring a pressure transfer tube between the compressor casing inner diameter and the transducer face which is approximately 0.35 inches in length. Thus the frequency response of the monitor pressure transducers is not as high as that of the control transducers. However, it is high enough ($\approx 9 \text{ KH}_2$) to detect frequencies associated with rotating stall. The monitor transducer installations are shown in Figure 21 viewed from inside the compressor casing.

In addition to the eight control and two monitor pressure transducers, two other pressure transducers were incorporated on the J-85. One of these transducers measured the static pressure rise across the compressor for use as the input reference pressure, ΔP_{ref} , to the rotating stall control system. Its function has been described in Section II. The other transducer was used to measure the dynamic pressure, q_0 , at the throat of the bellmouth upstream of the J-85 compressor. This transducer is not required by the stall control system. It was used simply to provide a measure of the mass flow through the compressor.

Various photographs of the J-85 engine with the rotating stall control mechanisms installed are shown in Figures 22 through 25. Most of the hardware apparent in these figures is auxiliary equipment for the original J-85 engine. The parts associated with the rotating stall control are labeled. Figure 22 shows an overall view of the engine. The small auxiliary hydraulic supply used to power the stall control servo is on the left. A detailed view showing all of the stall control installation except the control and monitor pressure transducers is given in Figure 23. A closeup view of the position feedback potentiometer and four of the monitor pressure transducers is shown in Figure 24. The functions of all of the labeled items except the emergency by-pass valve have been discussed earlier. This valve is part of a fail-safe system which automatically unloads the stall control servo and opens the bleed doors in the event of an electrical power or control system failure while the engine is operating. This system did not activate during the engine tests.

Some of the stall control tests on the J-85 engine were performed with a 180 degree circumferential distortion screen mounted just upstream of the compressor face. The screen is shown in Figure 25. The inlet bellmouth is removed in this photograph. During the tests, the bellmouth was installed as shown in Figures 22 and 23. The wire diameter in the distortion screen is 0.035 inches and the mesh size is 8 wires per inch, providing a porosity of 52.1 percent open area. The magnitude of the distortion was not measured. However, it falls within the range of values reported in Reference 3 where a series of distortion tests were performed on a J-85 engine. Screens of similar construction with mesh sizes of 7-1/2, 8-1/2 and 9 wires per inch (porosities = 57.4%, 49.8% and 39.7%, respectively) were tested in that work.

The distortion screen was positioned so that four of the control pressure transducers were in the wake of the screen and four were not. The four control transducers outside of the screen wake are labeled in Figure 25. The four transducers in the screen wake are not visible in this photograph. They are located circumferentially just below the labeled monitor pressure transducer.

B. ADJUSTMENT OF CONTROL SYSTEM VARIABLES

The prototype rotating stall control system has been designed so that several of the functions can be varied in order to optimize the performance. In the tests on the low speed annular cascade (Section III), it was possible to perform these adjustments on line; that is while the cascade was operating for lengthy periods in the presence of rotating stall. Such a procedure would probably lead to engine failure if it were used on the J-85. Thus the procedure used on this engine was to obtain magnetic tape records of the sensor signals required as inputs to the rotating stall control. These records were obtained for various on-schedule and off-schedule operating conditions including some where the compressor was forced into rotating stall for a brief time period. The stall control adjustments were then performed by using the taped records to simulate the engine.

There were three major adjustments required to optimize the stall control performance on the J-85. These were as follows.

- 1) Adjustment of the stall control servo so that its motion during on-schedule operation of the engine is identical to the motion of original J-85 feedback cable.
- 2) Selection of filter and gain characteristics for conditioning of the control pressure signals.
- 3) Selection of the gain and bias levels to be used in conditioning the reference pressure, ΔP_{REF}

Item 3 above depends on the selections made under Item 2. Item 1 is independent of Items 2 and 3. The items are discussed in the order listed.

Adjustment of the stall control servo motion was performed with the engine turned off. The original variable geometry system was moved by hand and the feedback loop in the stall control was adjusted to obtain static positions of the stall control servo which were the same as those of the original feedback cable. This adjustment procedure was then tested by comparing the position of the stall control servo with the position of the potentiometer on the variable geometry bellcrank during normal engine operation. The results are shown in Figure 26 along with records of some of the other variables on the engine. The

original mechanical feedback cable was left connected during this test. The stall control servo was operating but not connected to the fuel control system.

In Figure 26, six recorded traces are shown as a function of time. The time increases from left to right and its scale is indicated just below the second record from the top. Each record is discussed below starting with the top record as number one.

- (1) Engine Speed - This is a record of the engine speed in percent of design speed. It is obtained from a magnetic pickup which counts blade passage of the first stage rotor. The record has not been corrected for compressor inlet temperature.
- (2) Bleed Door Position - This is a record of the position of the linear potentiometer on the variable geometry bellcrank. It is representative of the bleed door position as well as the configuration of the inlet guide vanes since both are connected mechanically.
- (3) Stall Control Servo Position - This is a record of the position of the servo which is operated by the stall control system. Under normal engine operating conditions, it should follow exactly the same curve as the bleed door position (record number 2).
- (4) Compressor Static Pressure Rise, ΔP_{REF} - This is a record of the pressure difference between static pressure taps located on the outer casing upstream and downstream of the compressor. It is used as the input reference pressure to the stall control system. The function of this reference pressure was discussed in Sections II and III.
- (5) Compressor Inlet Dynamic Pressure, q_0 - This is a record of the dynamic pressure at the throat of the bellmouth upstream of the J-85 compressor. It is proportional to the square of the mass flow at the compressor inlet.
- (6) Conditioned System Reference Pressure, P_R - This is a record of the reference pressure that the control uses for comparison

with the amplitude of the unsteady pressure signals generated by the stall sensing pressure transducers within the compressor. It is obtained by filtering, amplifying (or attenuating), and biasing the compressor static pressure rise (record 4). The various conditioning functions have been described in Section III. In this particular record, the only conditioning was filtering of high frequency components. As indicated on the figure, the amplification factor was unity and the bias was set at zero.

The main feature illustrated by Figure 26 is that the stall control servo (record 3) is performing its required function by accurately tracking the position of the variable geometry bellcrank (record 2).

The rotating stall control operates by comparing the amplitude of conditioned signals, P_o , from control pressure transducers in the compressor with the magnitude of a conditioned reference pressure signal, P_R (record 6 in Figure 26). Prior to conditioning, the unsteady signals from the control transducers contain high frequency fluctuations caused by rotor blade passage and low frequency fluctuations associated with transient operation of the engine. Both of these components, which are associated with normal engine operation, could mask the presence of rotating stall. Thus, it is necessary to filter the control transducer signals to reduce or eliminate the high and low frequency components. The optimum filter characteristics were selected by observing the action of the control in response to tape recorded transducer signals from the engine operating under normal conditions and under stalled conditions. The filter characteristic finally selected is shown in Figure 27 as a solid line. The dashed line on the left of Figure 27 shows the low frequency portion of the filter curve used with a Brush Recorder System for displaying the test results. (Portions of the filters for the stall detection circuits were within the control system making it inconvenient to include these portions in the recorded data.)

As discussed in Section III, the stall control responds better to unsteady pressure signals from some locations in the compressor than from other locations. It was suggested in Section III that the gain in the detector input circuits be

adjusted selectively to take advantage of the signals which provide the best control response. This was done, again with the use of the tape recorded signals, and the results are listed in Table I. The gain selections are for the signals after filtering (see Figure 27).

TABLE I

DETECTOR CHANNEL GAINS

Control Transducer Location in J-85
Compressor Casing

Axial	Circumferential	Detector Gain
No. 1 Rotor Mid Chord	Top Right	10
No. 1 Rotor Mid Chord	Left	8
No. 1 Stator Quarter Chord	Top Right	5
No. 1 Stator Quarter Chord	Left	5
No. 2 Rotor Trailing Edge	Top Right	10
No. 2 Rotor Trailing Edge	Left	5
No. 2 Stator Trailing Edge	Top Right	7.5
No. 2 Stator Trailing Edge	Left	10

The tape recorded signals used to select detector channel gains were obtained with the engine operating with a clean inlet (no distortion screen). Nevertheless, the detector gains listed in Table I show a variation with circumferential location. (The highest gains correspond to the best signal quality for stall detection.) The reason for the circumferential variation in transducer signal quality is unknown.

The final adjustments to the stall control system involve the conditioning of the reference pressure signal, ΔP_{ref} , shown in record 4 of Figure 26. In general, it is desired that the magnitude of the reference pressure after conditioning vary with engine speed and inlet air density in the same way as the conditioned signals from the control pressure transducers under normal unstalled operating conditions. The engine test cell at Calspan does not allow for control of inlet air density. However, the variation with engine speed can be checked. This has been done and the results are shown in Figures 28 and 29.

Figure 28 shows the variation with engine speed of the unconditioned reference pressure, ΔP_{REF} , along with the inlet dynamic pressure, q_0 . Both of these quantities were obtained from records such as those shown in Figure 26, with the engine operating on its normal schedule. The ΔP_{REF} curve in Figure 28 requires adjusting (conditioning) to provide a proper reference level for the signals from the control pressure transducers. The conditioned reference level, P_R , must be large enough so that the control does not take action under normal engine operating conditions. At the same time, P_R must be small enough that the occurrence of rotating stall will be detected and action by the control will be initiated. As explained in Section III (see Figure 6), conditioning of ΔP_{REF} is accomplished by selecting bias and gain levels for the detector circuit in the rotating stall control. The results are shown in Figure 29.

The variation of the conditioned system reference pressure, P_R , with engine speed is shown in Figure 29. Also shown in this figure is a curve labeled the on-schedule detection level, P_D , which represents the combined background noise during normal engine operation from all eight control transducers signals after these signals have been conditioned. As noted above, the reference pressure curve, P_R , must be above the normal background level curve to avoid unwarranted action by the stall control system. The P_D curve was obtained by determining the reference voltage level which first triggers the stall control when tape recorded signals from the eight pressure transducers during normal engine operation are used as inputs to the stall control system.

As illustrated in Figure 29, the system reference pressure, P_R , has been adjusted to lie above the detection level curve by an approximately constant amount in the speed range between 50 and 75 percent of rated engine speed. This is the engine speed range of interest for the current tests since the configuration of the J-85 engine limits operation of the stall control to this range (see Section IV-A). The divergence of the P_R and P_D curves at engine speeds above 75 percent is desirable since operation of the stall control in this range could result in stall of the rear stages in the J-85 compressor.

After the P_R curve in Figure 29 had been selected and it was demonstrated that normal engine operation did not trigger the stall control, tape recorded

signals obtained during stall at approximately 50 and 60 percent of rated engine speed were used to ensure that control action was initiated for these conditions. The results of these tests were satisfactory so final on-line tests were performed with the stall control in full operation on the engine. No further adjustments were made during the on-line tests of the control. Specifically, the tests with and without inlet distortion used the same settings of the variables in the rotating stall control system.

C. STALL CONTROL TESTS

Stall control tests were performed on the J-85 engine with a clean inlet and also with a 180 degree circumferential distortion screen in the inlet (Figure 25). The J-85 was stalled in two ways; by closing the bleed doors at constant engine speed, and by decelerating the engine with the bleed doors partially closed at the beginning of the deceleration. A total of 41 compressor stalls were recorded at corrected engine speeds between 48 and 72 percent of the rated speed. During these tests, data were recorded directly on Brush Recorder charts and also on a 14 channel Sangamo FM tape recorder. The tape recorder was operated at 60 ips (20 KHz bandwidth) to obtain records which could be expanded in time by playback at slower speeds. The direct Brush records are presented first to illustrate the overall performance of the stall control system. Some of the expanded time records are presented later to illustrate the detailed signals from the control pressure transducers.

Before proceeding into the presentation of the results, a few general comments applicable to all of the data will be made. In the process of testing the control on the J-85 engine, records were taken of the performance under normal unstalled conditions and also under conditions when the compressor was forced into rotating stall. The normal on-schedule tests were performed to ensure that the stall control system allowed the engine to follow the schedule dictated by the fuel control system. The strip records of these tests are lengthy and are not reproduced herein. However, the data are summarized at the end of this section in graphical form. The data records which are presented are for cases where the compressor was forced into rotating stall. For the sake of clarity and conciseness only a portion of these records are presented. However, the selected records are representative of the performance attained.

Figures 30 through 33 are multi-channel strip recorder charts which illustrate the performance of the control system when the compressor is forced into rotating stall. In each of these figures, ten recorded traces are shown as a function of time. The time increases from left to right and the time scale is held constant between figures. The chart length corresponding to one second is indicated just below the second record from the top in each figure. Each record is discussed below, starting with the top record as number one. (Some of these records have been discussed earlier in reference to Figure 26.)

- (1) Engine RPM (Uncorrected) - This is record of the engine speed in percent of design speed. It is obtained from a magnetic pickup which counts blade passage of the first stage rotor. The record has not been corrected for compressor inlet temperature.
- (2) Bleed Door Position - This is a record of the position of the linear potentiometer on the variable geometry bellcrank. It is representative of the bleed door position as well as the configuration of the inlet guide vanes since both are connected mechanically.
- (3) Stall Control Servo Position - This is a record of the position of the servo which is operated by the stall control system. Under normal engine operating conditions, it should follow exactly the same curve as the bleed door position (see Figure 26). However, when the control is responding to the occurrence of rotating stall, this servo operates to generate an error signal in the mechanical feedback cable to the fuel control system. In this mode of operation, servo response is apparent only during rapid transient motion of the bleed doors. Moreover the direction of motion is opposite to that desired of the bleed door response (record 2).
- (4) Compressor Static Pressure Rise, ΔP_{REF} - This is a record of the pressure difference between static pressure taps located on the outer casing upstream and downstream of the compressor. The control system reference pressure, P_R , is derived from ΔP_{REF} as explained in Section IV-B.

- (5) Compressor Inlet Dynamic Pressure, q_0 - This is a record of the dynamic pressure at the throat of the bellmouth upstream of the J-85 compressor. It is proportional to the square of the mass flow at the compressor inlet.
- (6) Off-Schedule Command - This command is an arbitrary signal generated by the operating engineer. It is used to close the bleed doors (and open the inlet guide vanes) in order to force the compressor into rotating stall. In some of the tests (Figures 30 and 31) this command was used to stall the compressor by slowly closing the bleed doors while engine speed was held constant. In other tests (Figures 32 and 33), the off-schedule command was used to preset the bleed door closure at the beginning of an engine deceleration. The command was then held fixed and deceleration of the engine forced the compressor into rotating stall.
- (7), (8), (9), and (10) Detector Pressure Signals - These are records of the signals from four of the eight control pressure transducers mounted in the compressor outer casing. These signals along with signals from the other four transducers are used by the control system to detect the presence of rotating stall. If the amplitude of the fluctuations in any one of these signals becomes larger than the system reference pressure, P_R (Figure 29), the control opens the bleed doors until the fluctuation amplitude decreases below the reference level. After stall disappears for a specified time (1 second in these tests), the bleed doors return to their original position. The rate at which the bleed doors return is specified by the decay rate of the integrator in the control system. In these tests the time constant for the decay rate was 5.8 seconds. The recorded signals in records 7 through 10 have been filtered as indicated in Figure 27. Thus they contain lower frequencies than the fully conditioned signals seen by the control system. As noted previously, recording the signals in this way was simply a matter of convenience. In addition to frequency content, these signal amplitudes are less than those

seen by the control. The signals were recorded prior to the selective amplification used in the various detector channels (see Table I in Section IV-B). The differences between the recorded detector signals and the fully conditioned detector signals used by the control are irrelevant to judging the performance of the control system. The relevant question is, "Does the control take proper and rapid action to eliminate stall when it does occur?" This question can be answered by inspection of the results.

The vertical scales for all of the records discussed above are presented on the right side of each record. In some of the lower records on the figures, the recorder pen failed to write properly. In these cases the fault was in the recording system, not in the control system.

The results of the control system tests are presented in three steps. First, some records are presented to show the performance of the control when the compressor is stalled by closing the bleed doors at various constant engine speeds. Next is a discussion of the control performance when the engine is decelerated into a stalled condition for various initial values of bleed door closure. Finally, some records of the constant engine speed tests are presented with a greatly expanded time scale.

Figures 30 and 31 show the records obtained when the bleed doors were closed slowly to induce rotating stall at constant engine speed. Figure 30 is for the tests without inlet distortion and Figure 31 is for the tests with the 180 degree circumferential distortion screen mounted just upstream of the compressor face. Parts a and b of Figure 30 show results obtained at corrected engine speeds of 52.5 and 62.6 percent of design speed. An attempt was made to stall the compressor at a higher corrected engine speed (approximately 72 percent) but this test was discontinued when a bleed door closure of 66 percent was reached without causing stall in the compressor. This test series was the first performed with the control system in full operation on the engine and it was felt that the most prudent course of action was to limit the severity of the induced stalls by not closing the bleed doors too far. In later tests with the distortion screen installed, compressor

stall was induced at corrected engine speeds as high as 71.8 percent of design speed. The results of these tests are shown in parts a through d of Figure 31 for progressively higher engine speeds and bleed door closures.

On the left side of each part of Figures 30 and 31, the bleed doors are being closed slowly by increasing the magnitude of the off-schedule command. In this region the amplitudes of the detector pressure signals are small until rotating stall occurs. (Rotating stall inception is marked on these figures by a vertical dashed line.) At this point there is a sudden increase in these amplitudes and the control rapidly opens the bleed doors until the stall has disappeared. At low engine speeds, Figures 30(a) and 31(a), the increased amplitude in the pressure signals due to rotating stall is not very large. Nevertheless, it is large enough to trigger control action on the bleed doors. As the engine speeds for the tests are increased, the rotating stall which occurs becomes progressively more severe and the required control action on the bleed doors to eliminate stall becomes much larger. At the two highest engine speeds tested (Figures 31(c) and (d)), the stall control drove the bleed doors wide open (against the stops in the engine actuators).

The stall was particularly severe at the highest engine speed (Figure 31(d)). Its effect on the engine is apparent in the records of engine speed, compressor static pressure rise and compressor inlet dynamic pressure. The static and dynamic pressures dropped a significant amount almost immediately at inception while the engine speed dropped after a short delay. However, the control action on the bleed doors caused full recovery in all of these parameters. The severe stall shown in Figure 31(d) is the only one where there is an effect on engine speed. However, all of the stalls induced at engine speeds of 60 percent or higher produced an observable decrease in compressor static pressure rise and inlet dynamic pressure.

The rapid and effective action by the stall control system in eliminating rotating stall once it occurs is apparent in all of records shown in Figures 30 and 31. The presence of inlet distortion (Figure 31) does not appear to affect the performance of the control. After the rotating stall has been eliminated, the control allows the bleed doors to return to their original setting at a rate determined by the decay time constant in the integrator. For these tests the decay time constant

was 5.8 seconds. If the off-schedule command and the engine speed are held constant after the initial stall, the control will allow the bleed doors to close slowly until stall reoccurs. The time for the stall to reoccur varied from 14 seconds to more than 45 seconds for engine speeds up to 63 percent of design speed. Reoccurrence tests were not performed on the more severe stalls (Figures 31 (c) and (d)). Instead the off-schedule command was reduced before this happened. The reduction in the off-schedule command is apparent on the right side of the records in Figures 31 (c) and (d).

Following the series of stall control tests at constant engine speeds, the performance of the control was tested during engine decelerations. The results are shown in Figure 32 for the engine without inlet distortion and in Figure 33 for the engine with inlet distortion. The procedure used in these tests was to close the bleed doors a given amount with the engine speed held at approximately 70 percent of design speed. Then with the off-schedule command fixed at this preset bleed door closure, the engine was decelerated by moving the throttle to its idle position (approximately 50 percent engine speed). In the first tests (Figure 32), the throttle was decreased uniformly over a two to three second time period. In the latter tests (Figure 33), the throttle was chopped to idle position very rapidly. Initial bleed door settings of 10, 20, 30, 40 and 50 percent closed were used in these tests. Initial settings of 20 percent and greater were sufficient to induce rotating stall in the compressor at some point during the deceleration, with the larger initial closures inducing stall at the highest engine speeds. Parts a and b of Figures 32 and 33 illustrate the results obtained for initial bleed door settings of 30 and 50 percent closed, respectively.

In many of the deceleration tests, the compressor stalled a number of times during the deceleration with the control eliminating the stall almost immediately each time (Figures 32(b), 33(a), and 33(b)). The multiple compressor stalls during engine deceleration are caused by two factors. First, while the engine is decelerating, the control acts so fast to eliminate the initial stall that there is still time for the engine to decelerate further into a new stall which is also eliminated quickly by the control. Second, after deceleration has stopped (right side of Figures 32 and 33), the off-schedule command is still very large and the control allows the bleed doors to approach the position called for

by the off-schedule command. Rotating stall then keeps reoccurring and being eliminated until the off-schedule command is reduced. The latter type of stall, due to large continuous off-scheduling of the compressor, is an abnormal and severe test of the stall control system. It is equivalent to prescheduling the primary fuel control system for continuous engine operation beyond the compressor surge line and then requiring the stall control to override the primary control on a continuous basis. No engine would be designed to operate continuously in this fashion. Nevertheless, the stall control appears to function very well under such adverse conditions.

The final set of records (Figures 34, 35 and 36) are presented to illustrate the response speed of the stall control to inception of rotating stall. The time scale in these figures has been expanded greatly. These records were obtained by replaying at 1.88 ips the magnetic tape records of the tests which were recorded at 60 ips. The data records presented in Figures 34, 35 and 36 are for the same tests as those presented previously in Figures 31 and 32. The difference in the two sets of figures lies in the scale for the time base and in the selection of records for presentation. The top two records in Figures 34, 35 and 36 show the bleed door position and the compressor static pressure rise, ΔP_{REF} . The vertical scale for ΔP_{REF} has been magnified from that which was used previously. Its value is indicated on the right side of the record. The detector pressure signals generated by all of the control pressure transducers are shown in the next eight records. A description of these signals has been presented previously in the discussion of Figures 30 through 33. The final record at the bottom of each figure is from a monitor pressure transducer located near the rear of the compressor between the seventh stage stator blades (see Figure 18). This signal is not used by the stall control. It is included to illustrate the stability of the flow near the rear of the compressor. The monitor signal has been processed through the same filter system as the detector signals (Figure 27). The magnitude of the time scale in Figures 34 through 36 is constant. Its value is indicated just below the second record.

Expanded time scale records of the tests without inlet distortion are presented in Figure 34 while those for the tests with inlet distortion are presented in Figure 35. Figure 36 is a repeat of Figure 35(d) with reduced vertical gain for

the detector and monitor pressure signals. The stall was severe enough in this case to drive the recorder pens off-scale at the gain used in Figure 35.

A vertical dashed line labeled "Reference Time Zero" has been included on each of Figures 34 through 36 to indicate the approximate time at inception of rotating stall. The position of this line corresponds to the first indication of rotating stall in any of the detector pressure signals or in the monitor pressure signal. Inspection of the records shows that the duration of the stall, measured from time zero until stall has disappeared, varied between about 150 and 325 milliseconds. The longest durations of stall occurred with the mildest stall encountered, Figure 34(a), and with the severest stall encountered, Figures 35(d) and 36. Inspection of the bleed door position records shows that there is a delay between reference time zero and the time at which the bleed doors begin to open. With the most severe stall (Figures 35(d) and 36) the delay was approximately 30 milliseconds. At the same time the compressor static pressure rise began to drop after a delay of only 10 milliseconds. Thus, although the control opened the bleed doors fast enough to allow full recovery without damage or flameout there was a noticeable change in engine operating parameters. It would be desirable to increase the speed at which the bleed doors open to minimize these variations in engine operating parameters.

It is believed that the stall control system is capable of substantially faster action than that achieved on the J-85 with the current installation. A substantial portion of the delay in initial opening of the bleed doors can be attributed to the mechanical/hydraulic link between the stall control servo and the engine fuel control system. Moreover the rate at which the bleed doors open after they begin to move is limited by the engine fuel control system. In the tests on the J-85 engine, a rate limiting system was installed on the stall control servo to prevent it from operating so fast that mechanical failure might occur within the fuel control system. Analysis of the data records has shown that the more severe stalls generated stall control servo motions which reached the preset rate limit. This rate limit was more than twice as fast as that ultimately attained by the bleed doors after processing through the engine fuel control system. Thus it is concluded that the final response speed of the bleed doors was limited by the engine

fuel control system, not by the stall control system. It may be possible to shorten the duration of severe stalls to periods on the order of 100 milliseconds if the installation of the stall control system on the J-85 engine were modified to eliminate the closed-loop circuit through the engine fuel control.

The preceding paragraphs present the performance of the rotating stall control system in eliminating stall when the J-85 engine is forced into rotating stall by off-scheduling the bleed doors. In addition to these tests, the engine was also tested to ensure that the stall control system would allow the engine to follow the schedule dictated by the fuel control system when rotating stall did not occur. The results of these tests are shown in Figures 37 and 38 along with a summary of the bleed door positions observed at rotating stall inception in the previous tests. Figure 37 presents data obtained with undistorted inlet flow and Figure 38 presents data obtained with the 180 degree circumferential distortion screen mounted in the J-85 inlet. In these figures, bleed door position is plotted as a function of corrected engine speed. The on-schedule performance is shown on the right side of each figure.

For the on-schedule tests with undistorted inlet flow (Figure 37) the detectors in the stall control system were first turned off and the engine speed was varied over the range required to exercise the normal bleed door schedule. Next the stall detectors in the control were turned on and the process was repeated. The off-schedule command was set at zero for both of these tests so the bleed doors should follow the original schedule dictated by the fuel control system. The data presented in Figure 37 for on-schedule performance show no differences between the results with the stall detectors turned on and turned off. This indicates that normal unstalled engine operation does not trigger the stall control system.

Approximate limits for on-schedule operation of the bleed doors in the original engine are shown by dashed lines in the Figure 37. These limits were inferred from Figure 9-26 of T.O. 2J-J85-56-1 where the fully open and fully closed end points for the bleed door schedule are given as a function of engine speed and compressor inlet temperature. These scheduled end points have been joined by straight lines in Figure 37. It can be seen that measured bleed door positions fall within the schedule limits at the fully open and fully closed positions. There

is a small deviation from the inferred limits between the end points. However, tests on the engine before it was modified showed even larger deviations at times.

On-schedule test results for the engine with inlet distortion are shown on the right side of Figure 38. In this case, only data with the stall detectors turned on were taken. At the time of this test, we were beginning to encounter some high frequency noise in the output from the position feedback potentiometer on the engine. Thus the test was not repeated with the stall detectors turned off. The data which was taken deviate a small amount more from the schedule limits than did the data in Figure 37. However, the deviations are no larger than those observed in the original engine. Thus it is concluded that the on-schedule performance of the engine with the rotating stall control system is acceptable for the tests both with and without inlet distortion.

The data shown on the left sides of Figures 37 and 38 summarize the bleed door positions at which rotating stall occurred in all of the off-schedule tests. A distinction is made in the symbols for these data to indicate the different conditions for which the stall occurred. A legend for these symbols is shown at the top of each figure. Reentry stall is the stall which sometimes reoccurred after the initial stall had been eliminated by the control. As discussed previously, reentry stall occurs either through deceleration of the engine into a new stall regime or through maintaining the off-schedule command signal for long time periods after the initial stall has been cleared. In addition to the stall inception points in Figure 37, the unsuccessful attempt to stall the engine at 72 percent of rated speed is also shown. As explained earlier, this test was aborted after the bleed doors had been closed 66 percent.

For the tests with undistorted inlet flow, Figure 37, the stall inception points for the different conditions all lie approximately on one curve. With the distorted inlet flow, Figure 38, the stalls observed during rapid engine deceleration deviate measurably from the remainder of the stall inception points, with the largest deviation occurring for the greatest bleed door closure. The engine decelerations in the distorted flow tests were faster than those used for the clean inlet and the deceleration rate was highest at the inception points with the largest initial bleed door closures. Thus the inception data suggest that there is a delay

in inception during rapid decelerations. The bleed door position line drawn through the undistorted flow inception data in Figure 37 is reproduced in Figure 38 for comparison purposes. The comparison clearly shows that inlet distortion caused earlier inception (smaller bleed door closures) of rotating stall on the J-85 engine. In all cases, the bleed door boundary for inception of rotating stall is far removed from the on-schedule boundary programmed into the engine fuel control system.

In the process of performing the overall test program on the J-85 engine, only one problem was encountered. This problem was caused by the way that the stall control system is incorporated into the J-85 fuel control system. At present, the control is installed in the mechanical feedback loop between the bleed doors and the engine fuel control. With this installation, it was found that the position feedback potentiometer used to generate the proper on-schedule operation of the engine sometimes generated high frequency noise which the bleed doors followed. It is impossible to eliminate the effect of this noise by filtering since the use of filters in the closed-loop circuit creates enough phase lag to cause small oscillations in the feed-back loop. For the purpose of completing the tests reported above, a fail-safe system was installed which would allow the engine to be shut down safely in the event that this high frequency noise became a potential hazard during the tests.

During the test program, high frequency noise was observed in only one instance (during the on-schedule tests with inlet distortion) and in this case it was not severe enough to activate the fail-safe system. Thus the test program was completed successfully. However, the basic system reliability is still a problem in the closed-loop circuit. Therefore it is planned to revise the stall control system installation on the J-85 engine to eliminate the closed-loop circuit through the fuel control system. In addition to increasing reliability, the revised installation should allow more rapid response to inception of severe stalls than the current installation which is limited by the engine fuel control system.

In summary, the tests of the stall control system on the J-85 engine were completely successful. It was shown that the control is capable of

detecting and eliminating rotating stall in an operational jet engine. All of the rotating stalls which were induced on the engine were cleared rapidly by the control system without damage or flameout in the engine. The tests did suggest that the manner in which the stall control system is incorporated into the engine control system could be improved. It is planned to make such improvements and perform further stall control tests on the J-85 engine.

SECTION V

SUMMARY AND CONCLUSIONS

A prototype rotating stall control system has been installed and tested successfully on a low speed research compressor and on a J-85-5 turbojet engine. The control system is an improved version of one tested on the research compressor in a previous program (Reference 1).

On the low speed research compressor, the control was tested in the presence of circumferential inlet distortion. These tests were performed to demonstrate the ability of the improved control system to operate satisfactorily in the presence of inlet distortion and to aid in the selection of stall sensor configurations for the subsequent engine tests. The tests showed that with the proper types of sensors, the performance of the control is excellent. In many tests, the control system did not allow rotating stall to occur at all and in the remainder of the tests the stall was limited to a few intermittent stall cells of small amplitude.

The tests of the rotating stall control system on the J-85-5 engine were performed to demonstrate the performance of the control system on an operational compressor. The tests were performed under sea level static conditions, both with and without inlet distortion. On the engine, the stall control was installed to override the normal operating schedule of the compressor bleed doors and inlet guide vanes. The J-85 was stalled in two ways, first by closing the bleed doors at constant engine speed, and second by decelerating the engine with the bleed doors partially closed at the beginning of the deceleration. A total of 41 compressor stalls were recorded at corrected engine speeds between 48 and 72 percent of the rated speed. All of the rotating stalls which were induced on the engine were cleared rapidly by the control system without damage or flameout in the engine. The duration of the stalls which did occur were limited to 325 milliseconds or less. Thus it is concluded that the tests were successful in demonstrating that the control is capable of detecting and eliminating rotating stall in an operational jet engine. The tests did suggest that the manner in which the stall control system is incorporated into the engine control system could be improved. It is planned to make such improvements and perform further stall control tests on the J-85 engine.

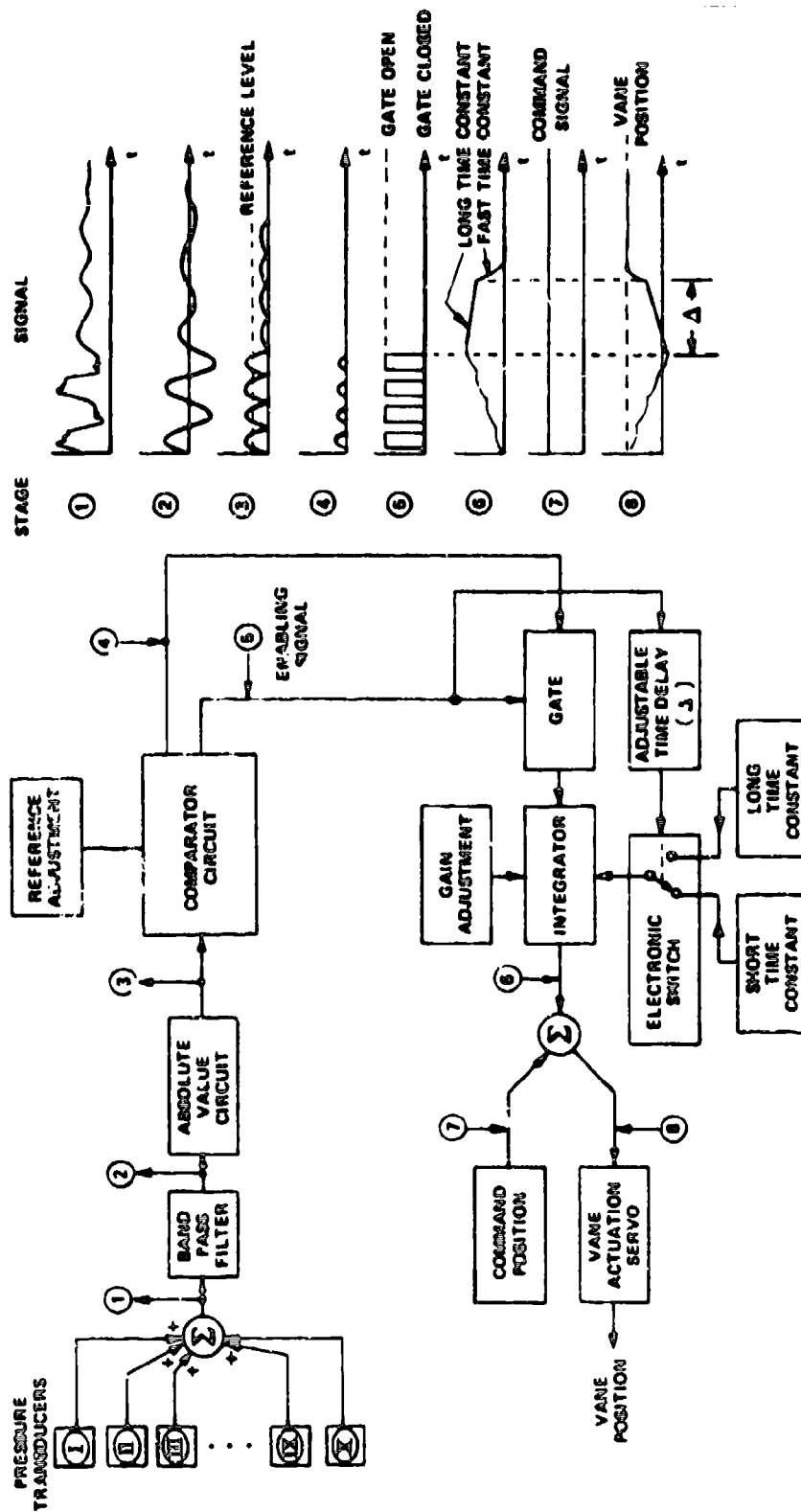
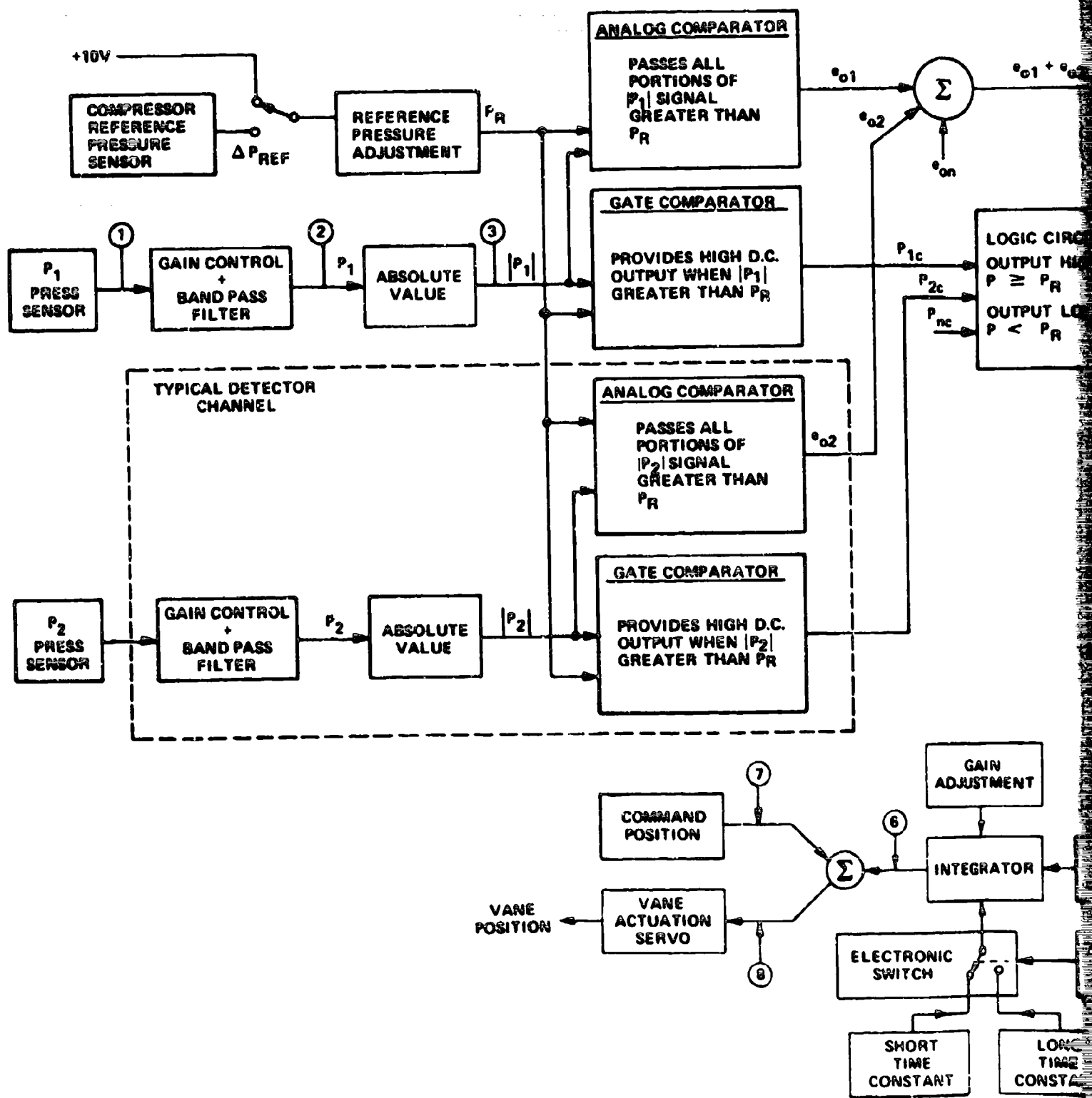


Figure 1 BLOCK DIAGRAM OF ORIGINAL ROTATING STALL CONTROL SYSTEM

Preceding page blank



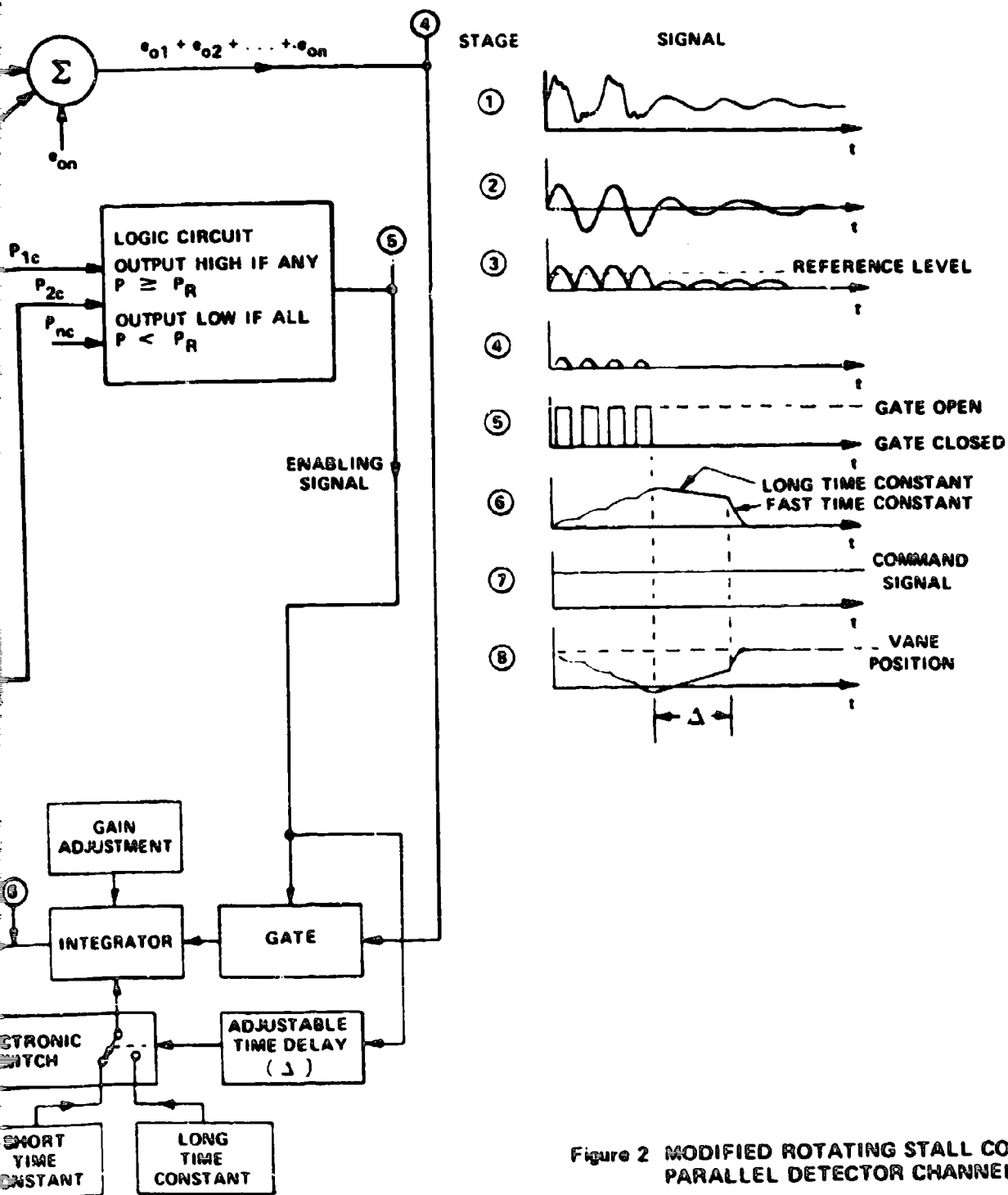


Figure 2 MODIFIED ROTATING STALL CONTROL WITH PARALLEL DETECTOR CHANNELS

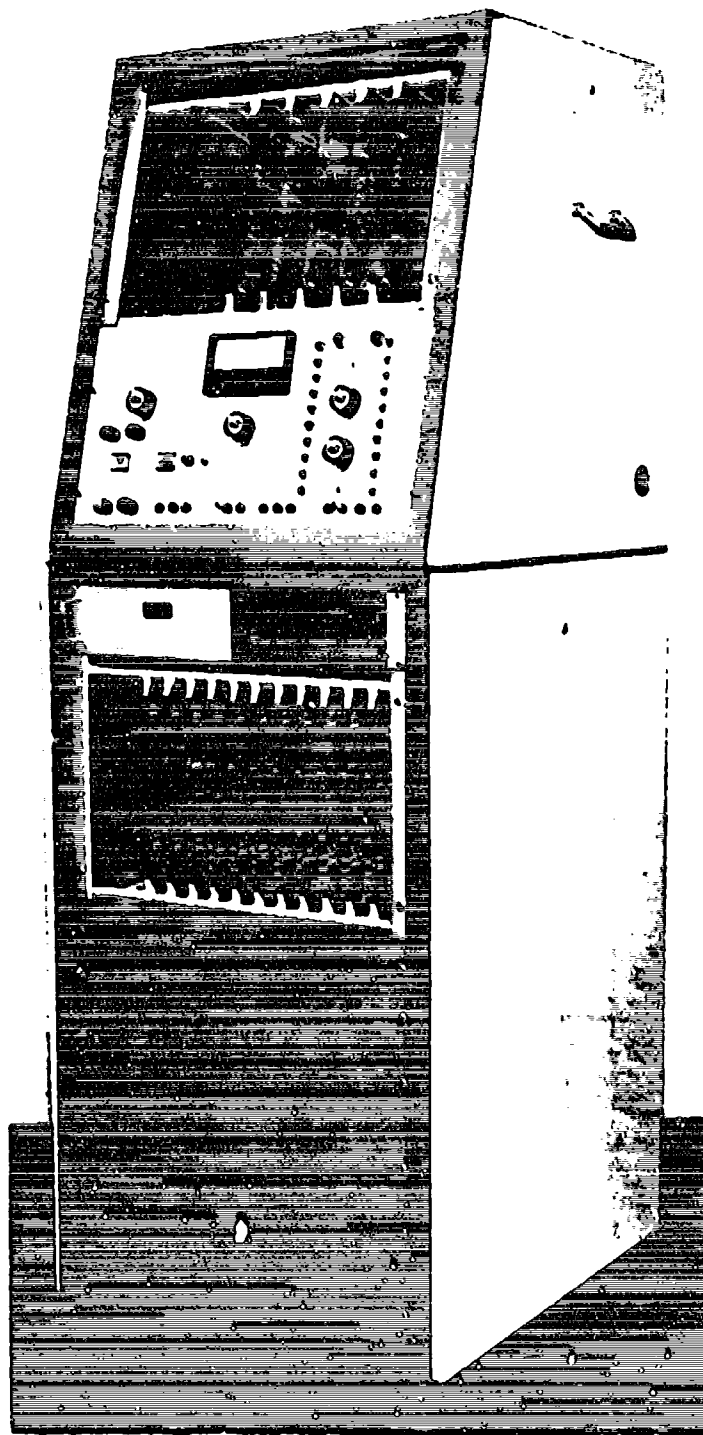


Figure 3 TEN CHANNEL ROTATING STALL CONTROL SYSTEM

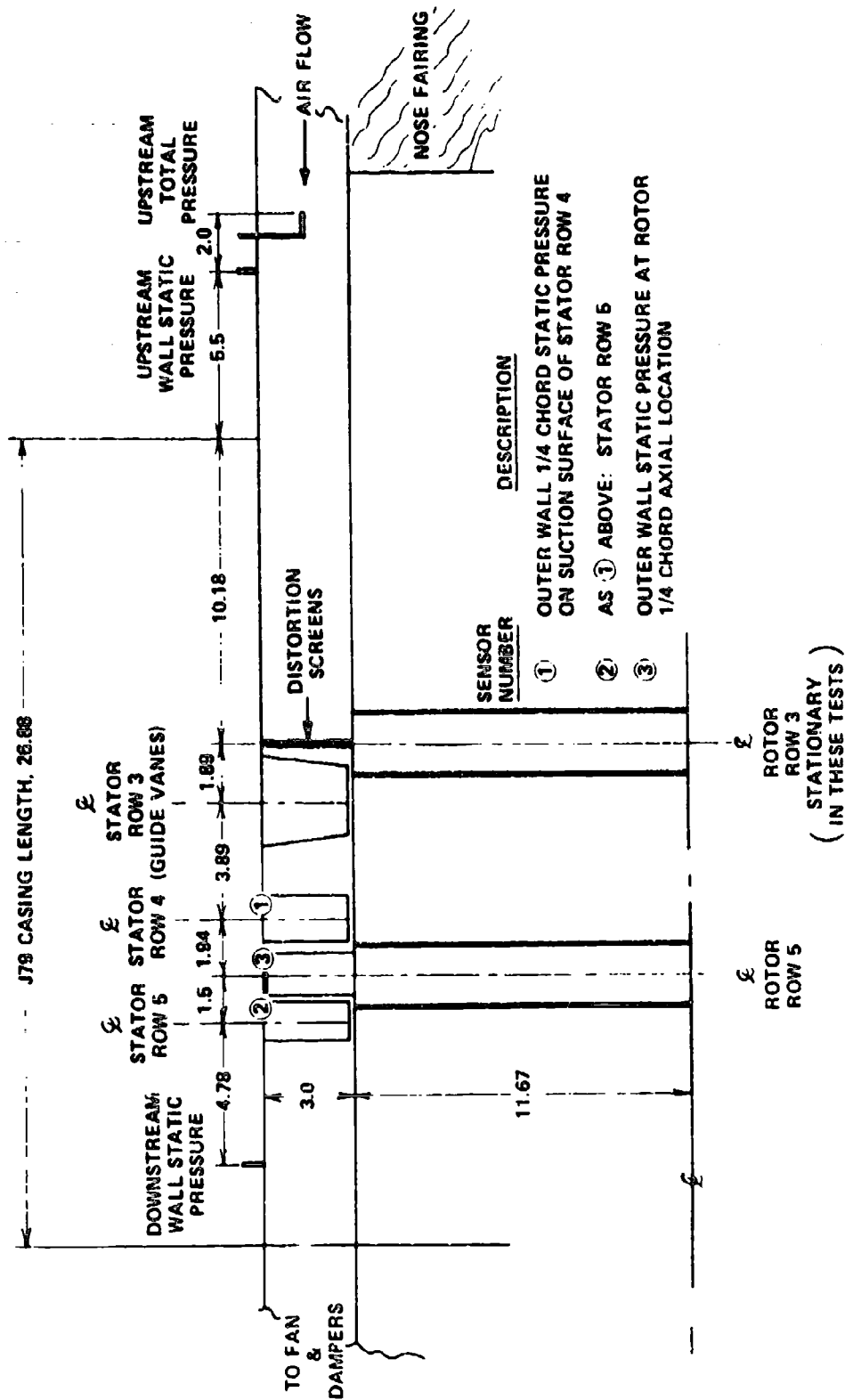
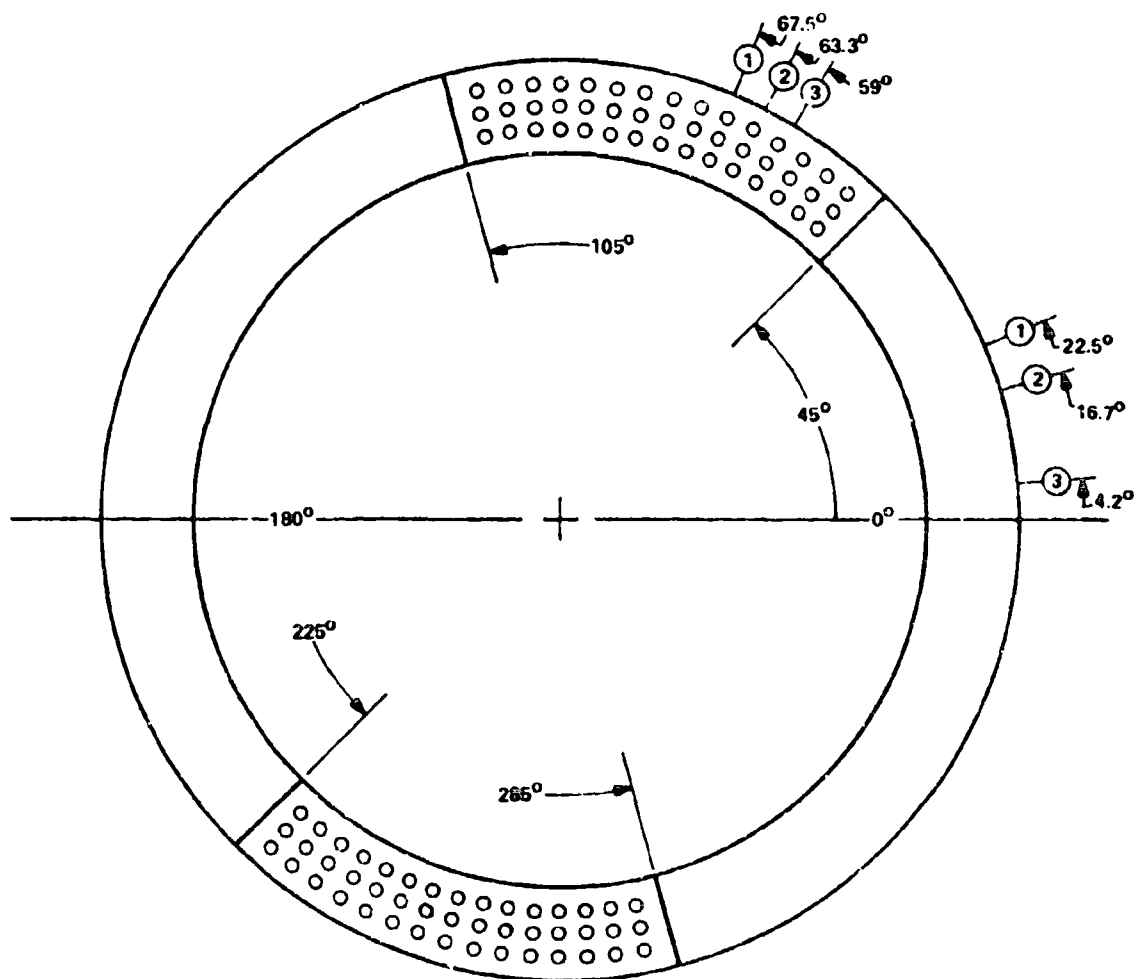


Figure 4 ANNULAR CASCADE CONFIGURATION USED IN TESTS OF STALL CONTROL WITH INLET DISTORTION



SENSOR NUMBER	DESCRIPTION
①	OUTER WALL 1/4 CHORD STATIC PRESSURE ON SUCTION SURFACE OF STATOR ROW 4
②	AS ① ABOVE: STATOR ROW 5
③	OUTER WALL STATIC PRESSURE ROTOR 1/4 CHORD AXIAL LOCATION

Figure 5 GEOMETRY OF DISTORTION SCREENS AND ROTATING STALL SENSORS (LOOKING UPSTREAM)

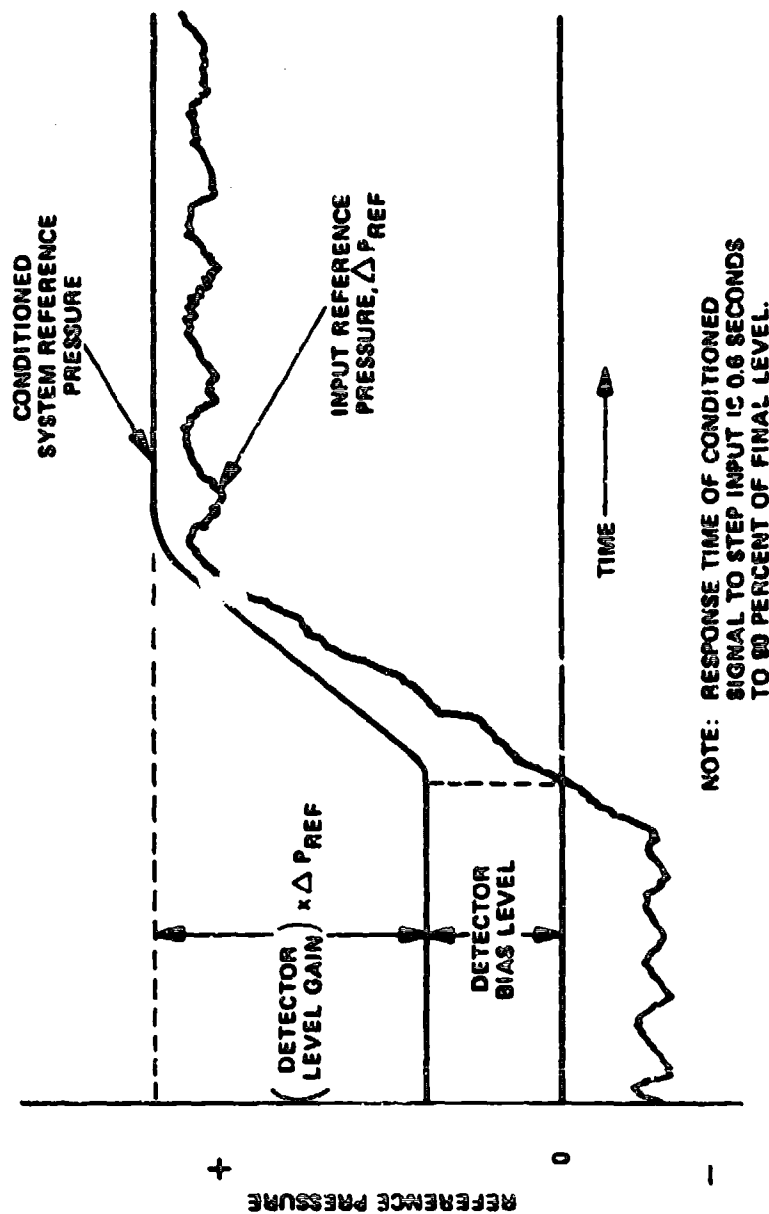
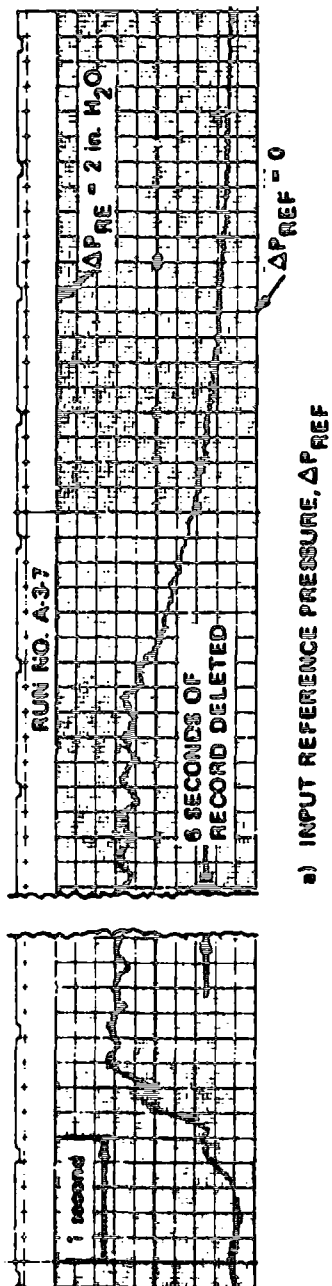
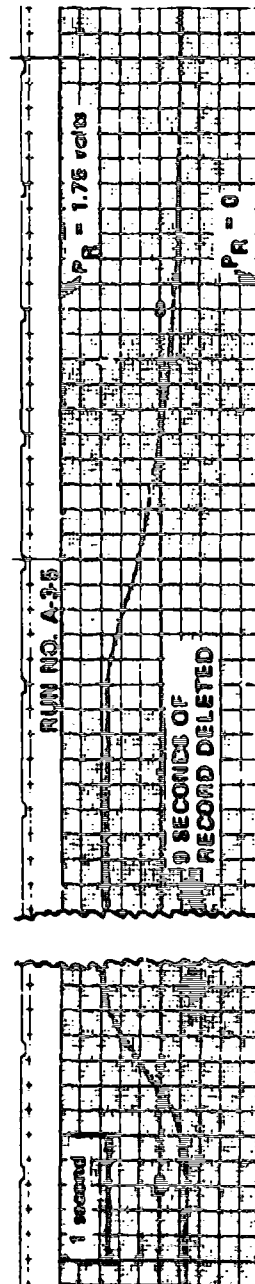


Figure 6 SKETCH SHOWING SIGNAL CONDITIONING OF INPUT REFERENCE PRESSURE TO REMOVE NEGATIVE AND SMALL POSITIVE REFERENCE VALUES AND HIGH FREQUENCY FLUCTUATIONS

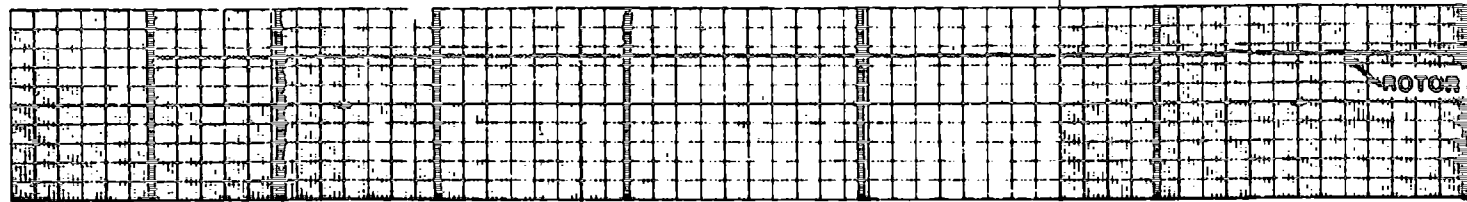


a) INPUT REFERENCE PRESSURE, ΔP_{REF}

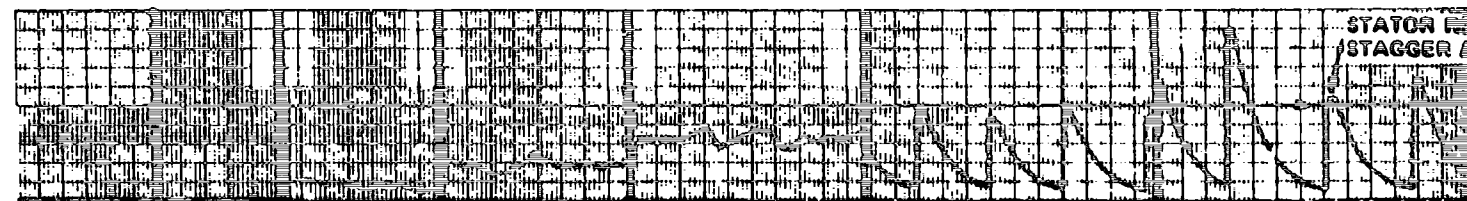


b) CONDITIONED SYSTEM REFERENCE PRESSURE, P_R

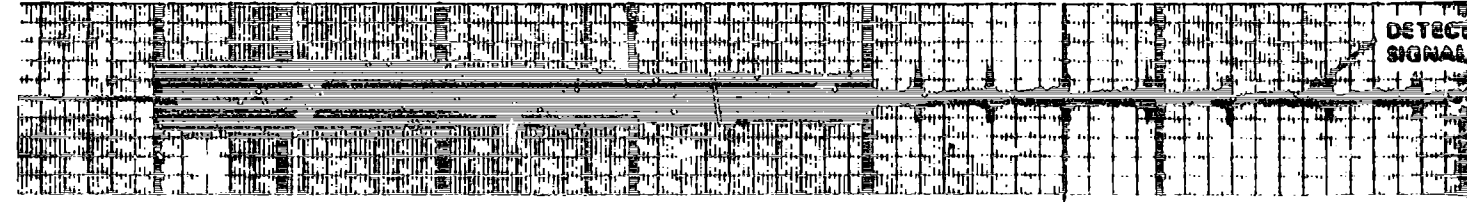
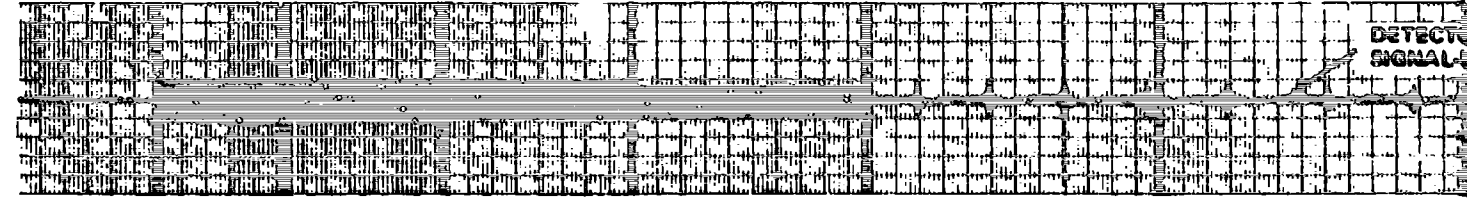
Figure 7 TYPICAL PERFORMANCE OF REFERENCE PRESSURE CONDITIONING SYSTEM



RUN NO. AA-1-1 AA-1-3 AA-1-4 AA-1-5 AA-1-6 AA-1-7



DETECTOR LEVEL GAIN 1000 500 400 300 200 100
DETECTOR BIAS LEVEL 60 50 40 30 20 10



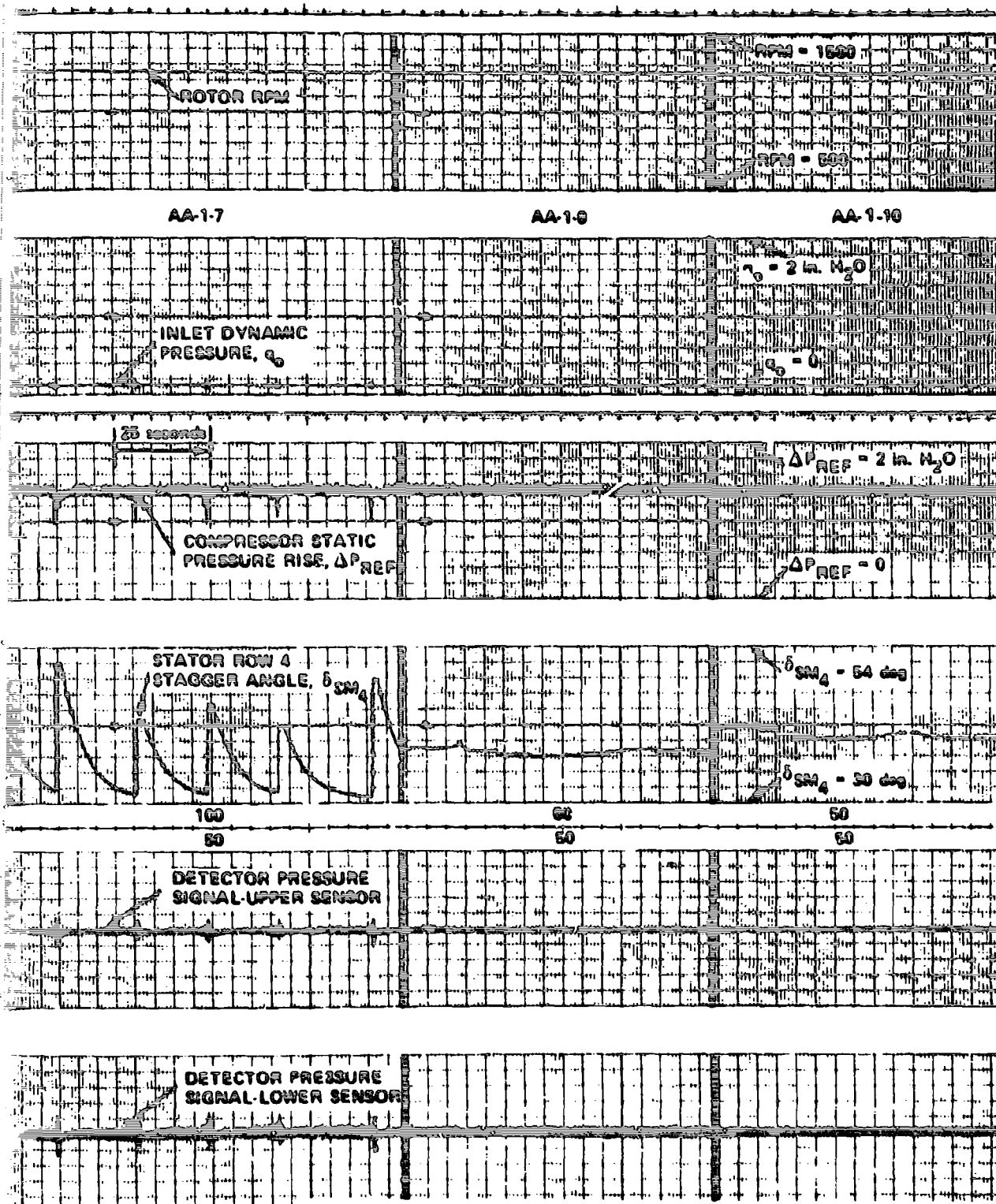


Figure 8

PERFORMANCE OF ROTATING STALL CONTROL AT VARIOUS DETECTOR
REFERENCE LEVELS WITH INTEGRATOR GAIN = 800

- (a) DETECTOR SIGNALS: SENSORS ①, OUTER WALL 1/4 CHORD STATIC, STATOR ROW 4
DETECTOR FILTER CORNER FREQUENCIES: LOW = 5 Hz, HIGH = WIDEBAND

RUN NO.

B-1-1

B-1-3

B-1-4

B-1-5

B-1-6

B-1-7

ROTOR RPM

INLET DYNAMIC
PRESSURE, q_0

COMPRESSOR ST
PRESSURE RISE,

STATOR ROW 4
STAGGER ANGLE, δ_{SM4}

DETECTOR LEVEL GAIN 1000

DETECTOR BIAS LEVEL

600

400

300

200

100

60

60

60

60

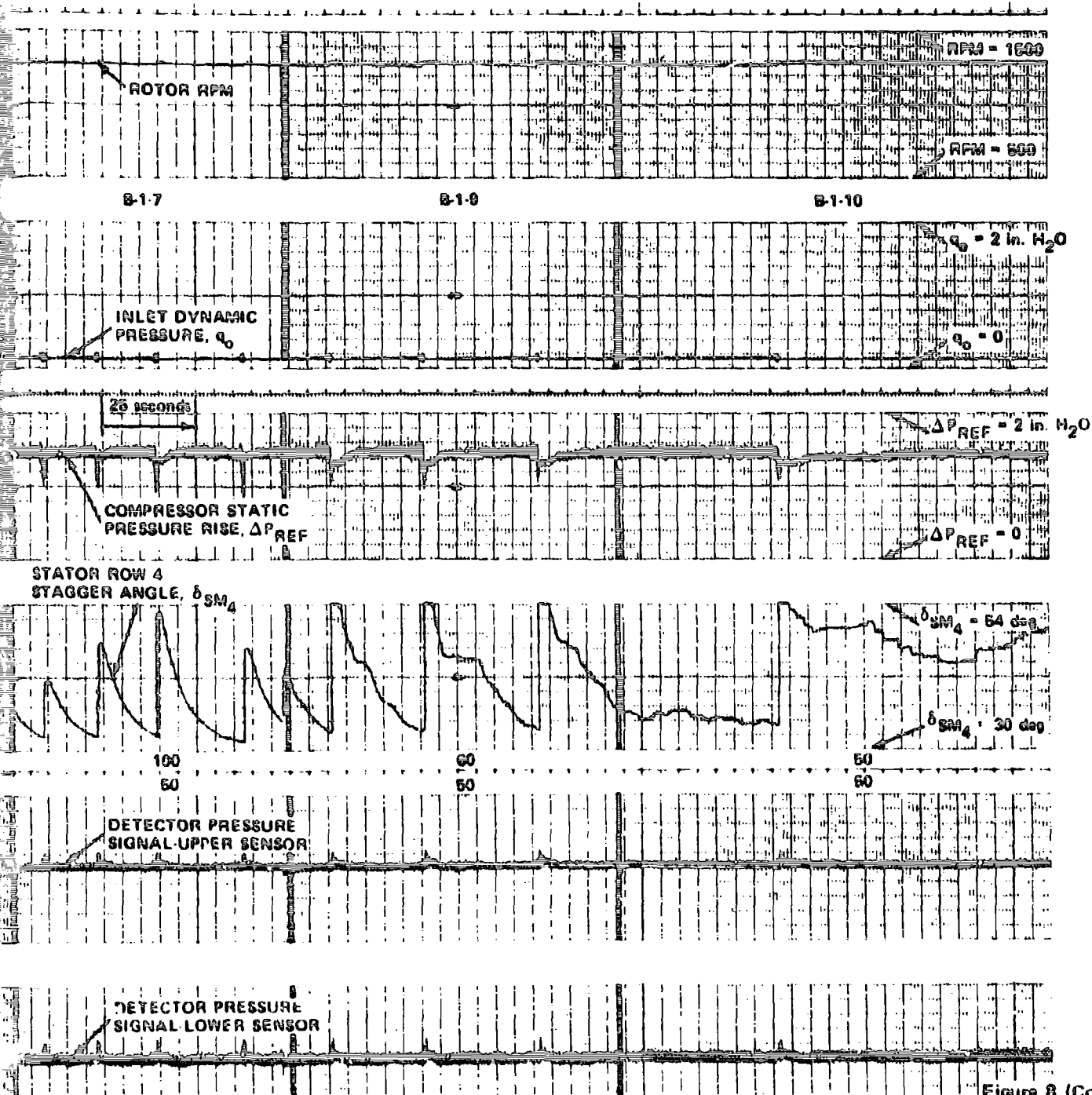
60

60

DETECTOR PRE
SIGNAL-UPPER

DETECTOR PRE
SIGNAL-LOWER

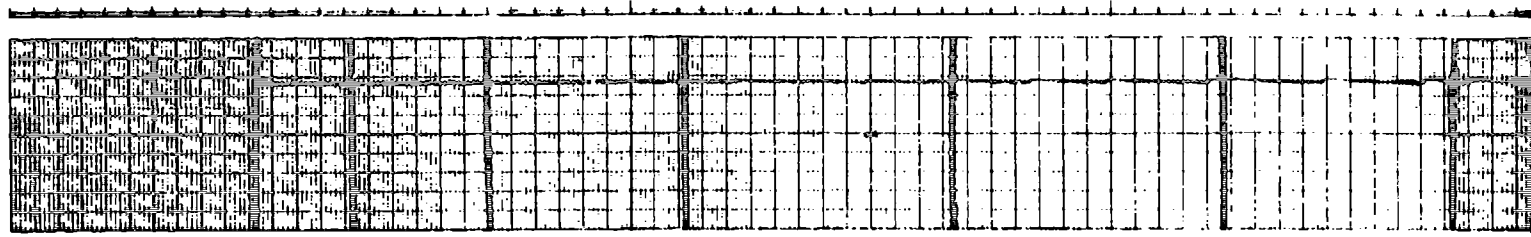
(b) DETECTOR
DETECTOR



PERFORMANCE OF ROTATING STALL CONTROL AT VARIOUS
DETECTOR REFERENCE LEVELS WITH INTEGRATOR GAIN = 800

Figure 8 (Cont.)

- (b) DETECTOR SIGNALS. SENSORS (2), OUTER WALL 1/4 CHORD STATIC, STATOR ROW 5
DETECTOR FILTER CORNER FREQUENCIES. LOW 1 Hz, HIGH > 6 Hz



RUN NO.

C-1-2

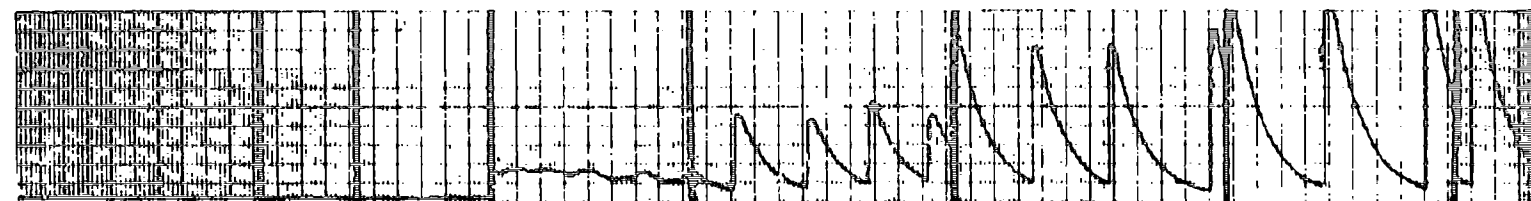
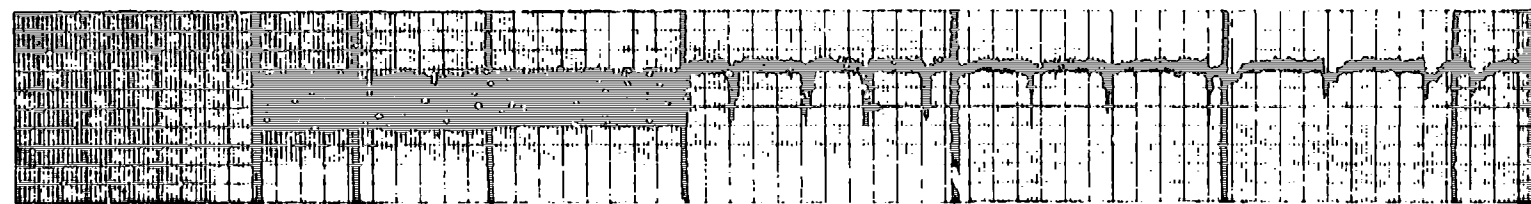
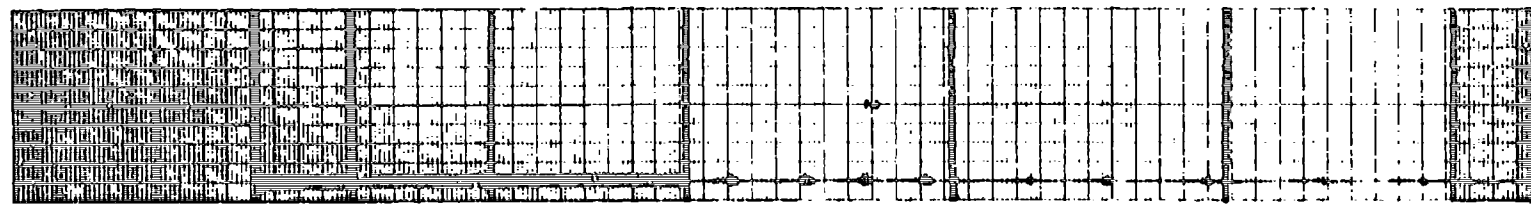
C-1-3

C-1-4

C-1-5

C-1-6

C-1-7



DETECTOR LEVEL GAIN

1000

600

400

300

200

100

DETECTOR BIAS LEVEL

60

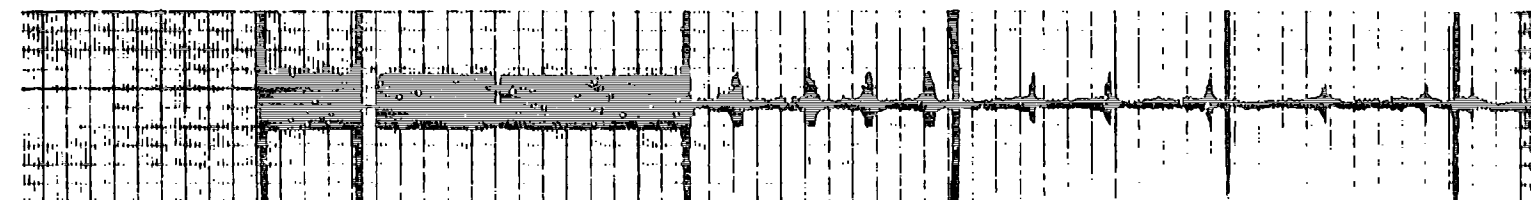
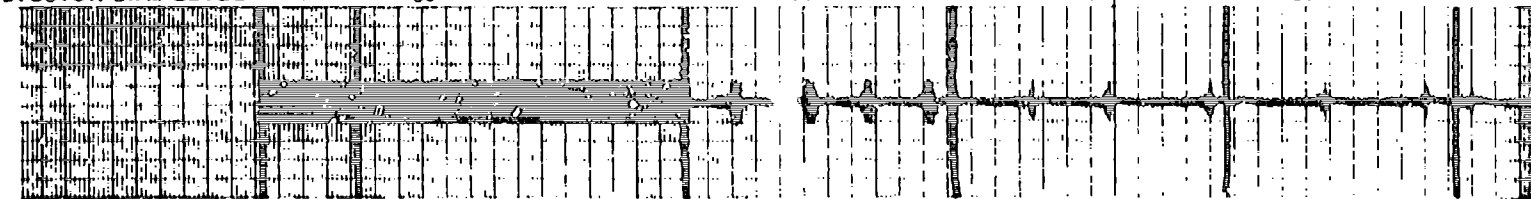
60

60

60

60

60



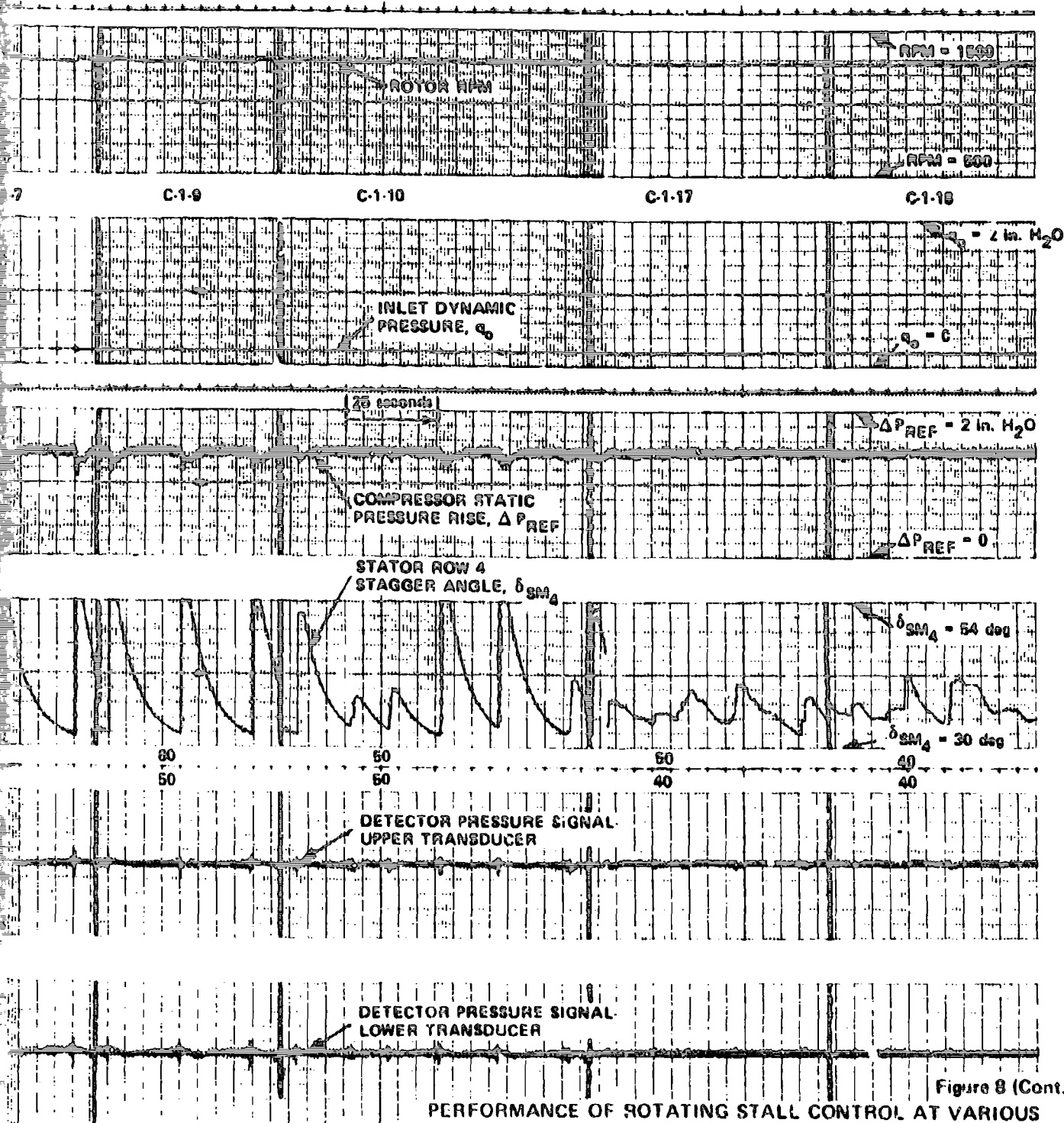
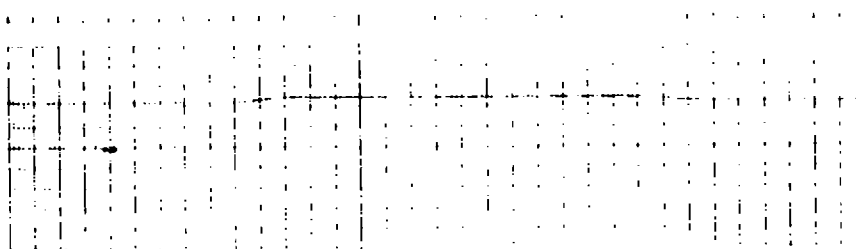


Figure 8 (Cont.)

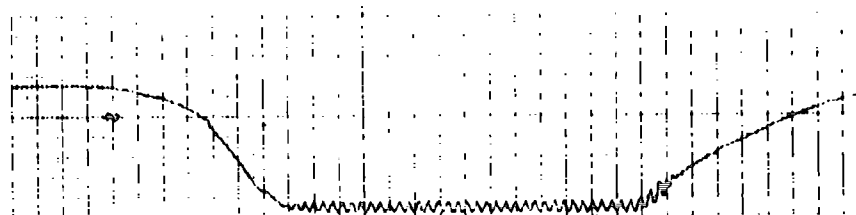
PERFORMANCE OF ROTATING STALL CONTROL AT VARIOUS
DETECTOR REFERENCE LEVELS WITH INTEGRATOR GAIN = 800

- (c) DETECTOR SIGNALS: SENSORS (3), ROTOR OUTER WALL
DETECTOR FILTER CORNER FREQUENCIES: LOW = 1 Hz, HIGH = 6 Hz

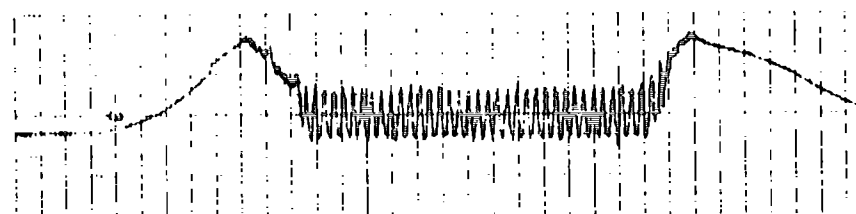


ROTOR RPM

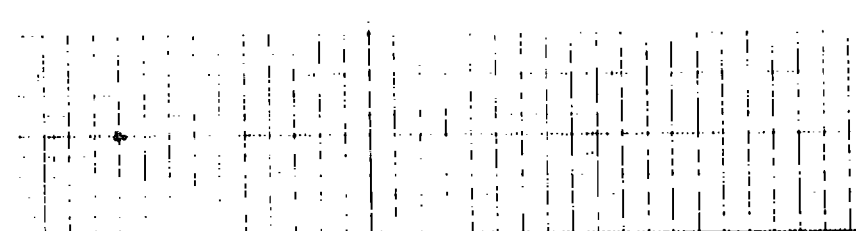
RUN NO. AA-2-1



INL
PR

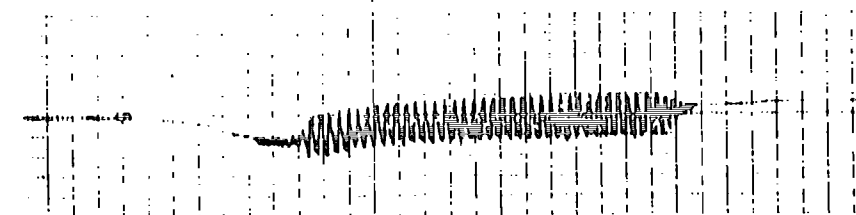


COMPRESSOR ST
PRESSURE RISE

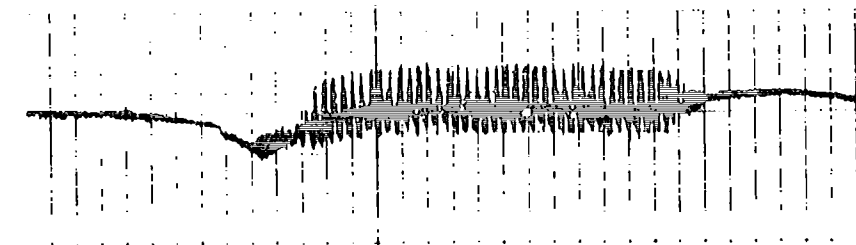


STATOR ROW 4
STAGGER ANGLE

CONTROL OFF



DETECTOR PRESSURE
SIGNAL UPPER SENSOR



DETECTOR PRESSURE
SIGNAL LOWER SENSOR

PE
RP

(a) DETECT
DETECT

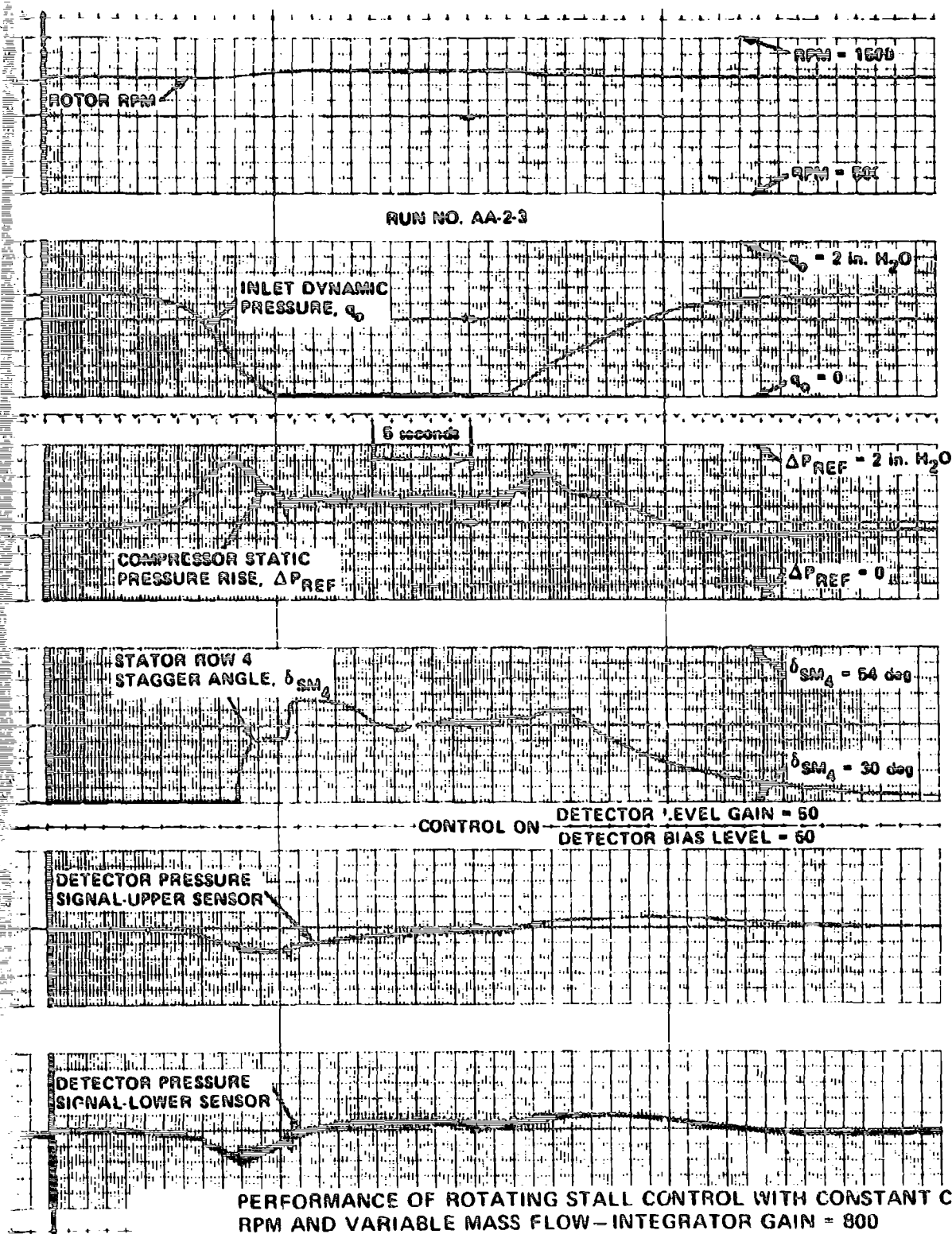
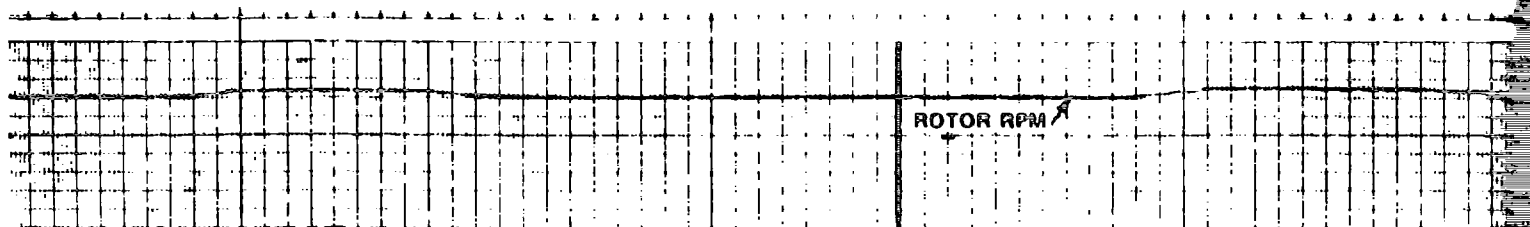


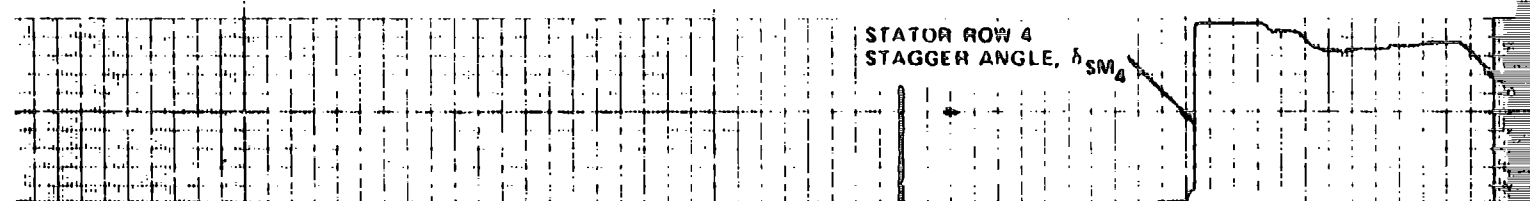
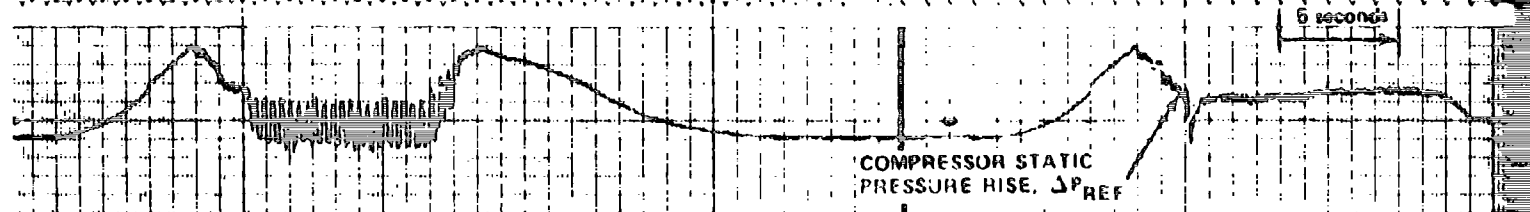
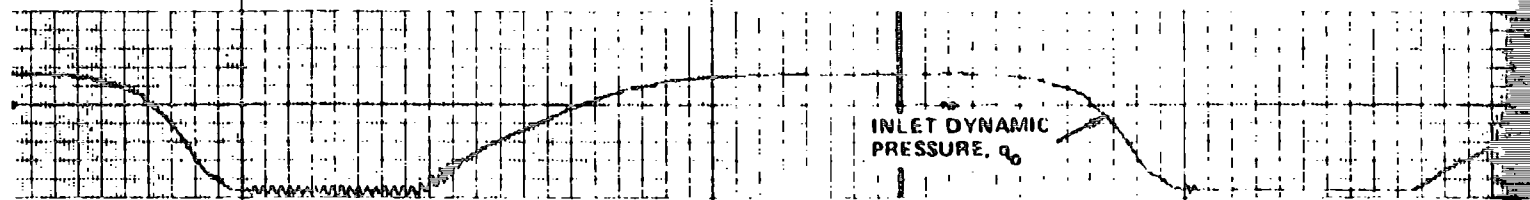
Figure 9

- (a) DETECTOR SIGNALS: SENSORS (1), OUTER WALL 1/4 CHORD STATIC, STATOR ROW 4
 DETECTOR FILTER CORNER FREQUENCIES: LOW = 5 Hz, HIGH = WIDEBAND



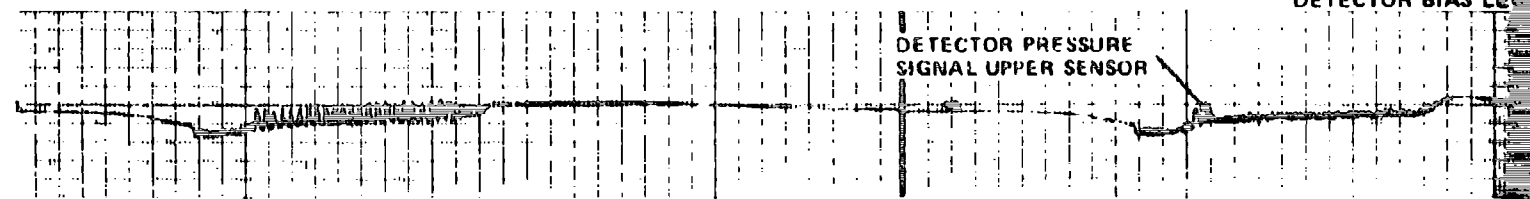
RUN NO. B-2-1

RUN NO. B-2-2



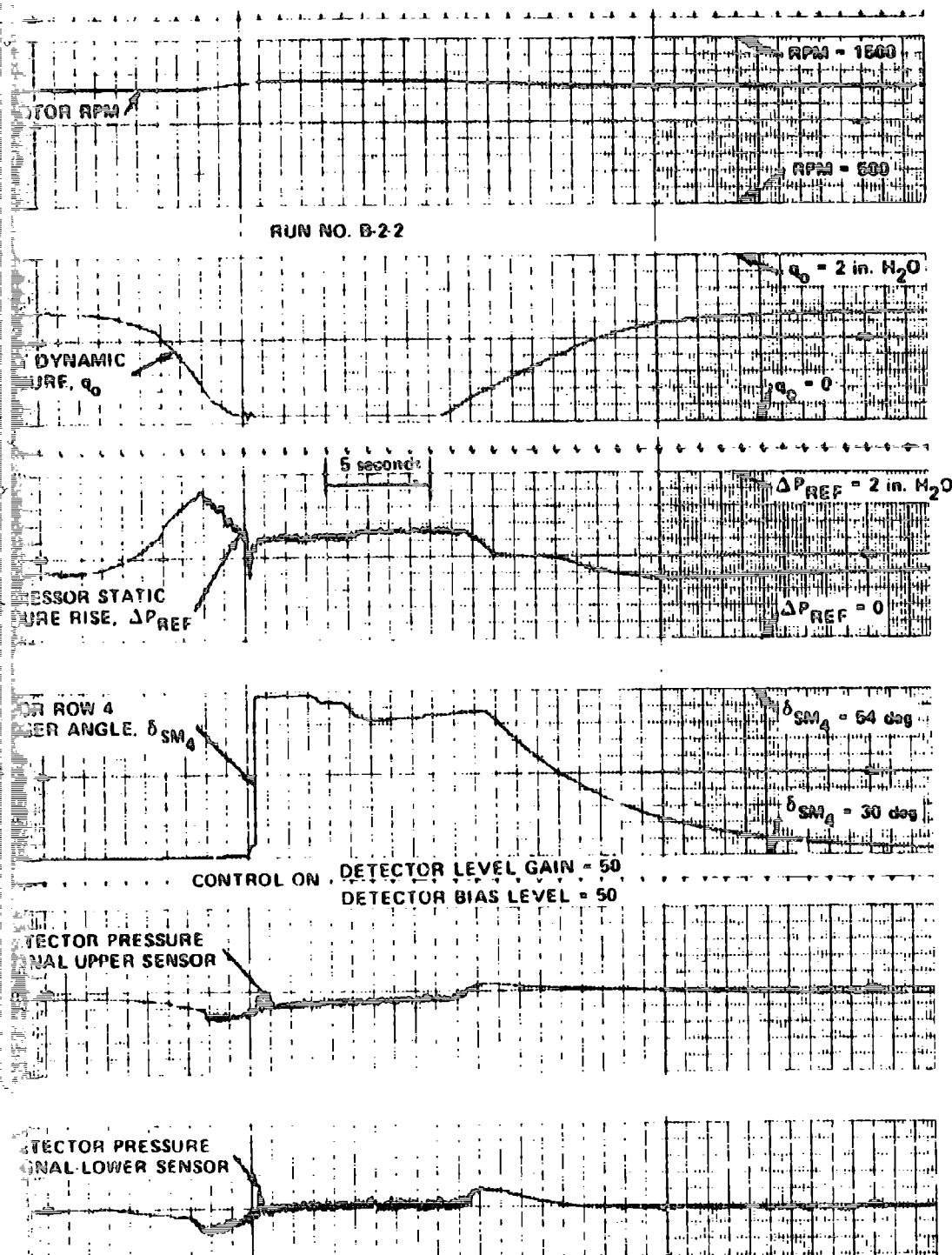
CONTROL OFF

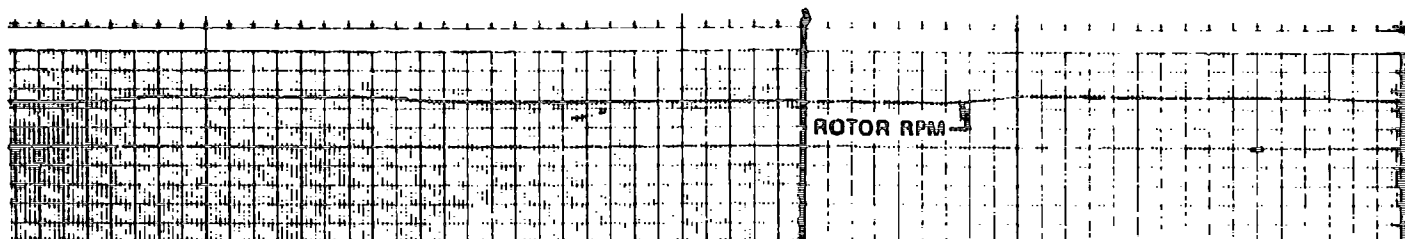
CONTROL ON DETECTOR LEVEL
DETECTOR BIAS LEV



PERFORM
COMPRES

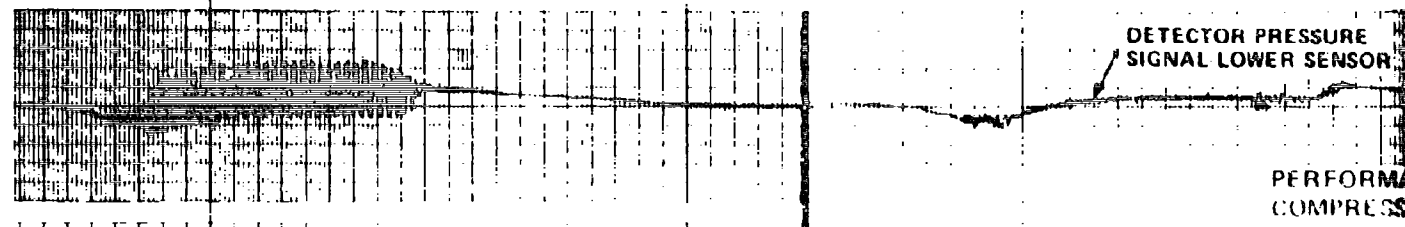
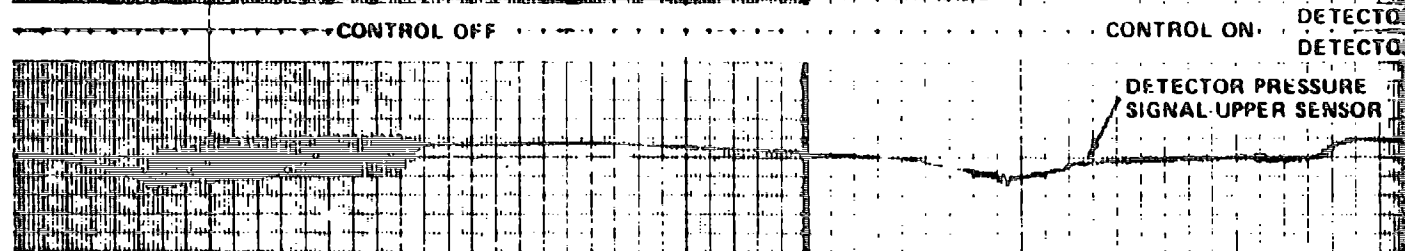
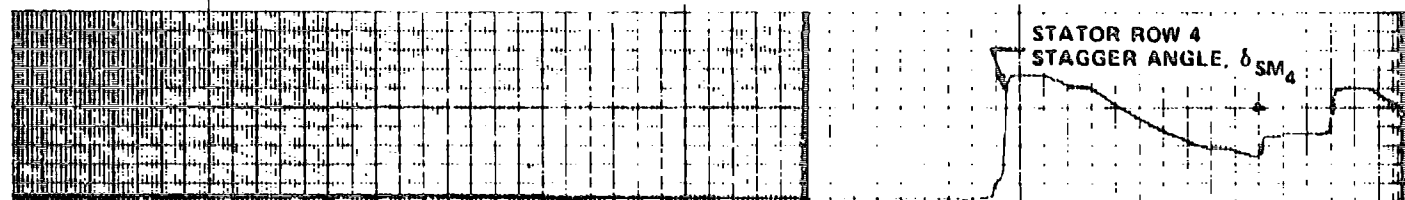
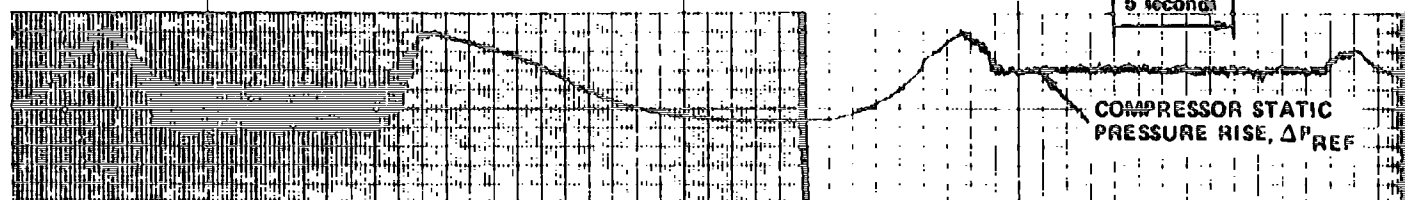
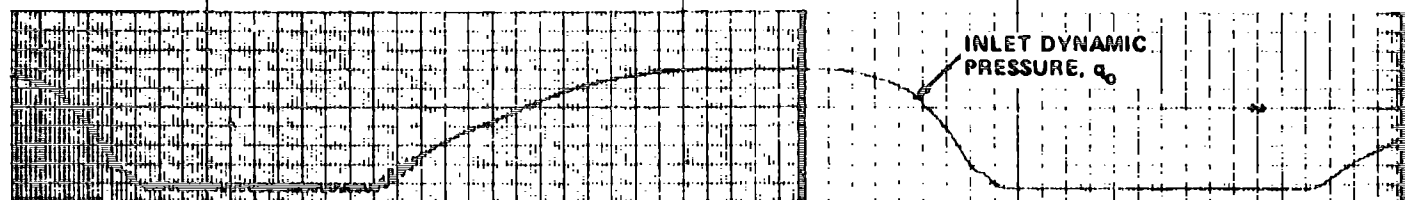
5) DETECTOR SIGNALS:
DETECTOR FILTER C





RUN NO. C-2-1

RUN NO. C-2-3



PERFORM
COMPRESS

(1) DETECTOR SIGNALS. S
DETECTOR FILTER CO

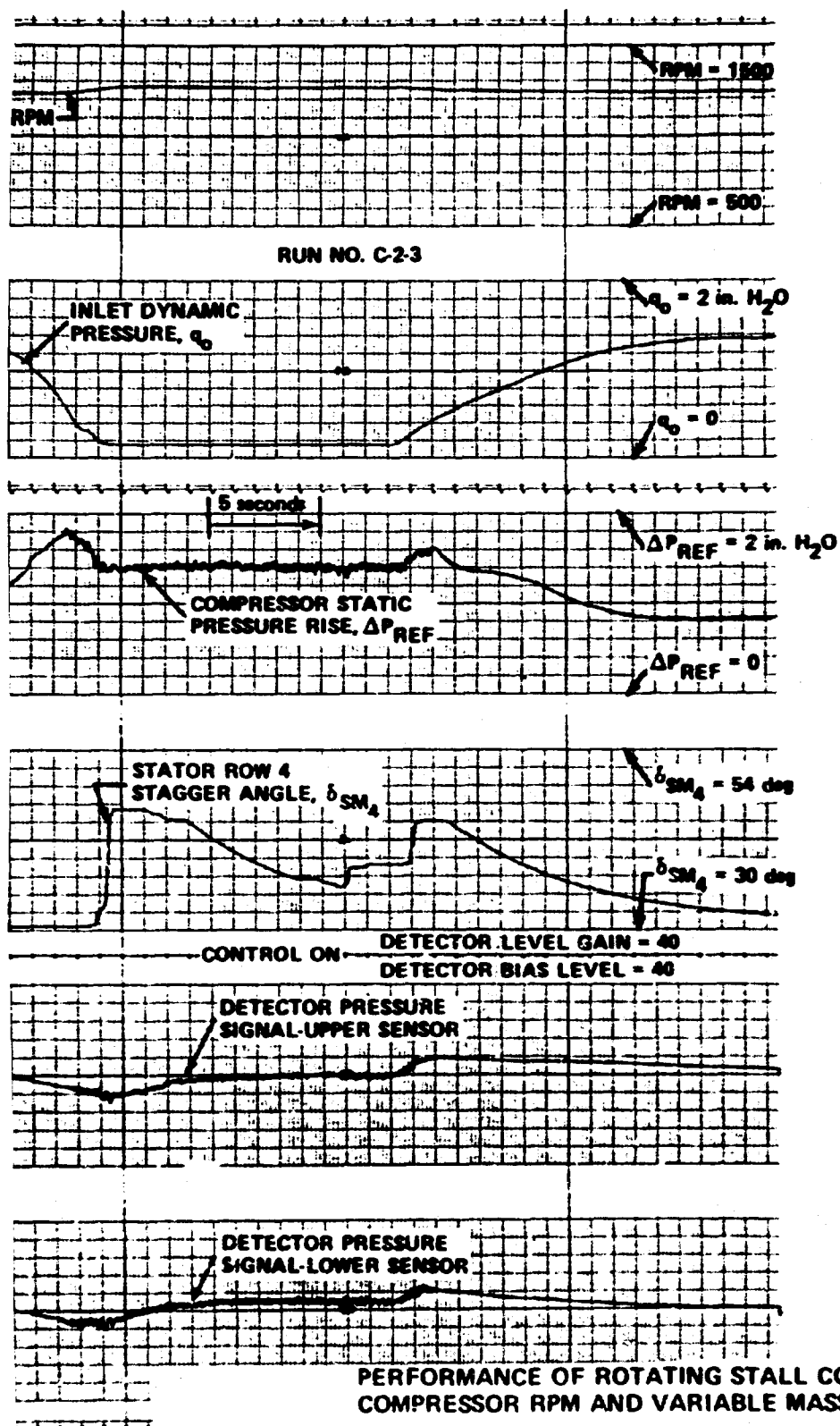
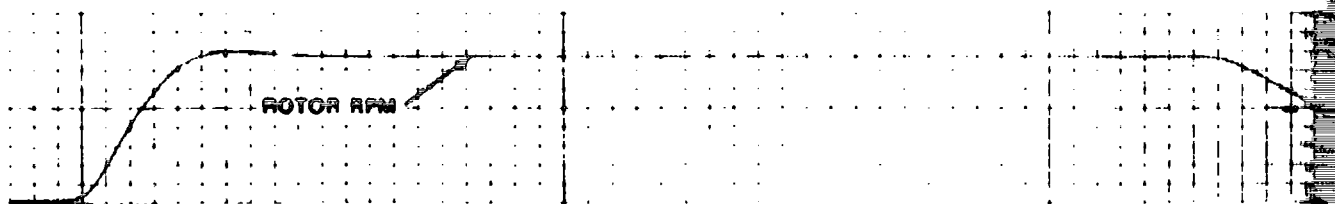


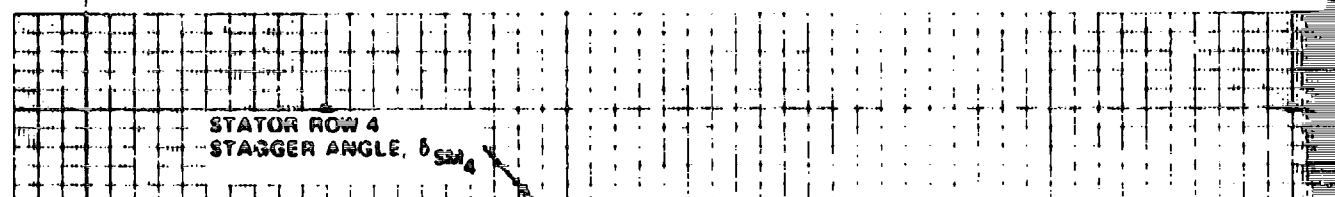
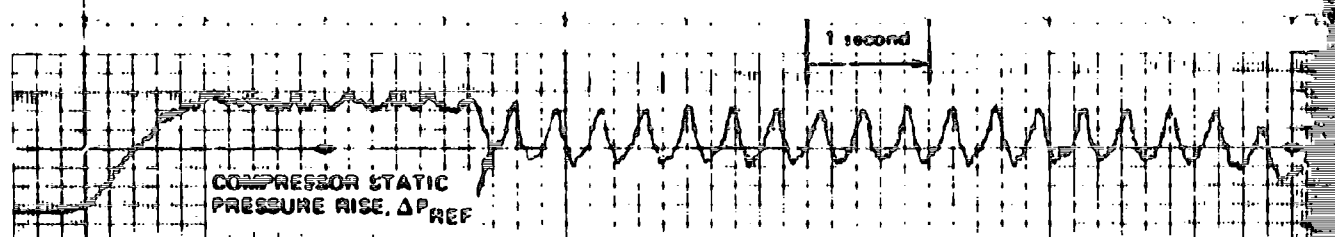
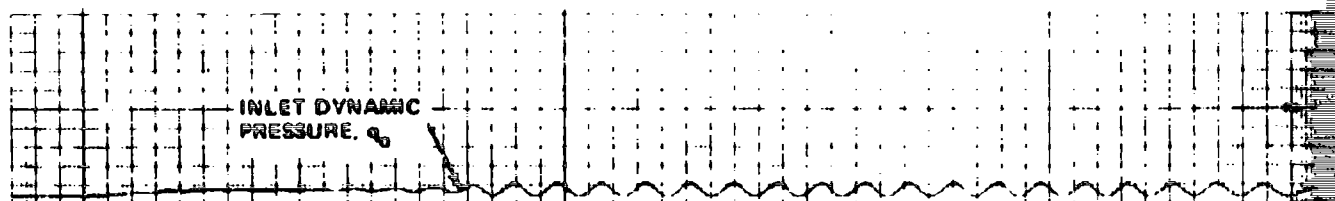
Figure 9 (Cont.)

PERFORMANCE OF ROTATING STALL CONTROL WITH CONSTANT COMPRESSOR RPM AND VARIABLE MASS FLOW—INTEGRATOR GAIN = 800

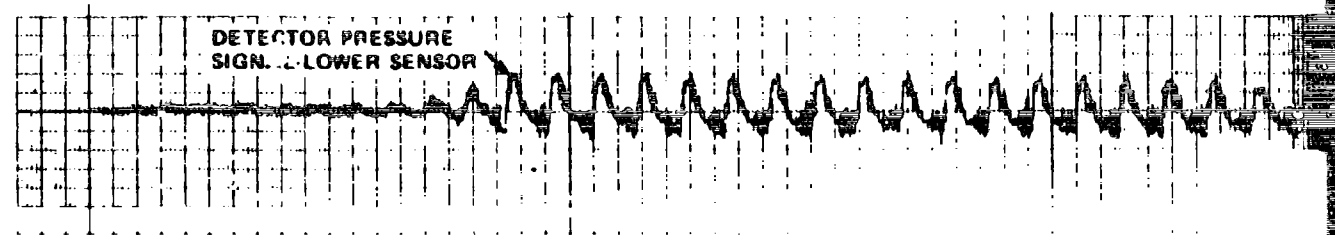
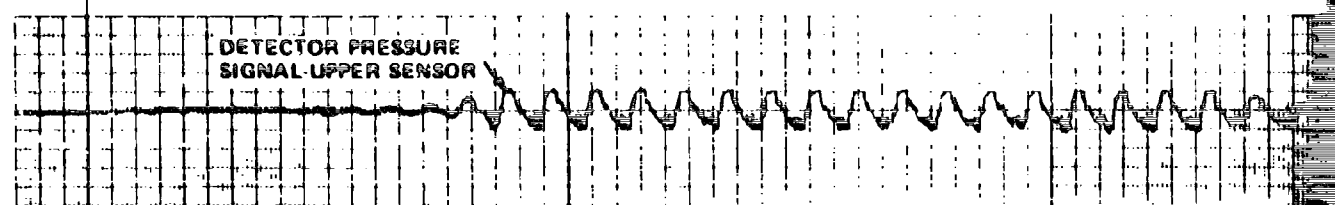
- (c) DETECTOR SIGNALS: SENSORS ③, ROTOR OUTER WALL
 DETECTOR FILTER CORNER FREQUENCIES: LOW = 1 Hz, HIGH = 6 Hz



RUN NO. AA-31



CONTROL OFF



DET
DET
CON

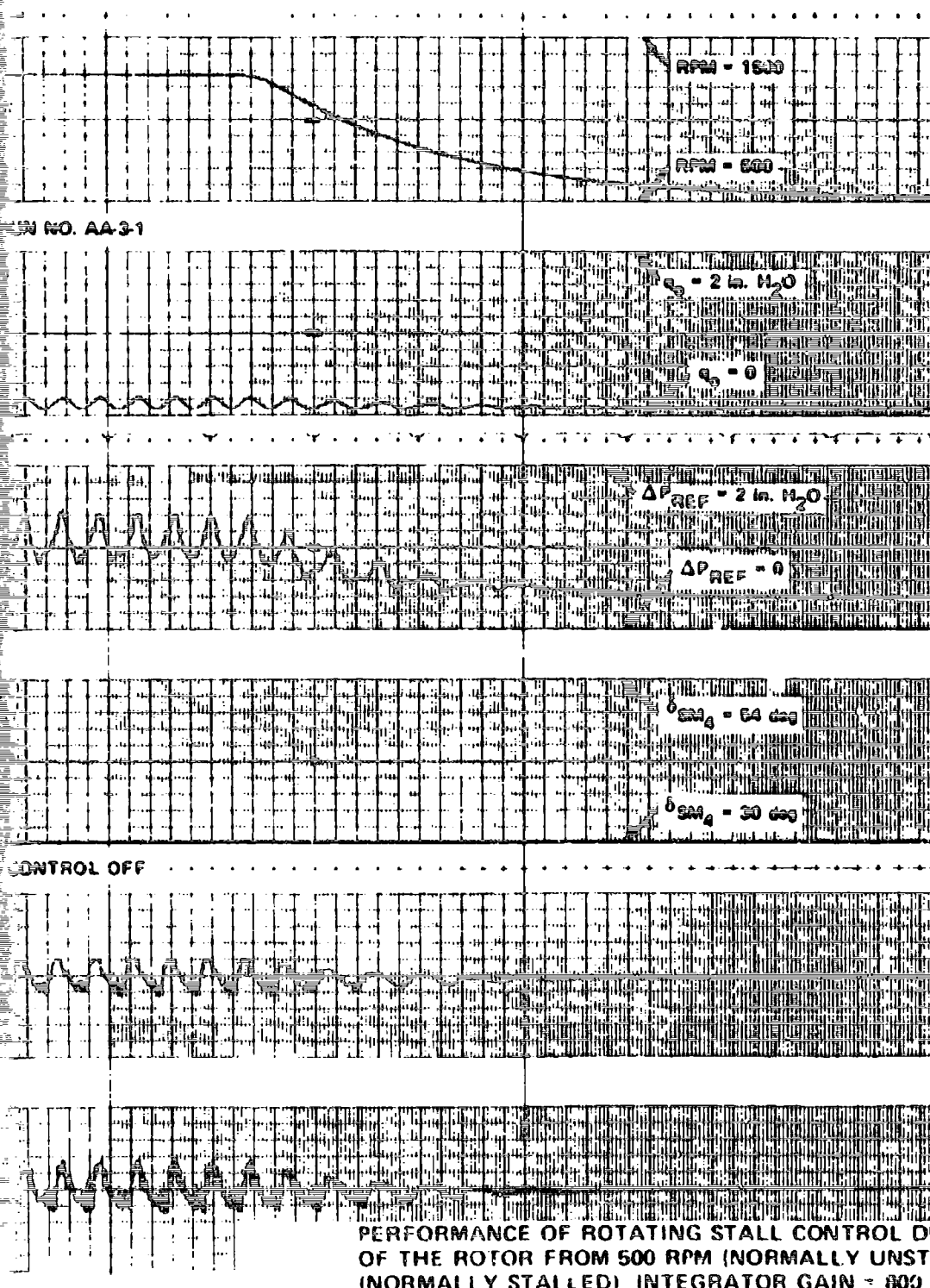
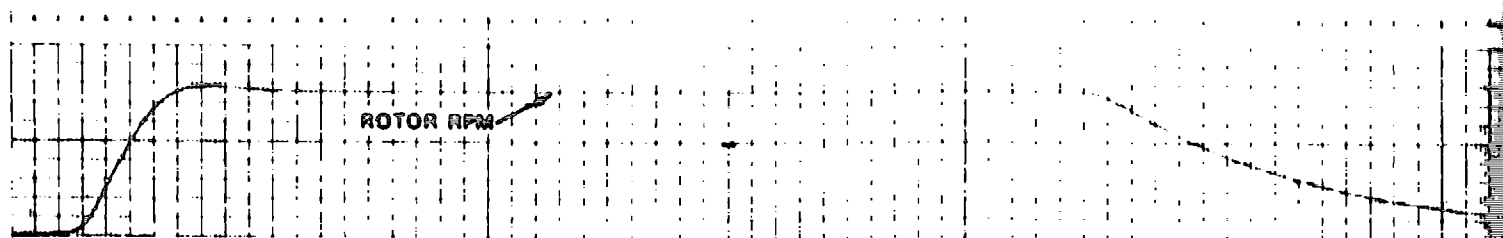


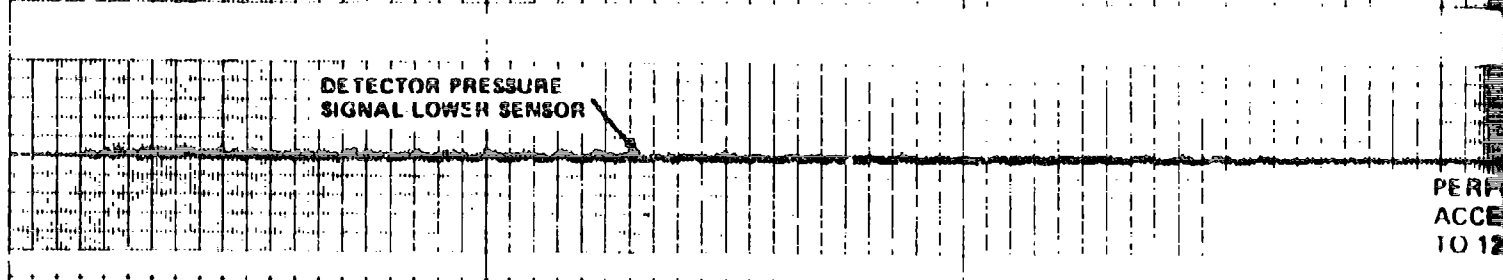
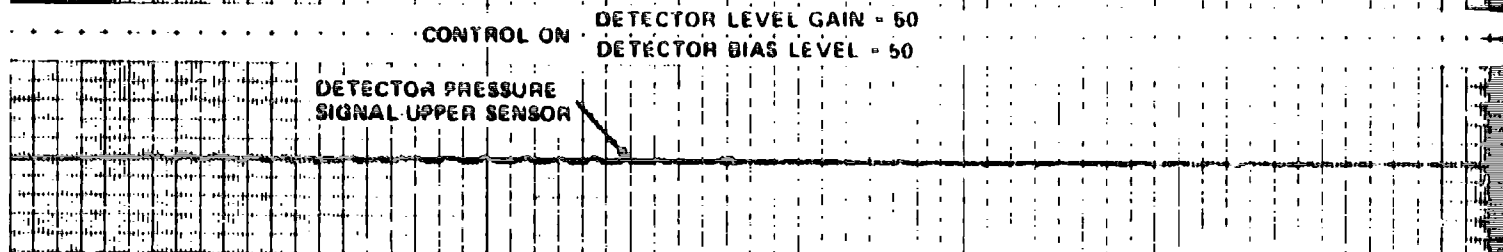
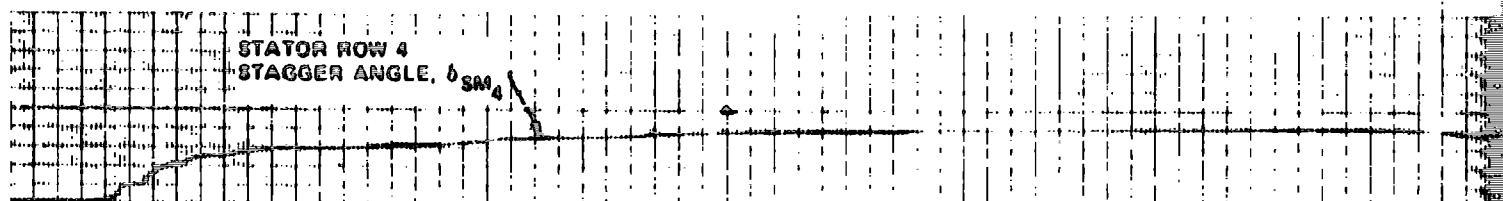
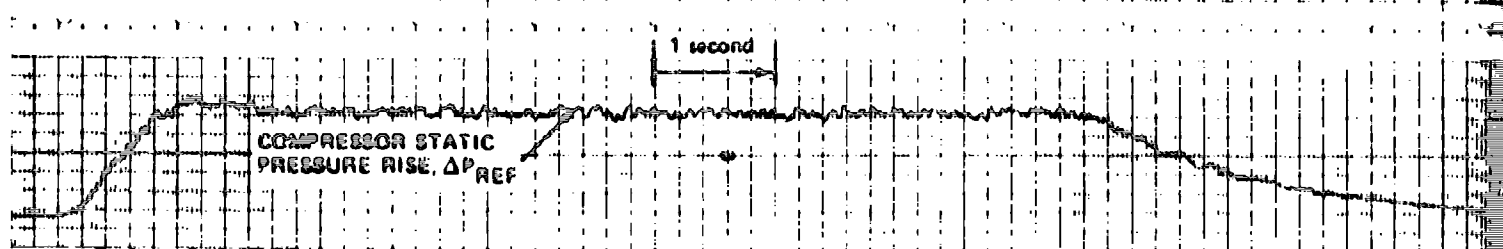
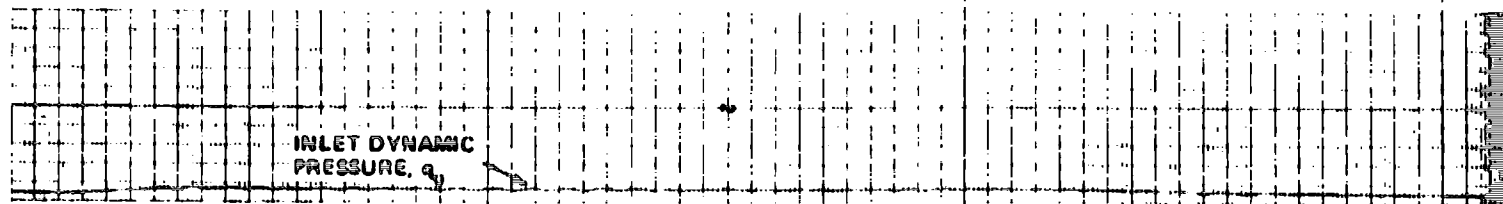
Figure 10

PERFORMANCE OF ROTATING STALL CONTROL DURING RAPID ACCELERATION OF THE ROTOR FROM 500 RPM (NORMALLY UNSTALLED) TO 1250 RPM (NORMALLY STALLED), INTEGRATOR GAIN = 800

- (a) DETECTOR SIGNALS: SENSORS (1), OUTER WALL 1/4 CHORD STATIC, STATOR ROW 4
 DETECTOR FILTER CORNER FREQUENCIES: LOW 5 Hz, HIGH = WIDEBAND
 CONTROL OFF



RUN NO. AA-3-2



PERF
ACCE
TO 12

(b) DETECTOR SIGN
DETECTOR FILT
CONTROL ON

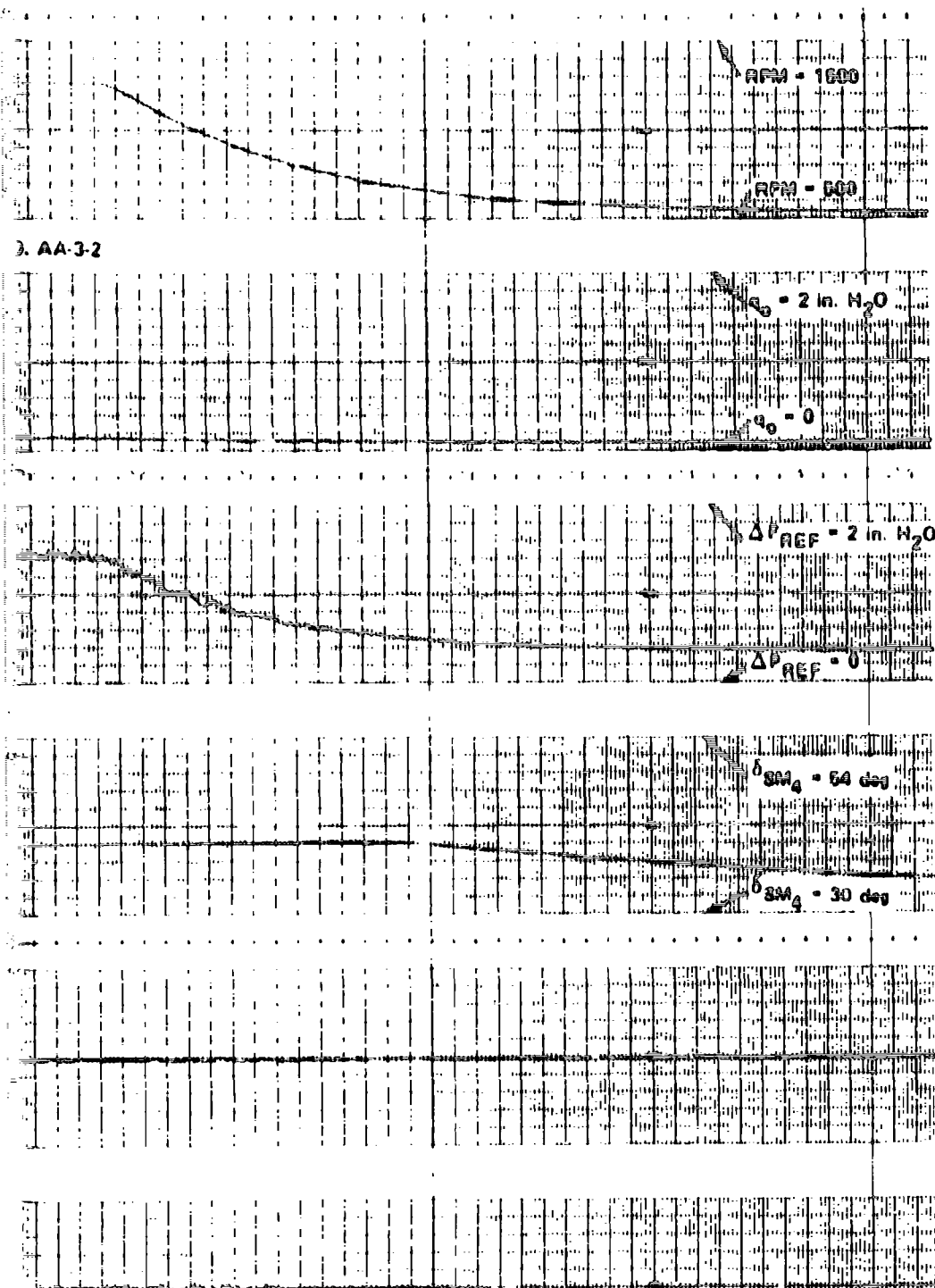
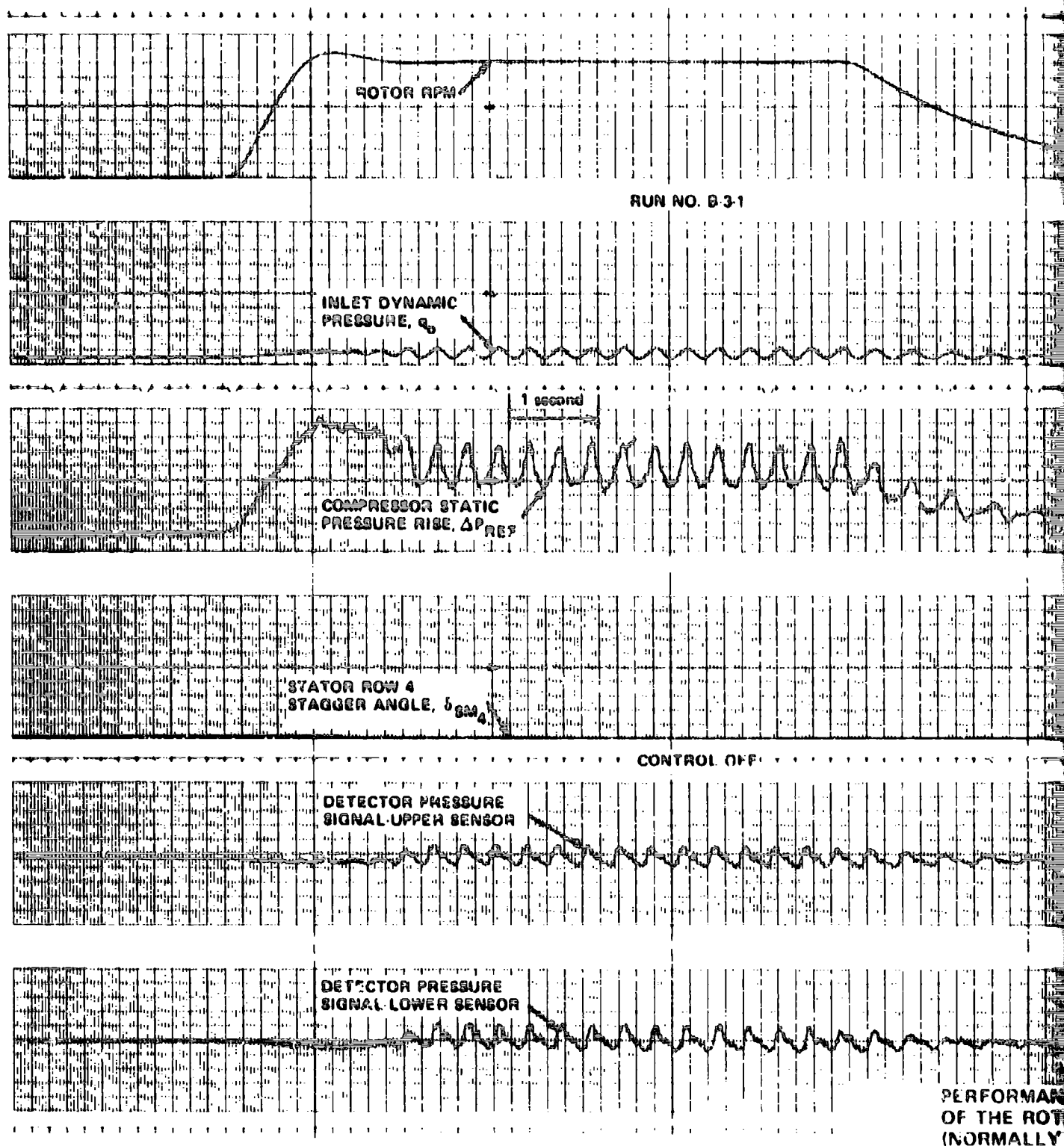


Figure 10 (Cont.)

PERFORMANCE OF ROTATING STALL CONTROL DURING RAPID
ACCELERATION OF THE ROTOR FROM 500 RPM (NORMALLY UNSTALLED)
TO 1250 RPM (NORMALLY STALLED), INTEGRATOR GAIN = 800

- (b) DETECTOR SIGNALS. SENSORS 1; OUTER WALL 1/4 CIRC. STATIC; STATOR ROW 4
DETECTOR FILTER CORNER FREQUENCIES LOW 5 Hz, HIGH WIDEBAND;
CONTROL ON



(H) DETECTOR SIGNAL
DETECTOR FILTER
CONTROL OFF

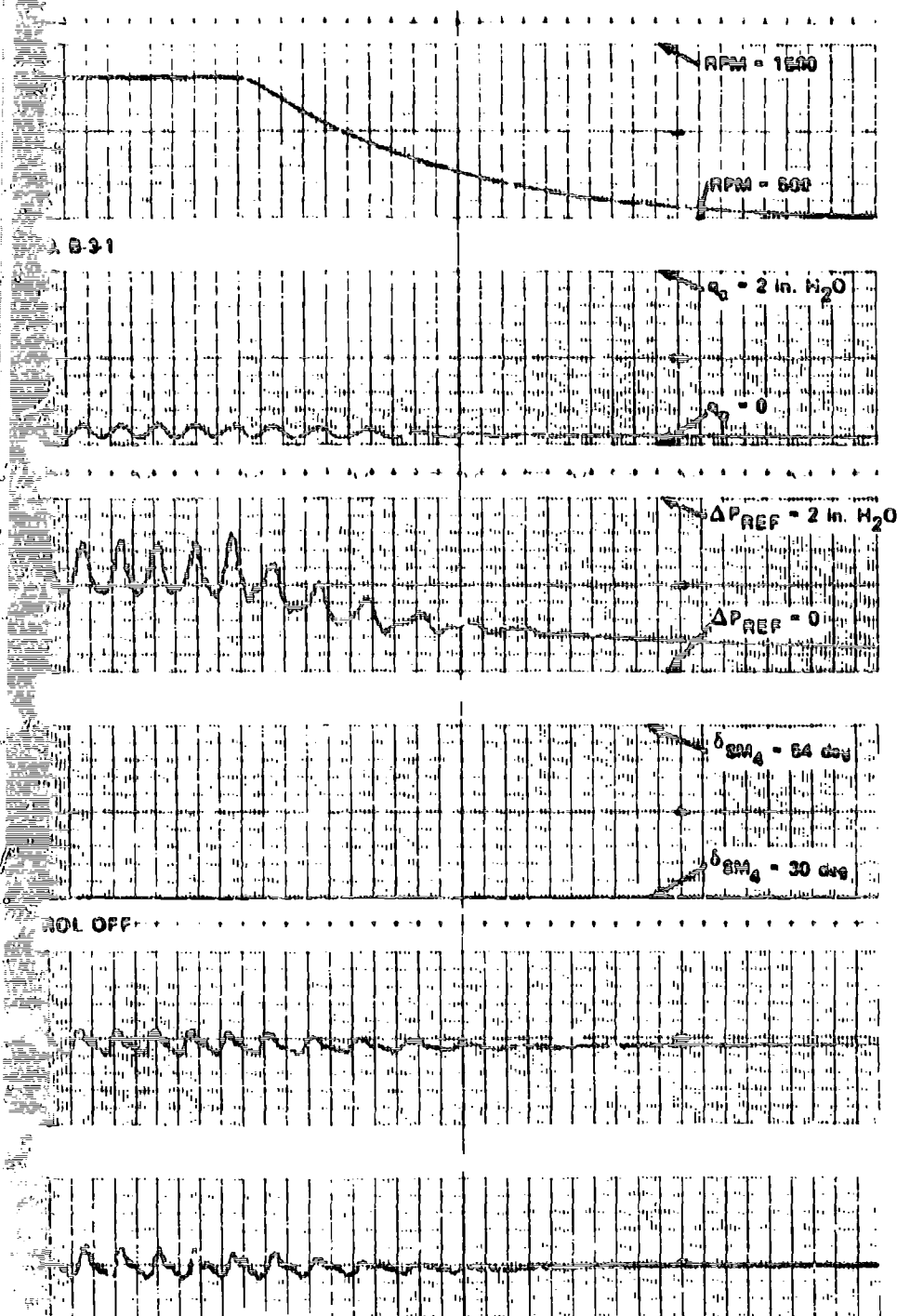
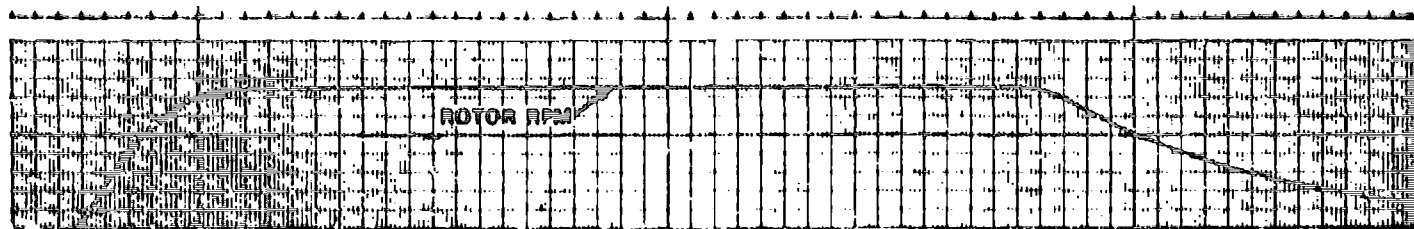


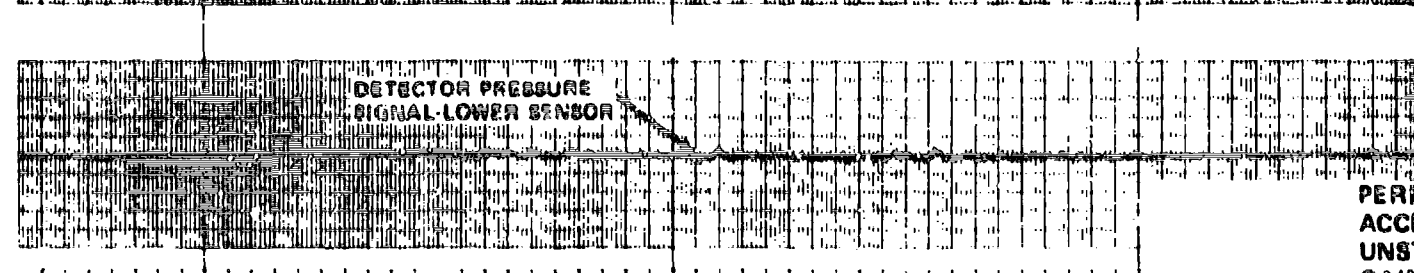
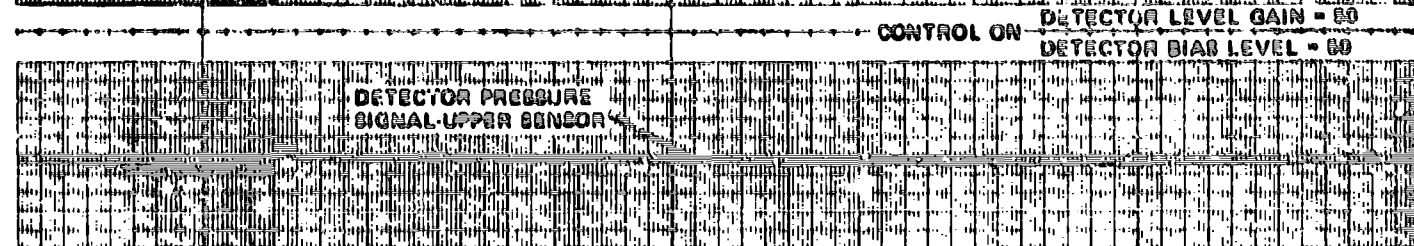
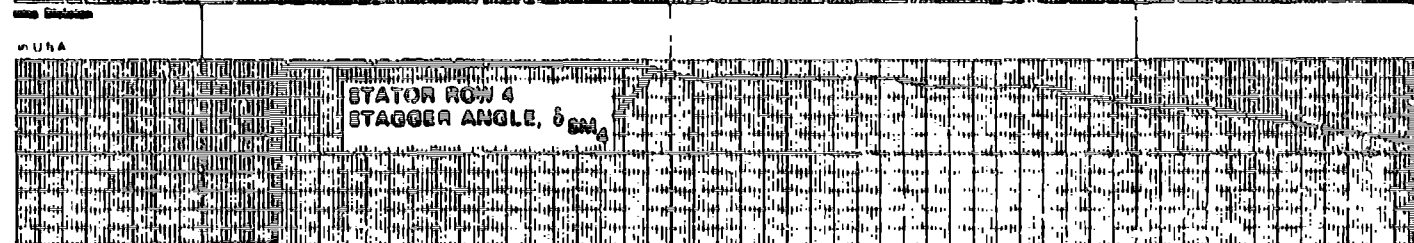
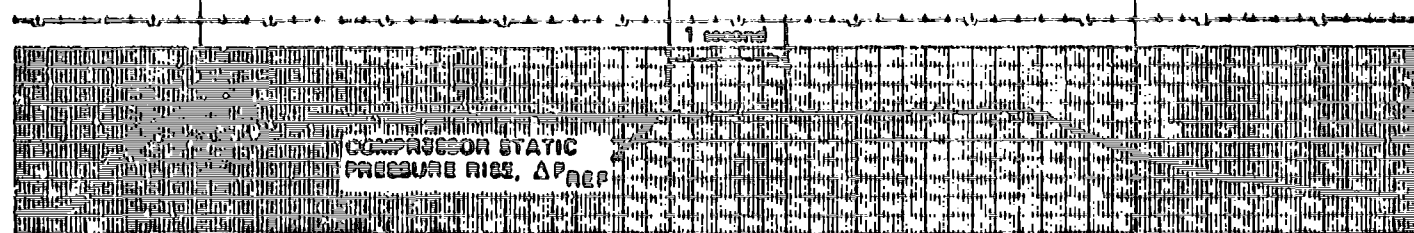
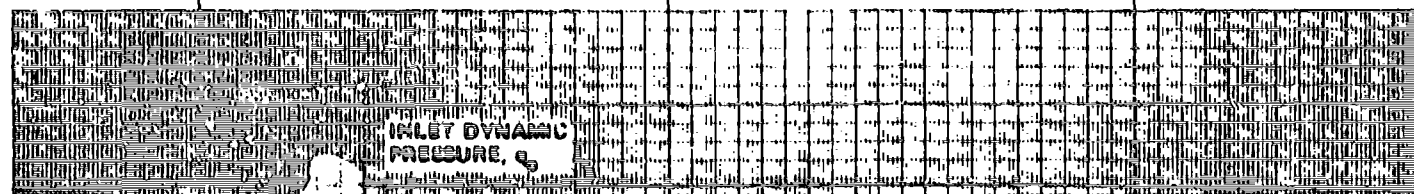
Figure 11

PERFORMANCE OF ROTATING STALL CONTROL DURING RAPID ACCELERATION OF THE ROTOR FROM 600 RPM (NORMALLY UNSTALLED) TO 1250 RPM (NORMALLY STALLED), INTEGRATOR GAIN = 800

- (a) DETECTOR SIGNALS: SENSORS (2), OUTER WALL 1/4 CHORD STATIC, STATOR ROW 5
 DETECTOR FILTER CORNER FREQUENCIES: LOW = 1 Hz, HIGH = 6 Hz:
 CONTROL OFF



RUN NO. B-32



PERF
ACCE
UNST
GAIN

(b) DETECTOR SIGNAL
DETECTOR FILTER
CONTROL ON

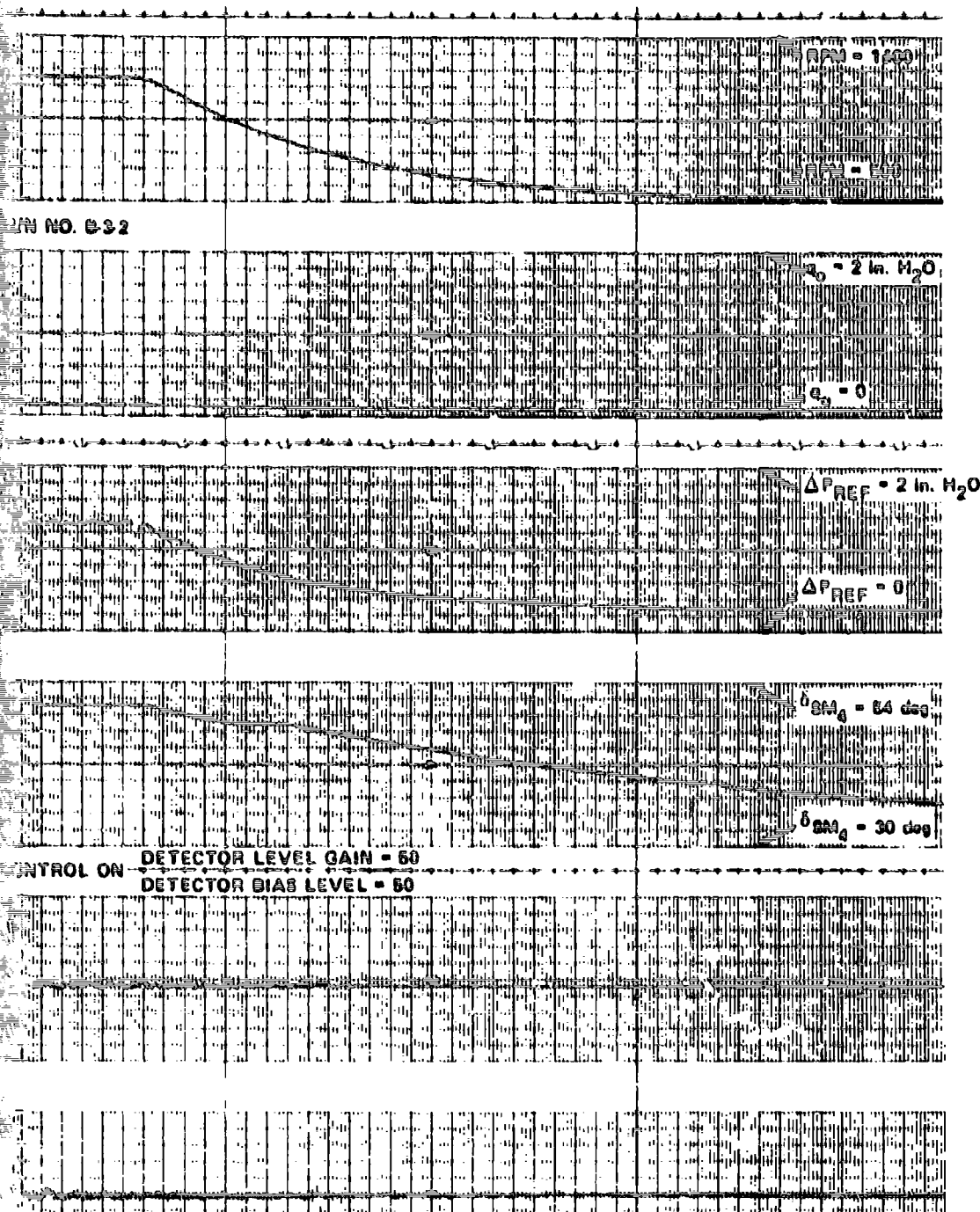
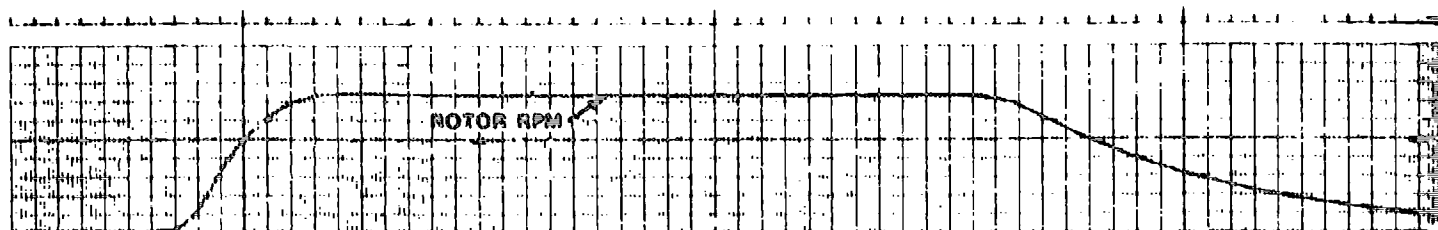


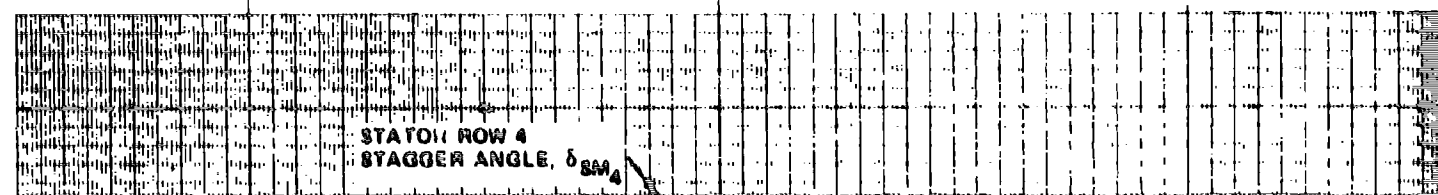
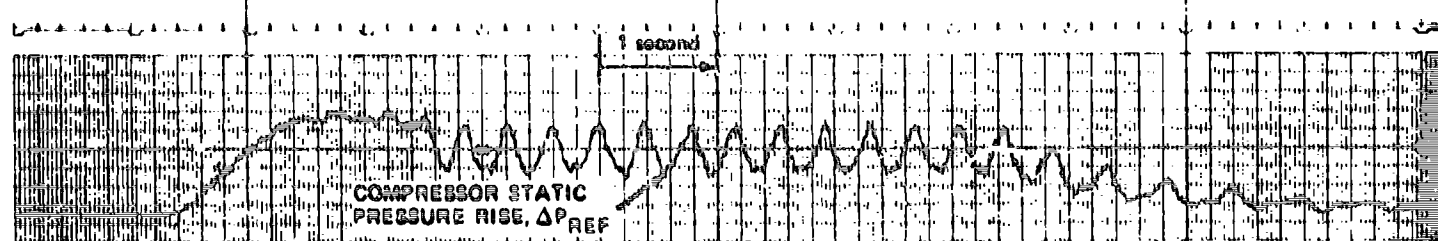
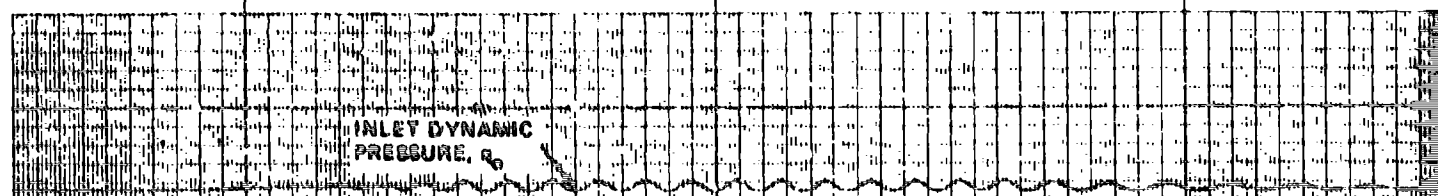
Figure 11 (Cont.)

PERFORMANCE OF ROTATING STALL CONTROL DURING RAPID
 ACCELERATION OF THE ROTOR FROM 500 RPM (NORMALLY
 UNSTALLED) TO 1260 RPM (NORMALLY STALLED), INTEGRATOR
 GAIN = 800

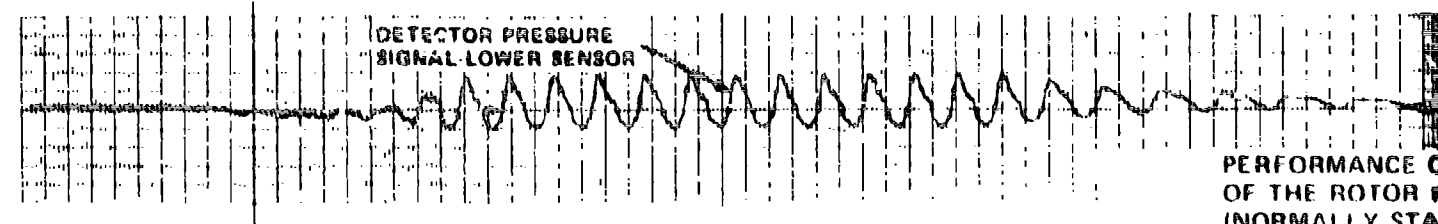
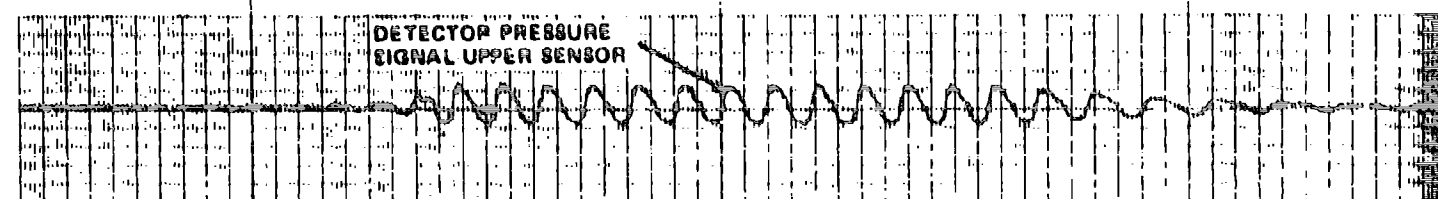
- (b) DETECTOR SIGNALS: SENSORS (2), OUTER WALL 1/4 CHORD STATIC; STATOR ROW 6
 DETECTOR FILTER CORNER FREQUENCIES: LOW 1 Hz, HIGH = 6 Hz
 CONTROL ON



RUN NO. C-3-1



CONTROL OFF



PERFORMANCE OF THE ROTOR (NORMALLY STALL)

(a) DETECTOR SIGNALS:
DETECTOR FILTER CO
CONTROL OFF

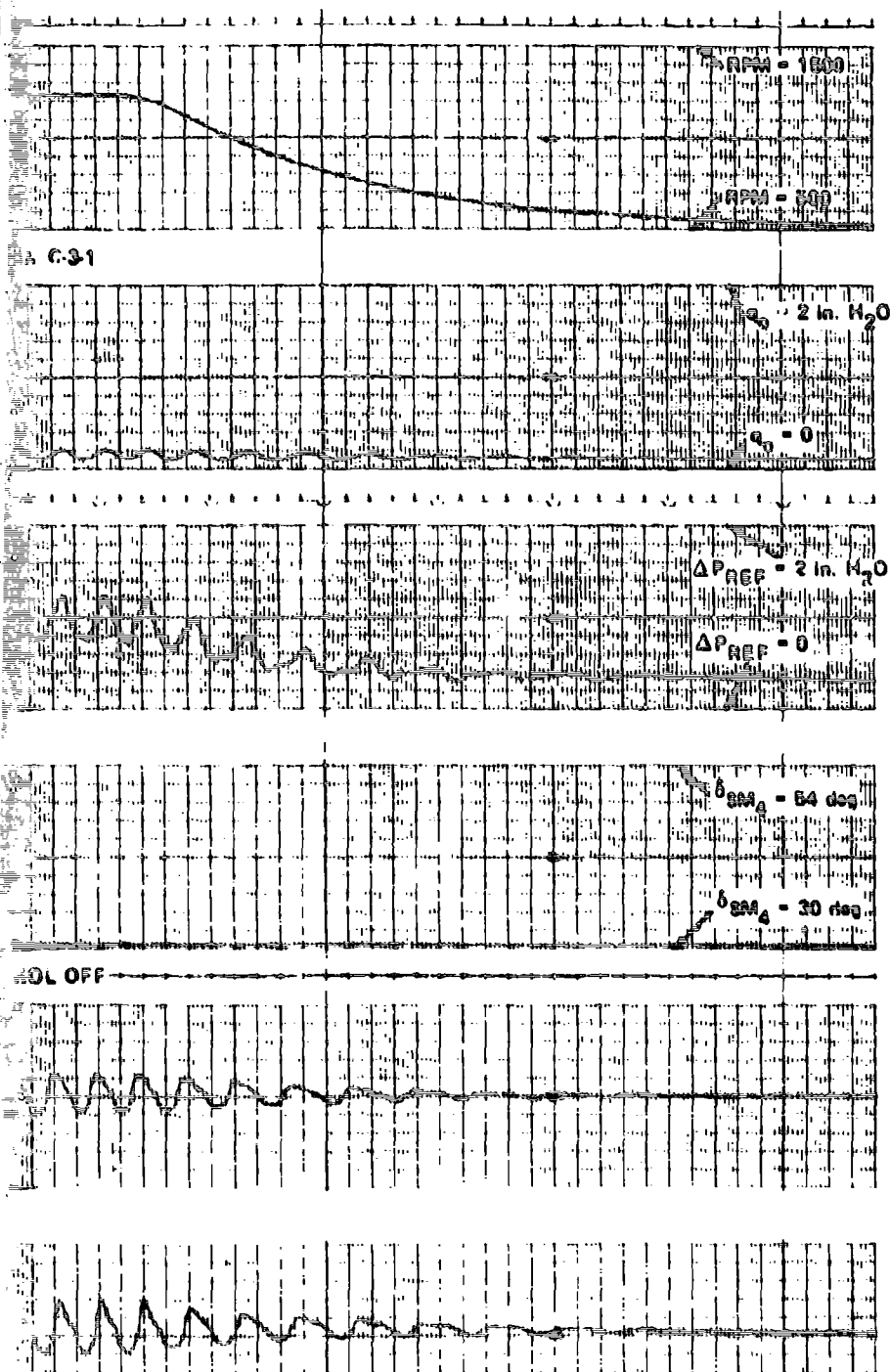
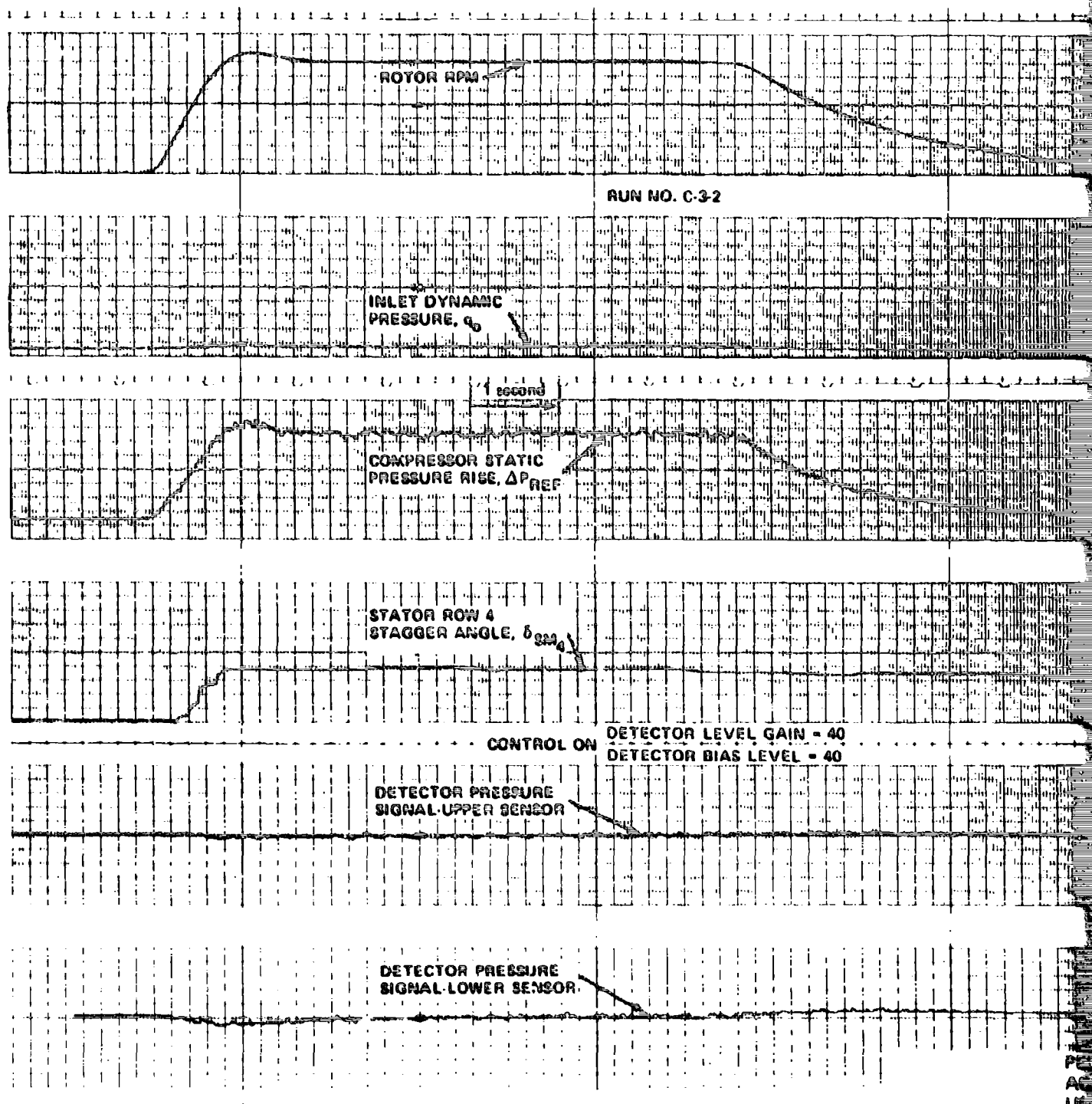


Figure 12
PERFORMANCE OF ROTATING STALL CONTROL DURING RAPID ACCELERATION
OF THE ROTOR FROM 500 RPM (NORMALLY UNSTALLED) TO 1200 RPM
(NORMALLY STALLED). INTEGRATOR GAIN = 800

- (a) DETECTOR SIGNALS SENSORS (3) ROTOR OUTER WALL
DETECTOR FILTER CORNER FREQUENCIES LOW = 1 Hz, HIGH = 6 Hz
CONTROL OFF



(b) DETECTOR SIGNAL
DETECTOR FAILURE
CONTROL ON

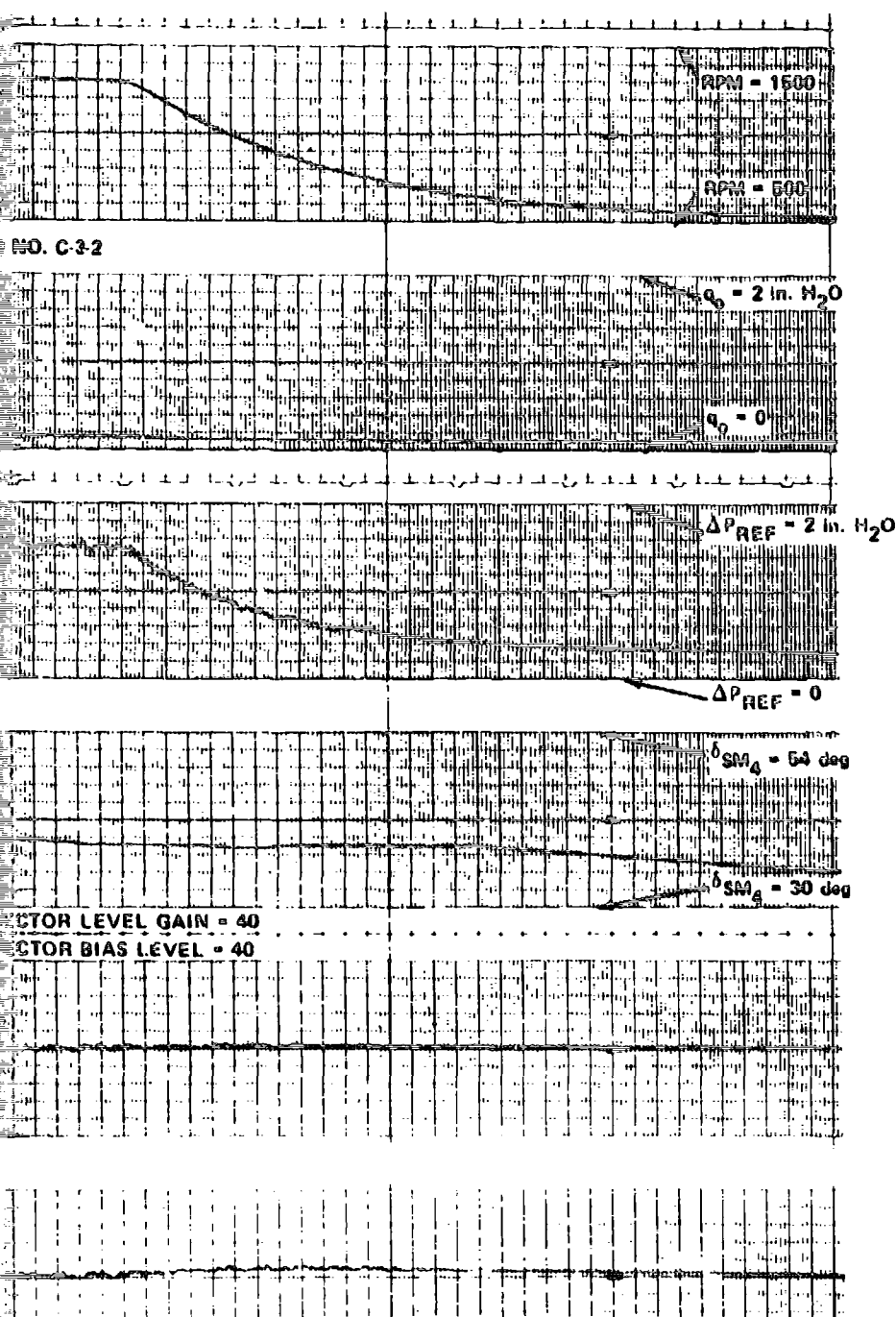
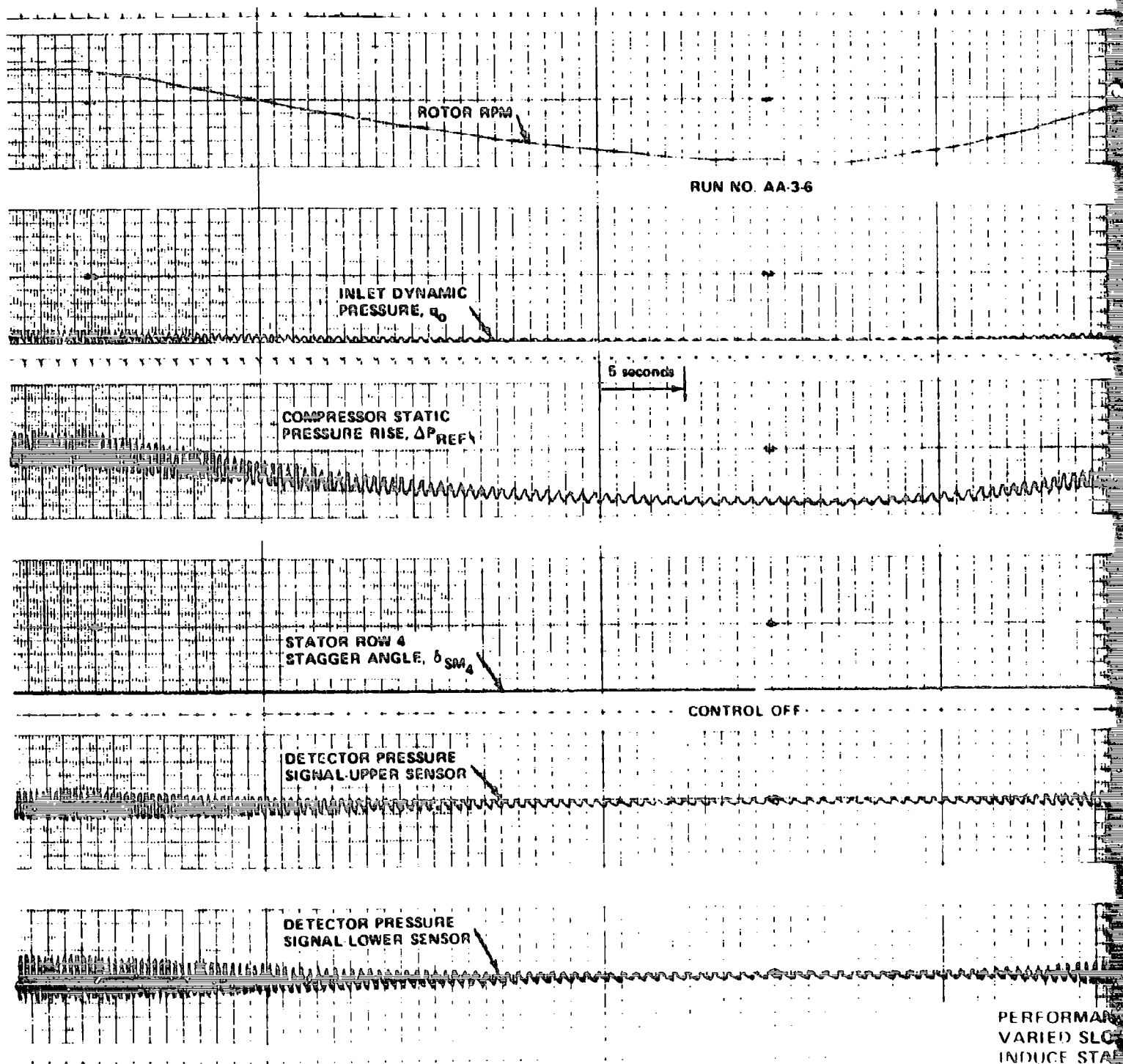


Figure 12 (Cont.)

PERFORMANCE OF ROTATING STALL CONTROL DURING RAPID ACCELERATION OF THE ROTOR FROM 500 RPM (NORMALLY UNSTALLED) TO 1250 RPM (NORMALLY STALLED), INTEGRATOR GAIN = 800

- (b) DETECTOR SIGNALS: SENSORS (3), ROTOR OUTER WALL
 DETECTOR FILTER CORNER FREQUENCIES: LOW 1 Hz, HIGH = 6 Hz:
 CONTROL ON



(1) DETECTOR SIGNAL
DETECTOR FILTER
CONTROL OFF

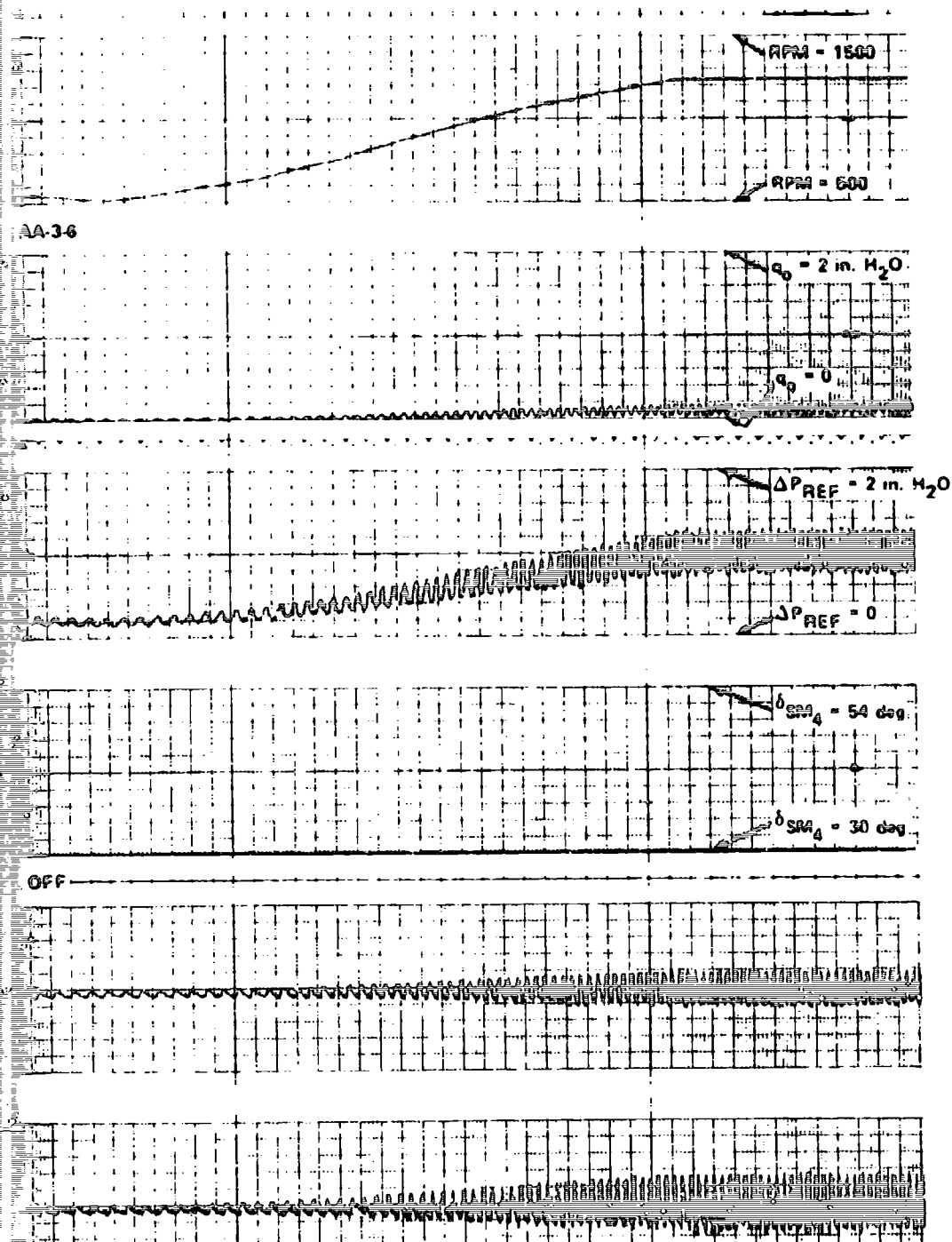
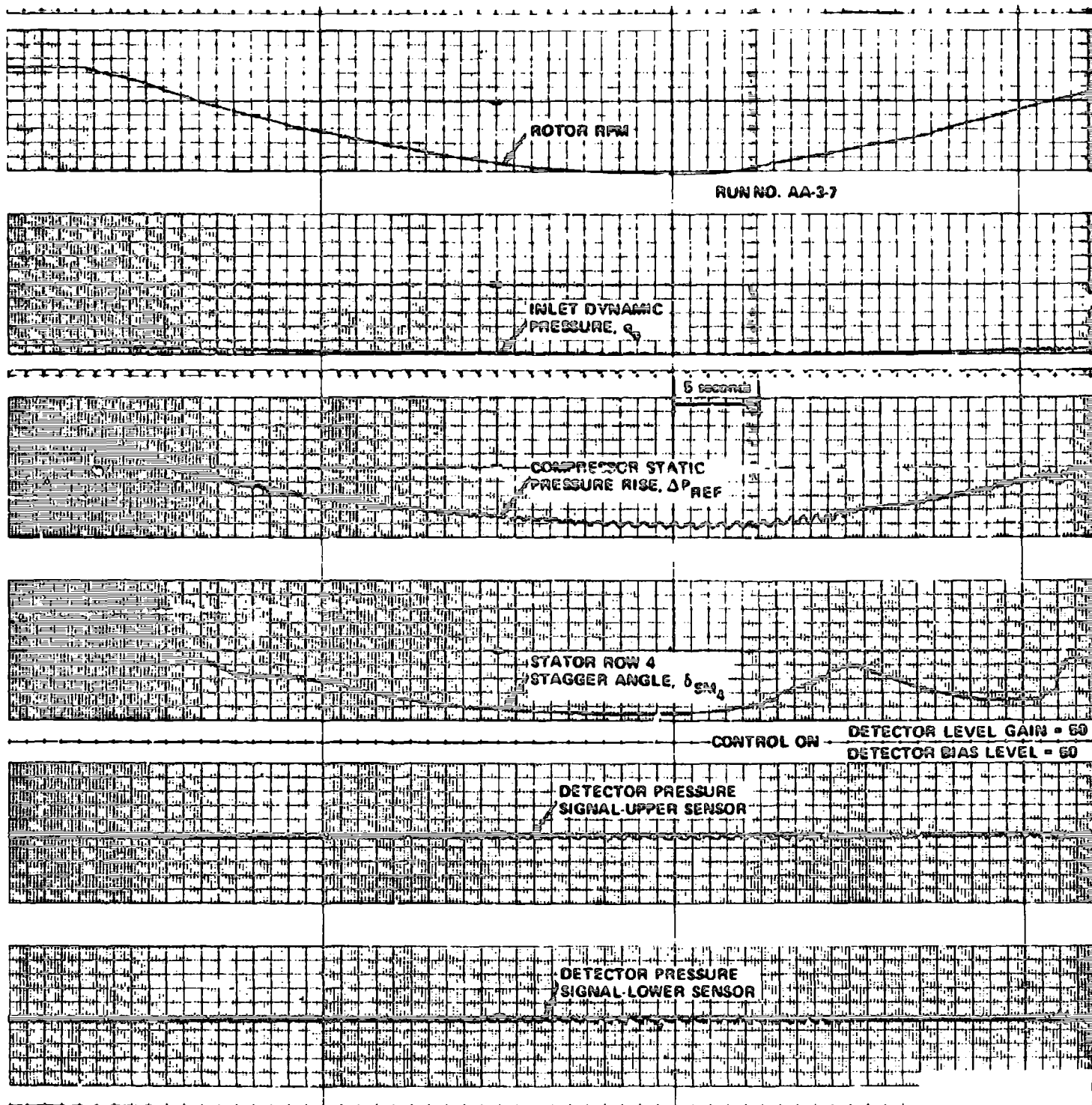


Figure 13

PERFORMANCE OF ROTATING STALL CONTROL AS ROTOR SPEED IS
VARIED SLOWLY UNDER DOWNSTREAM CONDITIONS WHICH NORMALLY
INDUCE STALL AT ALL RPM'S

- (a) DETECTOR SIGNALS: SENSORS (1), OUTER WALL 1/4 CHORD STATIC, STATOR ROW 4
DETECTOR FILTER CORNER FREQUENCIES: LOW = 5 Hz, HIGH = WIDEBAND:
CONTROL OFF



(b) DETECTOR SIG
DETECTOR FI
CONTROL ON

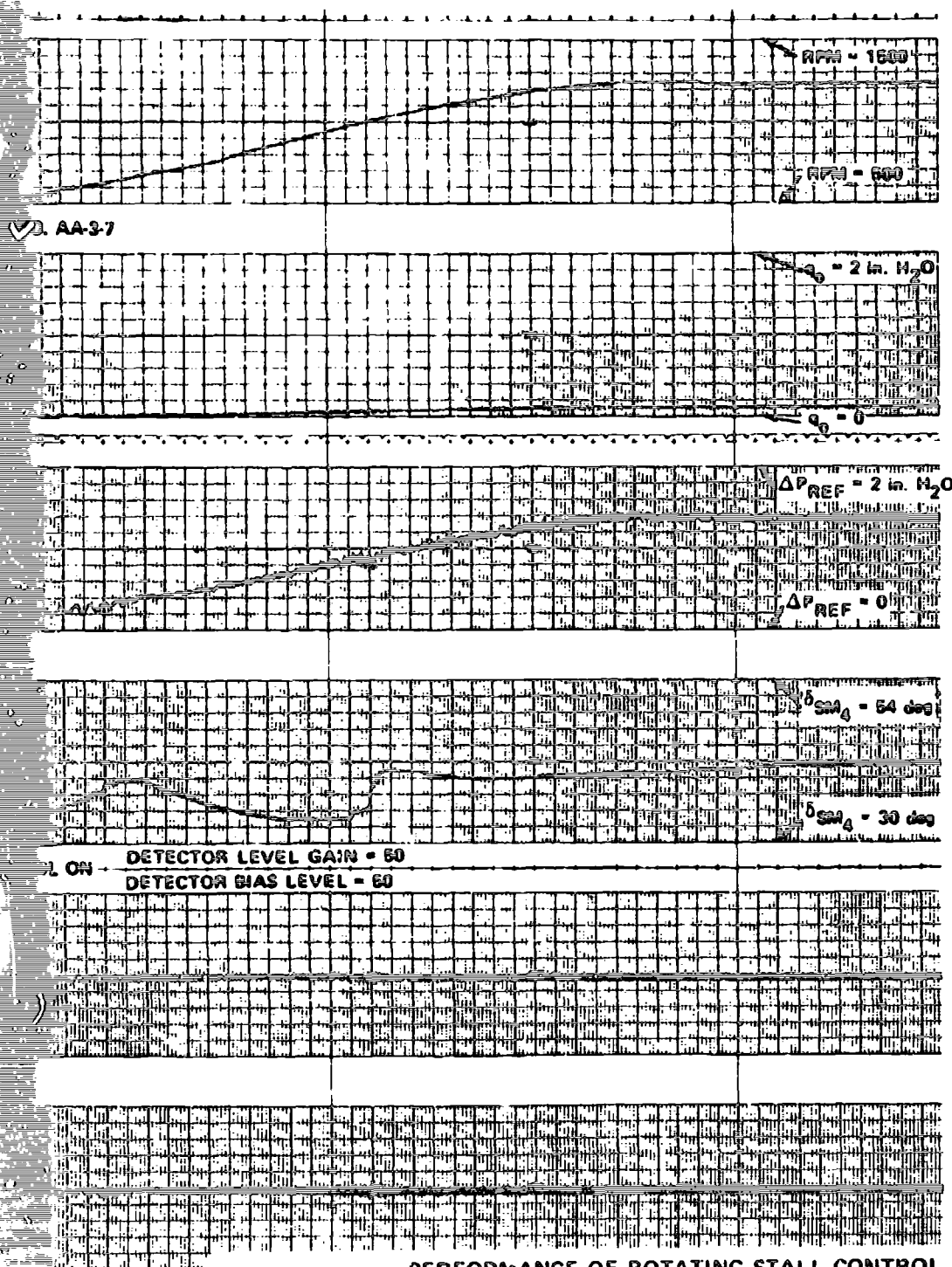


Figure 13 (Cont.)

PERFORMANCE OF ROTATING STALL CONTROL AS ROTOR SPEED IS VARIED SLOWLY UNDER DOWNSTREAM CONDITIONS WHICH NORMALLY INDUCE STALL AT ALL RPM's

- (b) DETECTOR SIGNALS: SENSORS (1), OUTER WALL 1/4 CHORD STATIC, STATOR ROW 4
 DETECTOR FILTER CORNER FREQUENCIES: LOW 5 Hz, HIGH = WIDEBAND:
 CONTROL ON

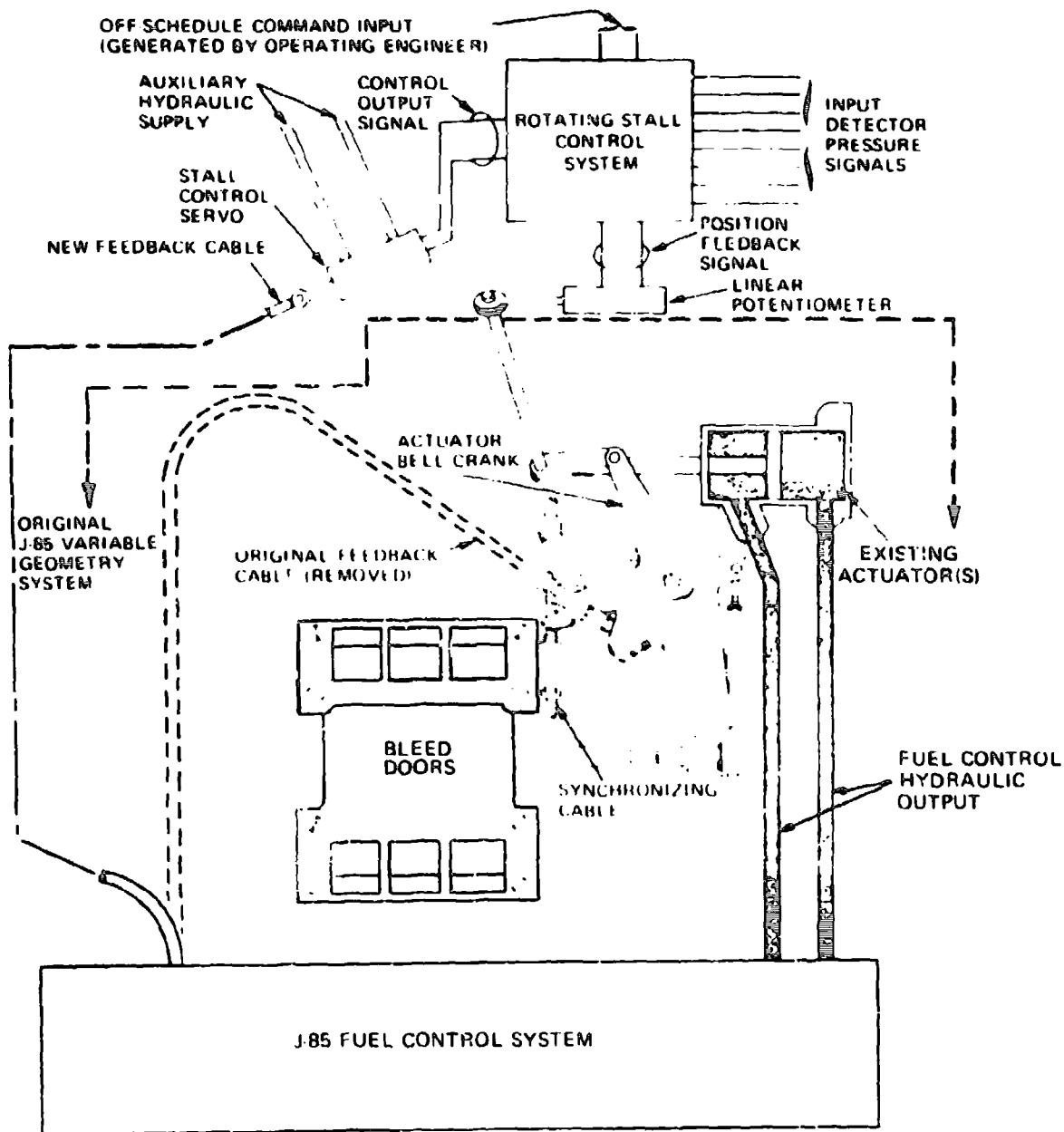
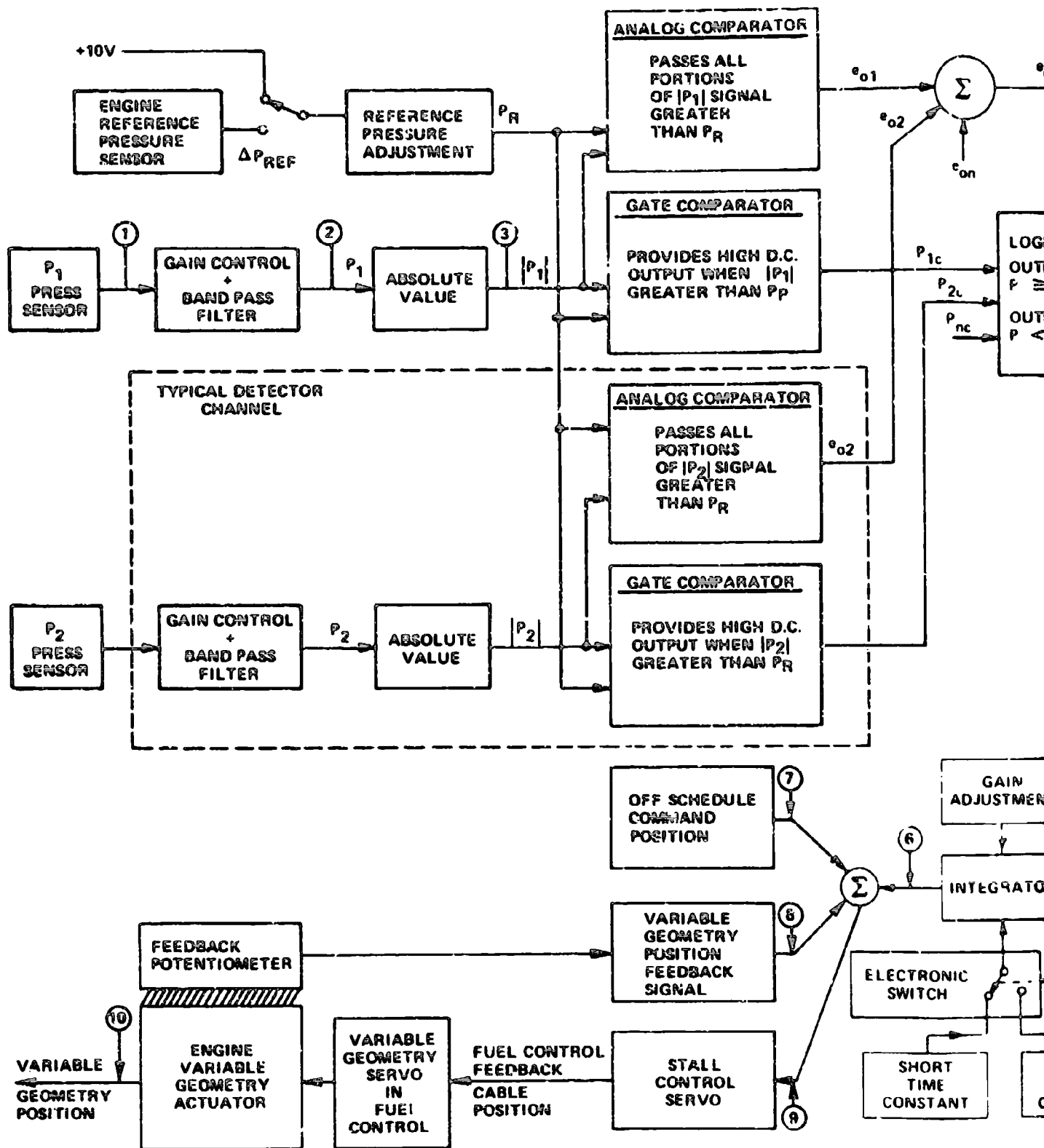


Figure 14 MODIFIED VARIABLE GEOMETRY SYSTEM INCORPORATING ROTATING STALL CONTROL ON J-85 ENGINE



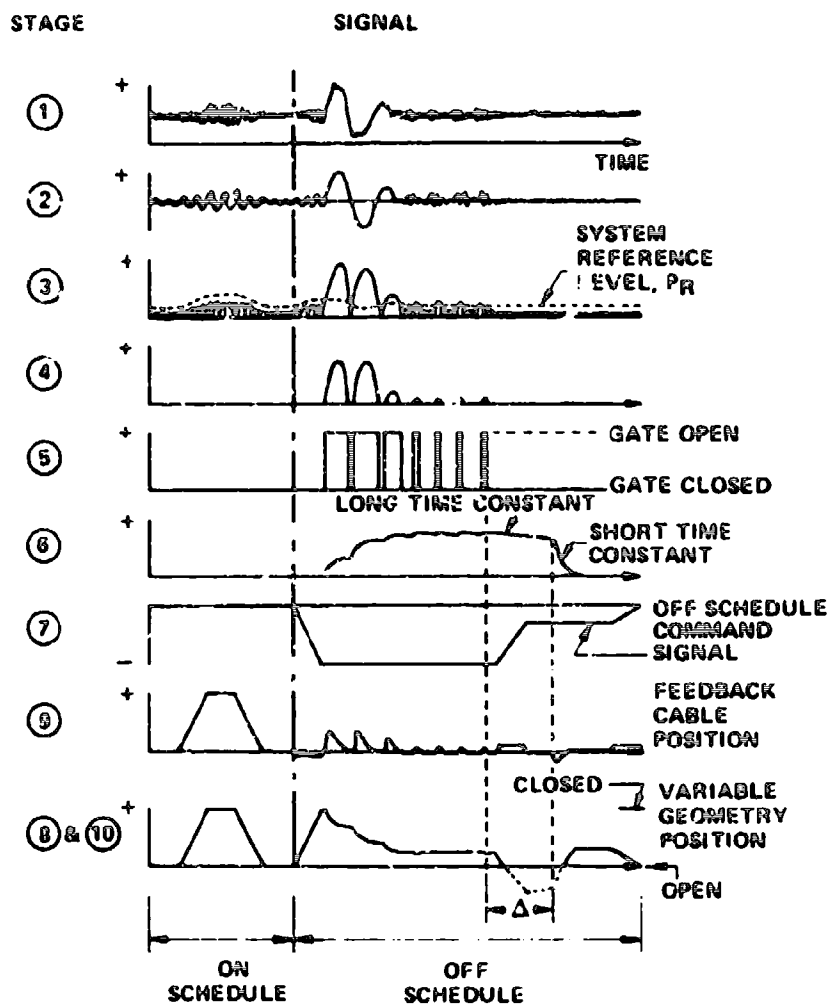
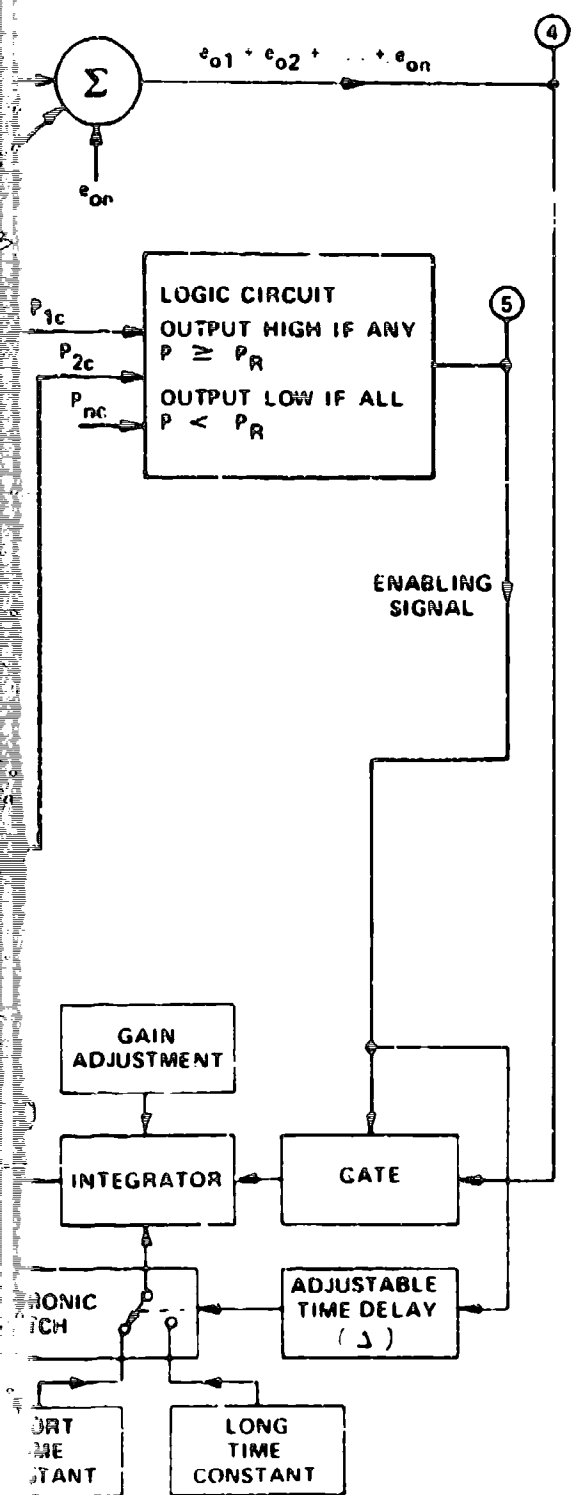


Figure 15

SCHEMATIC OF ROTATING STALL CONTROL
INSTALLATION ON J-85 ENGINE

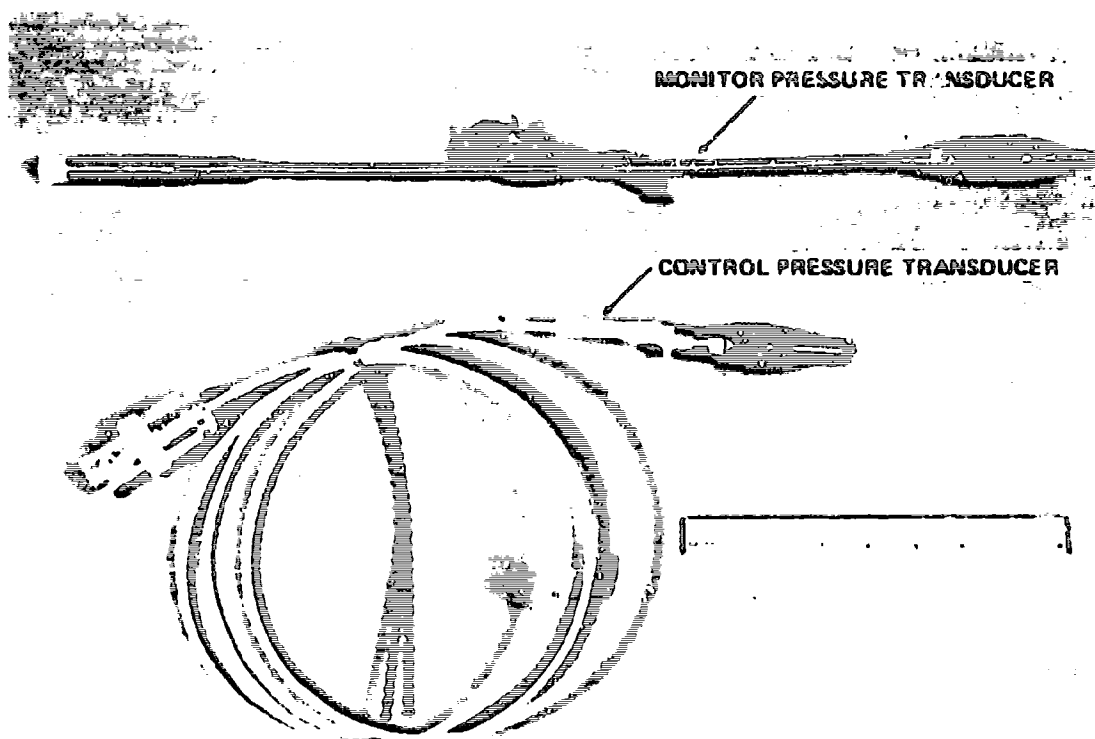


Figure 16 **PRESSURE TRANSDUCERS FOR J-85 ROTATING STALL CONTROL**

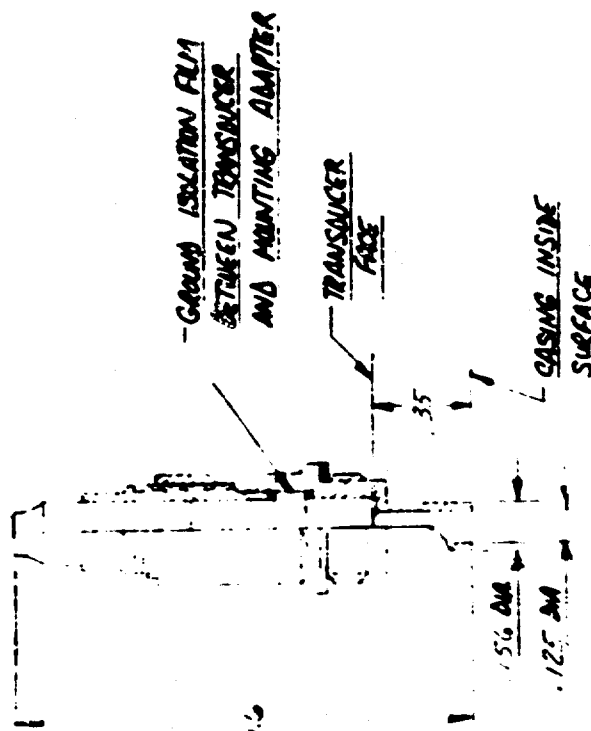
.125 DIA HARDLINE
CABLE CO-AXIAL
S, O₂ INSULATED

ELECTRICAL CONNECTOR
CO-AXIAL 10-92 JMF-2A

GROUND ISOLATION
FILM BETWEEN
TRANSDUCER AND
MOUNTING ADAPTER

.080 RECESS BETWEEN
TRANSDUCER FACE
AND CASING SURFACE

CENTRAL PRESSURE
TRANSDUCER
AXIAL LOCATION
NQ'S 1, 2, 3 & 4



HIGH TEMPERATURE
MONITOR PRESSURE
TRANSDUCER
AXIAL LOCATION
NO. 5

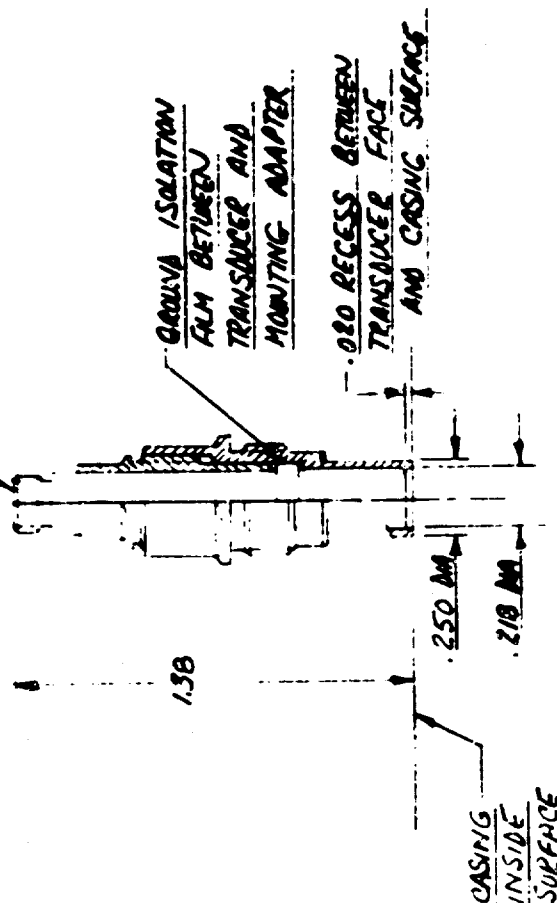


Figure 17 DETAIL OF PRESSURE TRANSDUCER CONFIGURATIONS

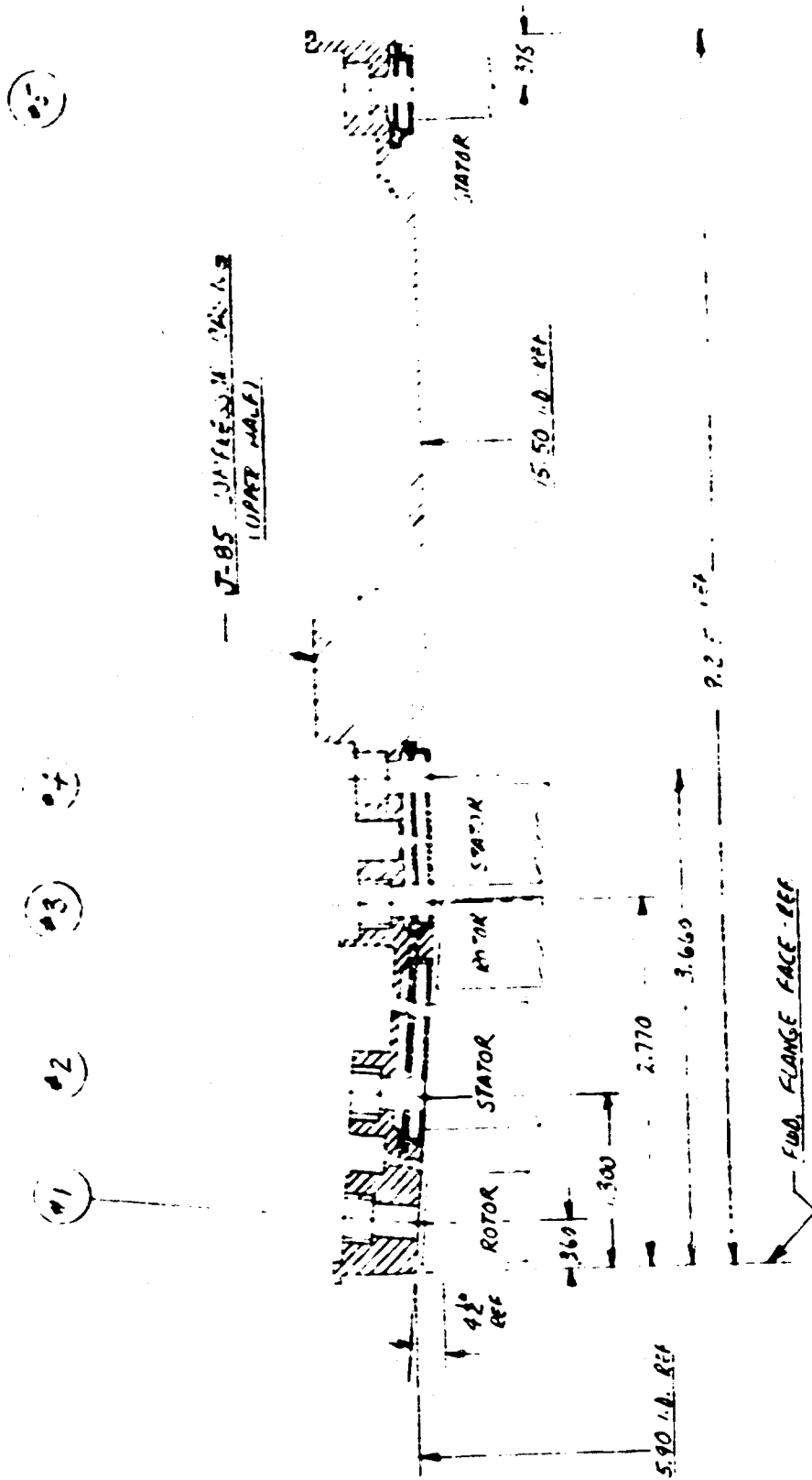
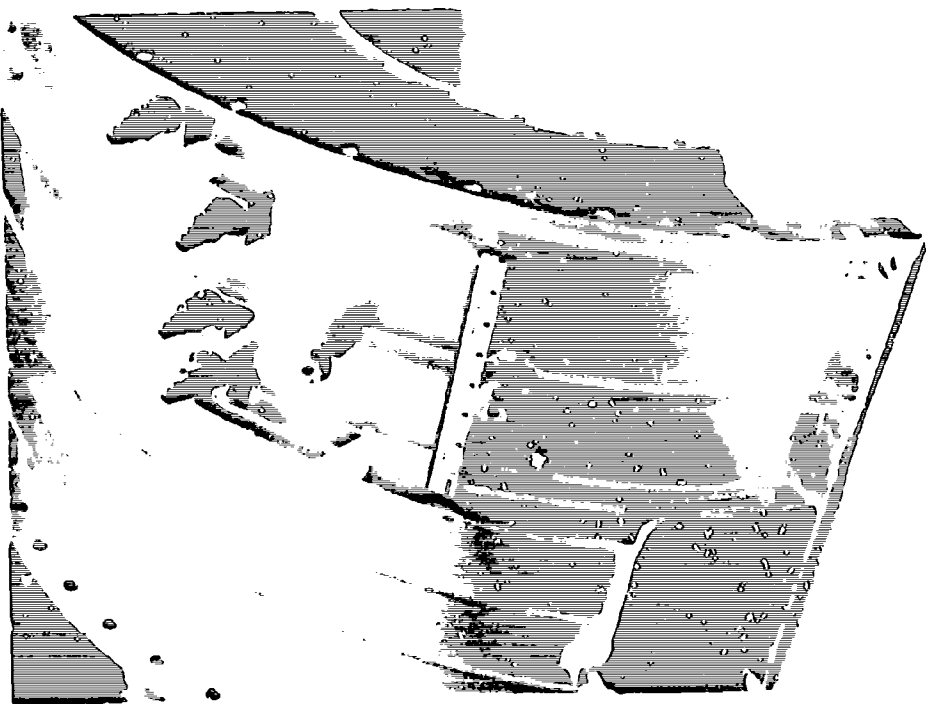
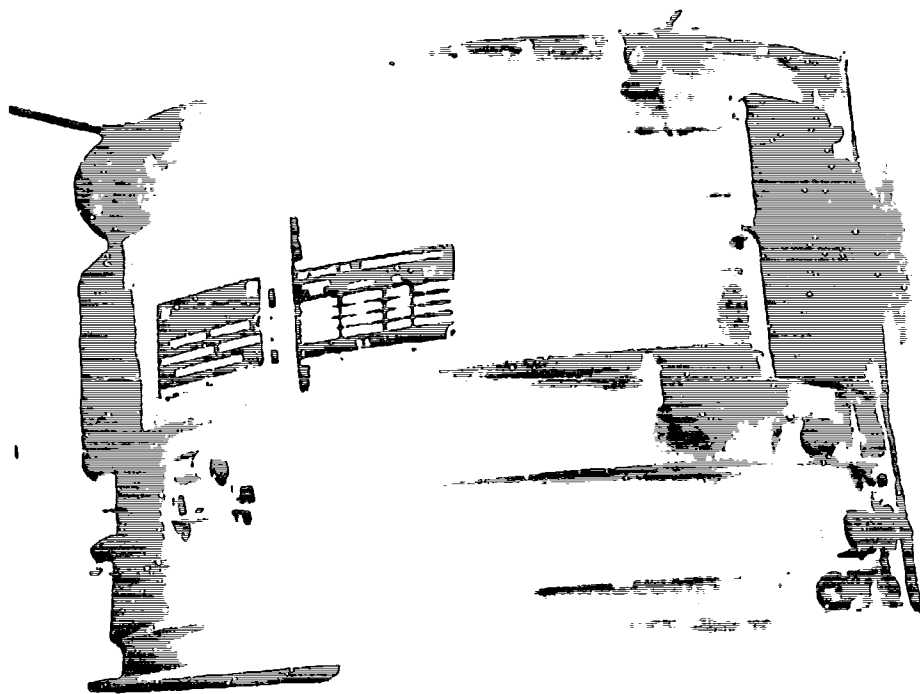


Figure 18 CROSS SECTION OF J-85 COMPRESSOR CASING SHOWING AXIAL LOCATIONS OF PRESSURE TRANSDUCERS

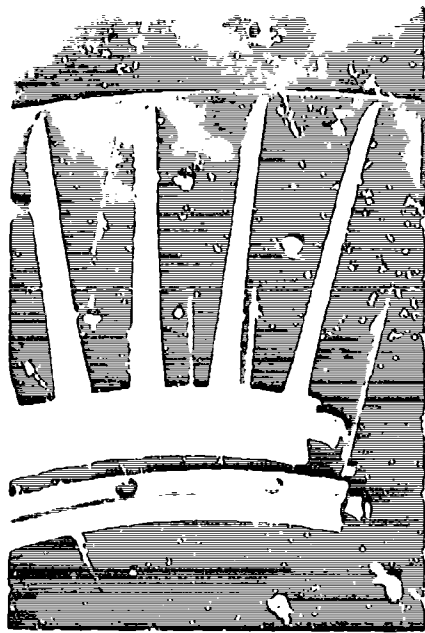


RIGHT SIDE

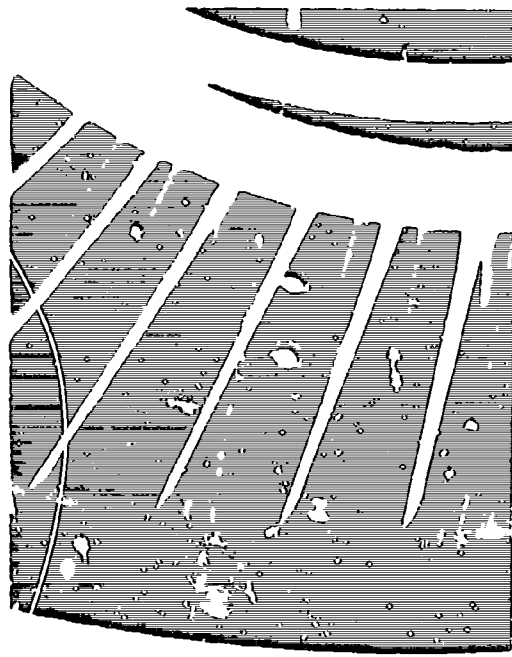


LEFT SIDE

Figure 19 PRESSURE TRANSDUCER INSTALLATIONS IN J85 COMPRESSOR
CASING VIEWED FROM OUTSIDE

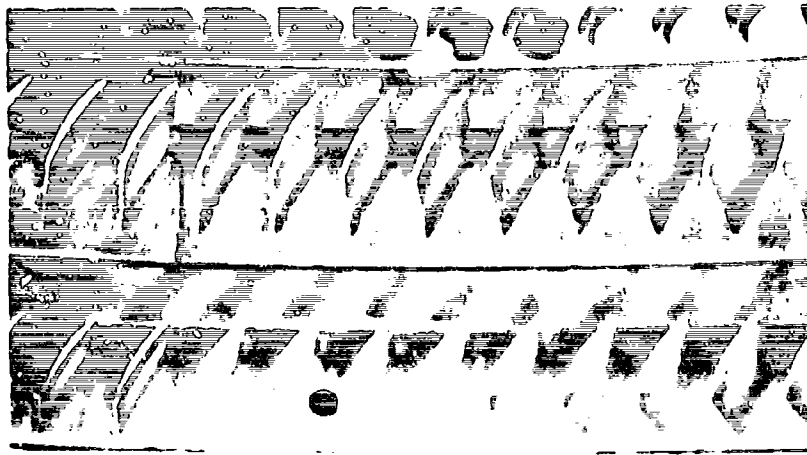


CONTROL TRANSDUCERS LEFT SIDE



CONTROL TRANSDUCERS RIGHT SIDE

Figure 20 CONTROL PRESSURE TRANSDUCER INSTALLATIONS IN J-85 COMPRESSOR CASING - VIEWED FROM INSIDE



LEFT SIDE INSTALLATION



UPPER INSTALLATION

Figure 21 MONITOR PRESSURE TRANSDUCER INSTALLATION IN J-85 COMPRESSOR CASING - VIEWED FROM INSIDE

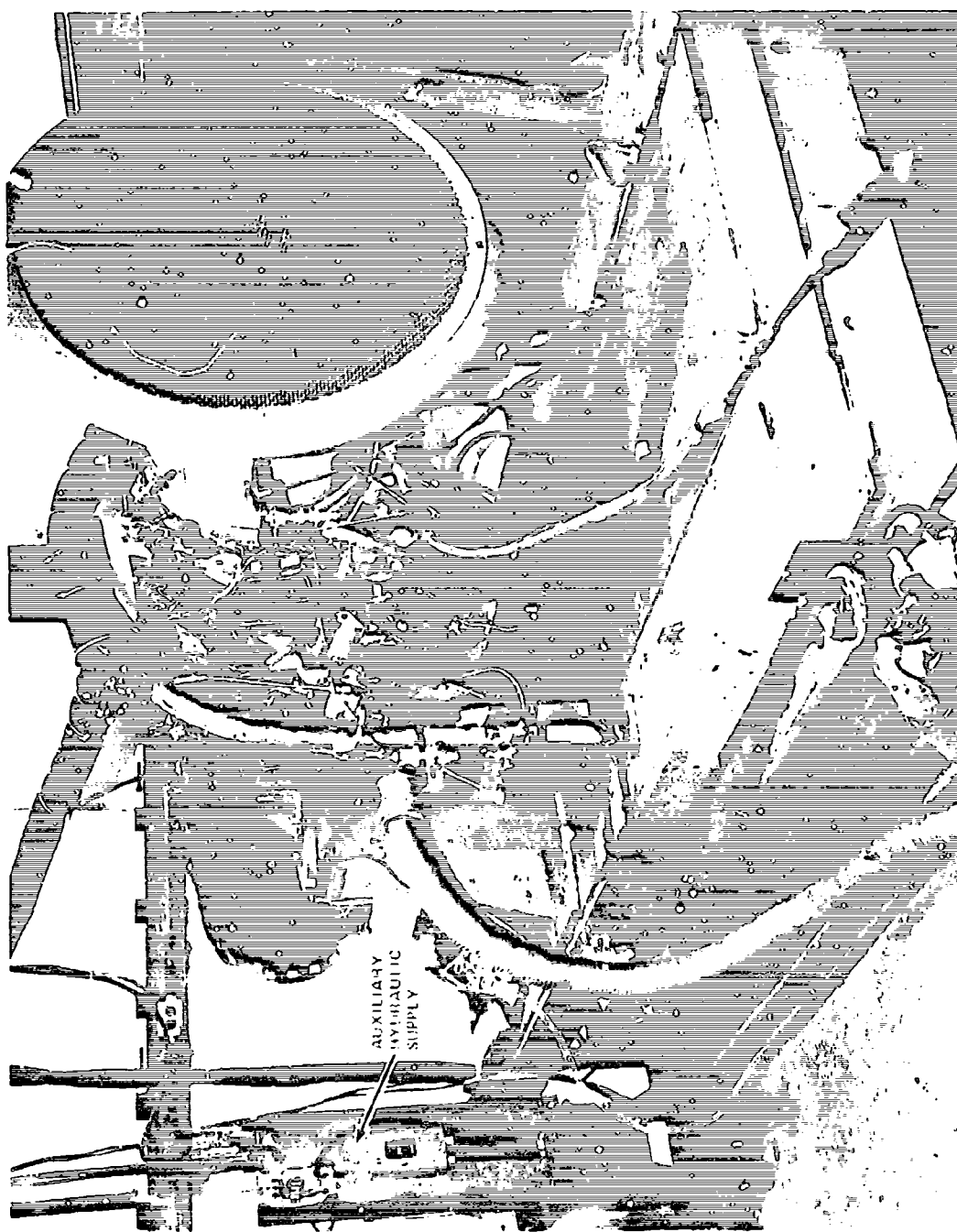


Figure 22 OVERALL VIEW OF J-85 ENGINE WITH ROTATING STALL CONTROL MECHANISM INSTALLED

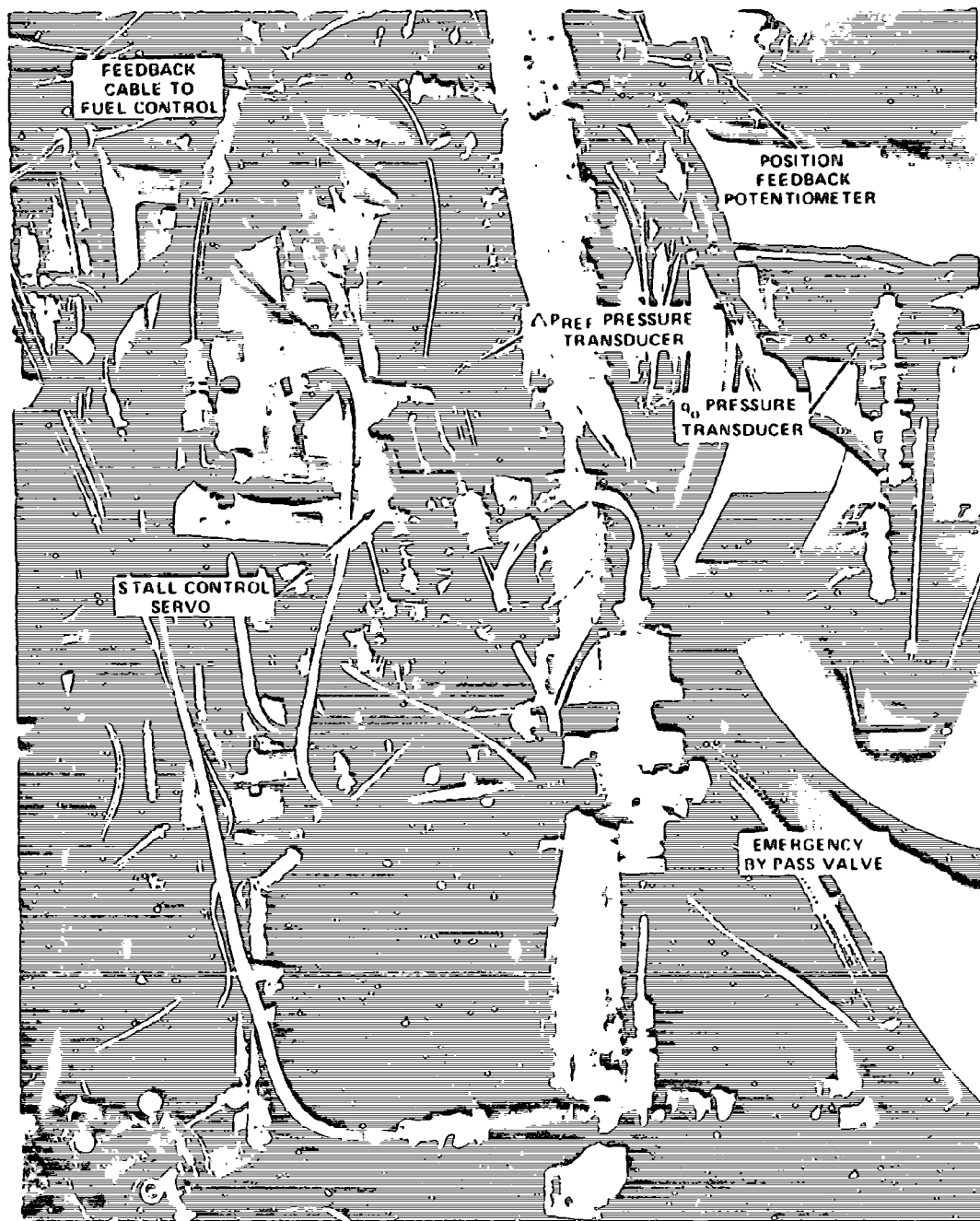


Figure 23 DETAILED VIEW OF STALL CONTROL MECHANISMS ON J 85 ENGINE

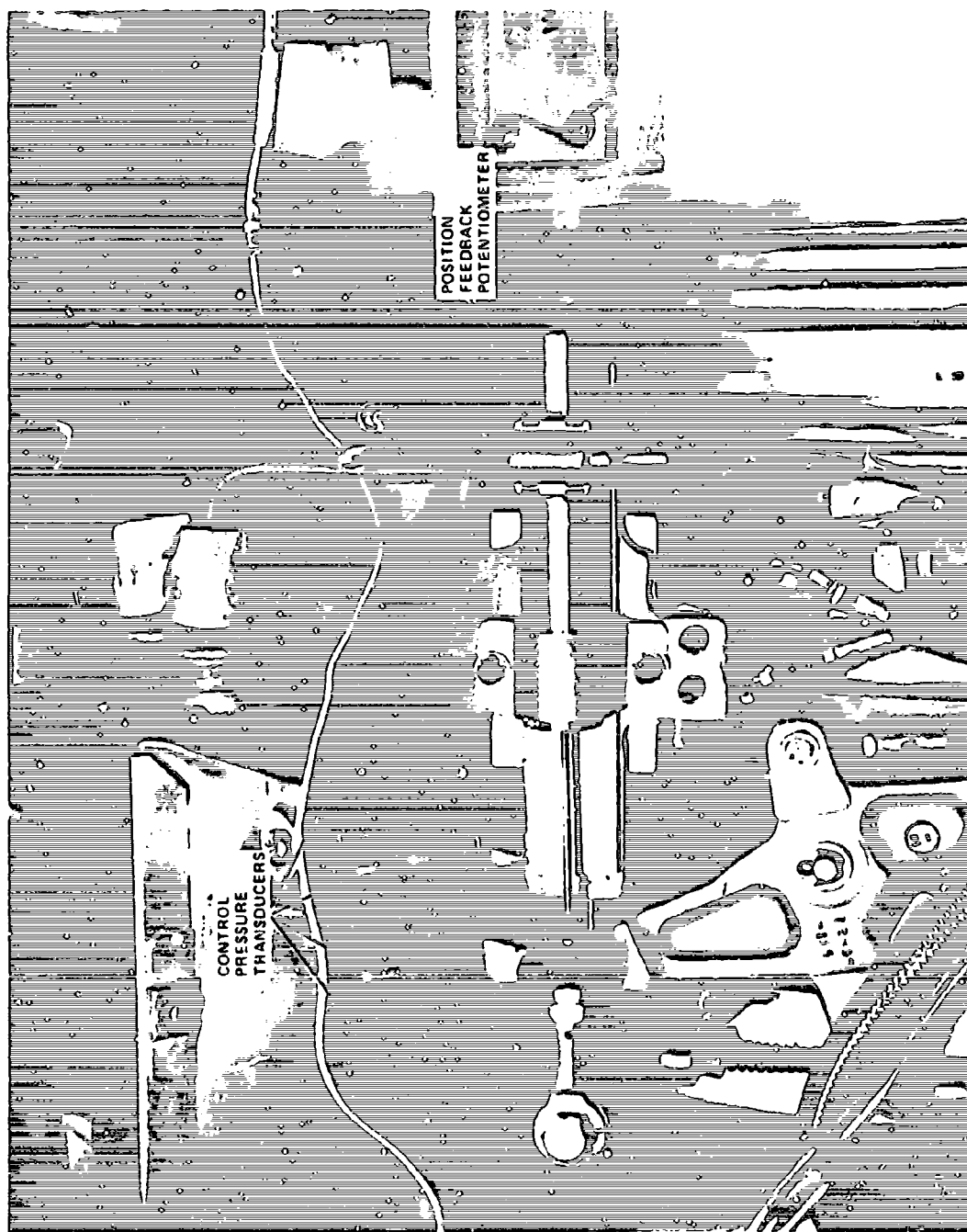


Figure 24 CLOSEUP VIEW OF POSITION FEEDBACK POTENTIOMETER AND SEVERAL PRESSURE TRANSDUCERS USED WITH STALL CONTROL SYSTEM ON J-85 ENGINE

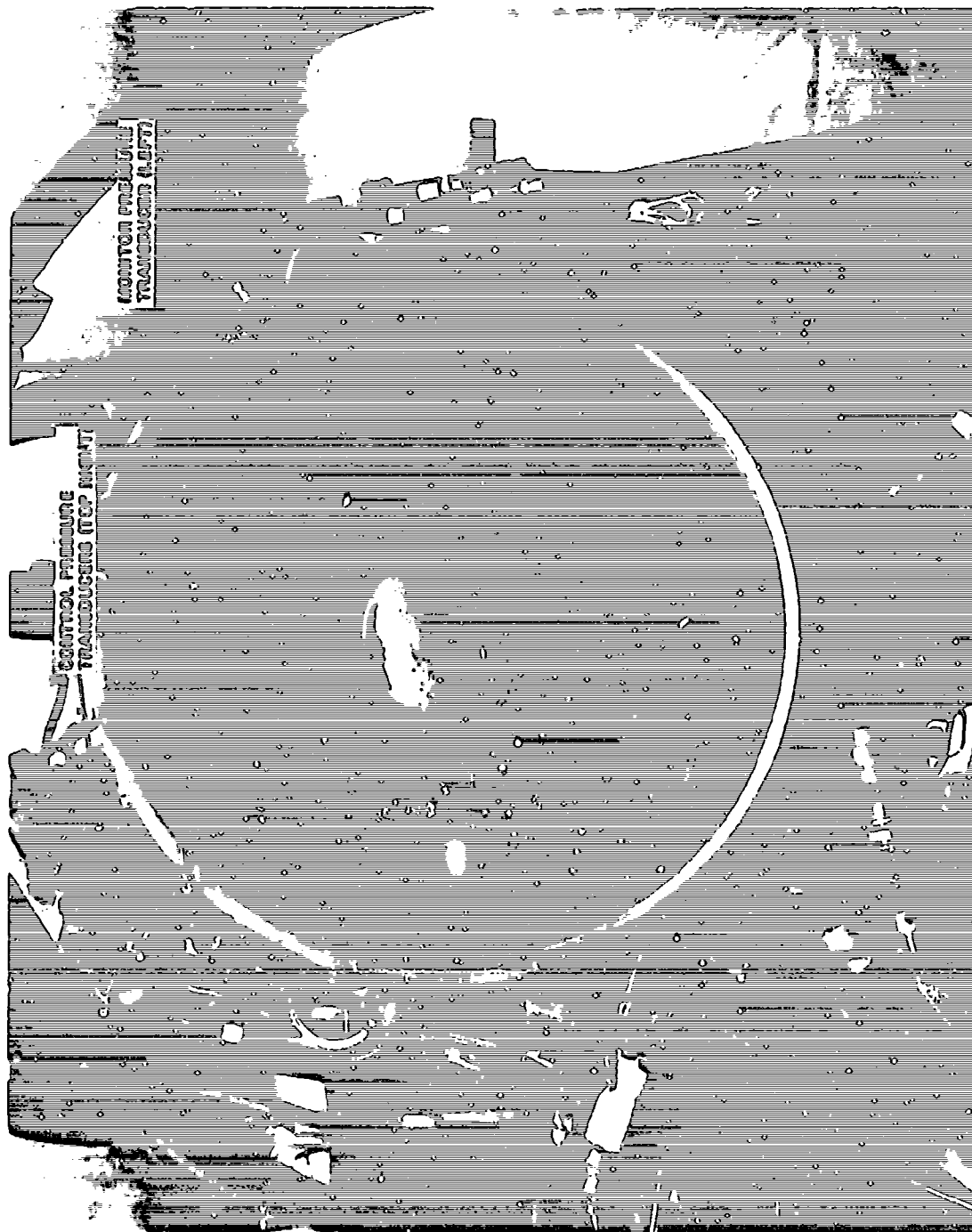
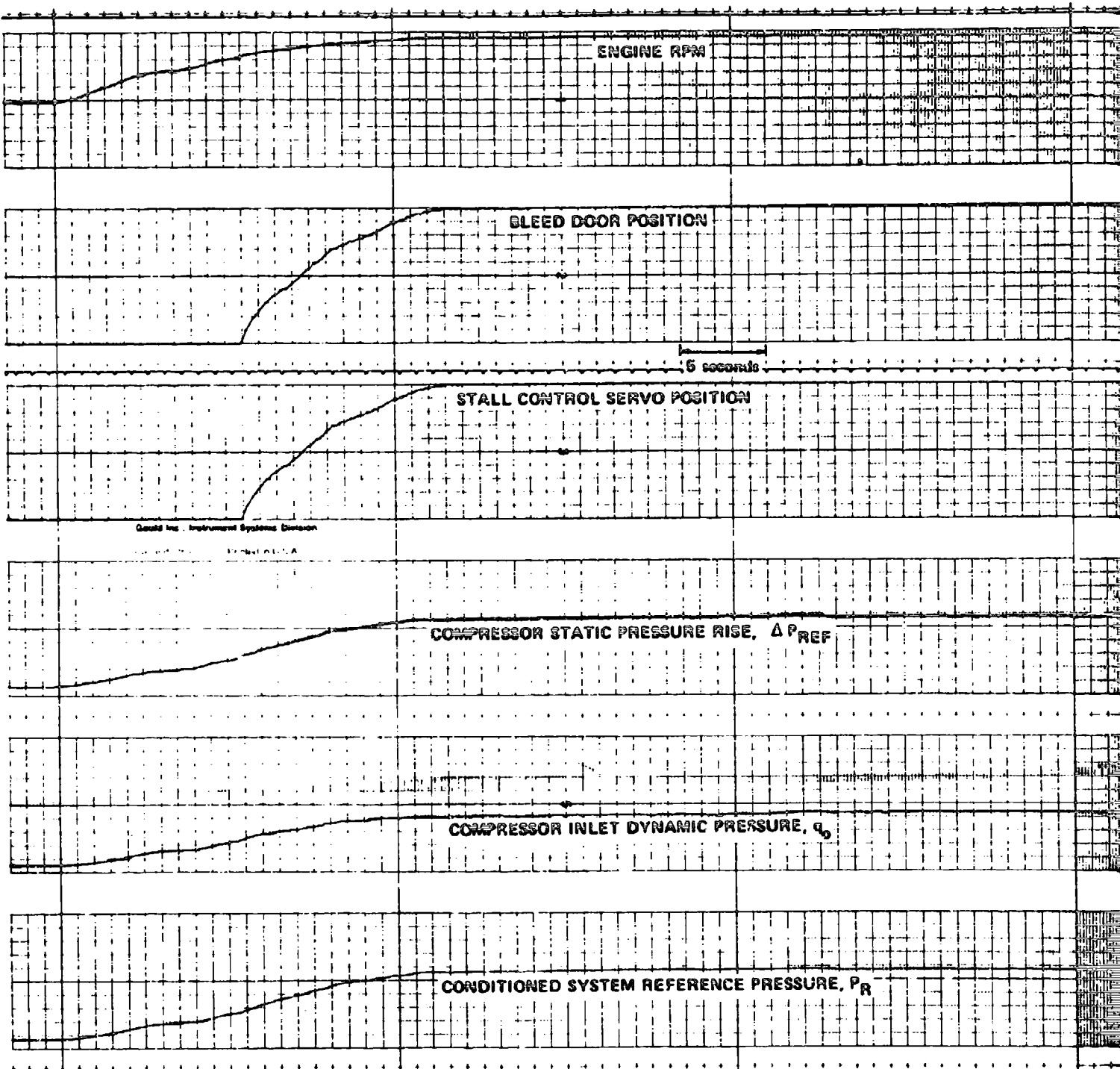


Figure 25 FRONT VIEW OF J-85 ENGINE WITH 180° DISTORTION SCREEN INSTALLED



DETECTOR LEVEL GAIN = 1.0, DETECTOR BIAS LEVEL = 0

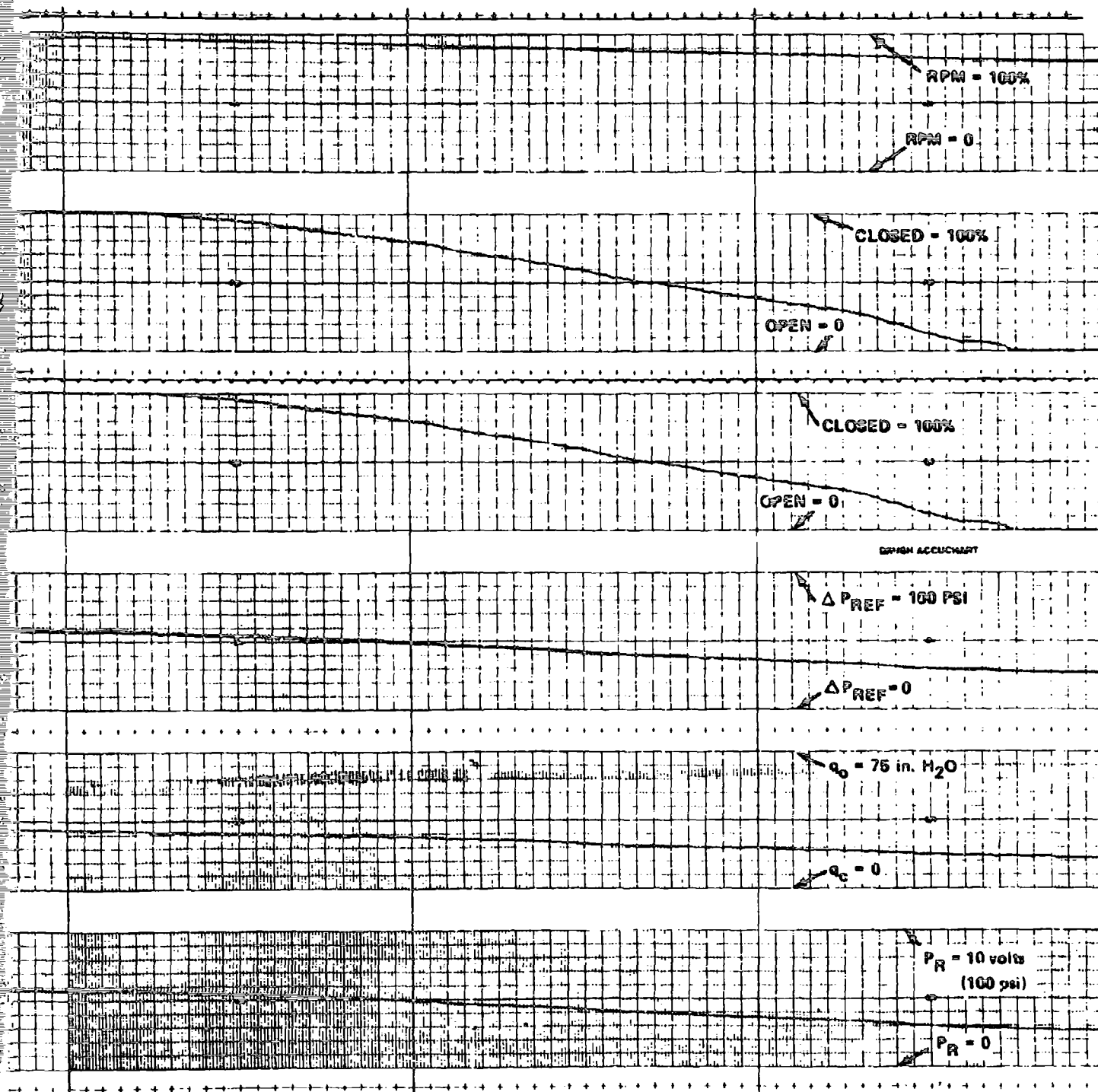


Figure 26 TRACKING PERFORMANCE OF STALL CONTROL SYSTEM ON J-85 ENGINE UNDER NORMAL ENGINE OPERATING CONDITIONS

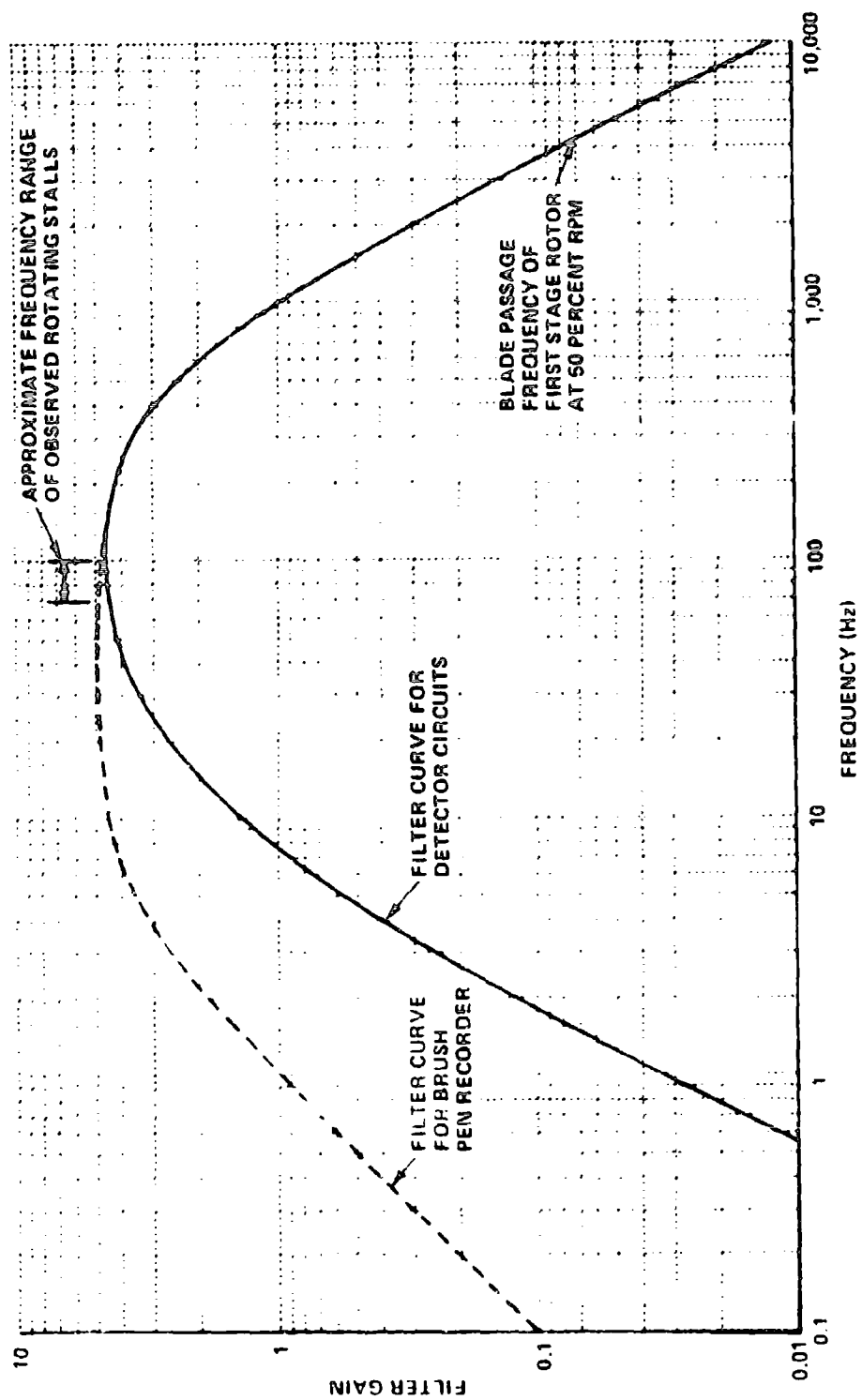


Figure 27 DETECTOR FILTER CHARACTERISTICS USED FOR STALL
CONTROL TESTS ON J85 ENGINE

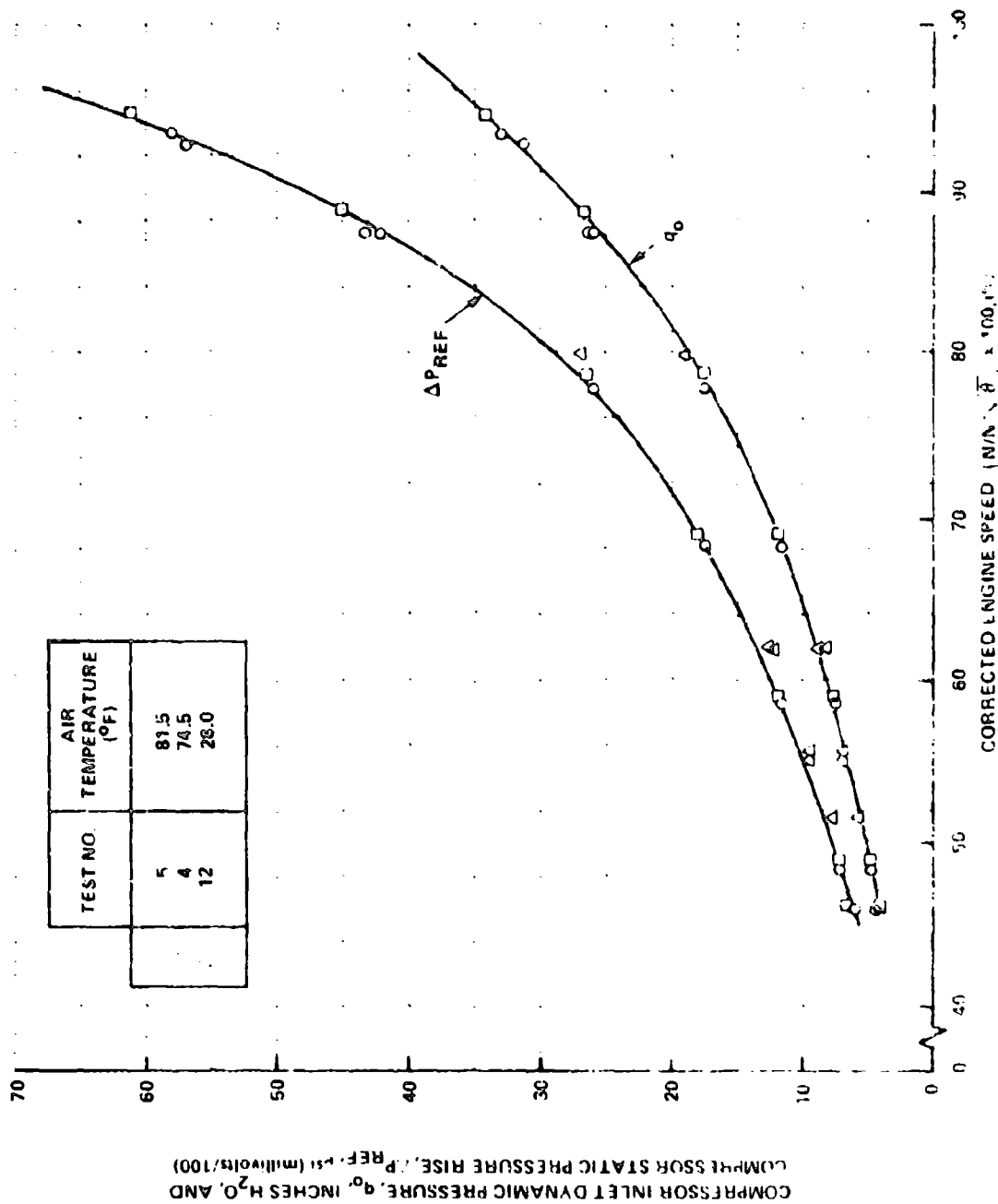


Figure 28. COMPRESSOR INLET DYNAMIC PRESSURE AND STATIC PRESSURE RISE
ON J15 ENGINE

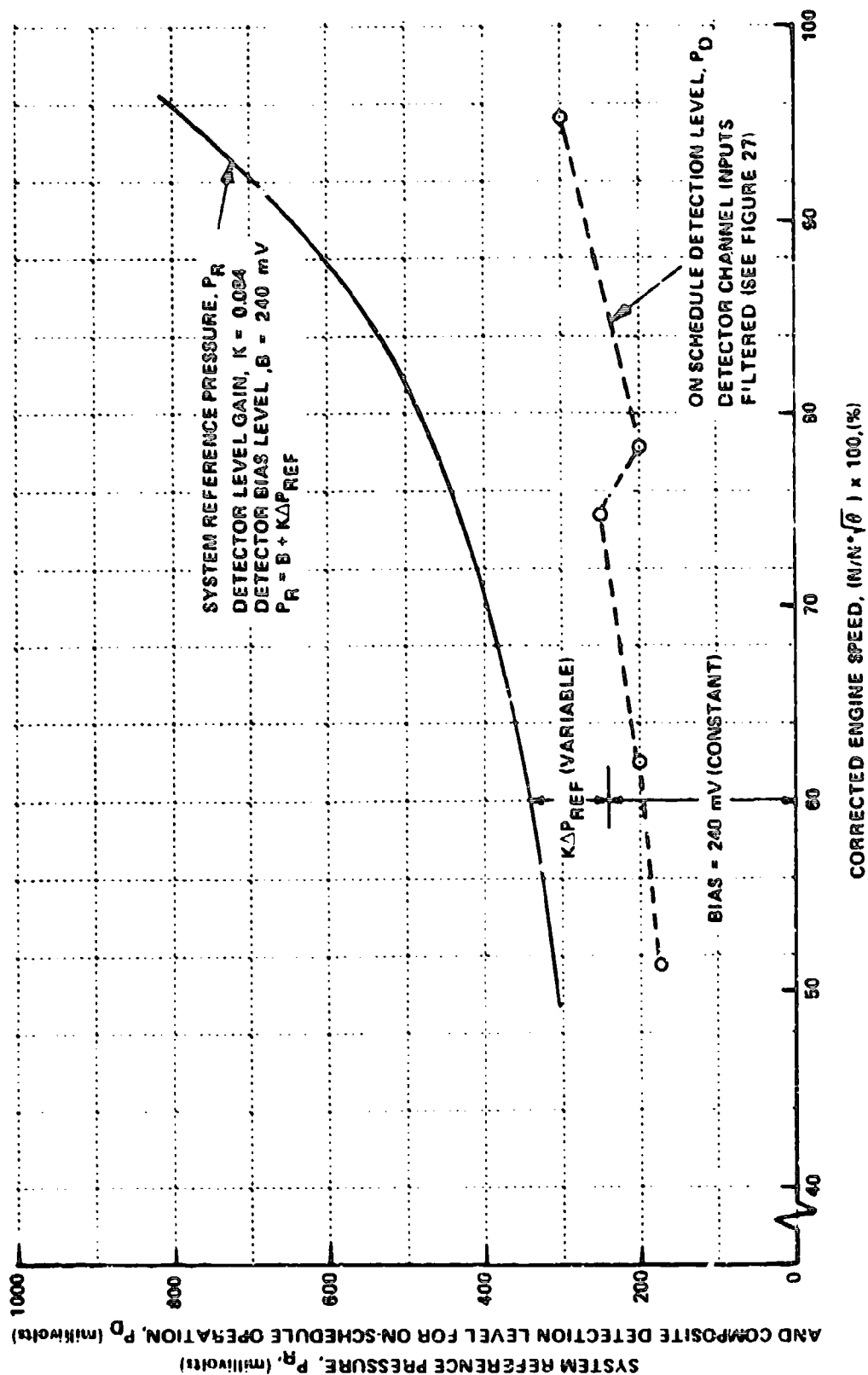
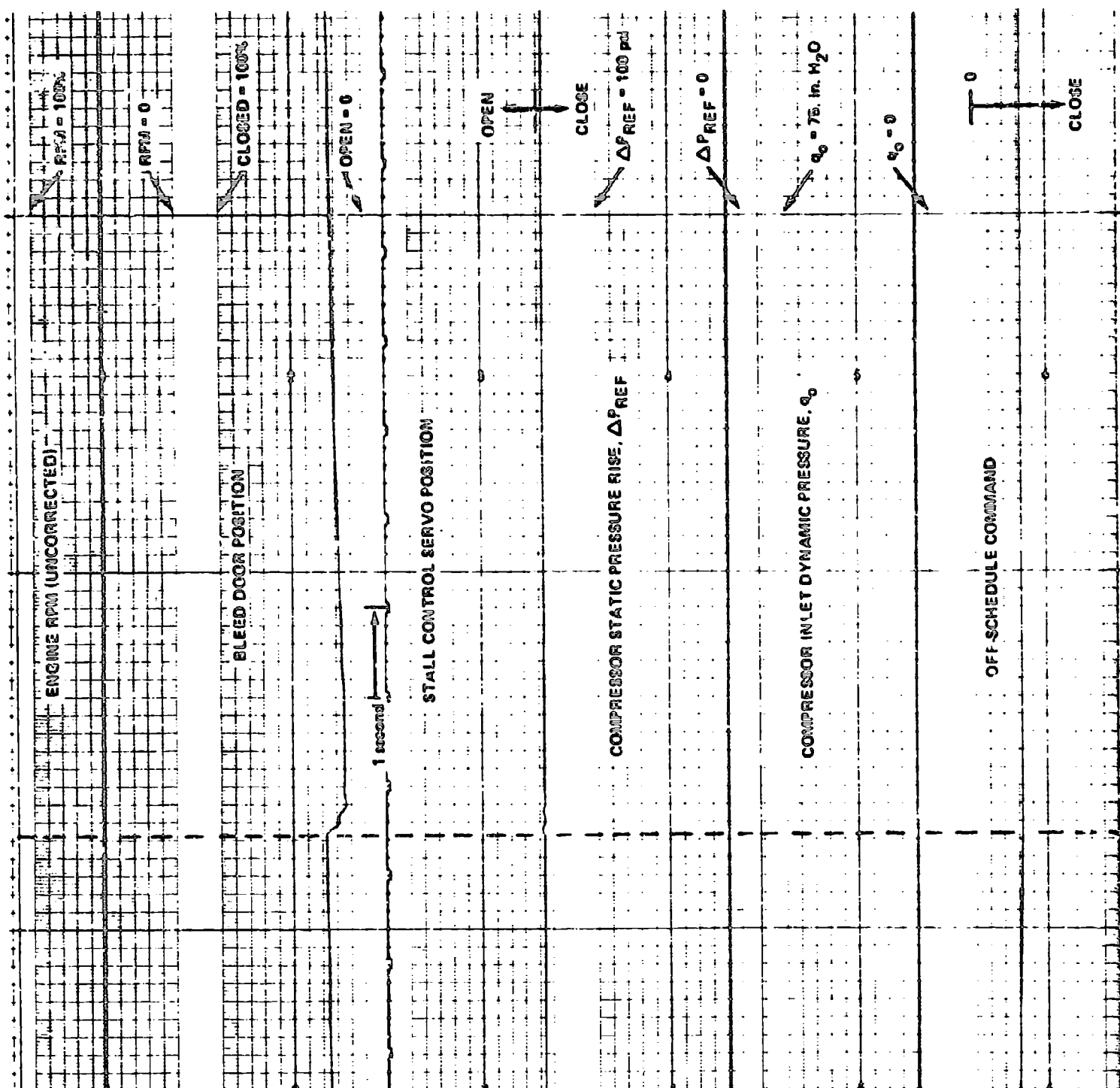
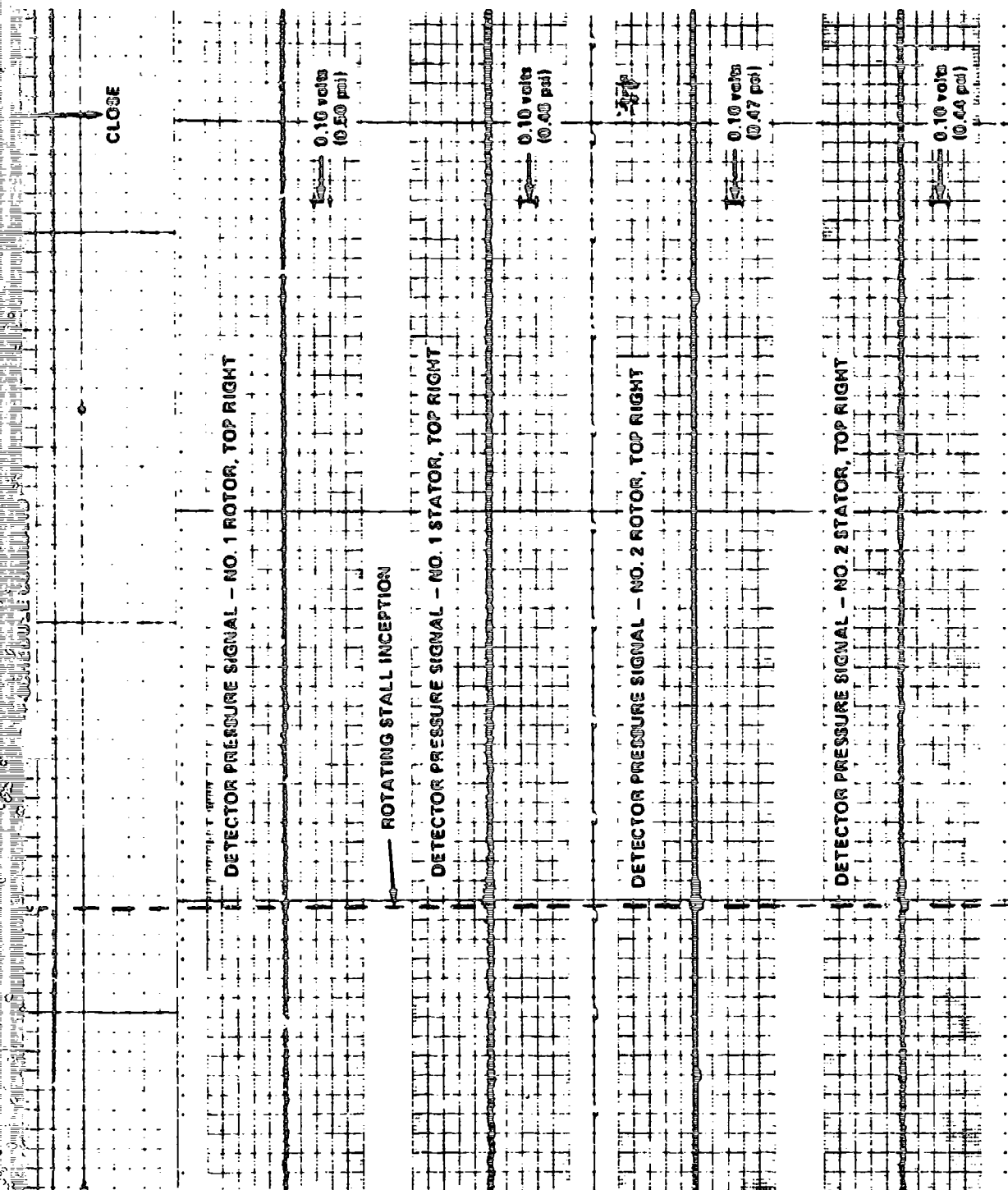


Figure 29 SYSTEM REFERENCE PRESSURE USED IN STALL CONTROL TESTS ON J85 ENGINE

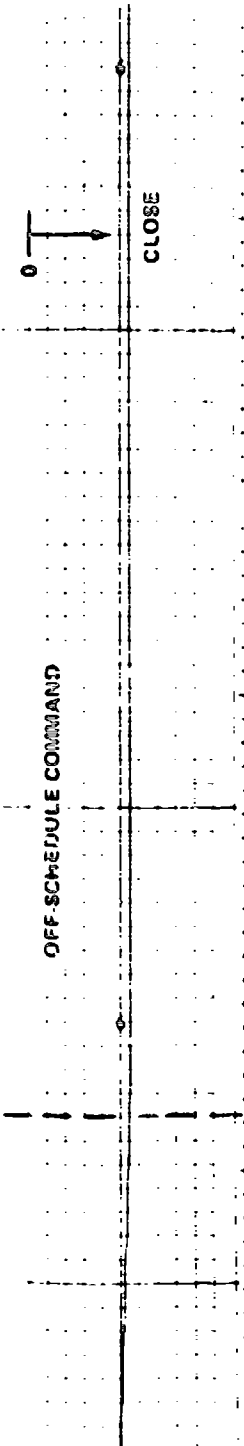
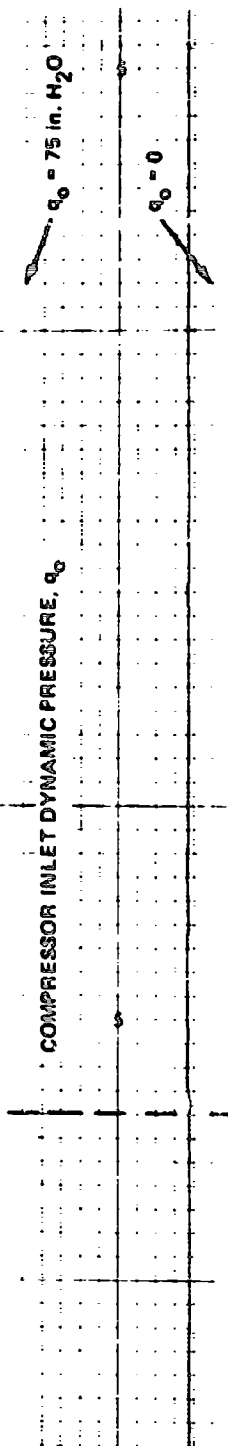
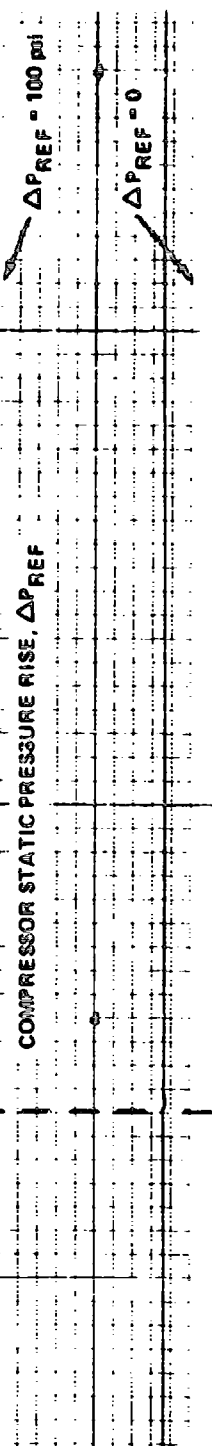
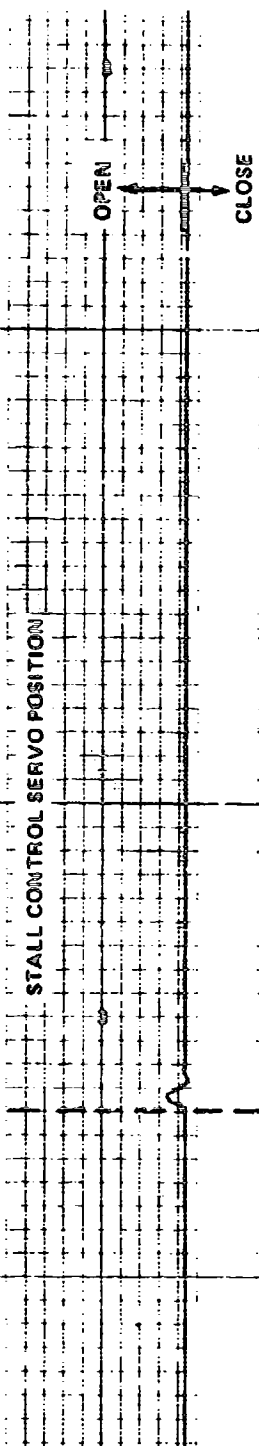
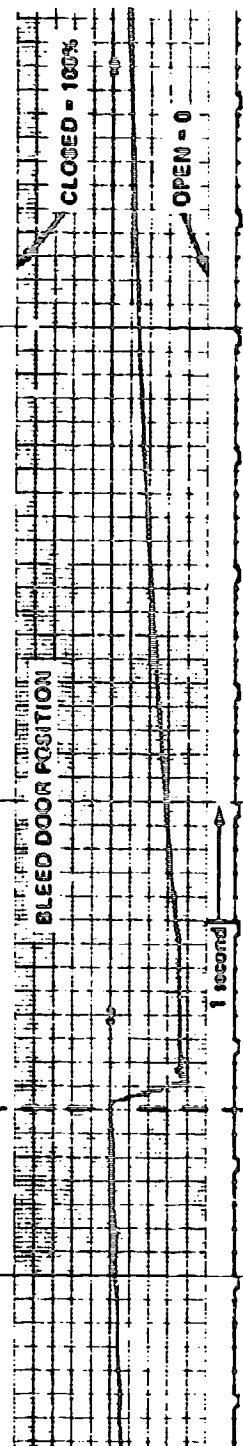
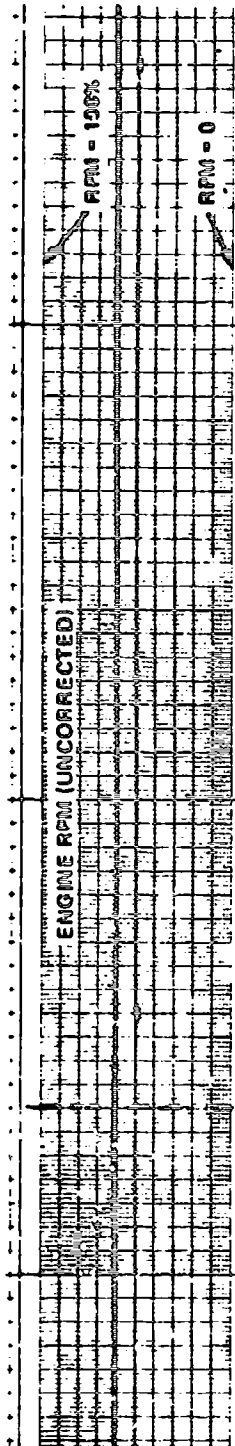


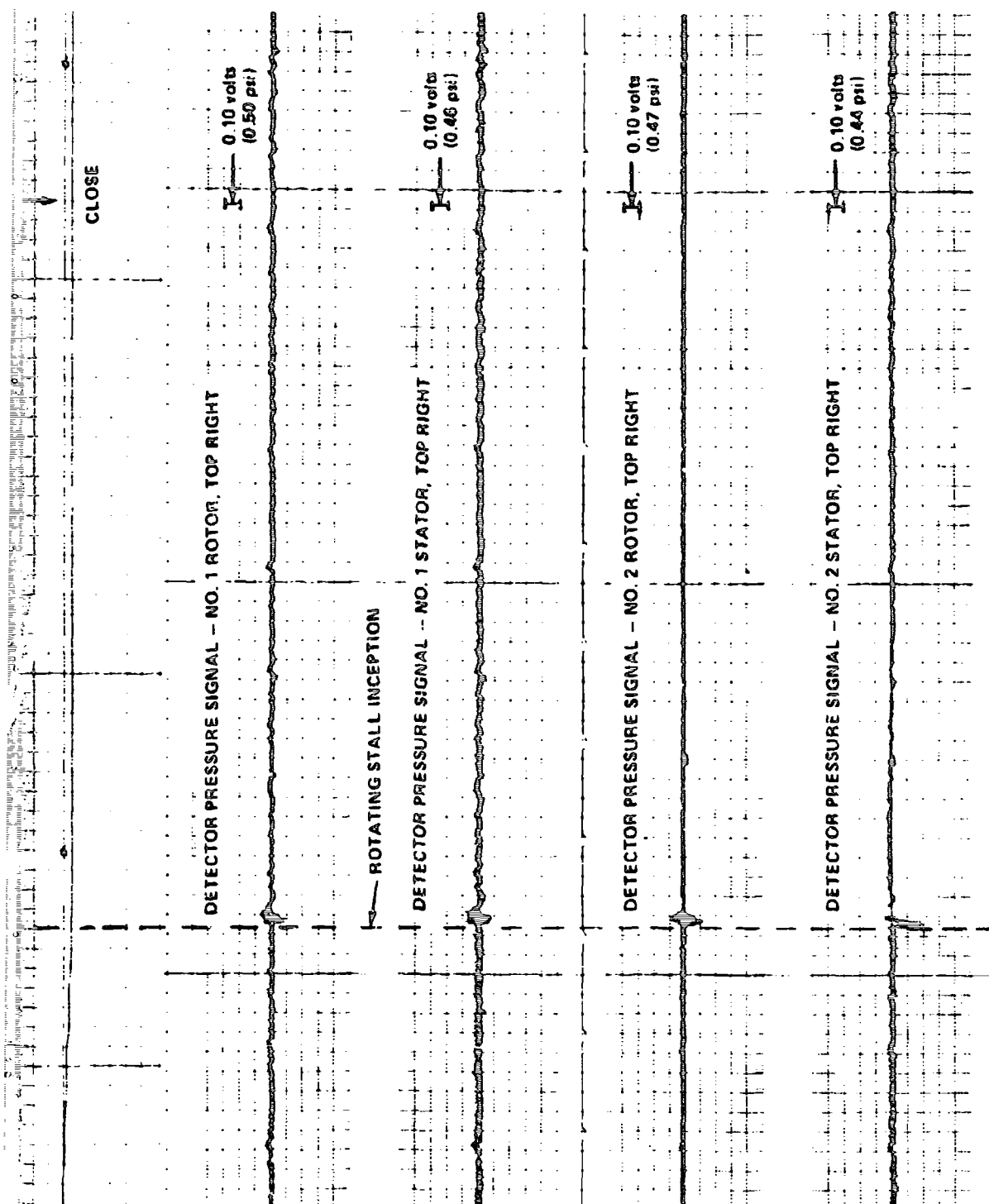


a) STALL TEST NO. 4(b) CORRECTED ENGINE SPEED, $(N/N_0 \sqrt{\rho/\rho_0}) = 52.5\%$

Figure 30

PERFORMANCE OF ROTATING STALL CONTROL ON J-85 ENGINE
COMPRESSOR STALLED BY CLOSING BLEED DOORS AT CONSTANT ENGINE SPEED
ENGINE TEST NO. 13: NO INLET DISTORTION





b) STALL TEST NO. 5, CORRECTED ENGINE SPEED, $(N/N \cdot \sqrt{\eta}) = 62.6\%$

Figure 30 (Cont.)

PERFORMANCE OF ROTATING STALL CONTROL ON J-85 ENGINE
COMPRESSOR STALLED BY CLOSING BLEED DOORS AT CONSTANT ENGINE SPEED
ENGINE TEST NO. 13: NO INLET DISTORTION

ENGINE RPM (UNCORRECTED)

RPM = 100%

RPM = 0

BLEED DOOR POSITION

CLOSED = 100%

OPEN = 0

1 second

STALL CONTROL SERVO POSITION

OPEN

CLOSE

COMPRESSOR STATIC PRESSURE RISE, ΔP_{REF}

$\Delta P_{REF} = 100$ psi

$\Delta P_{REF} = 0$

COMPRESSOR INLET DYNAMIC PRESSURE, q_0

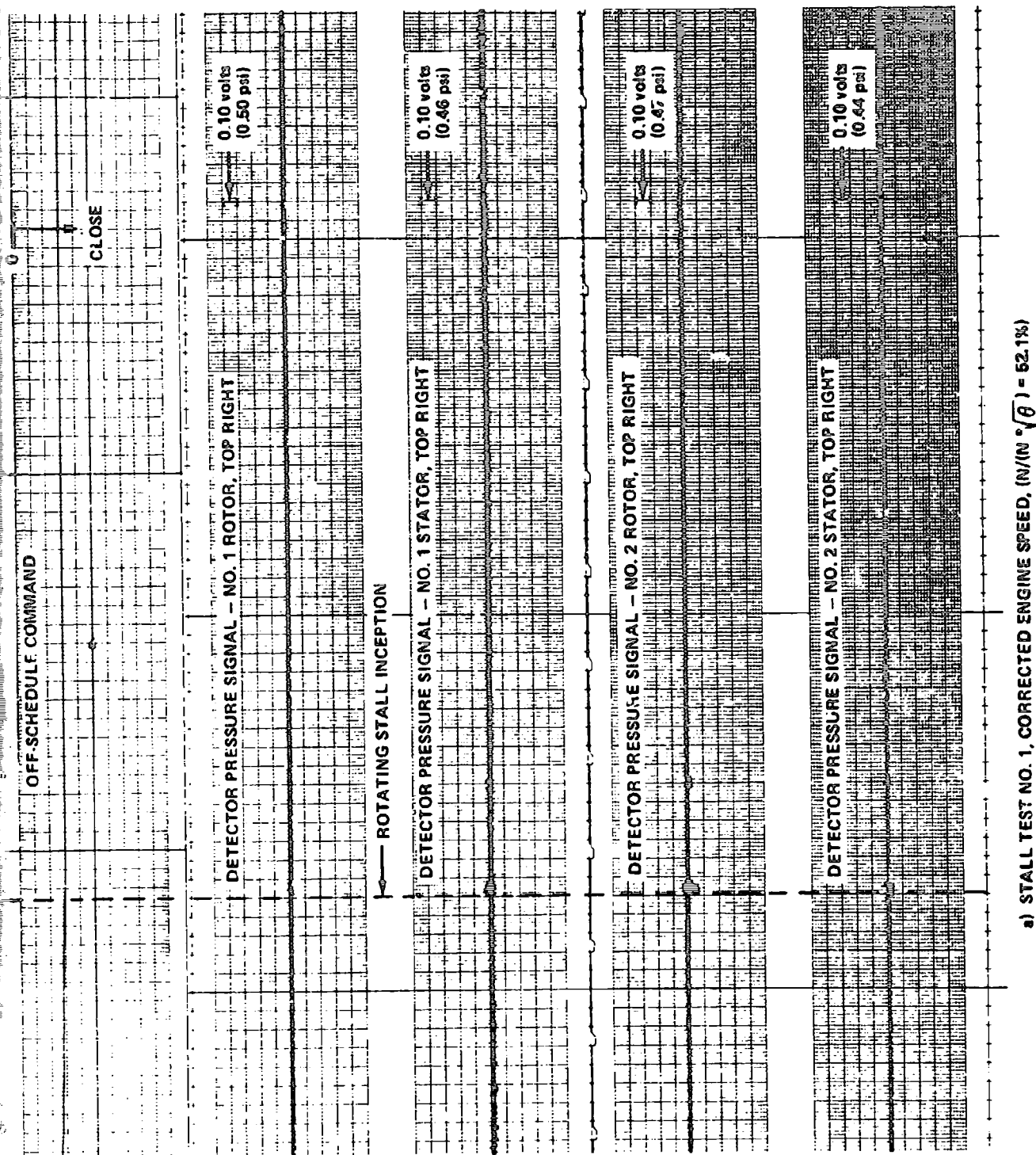
$q_0 = 75$ in. H_2O

$q_0 = 0$

OFF-SCHEDULE COMMAND

0

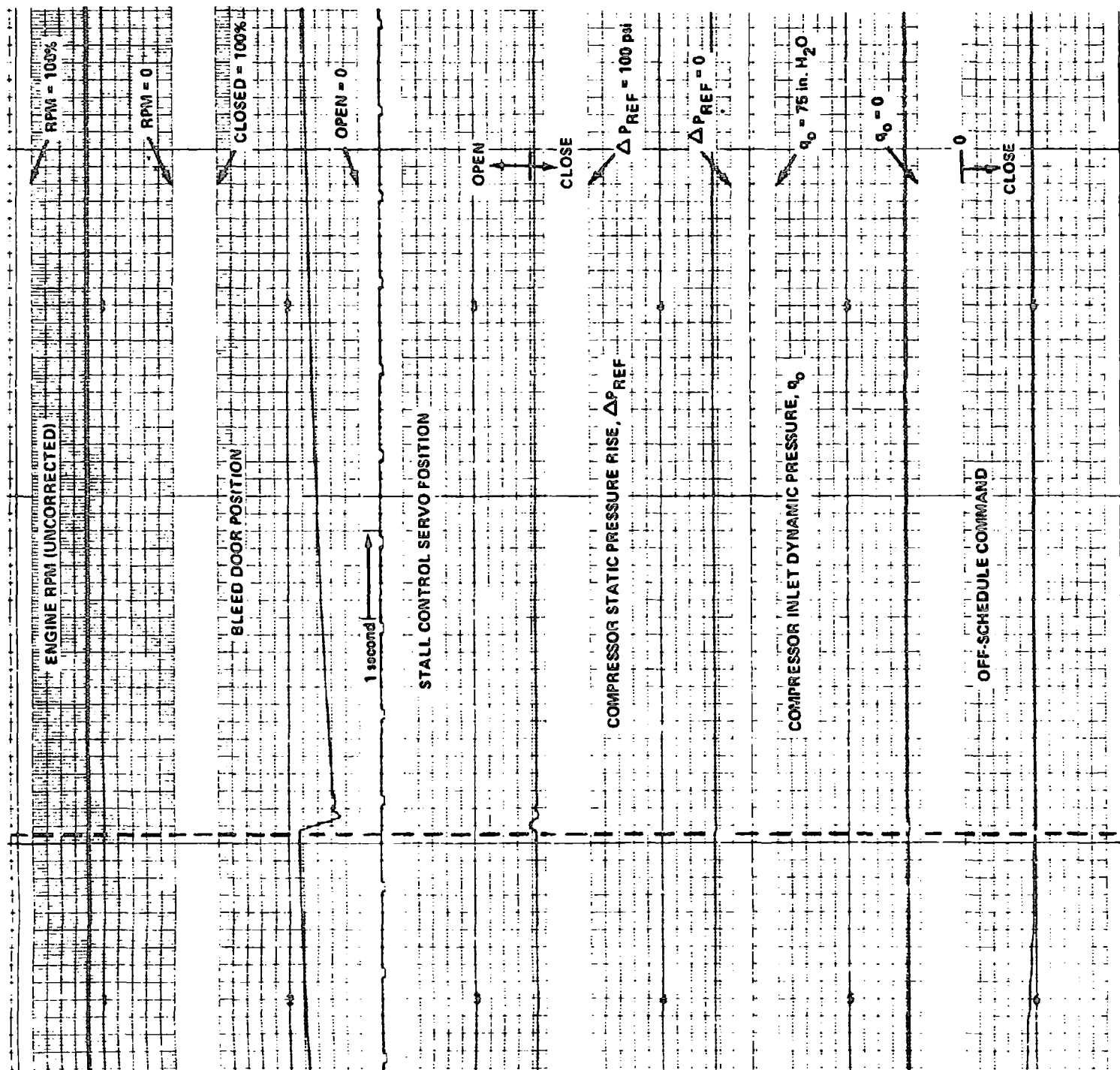
CLOSE

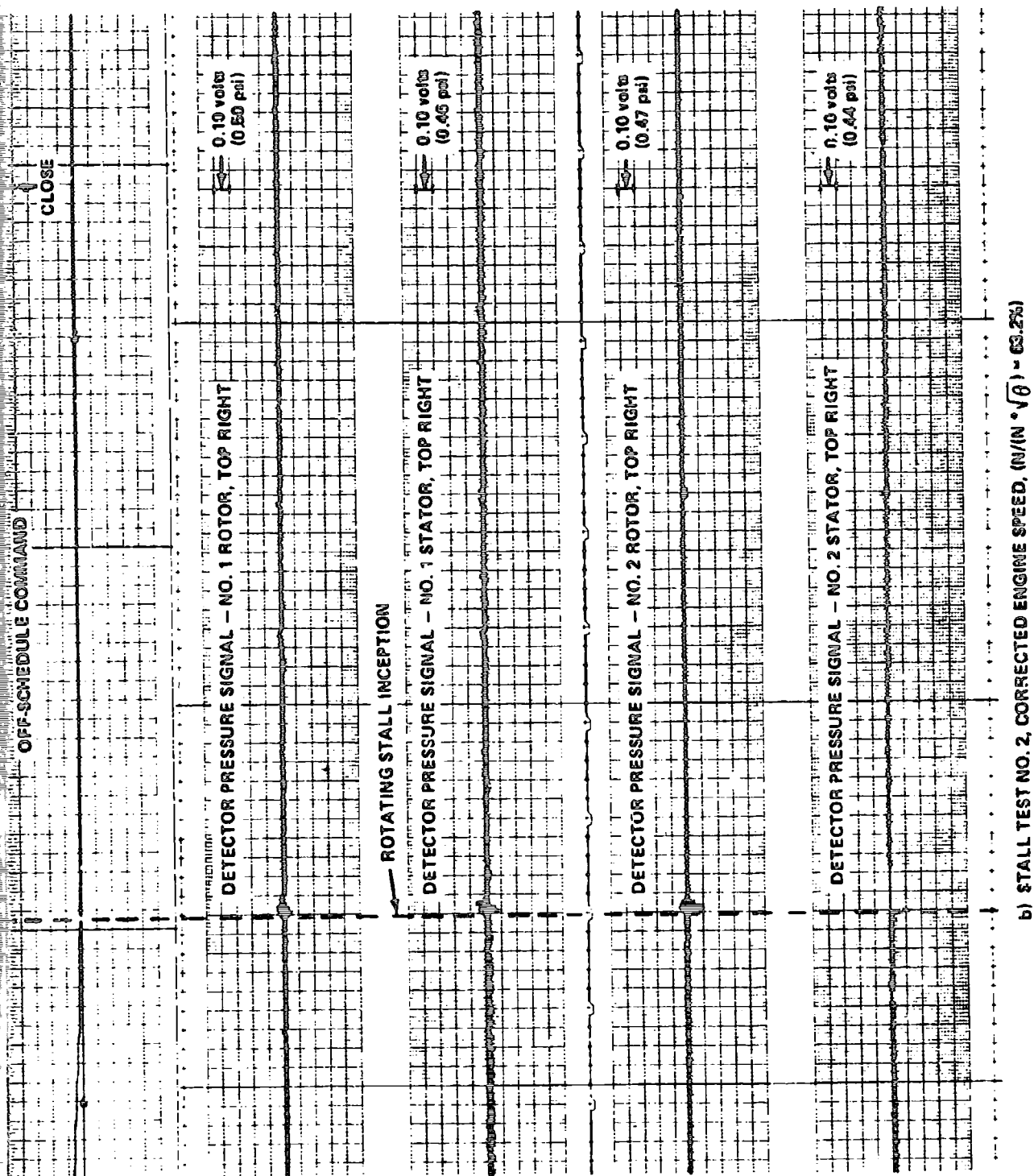


a) STALL TEST NO. 1, CORRECTED ENGINE SPEED, $(N/N^* \sqrt{\theta}) = 52.1\%$

PERFORMANCE OF ROTATING STALL CONTROL ON J-85 ENGINE
COMPRESSOR STALLED BY CLOSING BLEED DOORS AT CONSTANT ENGINE SPEED
ENGINE TEST NO. 14: 180° CIRCUMFERENTIAL INLET DISTORTION

Figure 31





b) STALL TEST NO. 2, CORRECTED ENGINE SPEED, $(N/N \cdot \sqrt{\theta}) = 63.2\%$

Figure 31 (Cont.)

PERFORMANCE OF ROTATING STALL CONTROL ON J-85 ENGINE
COMPRESSOR STALLED BY CLOSING BLEED DOORS AT CONSTANT ENGINE SPEED
ENGINE TEST NO. 14: 180° CIRCUMFERENTIAL INLET DISTORTION

ENGINE RPM (UNCORRECTED)

RPM = 100%

RPM = 0

BLEED DOOR POSITION

CLOSED = 100%

OPEN = 0

1 second

STALL CONTROL SERVO POSITION

OPEN

CLOSE

COMPRESSOR STATIC PRESSURE RISE, ΔP_{REF}

$\Delta P_{REF} = 100 \text{ psi}$

$\Delta P_{REF} = 0$

COMPRESSOR INLET DYNAMIC PRESSURE, q_0

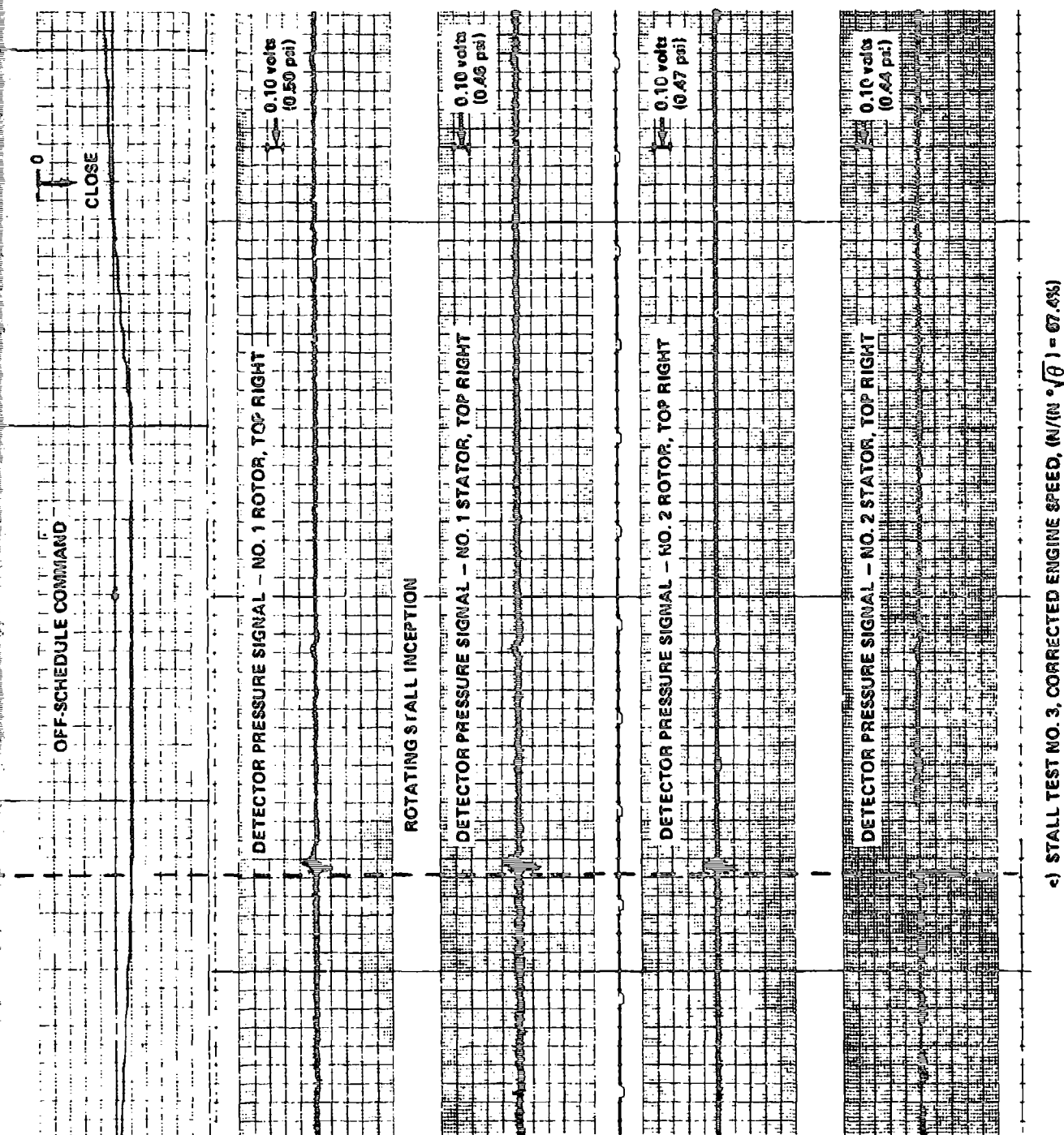
$q_0 = 75 \text{ in. H}_2\text{O}$

$q_0 = 0$

OFF-SCHEDULE COMMAND

T^0

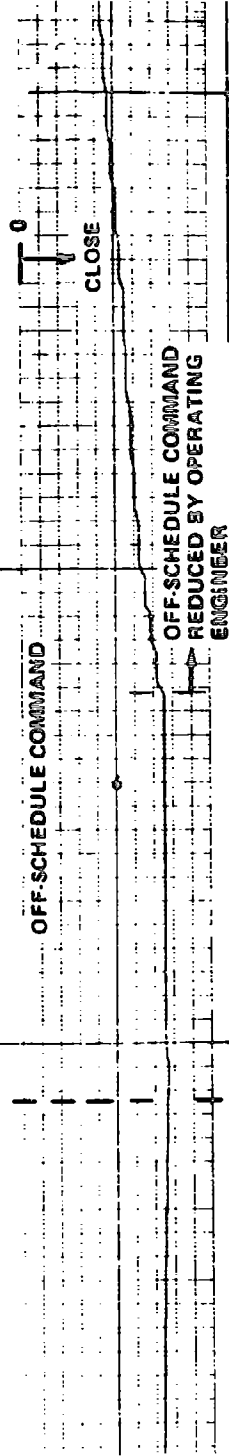
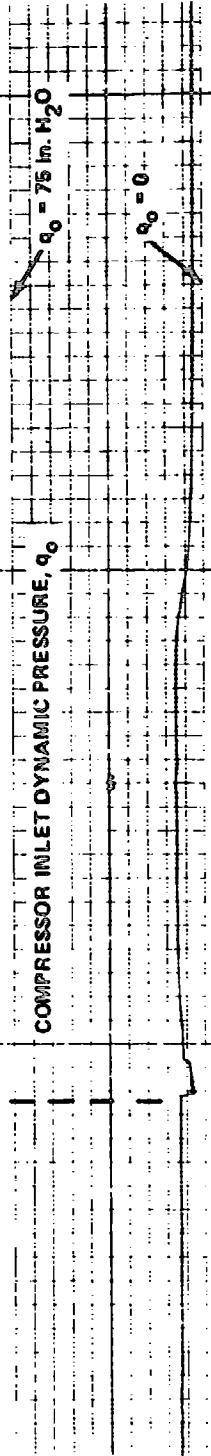
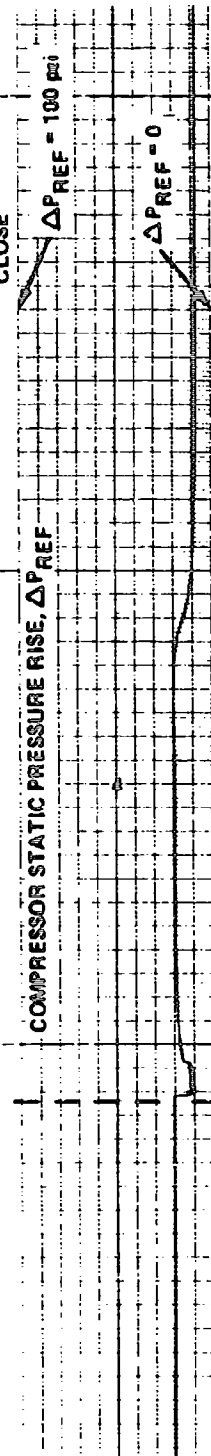
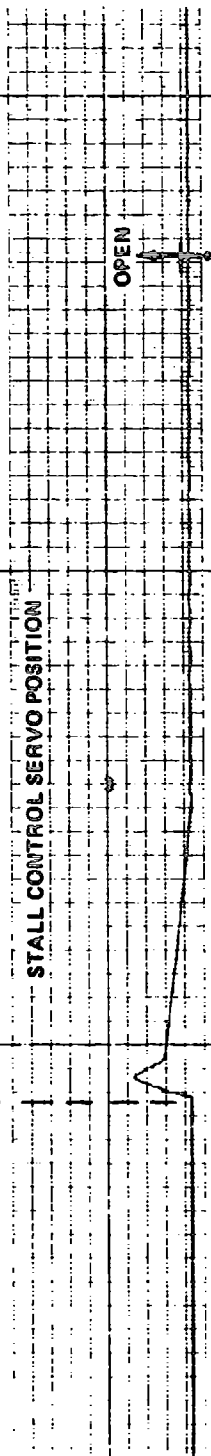
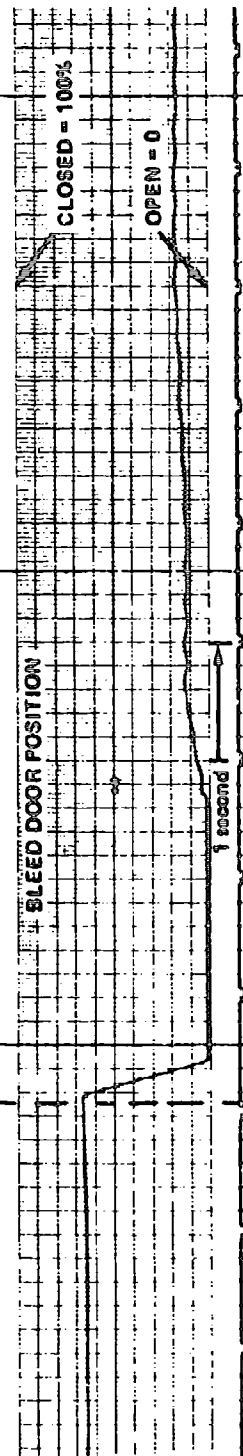
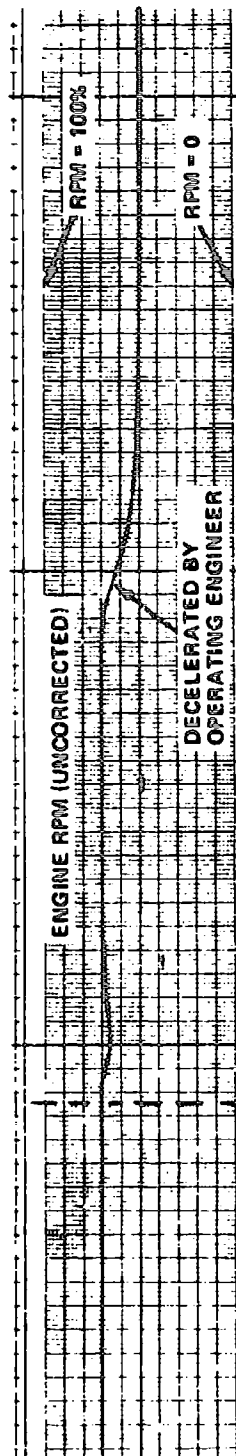
CLOSE

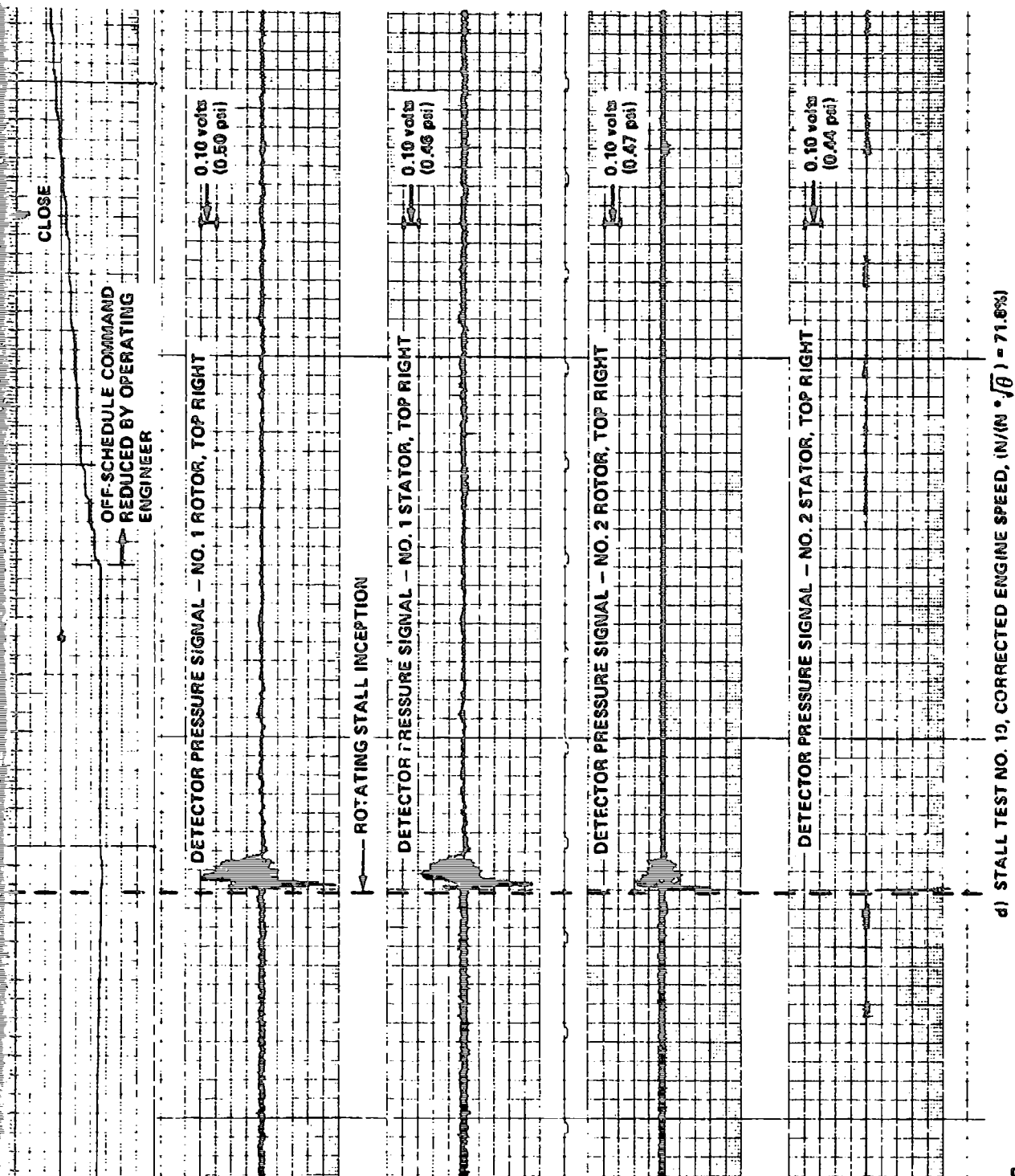


c) STALL TEST NO. 3, CORRECTED ENGINE SPEED, $(N/N \cdot \sqrt{\theta}) = 67.4\%$

Figure 31 (Cont.)

PERFORMANCE OF ROTATING STALL CONTROL ON J-85 ENGINE
COMPRESSOR STALLED BY CLOSING BLEED DOORS AT CONSTANT ENGINE SPEED
ENGINE TEST NO. 14: 180° CIRCUMFERENTIAL INLET DISTORTION

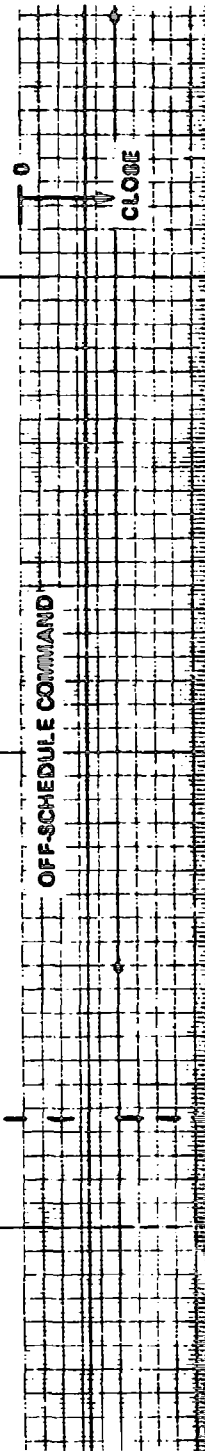
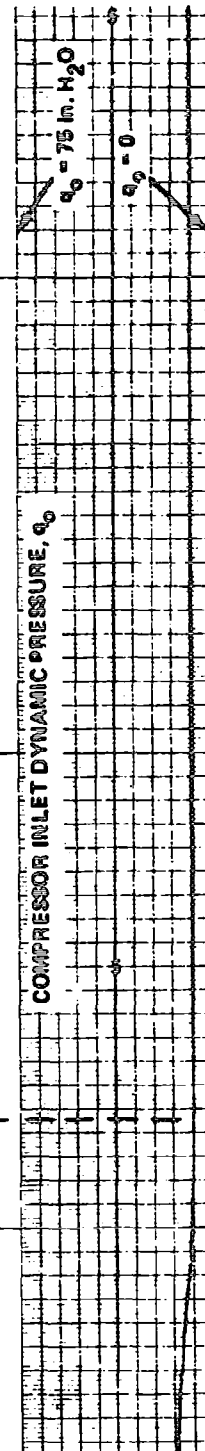
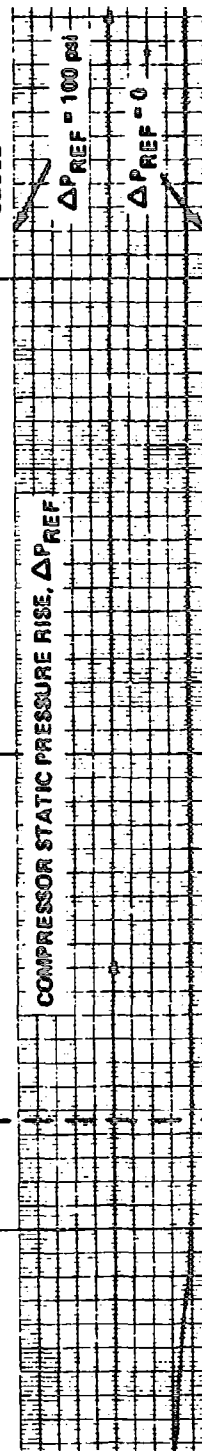
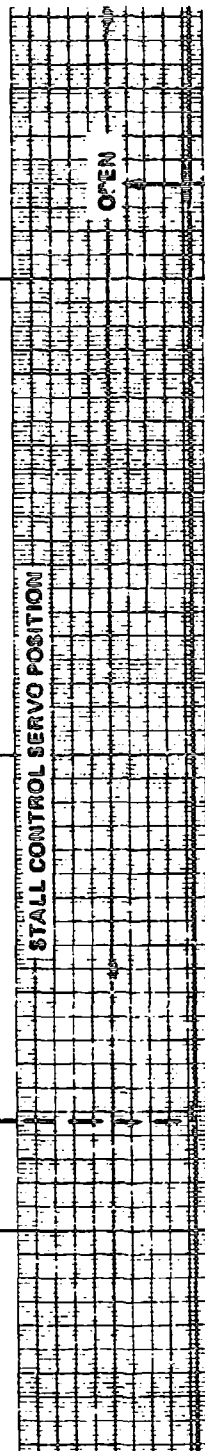
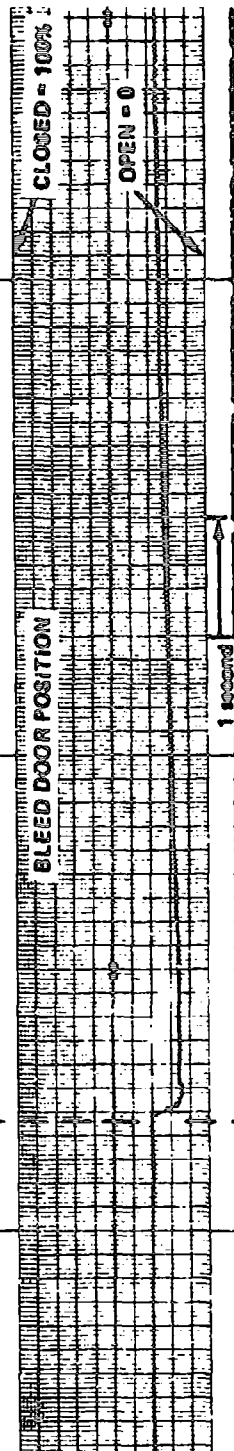
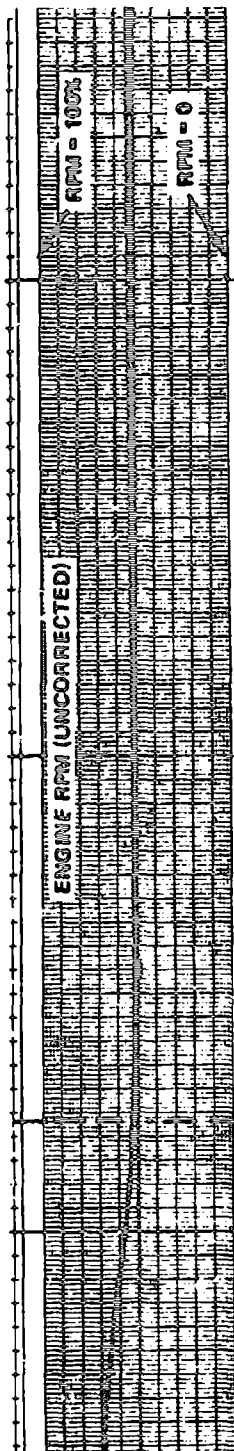


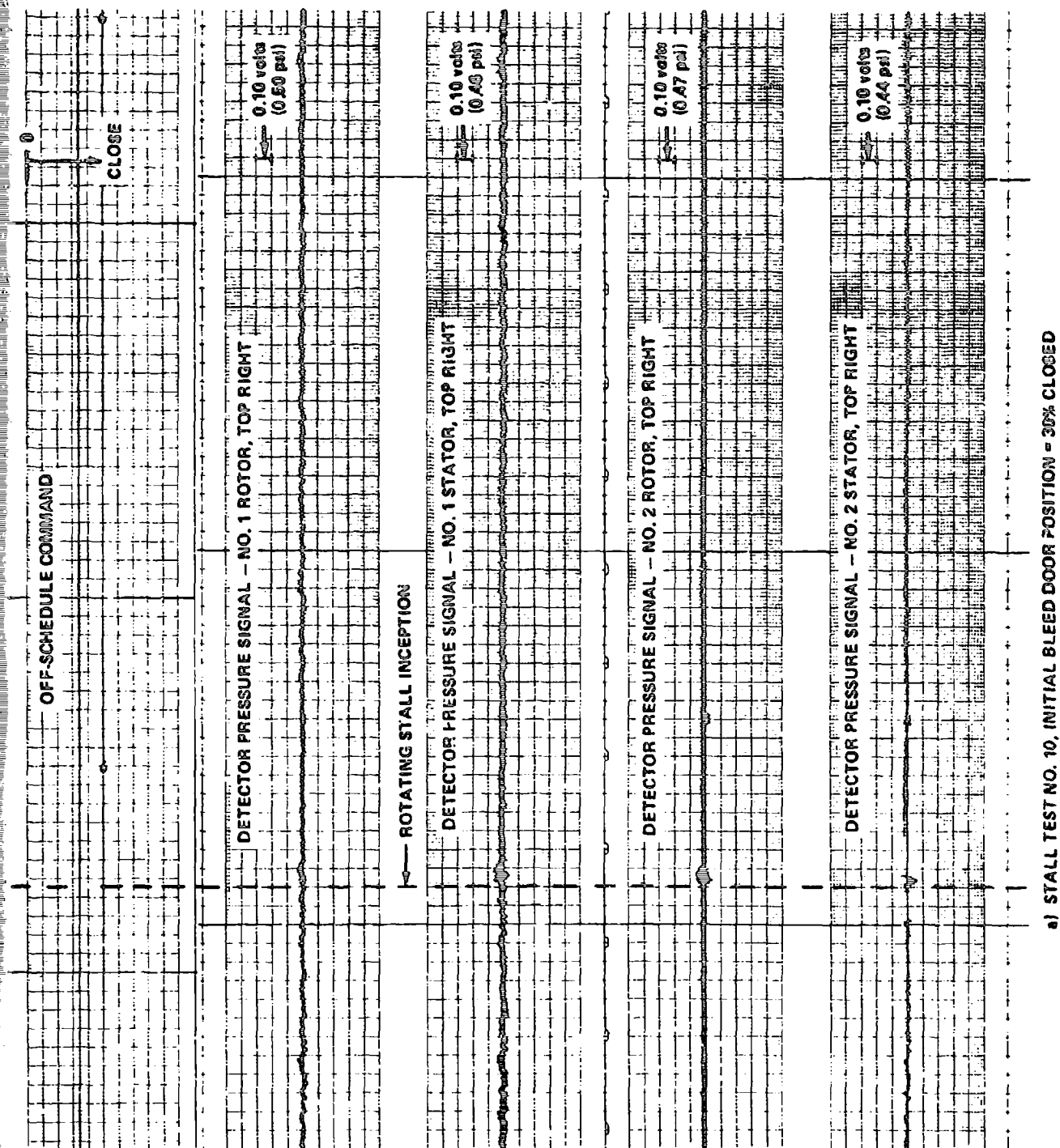


d) STALL TEST NO. 10, CORRECTED ENGINE SPEED, $(N/N \cdot \sqrt{\beta}) = 71.6\%$

Figure 31 (Cont.)

PERFORMANCE OF ROTATING STALL CONTROL ON J-85 ENGINE
COMPRESSOR STALLED BY CLOSING BLEED DOORS AT CONSTANT ENGINE SPEED
ENGINE TEST NO. 14: 180° CIRCUMFERENTIAL INLET DISTORTION

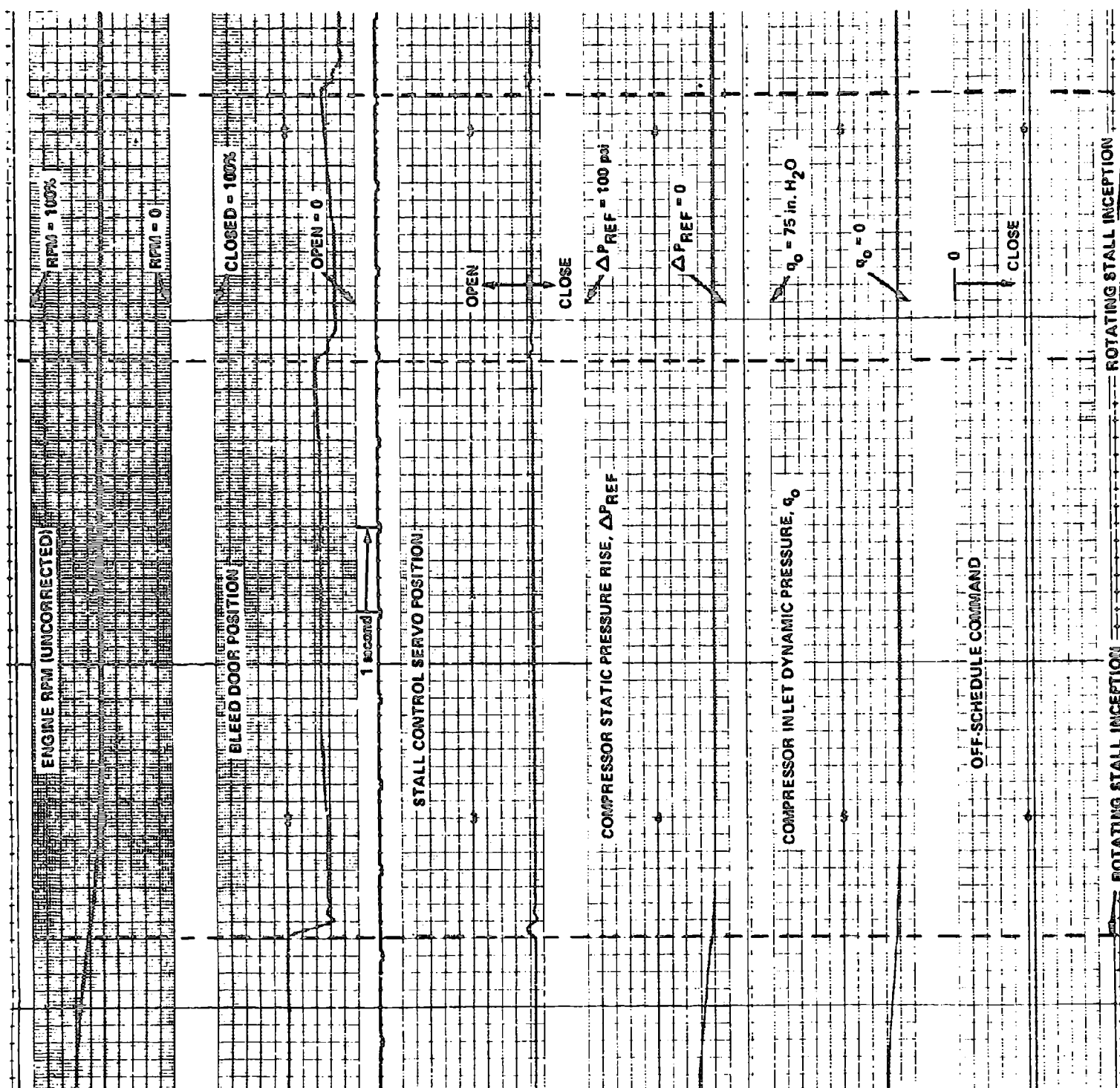


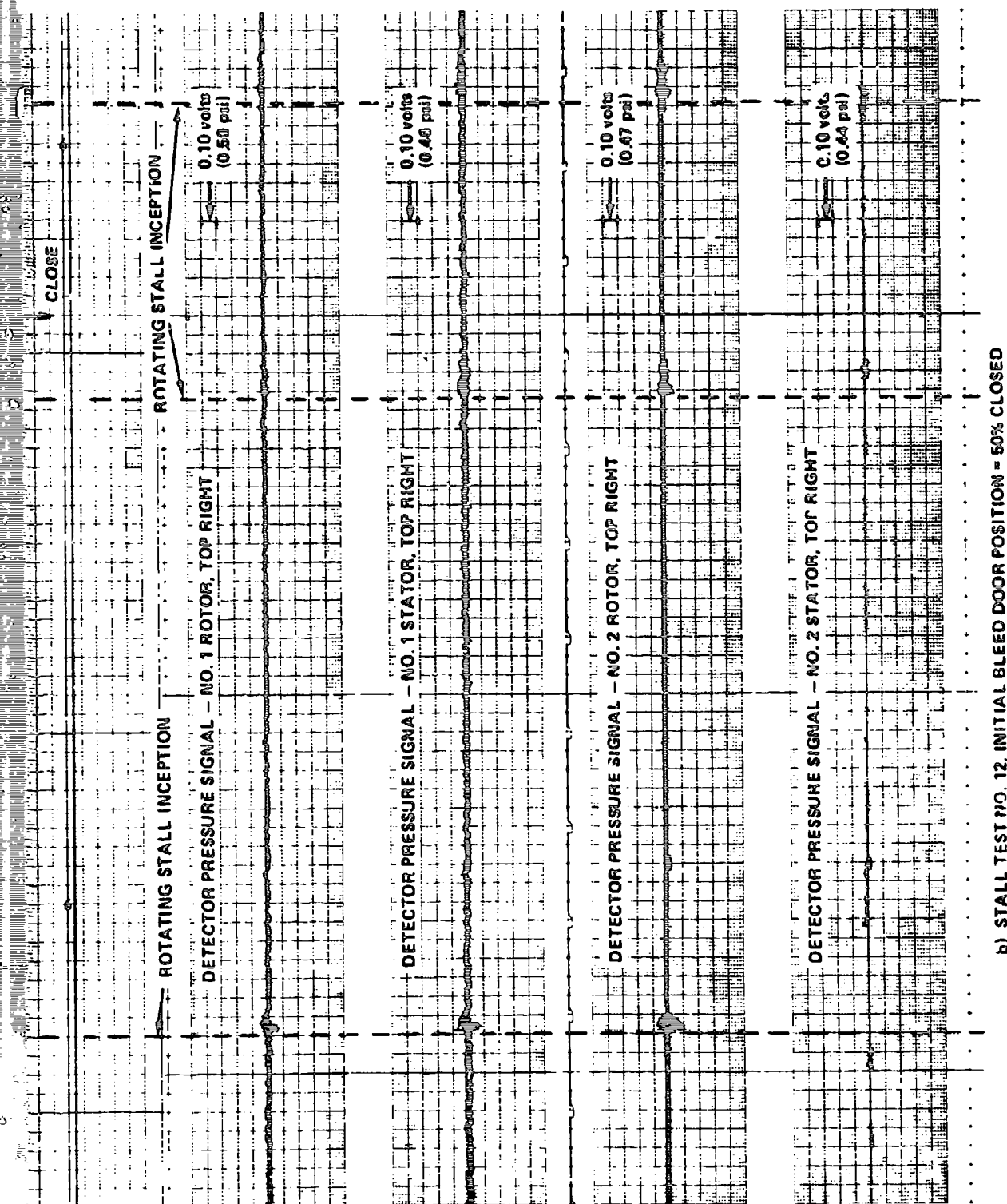


a) STALL TEST NO. 10, INITIAL BLEED DOOR POSITION = 30% CLOSED

PERFORMANCE OF ROTATING STALL CONTROL ON J-85 ENGINE
COMPRESSOR STALLED BY DECELERATING ENGINE WITH BLEED DOORS PARTLY CLOSED
ENGINE TEST NO. 13: NO INLET DISTORTION

Figure 32

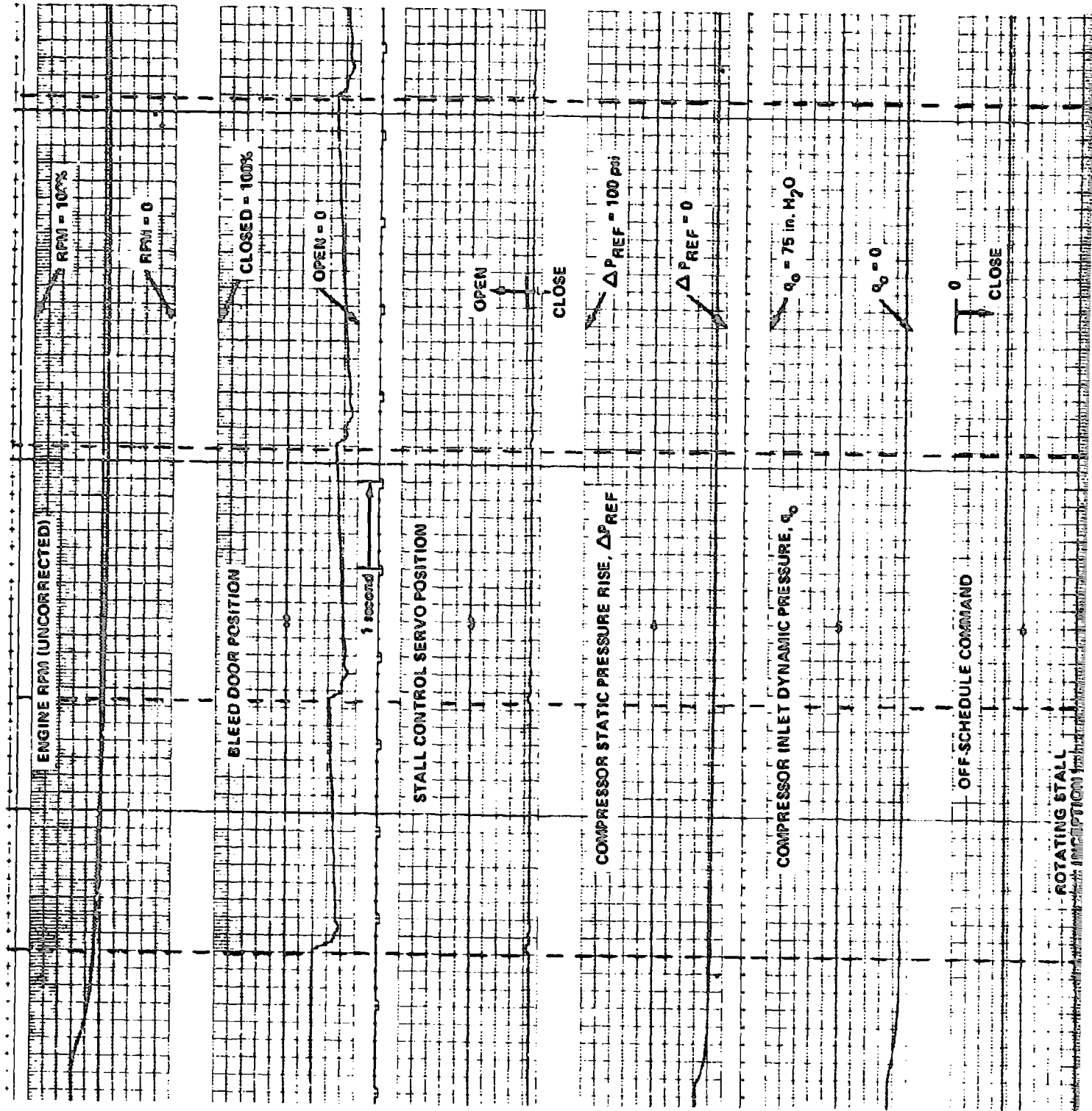


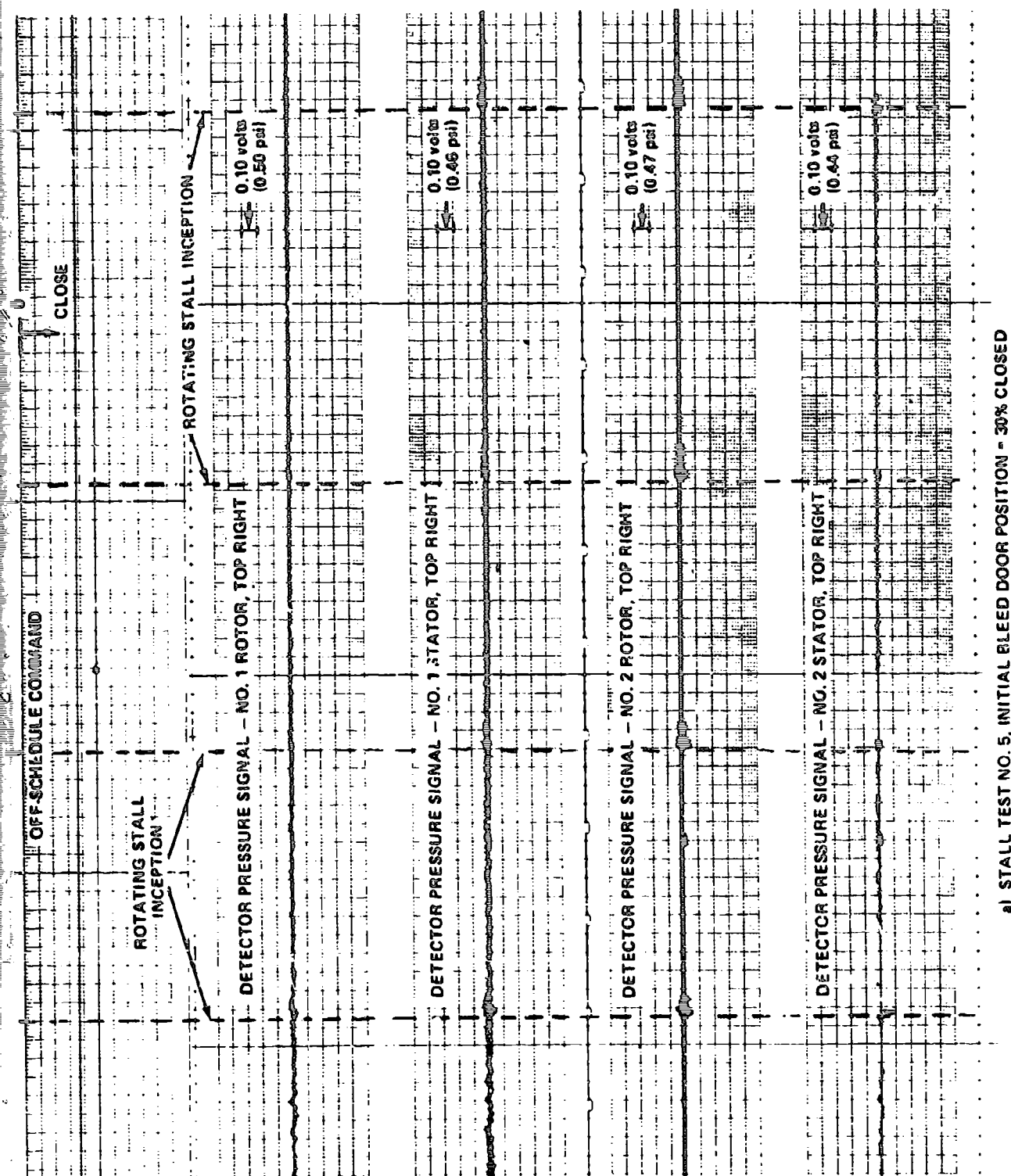


b) STALL TEST NO. 12, INITIAL BLEED DOOR POSITION = 50% CLOSED

Figure 32 (Cont.)

PERFORMANCE OF ROTATING STALL CONTROL ON J-85 ENGINE
 COMPRESSOR STALLED BY DECELERATING ENGINE WITH BLEED DOORS PARTLY CLOSED
 ENGINE TEST NO. 13: NO INLET DISTORTION

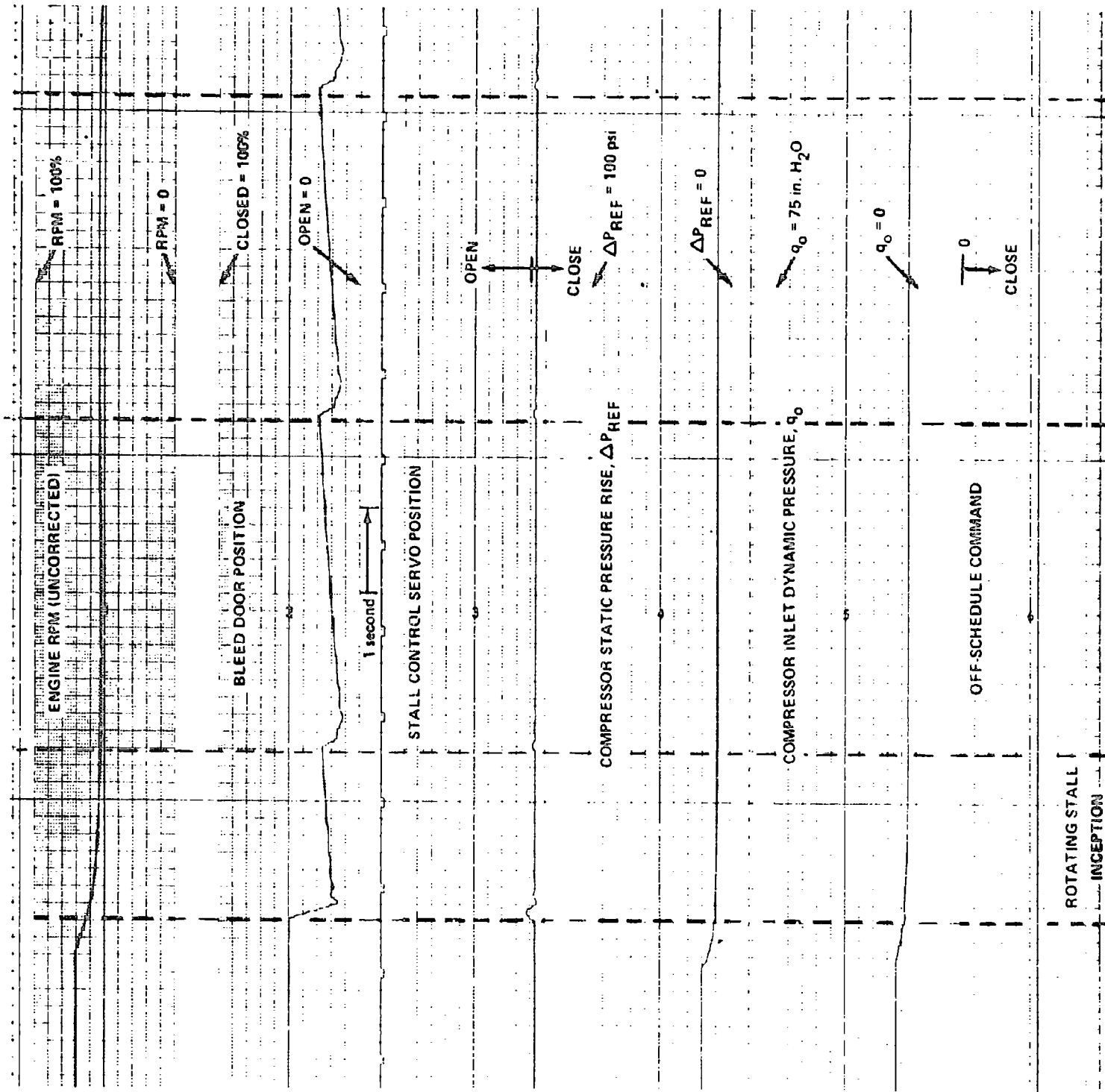


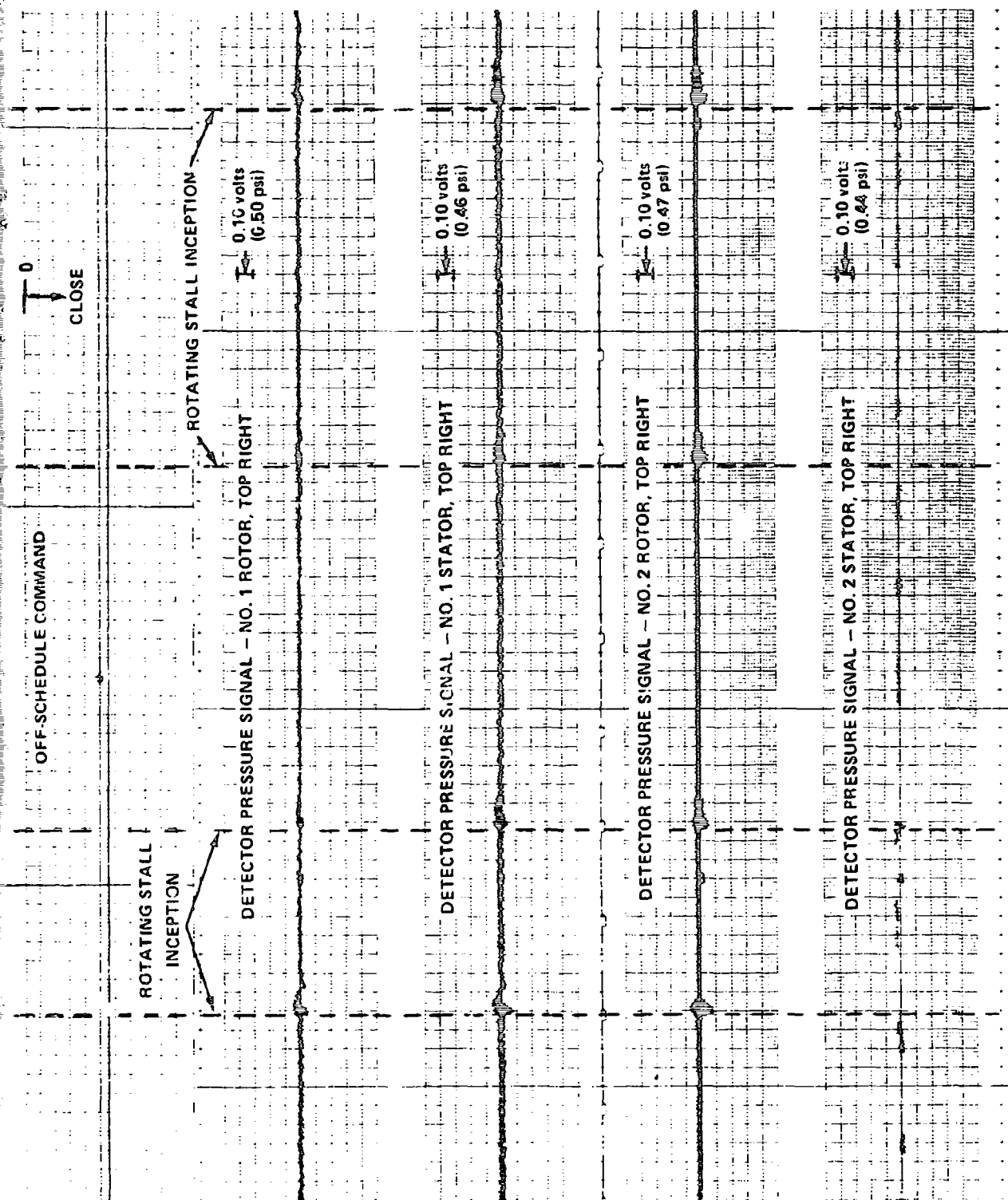


a) STALL TEST NO. 5, INITIAL BLEED DOOR POSITION - 30% CLOSED

PERFORMANCE OF ROTATING STALL CONTROL ON J-85 ENGINE
 COMPRESSOR STALLED BY DECELERATING ENGINE WITH BLEED DOORS PARTLY CLOSED
 ENGINE TEST NO. 14: 180° CIRCUMFERENTIAL INLET DISTORTION

Figure 33

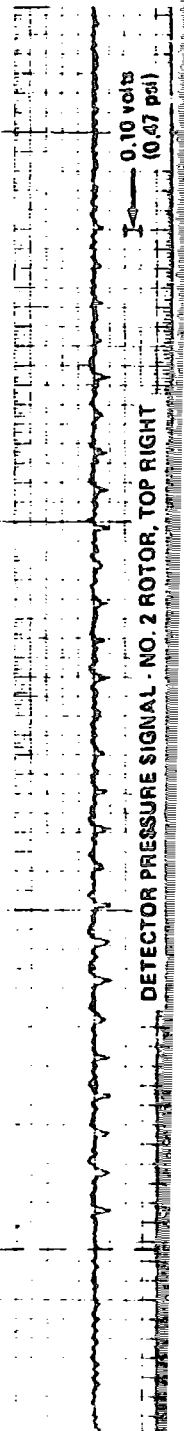
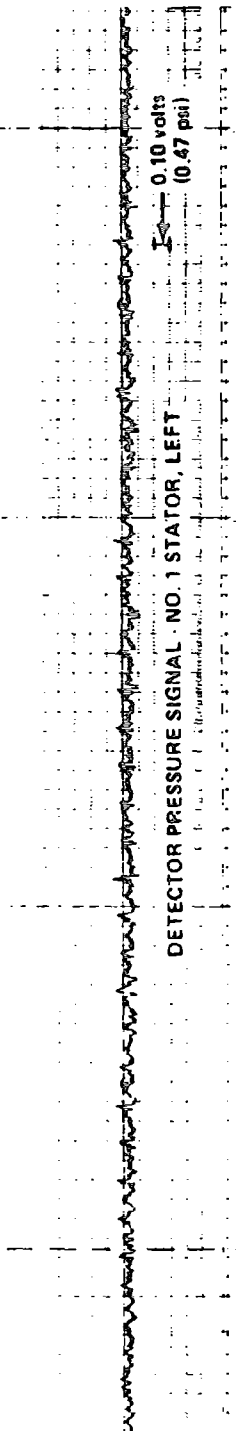
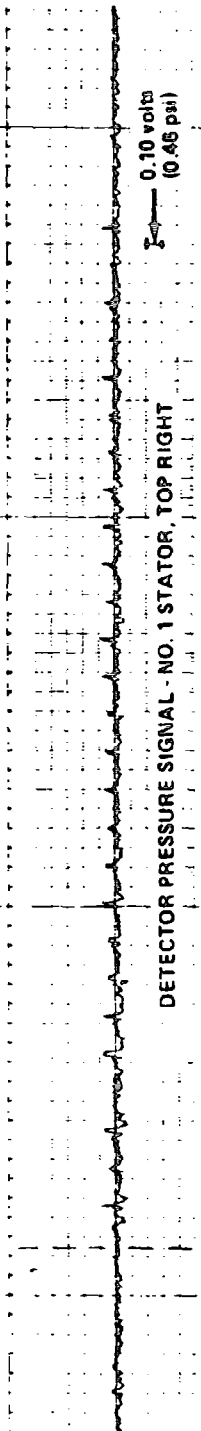
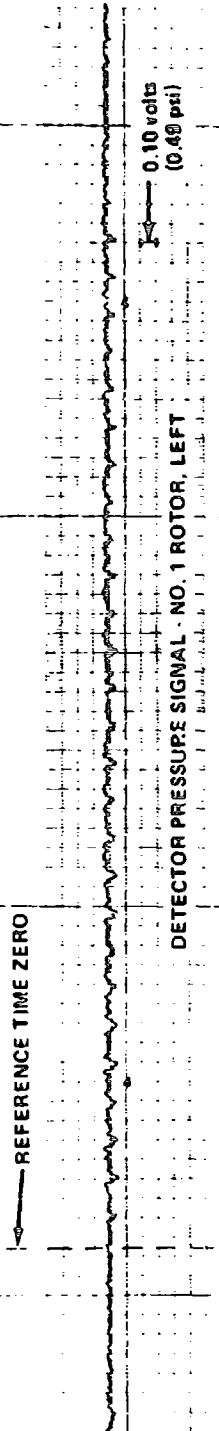
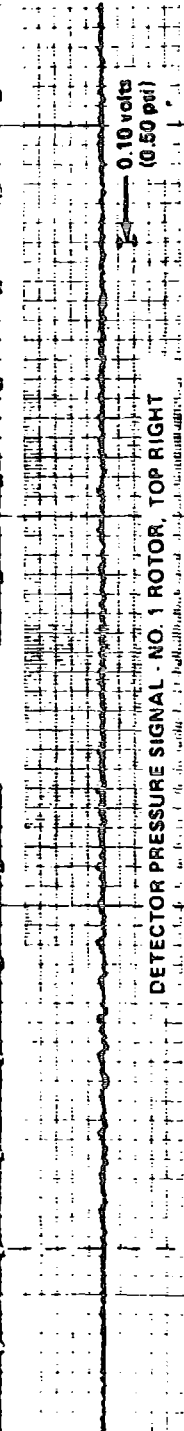
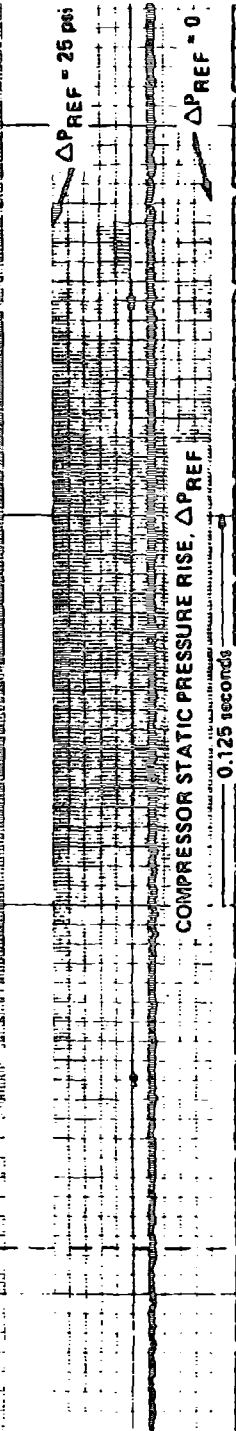
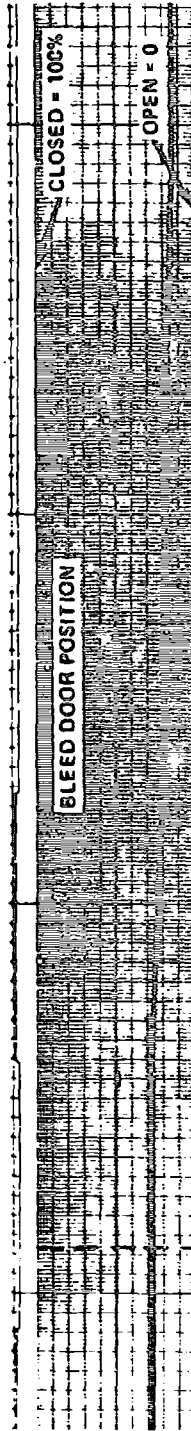




b) STALL TEST NO. 7, INITIAL BLEED DOOR POSITION = 50% CLOSED

Figure 33 (Cont.)

PERFORMANCE OF ROTATING STALL CONTROL ON J-85 ENGINE
 COMPRESSOR STALLED BY DECELERATING ENGINE WITH BLEED DOORS PARTLY CLOSED
 ENGINE TEST NO. 14: 180° CIRCUMFERENTIAL INLET DISTORTION



0.10 volts
(0.47 psi)

DETECTOR PRESSURE SIGNAL - NO. 2 ROTOR, TOP RIGHT

0.10 volts
(0.49 psi)

DETECTOR PRESSURE SIGNAL - NO. 2 ROTOR, LEFT

0.10 volts
(0.44 psi)

DETECTOR PRESSURE SIGNAL - NO. 2 STATOR, TOP RIGHT

0.10 volts
(0.47 psi)

DETECTOR PRESSURE SIGNAL - NO. 2 STATOR, LEFT
(RECORDER PEN INOPERATIVE)

NOT USED

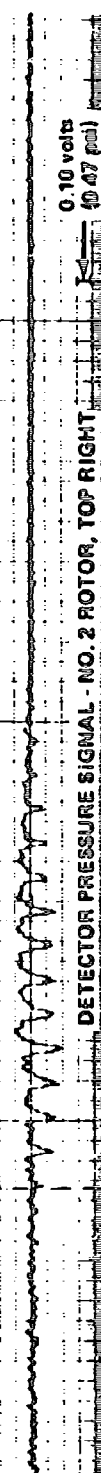
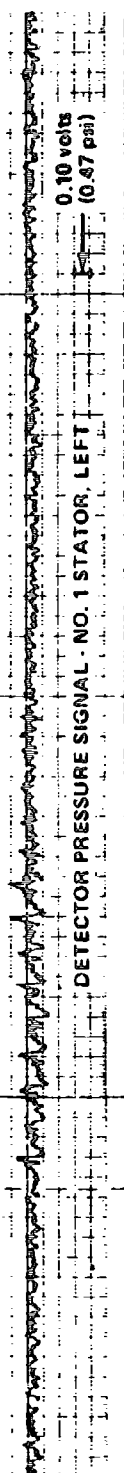
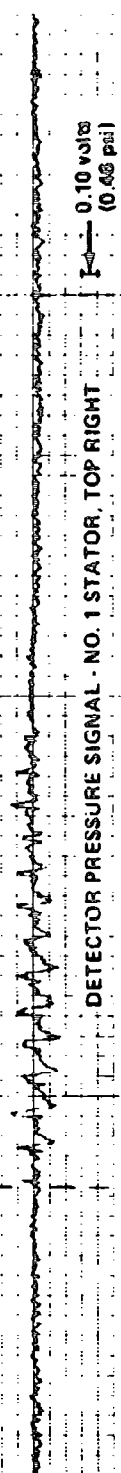
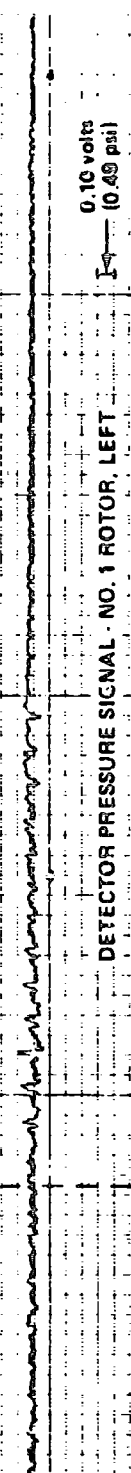
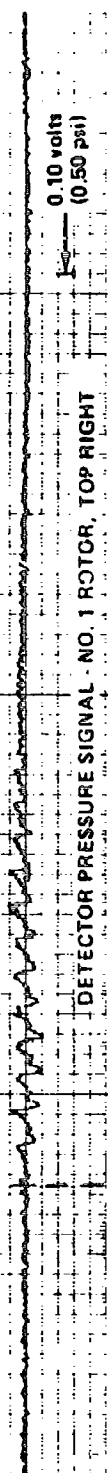
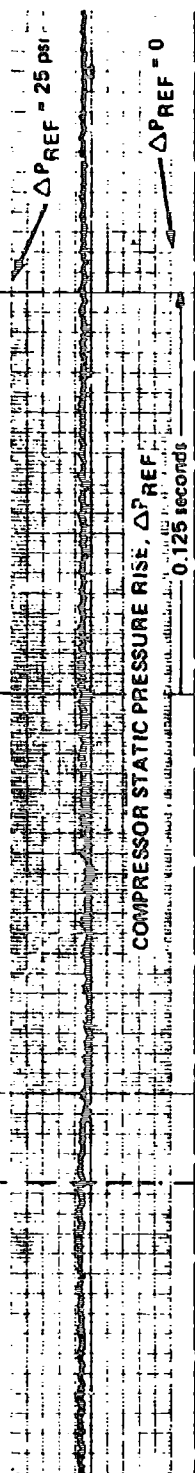
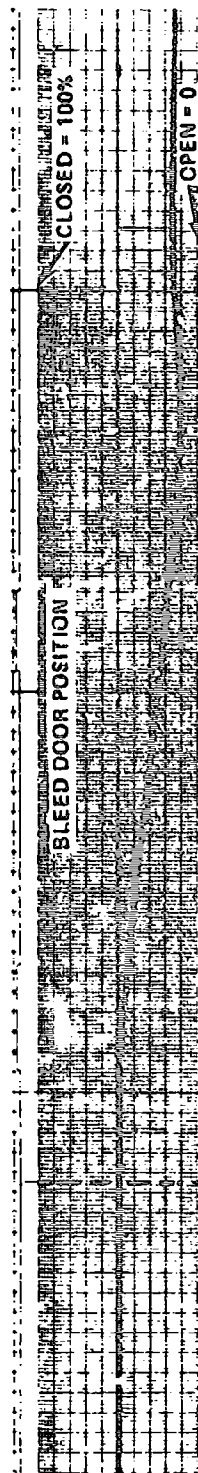
0.10 volts
(0.93 psi)

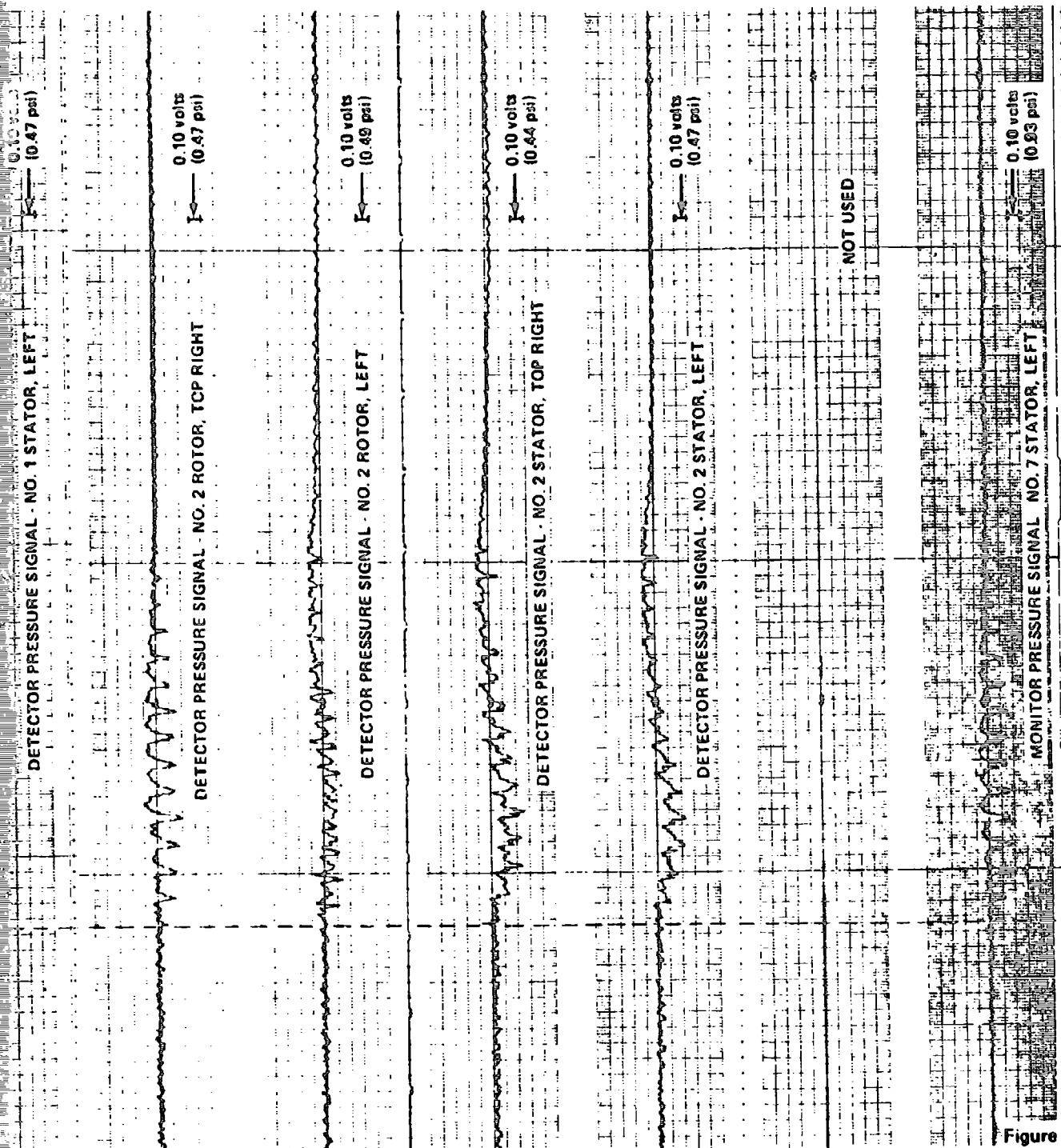
MONITOR PRESSURE SIGNAL - NO. 7 STATOR, LEFT

a) STALL TEST NO. 4(b), CORRECTED ENGINE SPEED, $(N/N^*\sqrt{\theta}) = 52.3\%$

Figure 34

ROTATING STALL DETECTOR SIGNALS (EXPANDED TIME SCALE)
ENGINE TEST NO. 13: NO INLET DISTORTION
COMPRESSOR STALLED BY CLOSING BLEED DOORS AT CONSTANT
ENGINE SPEED

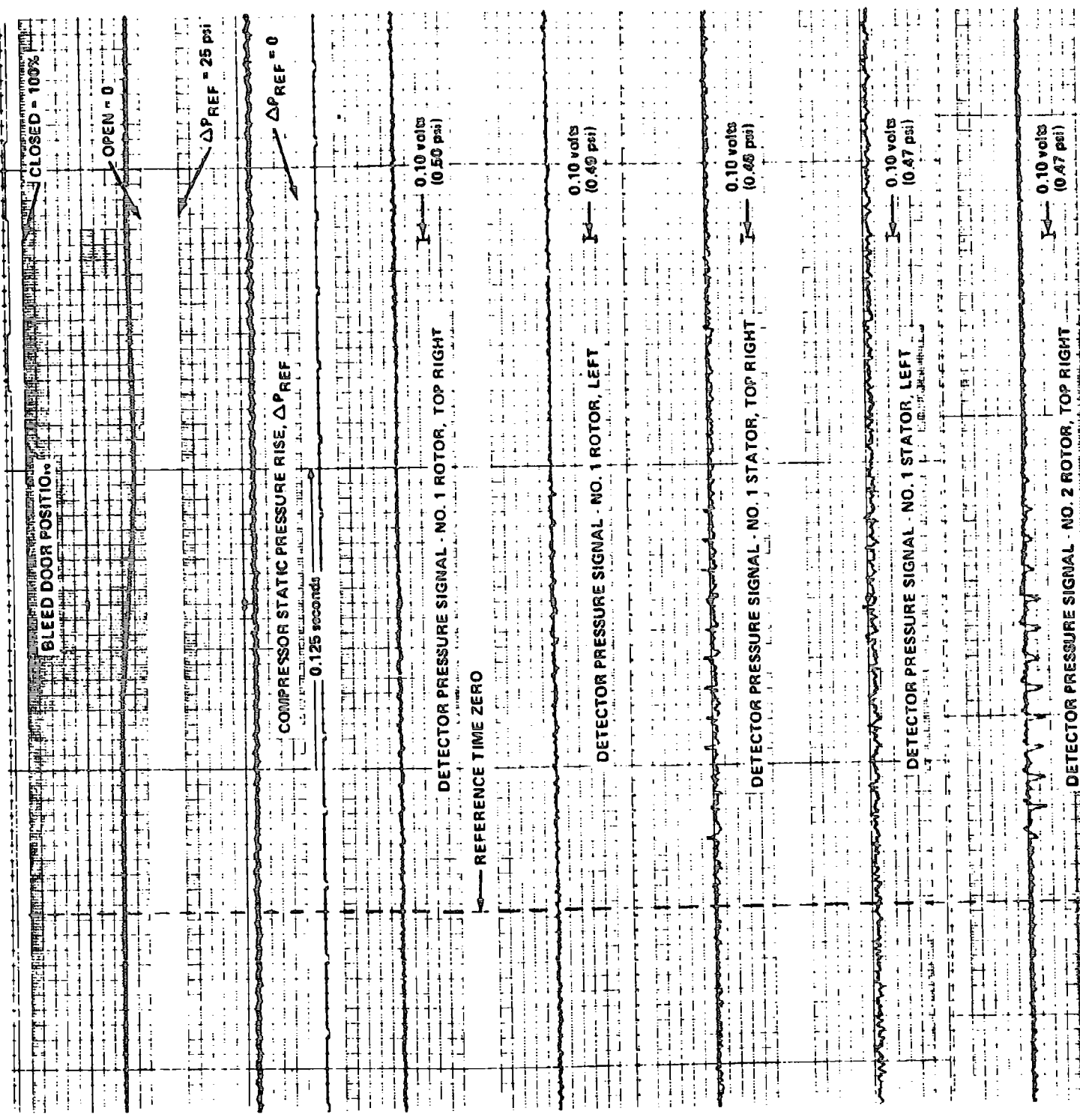


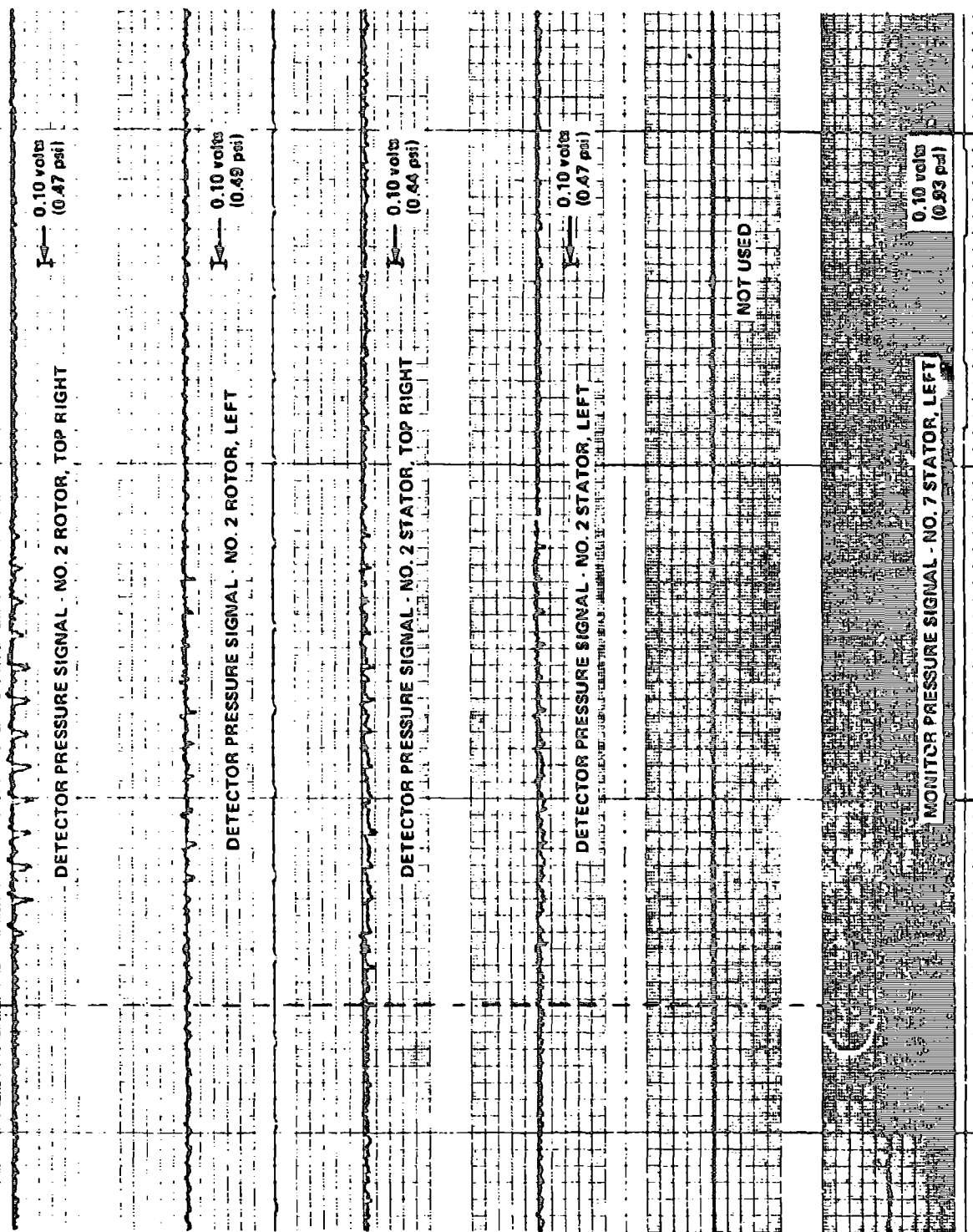


b) STALL TEST NO. 5, CORRECTED ENGINE SPEED, $(N/N^* \bar{b}) = 52.6\%$

Figure 34 (Cont.)

ROTATING STALL DETECTOR SIGNALS (EXPANDED TIME SCALE)
ENGINE TEST NO. 13: NO INLET DISTORTION
COMPRESSOR STALLED BY CLOSING BLEED DOORS AT CONSTANT
ENGINE SPEED





a) STALL TEST NO. 1, CORRECTED ENGINE SPEED, $(N/N^* \sqrt{\theta}) = 52.1\%$

Figure 35

ROTATING STALL DETECTOR SIGNALS (EXPANDED TIME SCALE)
ENGINE TEST NO. 14: 180° CIRCUMFERENTIAL INLET
DISTORTION—COMPRESSOR STALLED BY CLOSING
BLEED DOORS AT CONSTANT ENGINE SPEED

BLEED DOOR POSITION

CLOSED - 100%

OPEN = 0

$\Delta P_{REF} = 25 \text{ psi}$

COMPRESSOR STATIC PRESSURE RISE, ΔP_{REF}

0.125 seconds

$\Delta P_{REF} = 0$

DETECTOR PRESSURE SIGNAL - NO. 1 ROTOR, TOP RIGHT

0.10 volts
(0.50 psi)

REFERENCE TIME ZERO

DETECTOR PRESSURE SIGNAL - NO. 1 ROTOR, LEFT

0.10 volts
(0.40 psi)

DETECTOR PRESSURE SIGNAL - NO. 1 STATOR, TOP RIGHT

0.10 volts
(0.45 psi)

DETECTOR PRESSURE SIGNAL - NO. 1 STATOR, LEFT

0.10 volts
(0.47 psi)

DETECTOR PRESSURE SIGNAL - NO. 2 ROTOR, TOP RIGHT

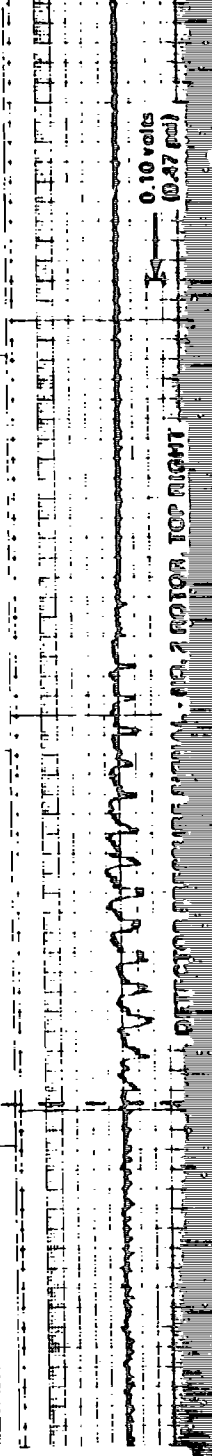
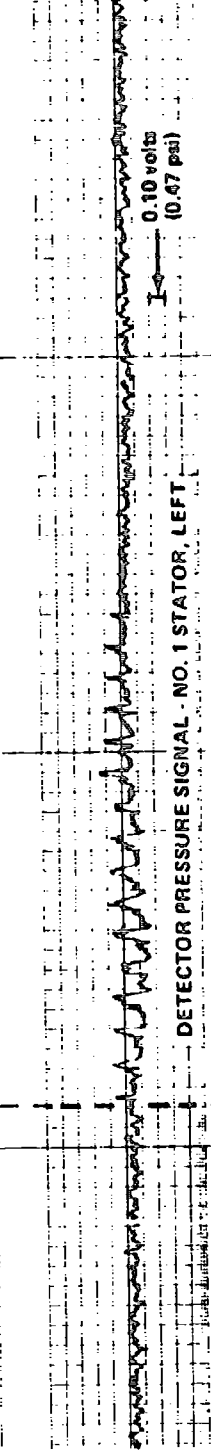
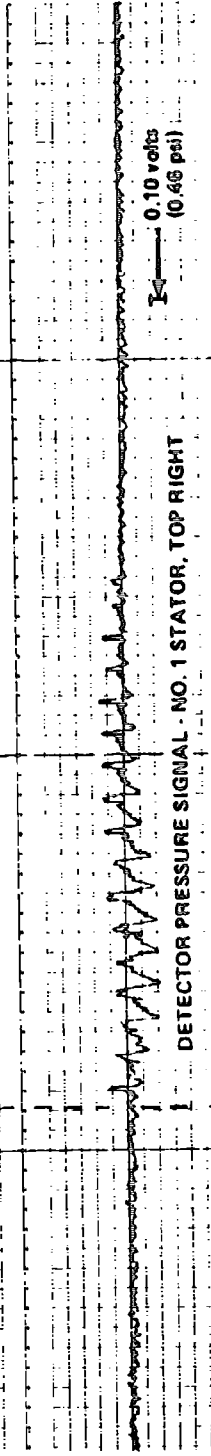
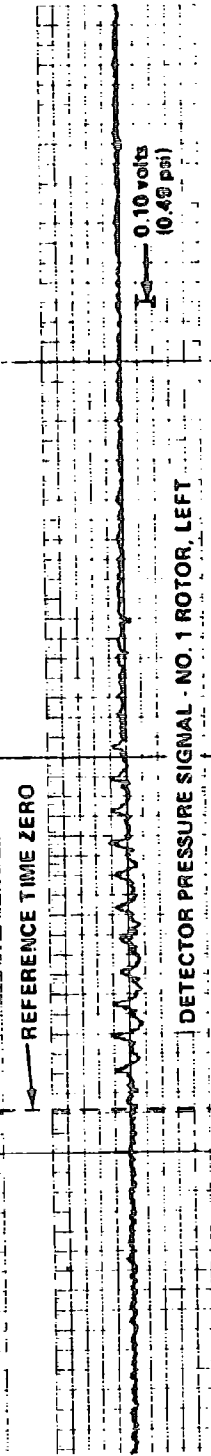
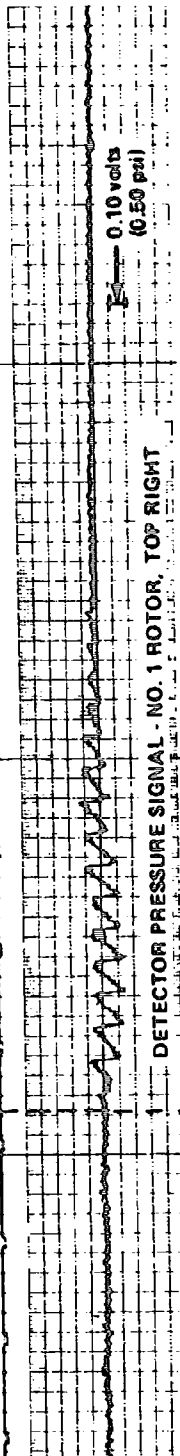
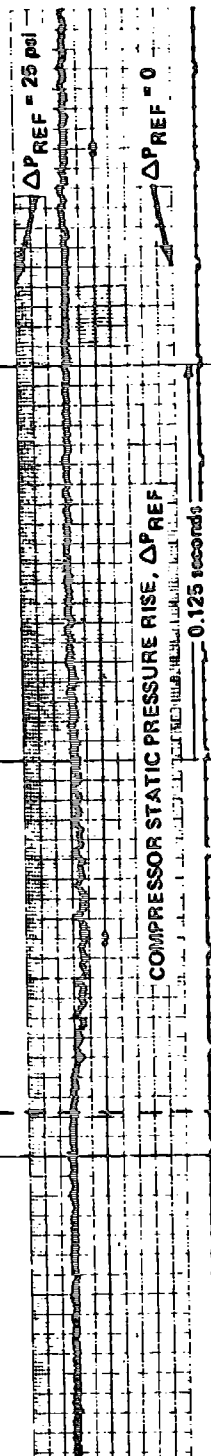
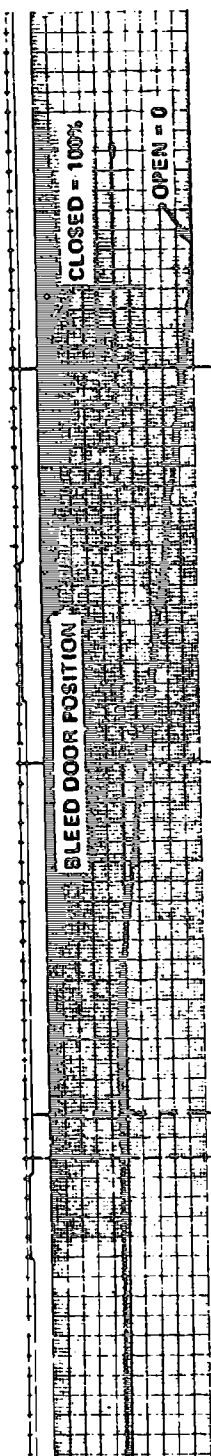
0.10 volts
(0.47 psi)

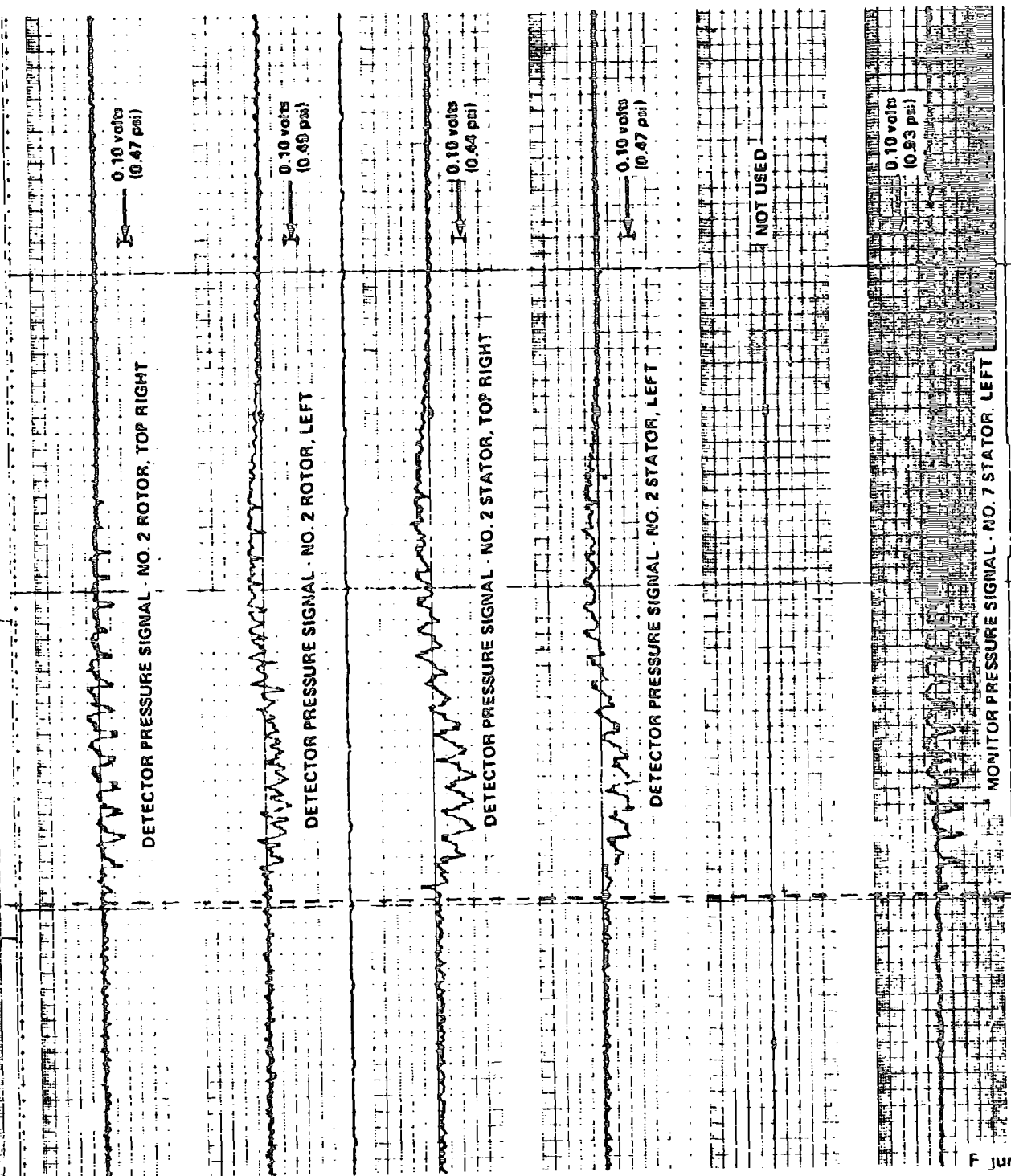


b) STALL TEST NO. 2, CORRECTED ENGINE SPEED, $(N/N^* f_{\theta}) = 63.2\%$

Figure 35 (Cont.)

ROTATING STALL DETECTOR SIGNALS (EXPANDED TIME SCALE)
ENGINE TEST NO. 14: 180° CIRCUMFERENTIAL INLET
DISTORTION—COMPRESSOR STALLED BY CLOSING
BLEED DOORS AT CONSTANT ENGINE SPEED





c) STALL TEST NO. 3. CORRECTED ENGINE SPEED, $(N_2/N_2^*) = 67.4\%$

F. Jure 35 (Cont.)

ROTATING STALL DETECTOR SIGNALS (EXPANDED TIME SCALE)
ENGINE TEST NO. 14: 180° CIRCUMFERENTIAL INLET
DISTORTION—COMPRESSOR STALLED BY CLOSING
BLEED DOORS AT CONSTANT ENGINE SPEED

BLEED DOOR POSITION

CLOSED = 100%

OPEN = 0

COMPRESSOR STATIC PRESSURE RISE, ΔP_{REF}

$\Delta P_{REF} = 25 \text{ psi}$

$\Delta P_{REF} = 0$

0.125 seconds

DETECTOR PRESSURE SIGNAL - NO. 1 ROTOR, TOP RIGHT

0.10 volts
(0.50 psi)

DETECTOR PRESSURE SIGNAL - NO. 1 ROTOR, LEFT

0.10 volts
(0.49 psi)

DETECTOR PRESSURE SIGNAL - NO. 1 STATOR, TOP RIGHT

0.10 volts
(0.46 psi)

REFERENCE TIME ZERO

DETECTOR PRESSURE SIGNAL - NO. 1 STATOR, LEFT

0.10 volts
(0.47 psi)

DETECTOR PRESSURE SIGNAL - NO. 2 ROTOR, TOP RIGHT

0.10 volts
(0.47 psi)

0.10 volts
(0.47 psi)

DETECTOR PRESSURE SIGNAL - NO. 2 ROTOR, TOP RIGHT

0.10 volts
(0.49 psi)

DETECTOR PRESSURE SIGNAL - NO. 2 ROTOR, LEFT

0.10 volts
(0.47 psi)

DETECTOR PRESSURE SIGNAL - NO. 2 STATOR, TOP RIGHT

0.10 volts
(0.47 psi)

DETECTOR PRESSURE SIGNAL - NO. 2 STATOR, LEFT

NOT USED

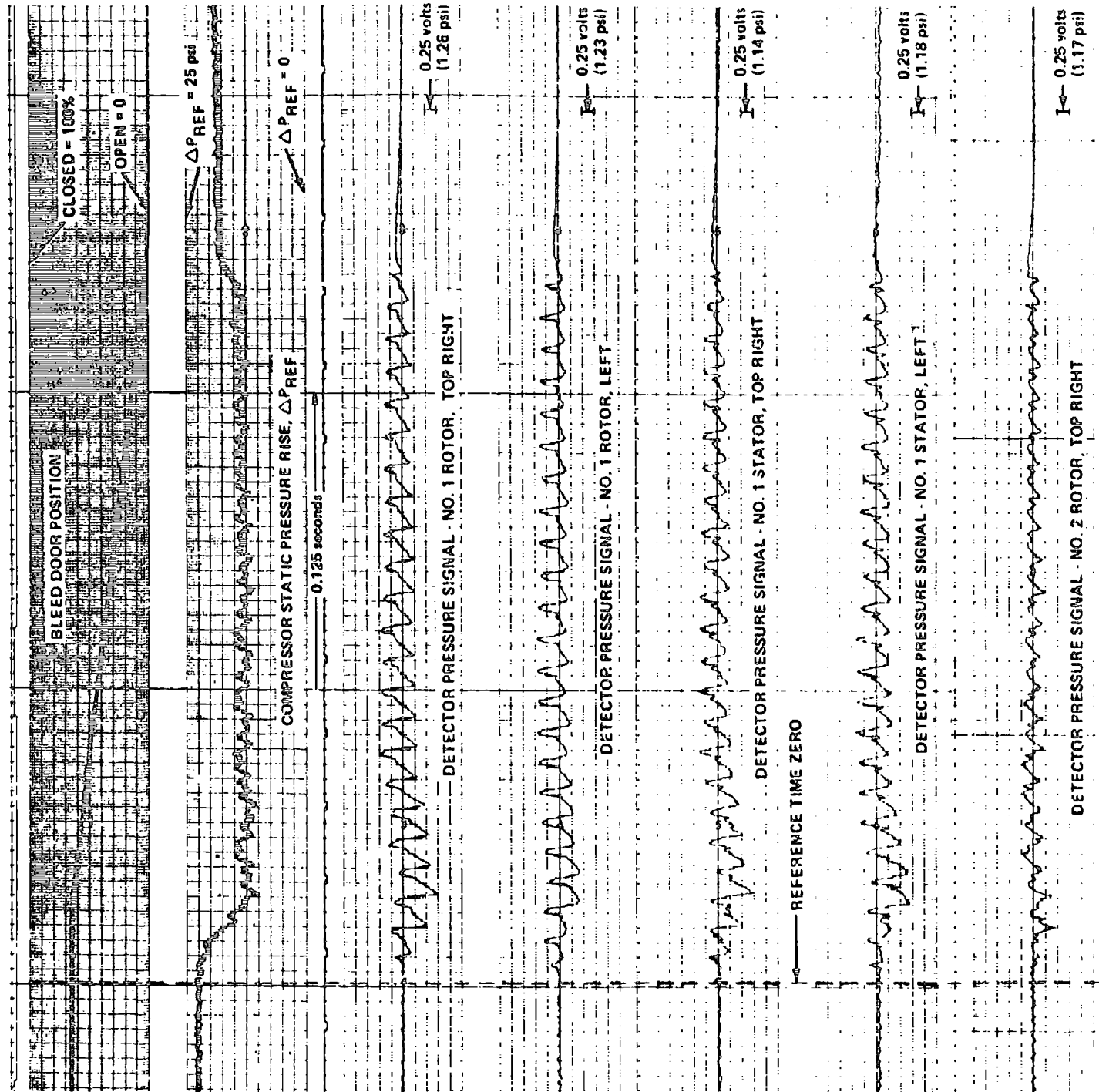
0.10 volts
(0.93 psi)

MONITOR PRESSURE SIGNAL - NO. 7 STATOR, LEFT

d) STALL TEST NO. 10, CORRECTED ENGINE SPEED, $(N/N^* \sqrt{\beta}) = 71.8\%$

Figure 35 (Cont.)

ROTATING STALL DETECTOR SIGNALS (EXPANDED TIME SCALE)
ENGINE TEST NO. 14: 180° CIRCUMFERENTIAL INLET
DISTORTION COMPRESSOR STALLED BY CLOSING
BLEED DOORS AT CONSTANT ENGINE SPEED



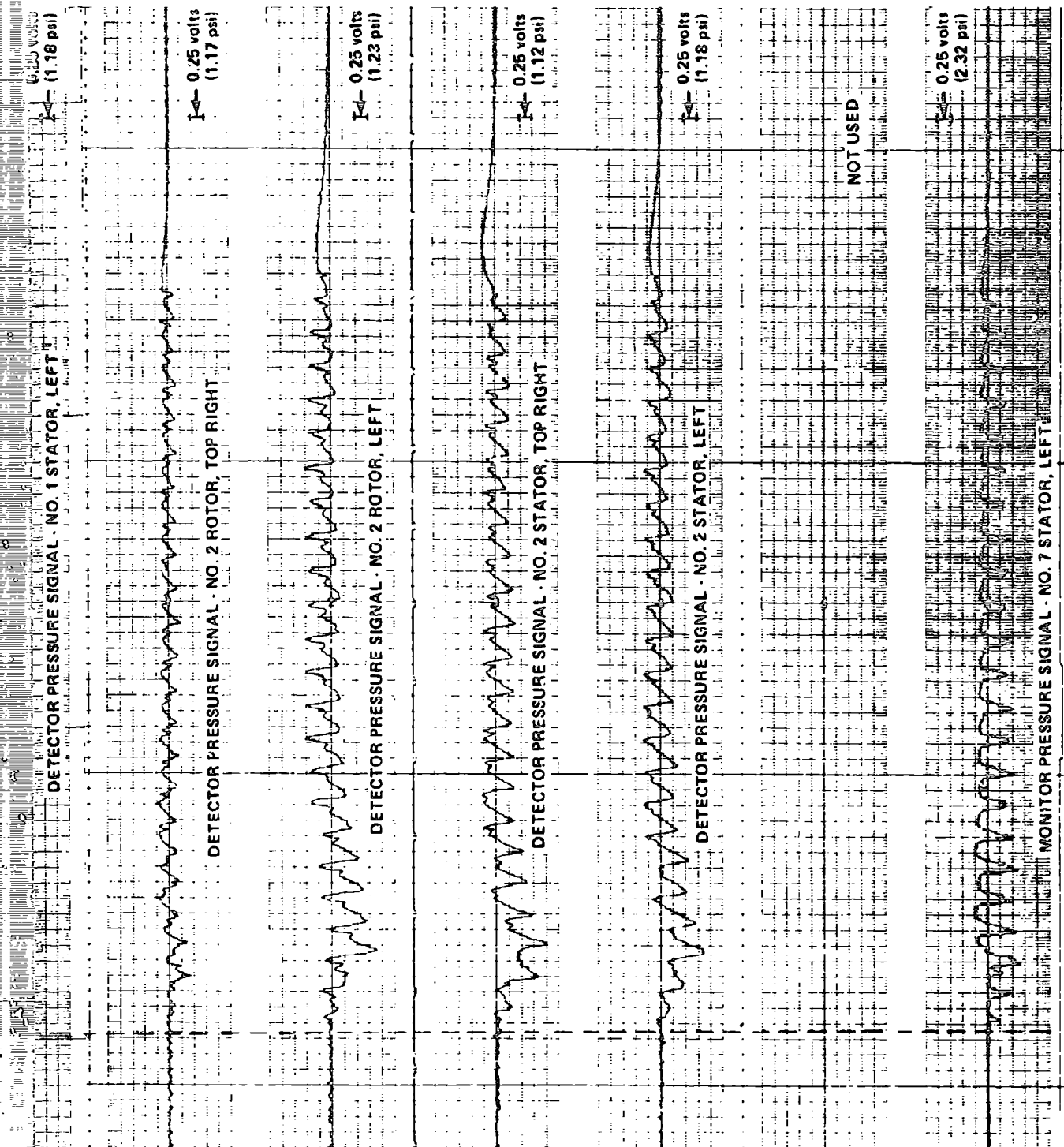


Figure 36

ROTATING STALL DETECTOR SIGNALS (EXPANDED TIME SCALE - REDUCED VERTICAL GAIN) - ENGINE TEST NO. 14, STALL TEST NO. 10: 180° CIRCUMFERENTIAL INLET DISTORTION
COMPRESSOR STALLED BY CLOSING BLEED DOORS AT CONSTANT ENGINE SPEED ($\sqrt{\theta} = 71.8\%$)

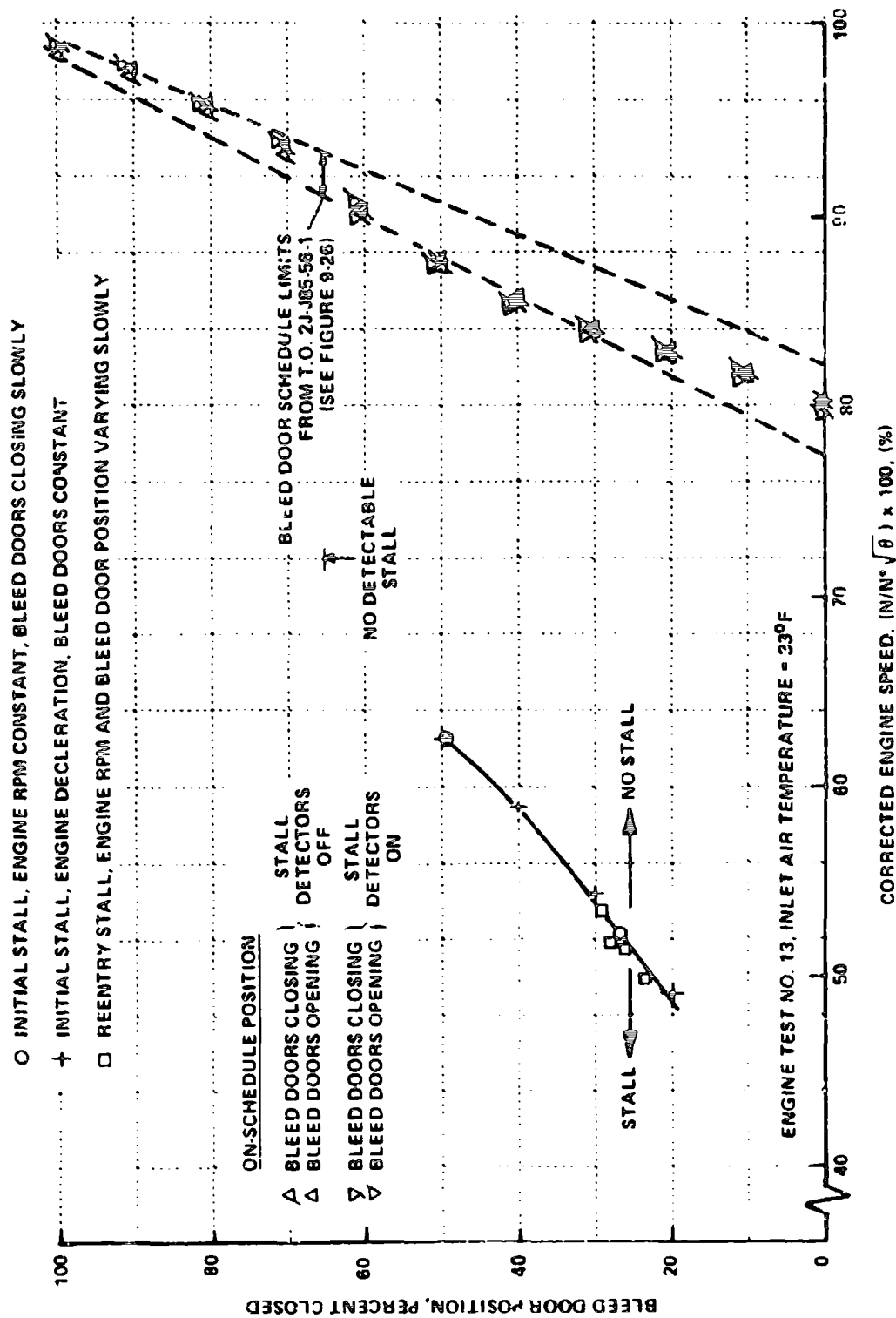


Figure 37 BLEED DOOR POSITION AT ROTATING STALL INCEPTION ON J85 ENGINE WITH UNDISTORTED INLET FLOW

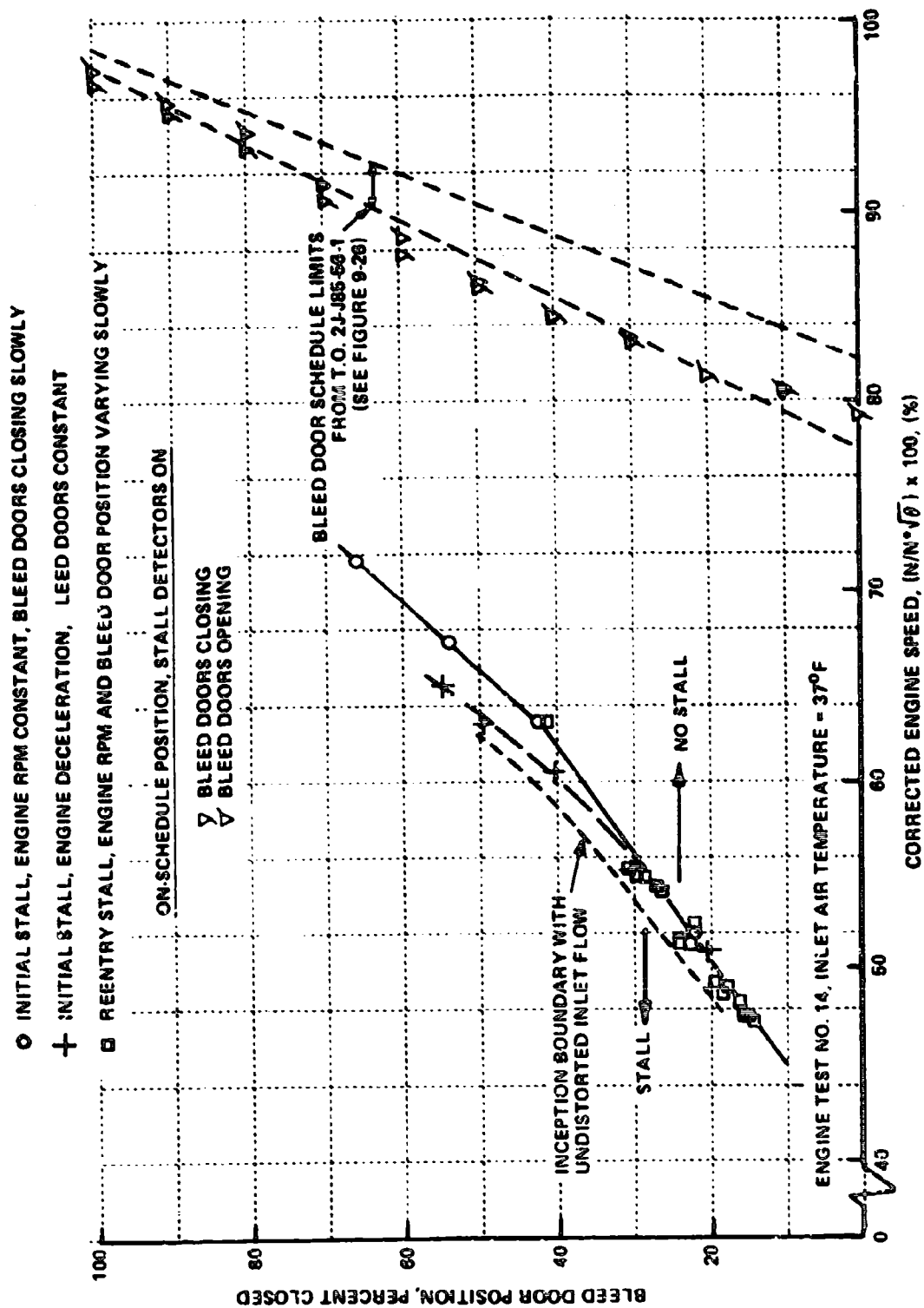


Figure 38 BLEED DOOR POSITION AT ROTATING STALL INCEPTION ON J85 ENGINE WITH 180 DEGREE CIRCUMFERENTIAL INLET DISTORTION

REFERENCES

1. Ludwig, G.R., Nenni, J.P. and Arendt, R.H., Investigation of Rotating Stall in Axial Flow Compressors and the Development of a Prototype Rotating Stall Control System, AFAPL-TR-73-45, May 1973.
2. Ludwig, G.R., Nenni, J.P. and Rice, R.S., Jr., An Investigation of Rotating Stall Phenomena in Turbine Engine Compressors, AFAPL-TR-70-26, May 1970.
3. Calogeras, J.E., Mehlic, C.M., and Burstadt, P.L., Experimental Investigation of the Effect of Screen-Induced Total Pressure Distortion on Turbojet Stall Margin, NASA Technical Memorandum TMX-2239, March 1971.

UNCLASSIFIED

SECURITY CLASSIFICATION OF THIS PAGE (When Data Entered)

REPORT DOCUMENTATION PAGE		READ INSTRUCTIONS BEFORE COMPLETING FORM	
1. REPORT NUMBER	2. GOVT ACCESSION NO.	3. RECIPIENT	4. LOG NUMBER
AFAPL-TR-76-48 -Volume III			
5. TITLE (and Subtitle)		6. TYPE OF REPORT & PERIOD COVERED	
Investigation of Rotating Stall Phenomena in Axial Flow Compressors		Final, May 73 - May 76	
Vol. III - Development of a Rotating Stall Control System		7. PERFORMING ORG. REPORT NUMBER	
		XE-5315-A-12	
8. AUTHOR(s)		9. CONTRACT OR GRANT NUMBER(s)	
Gary R. Ludwig Rudy H. Arendt		F33615-73-C-2046	
10. PERFORMING ORGANIZATION NAME AND ADDRESS		11. PROGRAM ELEMENT, PROJECT, TASK AREA & WORK UNIT NUMBERS	
Calspan Corporation P. O. Box 235 Buffalo, New York 14221		30660334	
12. CONTROLLING OFFICE NAME AND ADDRESS		13. REPORT DATE	
U.S. Air Force Aero-Propulsion Laboratory Air Force Systems Command Wright-Patterson AFB, OH 45433		June 1976	
		14. NUMBER OF PAGES	
		156	
15. MONITORING AGENCY NAME & ADDRESS (if different from Controlling Office)		16. SECURITY CLASS. (of this report)	
		Unclassified	
		17. DECLASSIFICATION DOWNGRADING SCHEDULE	
18. DISTRIBUTION STATEMENT (of this Report)			
19. DISTRIBUTION STATEMENT (of the abstract entered in Block 20, if different from Report)			
Approved for public release; distribution unlimited.			
20. SUPPLEMENTARY NOTES			
21. KEY WORDS (Continue on reverse side if necessary and identify by block number)			
Rotating Stall Fluid Mechanics Compressor Jet Engines Cascade Acoustics Control Systems Noise			
22. ABSTRACT (Continue on reverse side if necessary and identify by block number)			
<p>This report presents the results of a research program that had two major objectives. The first objective was the development of a prototype rotating stall control system which was tested both on a low speed rig and a J-85-5 engine. The second objective was to perform fundamental studies of the flow mechanisms that produce rotating stall, surge and noise in axial flow compressors and thereby obtain an understanding of these phenomena that would aid attaining the first objective. The work is reported in three separate volumes. Volume I</p>			

DD FORM 1 JAN 73 1473 EDITION OF 1 NOV 68 IS OBSOLETE

UNCLASSIFIED


SECURITY CLASSIFICATION OF THIS PAGE (When Data Entered)

UNCLASSIFIED

SECURITY CLASSIFICATION OF THIS PAGE(When Data Entered)

20. (Cont'd)

covers the fundamental theoretical and experimental studies of rotating stall; Volume II covers the theoretical and experimental studies of discrete-tone aerodynamic noise generation mechanisms in axial flow compressors; and Volume III covers the development and testing of a prototype rotating stall control system on both the low speed test rig and the J-85-5 engine.

ACCESSION for	
NTIS	Wallo Section <input checked="" type="checkbox"/>
DTIC	Detl Section <input type="checkbox"/>
UNANNOUNCED	<input type="checkbox"/>
JUSTIFICATION	
BY	
DISTRIBUTION/AVAILABILITY CODES	
Dist.	AVAIL. and/or SPECIAL
	

1a

UNCLASSIFIED

SECURITY CLASSIFICATION OF THIS PAGE(When Data Entered)